Lawrence Berkeley National Laboratory
Recent Work

Title

ALL INORGANIC AMBIENT TEMPERATURE RECHARGEABLE LITHIUM BATTERY: FINAL REPORT

Permalink

https://escholarship.org/uc/item/2jw6n7z0

Authors

Kuo, H.F.
Dey, A.N.
Schlaikjer, C.

Publication Date

1987-10-01

eScholarship.org Powered by the California Digital Library
University of California

LBL-24295
UC-210

Lawrence Berkeley Laboratory
UNIVERSITY OF CALIFORNIA

APPLIED SCIENCE DIVISION

RECEIVED
LAWRENCE
BERKELEY LABORATORY

APR 19 1988

LIBRARY AND
DOCUMENTS SECTION

All Inorganic Ambient Temperature Rechargeable Lithium Battery: Final Report

H.C. Kuo, A.N. Dey, C. Schlaikjer,
D. Foster, and M. Kallianidis

October 1987

APPLIED SCIENCE DIVISION

Prepared for the U.S. Department of Energy under Contract DE-AC03-76SF00098

LBL-24295

DISCLAIMER

This document was prepared as an account of work sponsored by the United States Government. While this document is believed to contain correct information, neither the United States Government nor any agency thereof, nor the Regents of the University of California, nor any of their employees, makes any warranty, express or implied, or assumes any legal responsibility for the accuracy, completeness, or usefulness of any information, apparatus, product, or process disclosed, or represents that its use would not infringe privately owned rights. Reference herein to any specific commercial product, process, or service by its trade name, trademark, manufacturer, or otherwise, does not necessarily constitute or imply its endorsement, recommendation, or favoring by the United States Government or any agency thereof, or the Regents of the University of California. The views and opinions of authors expressed herein do not necessarily state or reflect those of the United States Government or any agency thereof or the Regents of the University of California.

LBL-24295

ALL INORGANIC AMBIENT TEMPERATURE RECHARGEABLE LITHIUM BATTERY

Final Report

October 1987

by

H.C. Kuo
A.N. Dey
C. Schlaikjer
D. Foster
M. Kallianidis

Duracell Inc.
Duracell Research Center
37 A Street
Needham, Massachusetts 02194

for

Technology Base Research Project
Lawrence Berkeley Laboratory
University of California
Berkeley, California 94720

This work was supported by the Assistant Secretary for Conservation and Renewable Energy, Office of Energy Storage and Distribution of the U.S. Department of Energy under Contract No. DE-AC03-76SF00098, Subcontract No. 4507410 with the Lawrence Berkeley Laboratory.

SUMMARY

Duracell Inc. developed an ambient temperature lithium rechargeable system using the inorganic SO_2 electrolyte in 1980. The system had porous carbon as the positive electrode, SO_2 as depolarizer and $Li_2B_{10}Cl_{10}$ or $LiGaCl_4$ as electroltyte salt. The system made in D cells delivered a cycle life of 50-140 at 10 to 20% depth and only 10-30 cycles on deep discharge. Degradation of the carbon electrode was believed to be the problem of poor cycle life.

In addition to poor cycle life, the lithium salts, $Li_2B_{10}Cl_{10}$ and $LiGaCl_4$ were also very expensive. The development efforts were continued with the exploration of new low cost electrolyte salts and other positive electrode materials. Various lithium and other alkali or alkaline-earth metal salts were found readily soluble in SO_2 and form highly conductive electrolytes. A conductivity of about 1×10^{-1} $ohm^{-1}cm^{-1}$ was obtained with the solvated $LiAlCl_4$-xSO_2 electrolytes. The solvated electrolytes can also provide excellent lithium stability and cycling efficiency. Lithium cycling efficiencies of over 96% were obtained. Studies of various solid positive materials has also identified that $CuCl_2$ is one of the promising materials for use in the inorganic electrolyte system. Cells using porous carbon and solid active materials such as $CuCl_2$ as positive electrodes were evaluated with various new SO_2 electrolytes.

Li/carbon system with $LiAlCl_4$-xSO_2 electrolyte shows an OCV of 3.2 V and the cell reaction is different from the regular Li/carbon cells with $Li_2B_{10}Cl_{10}/SO_2$ or $LiGaCl_4/SO_2$ electrolytes. The system has a

theoretical energy density of 524 W/kg. In experimental prismatic cells, the system delivered over 200 cycles on 100% DOD. The 2/3A size prototype wound cells delivered about 40-60 cycles on 100% DOD and near 200 cycles on 50% DOD. A practical energy density of about 100 W/kg has been obtained with the prototype 2/3A cells and higher energy density is anticipated for larger sizes of cells.

$Li/CuCl_2$ with inorganic SO_2 electrolytes has OCV of 3.4 V with a theoretical energy density of 606 Wh/Kg to a cut-off of 2.6 V(first electron discharge). Over 400 cycles at 2 mA/cm^2 discharge rate and 1 mA/cm^2 charge rate has been demonstrated in experimental cells. Cells discharged to 2.2 V with the reduction of $CuCl_2$ to Cu delivered less cycle life. 2/3A size prototype wound cells delivered only 15-20 cycles which was probably due to poor fabrication process of the positive electrode.

The capability of taking overcharge is one of the important advantages of the inorganic electrolyte systems. All active chemicals present in the systems are inherently reversible. Experiments to demonstrate the overcharge capability and to investigate the balancing reactions were carried out. Oxidation of the electrolyte salt and the recombination of the overcharge products provide the balancing function. The amount of overcharge which the cell can sustain is limited by the chemical stability of the separator to the overcharge products.

Capacity fade, developmemt of internal shorts and instability of the separator with the overcharge products are the major problems of the prototype wound cells. Further studies of the inorganic rechargeable system to improve the cycle life, energy density and the stability of the separator are recommended.

CONTENTS

LIST OF TABLES

TABLE OF FIGURES

I. INTRODUCTION

Having the advantages of high energy density and good charge retention, rechargeable lithium batteries have been of interest to many companies and research organizations within the last 15 years. Various lithium rechargeable systems with different positive electrodes and electrolytes have been reported in literature. Most systems which have been evaluated or are currently under development are using electrolytes with organic solvents. Organic electrolytes usually have significantly lower conductivity compared to aqueous systems. In addition, due to the high chemical activity of the plated lithium and the instability of most electrolyte solvents toward oxidation and reduction, problems of poor rate capability and poor lithium plating have been observed.

Duracell Inc. has demonstrated the feasibility of using totally inorganic electrolytes based on liquid SO_2 for the ambient temperature rechargeable lithium battery. The system has lithium as the negative electrode and porous carbon as the positive electrode with SO_2 as the depolarizer and electrolyte solvent. The reversibilities of the lithium electrode and the carbon/SO_2 electrode have been well established. (3,4) The system is capable of delivering an initial energy density of about 330 Wh/Kg. The all-inorganic SO_2 electrolyte has high electrical conductivity,

excellent chemical and electrochemical stability, and is believed superior to other electrolyte systems containing organic solvents.

A four year cost-shared joint program with the Department of Energy was initiated in October 1980 to investigate the SO_2-based electrolytes and to develop an ambient temperature rechargeable lithium battery for future energy storage applications. The ultimate goal of this program is to develop a battery having an energy density over 150 wh/kg with cycle life of 500 to 800 at 80 to 100% depth of discharge. The near term objective is to obtain a cycle life of 100-200 at 50% to 80% depth of discharge.

During the four years, SO_2 electrolytes with various inorganic salts and various positive electrodes made of porous carbon and solid active materials were evaluated. Promising systems having good rechargeability and high energy density, such as $Li/CuCl_2$ and $Li/LiAlCl_4$-SO_2/carbon were identified. This report summarizes the progress achieved in the program.

II. ELECTROLYTE STUDY

Introduction

In the initial stage of the program, $Li_2B_{10}Cl_{10}$ was used as an electrolyte salt for the totally inorganic rechargeable Li/SO_2 system with a porous carbon positive electrode. $Li_2B_{10}Cl_{10}$ salt is soluble in liquid SO_2 and provides a highly conductive solution. The $B_{10}Cl_{10}^{=}$ anion has very good chemical and thermal stability [5,6]. A 0.5 M electrolyte has a conductivity of 2×10^{-2} $ohm^{-1}cm^{-1}$ at $20^{o}C$ as shown in Figure 1. On cathodic polarization to lithium potential, lithium metal can be plated. On anodic polarization to about 3.6 v. vs Li, $B_{10}Cl_{10}^{=}$ is oxidized with one electron transfer to generate $B_{10}Cl_{10}^{-}$ which can be reduced electrochemically back to $B_{10}Cl_{10}^{=}$. The rechargeability of the lithium electrode and the porous carbon/SO_2 electrode in this electrolyte had been studied previously [3,7]. However, since the $Li_2B_{10}Cl_2$ was quite expensive, a program was carried out to explore other electrolyte salts to be used for the inorganic rechargeable lithium system. The details and the results are described in following.

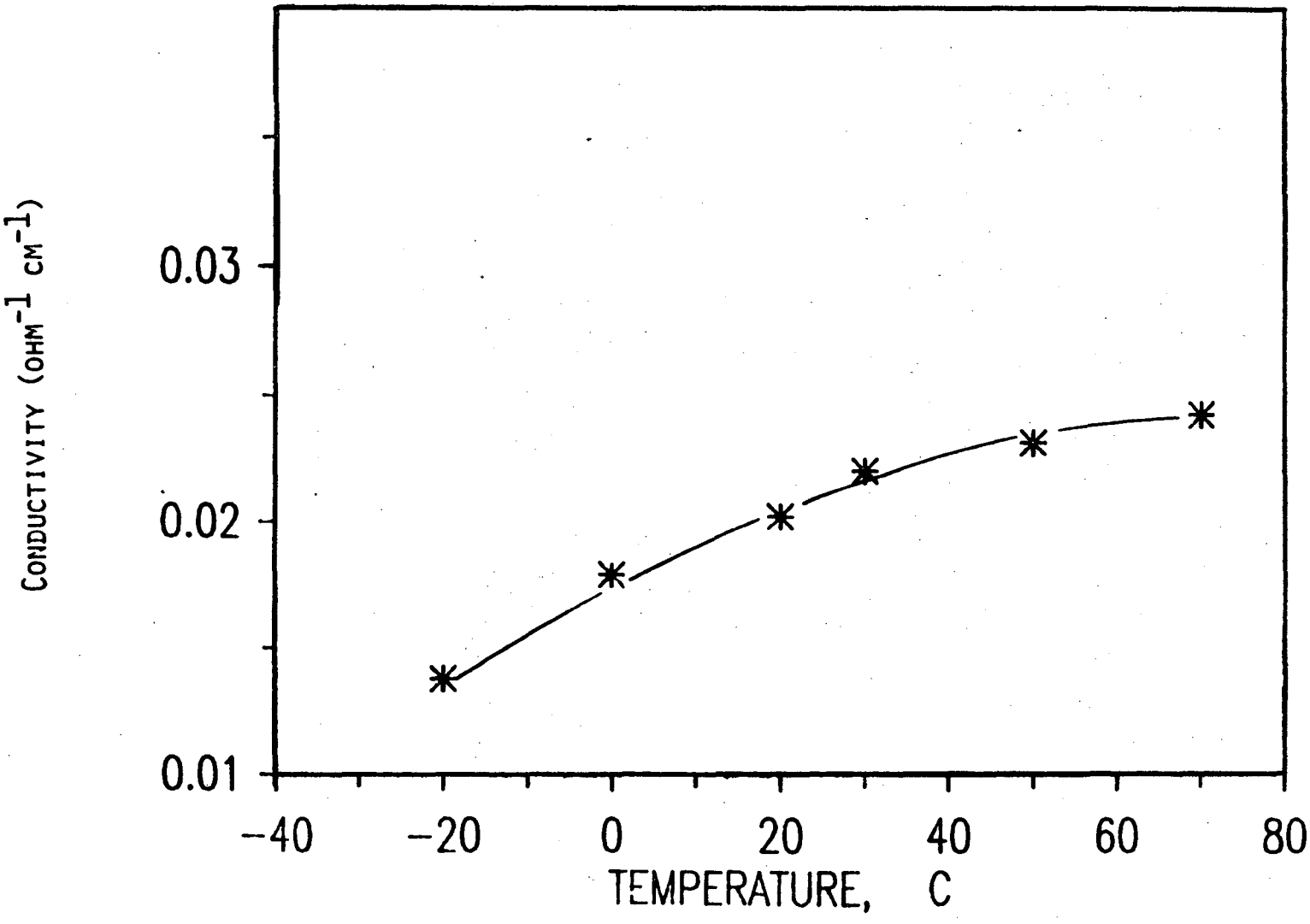

FIGURE 1. Conductivity of 0.6 N $Li_2B_{10}Cl_{10}/SO_2$ Electrolyte.

A. Exploration of New Electrolyte Salts

1. Experimental

a. Preliminary Screening of New Electrolyte Salts

Preliminary screening tests of potential new inorganic salts suitable for making the SO_2 electrolytes were carried out using heavy wall glass tubes, 1 inch in diameter and 3 inches in length, as shown in Figure 2. The tube contained a lithium electrode and a porous carbon electrode about 1 cm^2 in area which were electrically connected to the outside using nickel wires punctured through a rubber stopper. The rubber stopper was held in position against the pressure of the SO_2 electrolyte in the tube with a clamp device.

High purity inorganic salts of analytical or research grade were used to make the electrolyte. The salts were pre-dried under vacuum and stored in a dry box. Preweighed salt was first added to the tube and the tube sealed with the stopper. The tube was then removed from the dry box, evacuated and filled with pure SO_2 (less than 30 ppm water). Some electrolytes contained composite salts such as $LiGaCl_4$ or $LiAlCl_4$ and were made by mixing the equivalent amounts of the component salts.

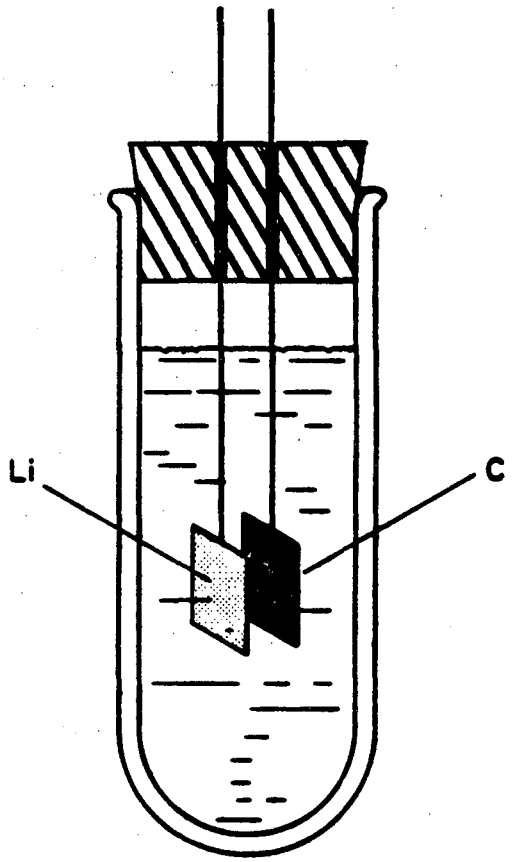

GLASS TESTING CELL

FIGURE 2. Glass Cell for Preliminary Test of the Electrolyte Salts.

After the tube was filled with SO_2, the usefulness of the electrolyte was judged by visual observations of solubility of the salt, color degradation, lithium stability, measurements of the open circuit voltage and the short circuit current of the two electrodes, discharge capacity and voltage of the cell at 1 ma/cm_2 rate, and the cycling performance.

b. Physical and Electrochemical Properties of The Electrolytes

The conductivity of various promising electrolytes were measured at various temperatures using a stainless steel cell containing two 1 cm^2 platinized platinum electrodes and spaced 1cm apart. The internal surface of the vessel was coated with Teflon. The cover had a Teflon O-ring seal with screws for mounting the cell body which was able to withstand the vapor pressure of the SO_2 within the temperature range of measurement. After filling with electrolyte, the cell was immersed in a constant temperature bath for at least 24 hrs. The conductivity was measured using a Genrad Model 1657RLC after the temperature of the cell reached equilibrium.

The electrochemical stabilities of the electrolytes were characterized using PAR 173 potentiostat with PAR Model 175 function generator.

2. Results and Discussion

a. Screening of the Electrolyte Salts

Table 1 summarizes the electrolyte salts which were evaluated. High short circuit current implied a high conductivity. Low short circuit current indicated either a low conductivity or high polarization of the carbon cathode. Most salts were found to have poor solubility in liquid SO_2. The high open circuit voltage (OCV) shown by some electrolytes might have been due to the formation of $SOCl_2$ or other compounds in-situ. The rechargeability of the carbon electrode in these electrolytes having high OCV was also very poor. Only $LiGaCl_4$ was found to have good solubility and to provide good discharge capacity with the porous carbon electrode. $LiAlCl_4$ was also readily soluble in SO_2 and gave a clear stable electrolyte. However, the porous carbon electrode performed poorly and gave a low discharge capacity.

b. Physical and Electrochemical Properties of the Electrolytes

$LiGaCl_4/SO_2$ Electrolyte

$LiGaCl_4/SO_2$ electrolyte can be prepared by dissolving $LiGaCl_4$ salt or the equivalent amounts of the component salts,

TABLE 1. PRELIMINARY EVALUATION OF THE ELECTROLYTE SALTS

SALTS	CONCENTRATION	OCV	SHORT CIRCUIT CURRENT	CAPACITY	COMMENTS
$LiGaCl_4$	1.0M	2.91v		40mAh	Colorless
$Li_2O.2GaCl_3$	0.5M	2.97v			
$LiClO_4$		2.90V			Poor solubility
$LiAlCl_4$	1.0M	3.26v	30mA	6mAh	Colorless
$LiAlBr_4$		3.21v	65mA		Brown, reacted with SO_2
$LiInCl_4$	1.0M	2.89v	310mA	20mAh	Poor recharge
Li_3InCl_6	1.0M	2.87v	17mA		
$LiTaCl_6$	1.0M	3.60v	60mA	10mAh	Poor recharge
$LiNbCl_6$	1.0M	3.62v	640mA	7mAh	Poor recharge
$LiAlF_6$		2.97v	6 mA		Poor Solubility*
$LiSbCl_6$		3.62v	430mA	<5 mAh	Poor recharge
Li_3SbCl_6		3.62v		<5 mAh	Poor recharge
$LiNO_3$					Not soluble
$LiMoO_4$		2.9v			Poor solubility
Li_2SO_4		2.9v			Poor solubility
Li_3PO_4		2.9v			Poor solubility
Li_3AlF_6		2.9v			Poor solubility
$LiBF_4$		2.9v			Poor solubility
$LiAsF_6$		3.2v			Poor solubility
$LiPF_6$		2.9v			Poor solubility

*Visually over 90% of the salt was not dissolved after stirring and overnight storage.

TABLE 1 (CONTINUED)

SALTS	CONCENTRATION	OCV	SHORT CIRCUIT CURRENT	CAPACITY	COMMENTS
LiF					Not soluble
LiBr					Not soluble
$LiTaOCl_4$		2.9v			Poor solubility
$LiNbOCl_6$		2.9v.			Poor solubility
$LiB(C_4H_9)_4$		2.9v.			Poor solubility

LiCl and $GaCl_3$ in liquid SO_2. Figure 3 shows the conductivity of 1 M $LiGaCl_4/SO_2$ electrolyte at various temperatures. On anodic polarization to above 4.0 V vs Li, the $LiGaCl_4$ salt is oxidized to generate chlorine as indicated in Figure 4,

$$GaCl_4^- \text{-------->} GaCl_3 + 1/2\ Cl_2 + e$$

Both $GaCl_3$ and Cl_2 are soluble in SO_2. This oxidation potential is well above the reversible potential of $SO_2/Li_2S_2O_4$(carbon), which provides a wide potential window for Li/SO_2 cell operation.

$LiAlCl_4/SO_2$ Electrolytes

In the preliminary electrolyte screening test it was found that $LiAlCl_4$ is readily soluble in liquid SO_2 and gives high conductivity. Although the electrolyte showed poor capacity for SO_2 discharge with a Shawinigan carbon electrode, it might well be suitable for use as an electrolyte for solid positive electrode materials. We also observed that a SO_2 solvated liquid electrolyte was also formed when $LiAlCl_4$ salt was contacted with SO_2 gas at atmospheric pressure. $LiAlCl_4/SO_2$ electrolytes with different SO_2 content were prepared for conductivity measurements. Figure 5 shows the conductivities of $LiAlCl_4$-xSO_2electrolytes with various

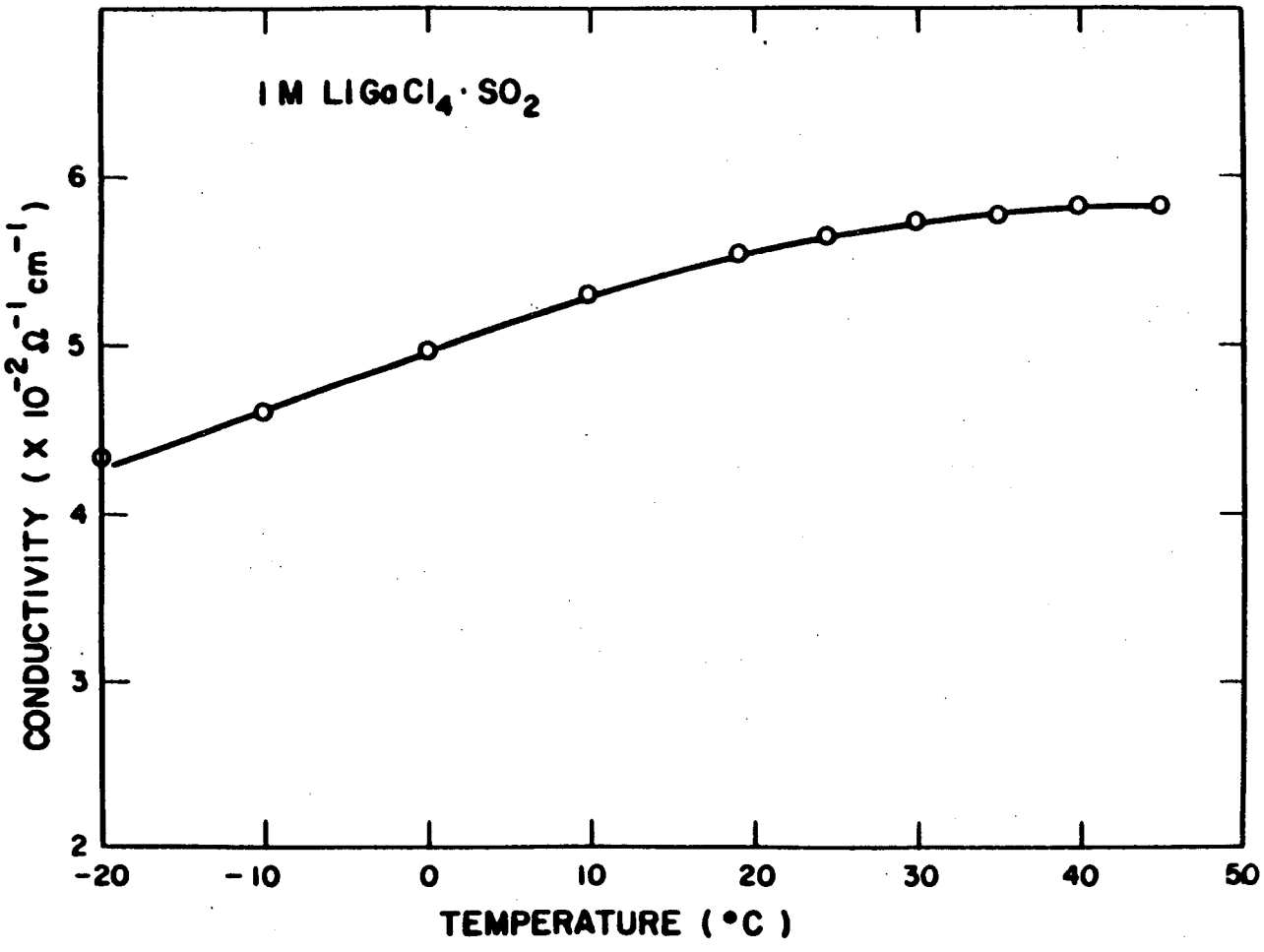

FIGURE 3. Conductivity of 1M $LiGaCl_4/SO_2$ Electrolyte.

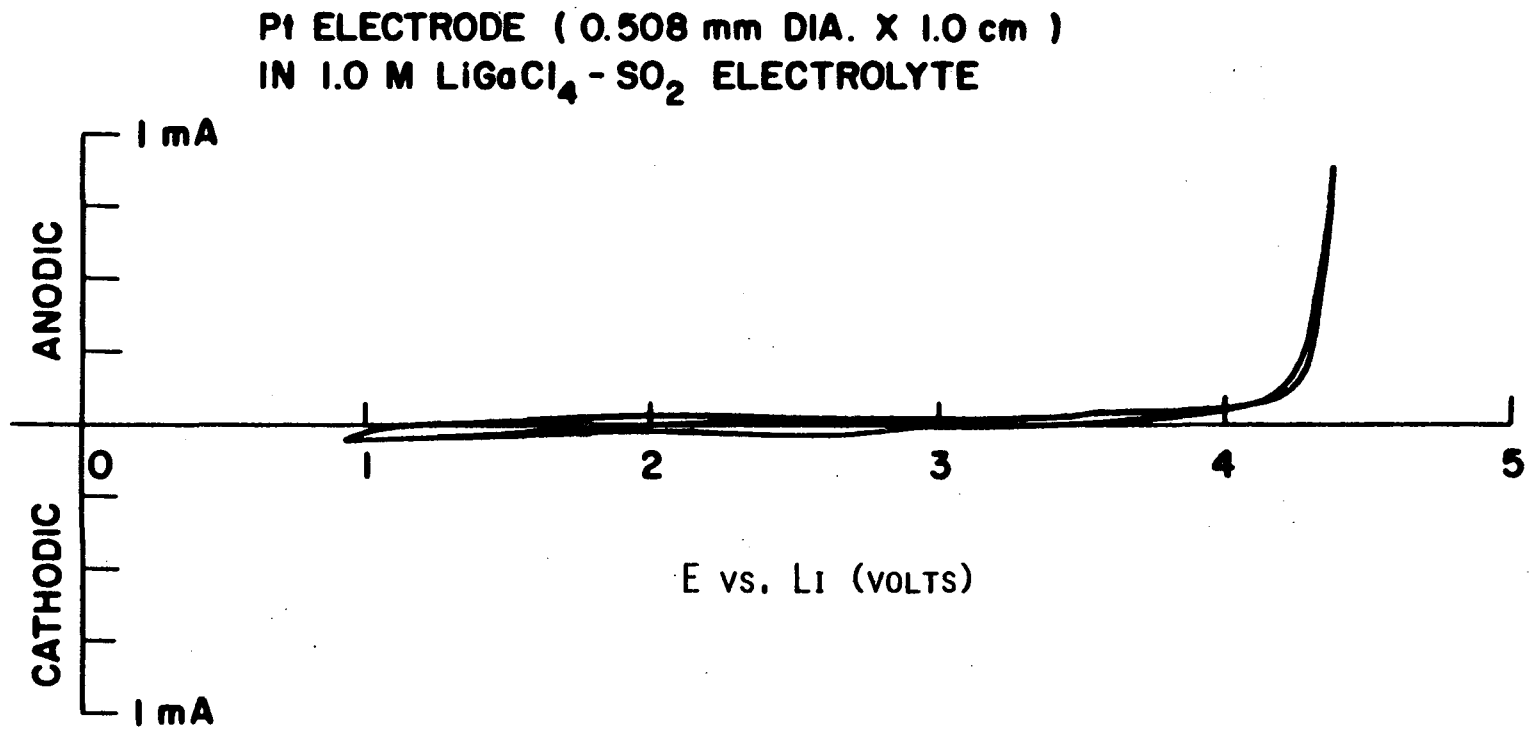

FIGURE 4. Electrochemical Characteristic of the 1M $LiGaCl_4/SO_2$ Electrolyte.

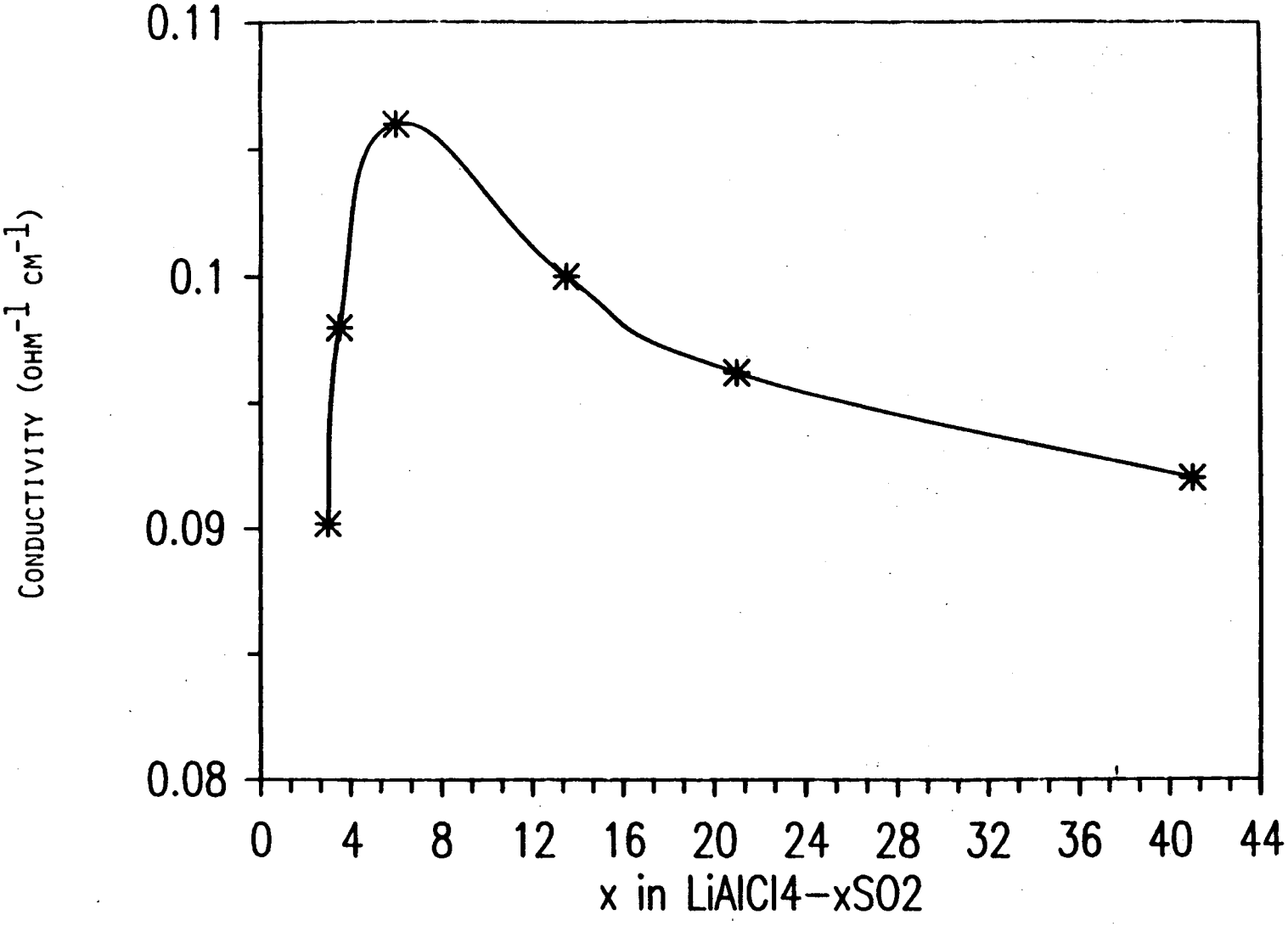

FIGURE 5. Conductivity of $LiAlCl_4/SO_2$ Electrolytes of Various Concentration Measured at 25°C.

SO_2 contents measured at 25°C. A maximum conductivity was obtained with $LiAlCl_4$-$6SO_2$. Figure 6 shows the temperature dependence of the conductivity of the electrolytes for several selected compositions. The electrolytes are highly conductive with a conductivity of about 1×10^{-1} $ohm^{-1}cm^{-1}$ at ambient temperature, which is comparable to that of aqueous electrolytes.

Solvated $LiAlCl_4$-$3SO_2$ is a super-cooled liquid at ambient temperature (20°C) when initially formed by reaction of stoichiometric amounts of LiCl, $AlCl_3$ and SO_2. It crystallizes when cool to about -10°C or when the equilibrium pressure of SO_2 above the liquid is released abruptly. The crystal has an orthorhombic structure[9] and melts at 24°C[10]. The freezing temperature of $LiAlCl_4$-xSO_2 electrolytes decreases with increasing the SO_2 content. The electrolyte of composition $LiAlCl_4$-$6SO_2$ remains in liquid state at temperature as low as -30°C.

The vapor pressure of SO_2 over the solvated electrolyte is significantly lower than that of pure liquid SO_2. The equilibrium pressure of SO_2 over the stoichiometric solvate $LiAlCl_4$-$3SO_2$ is less than 1 atm at ambient temperatures. Figure 7 exhibits the vapor pressure of the two solvated electrolytes, $LiAlCL_4$-$3SO_2$ and $LiAlCl_4$-$6SO_2$, measured at various temperatures.

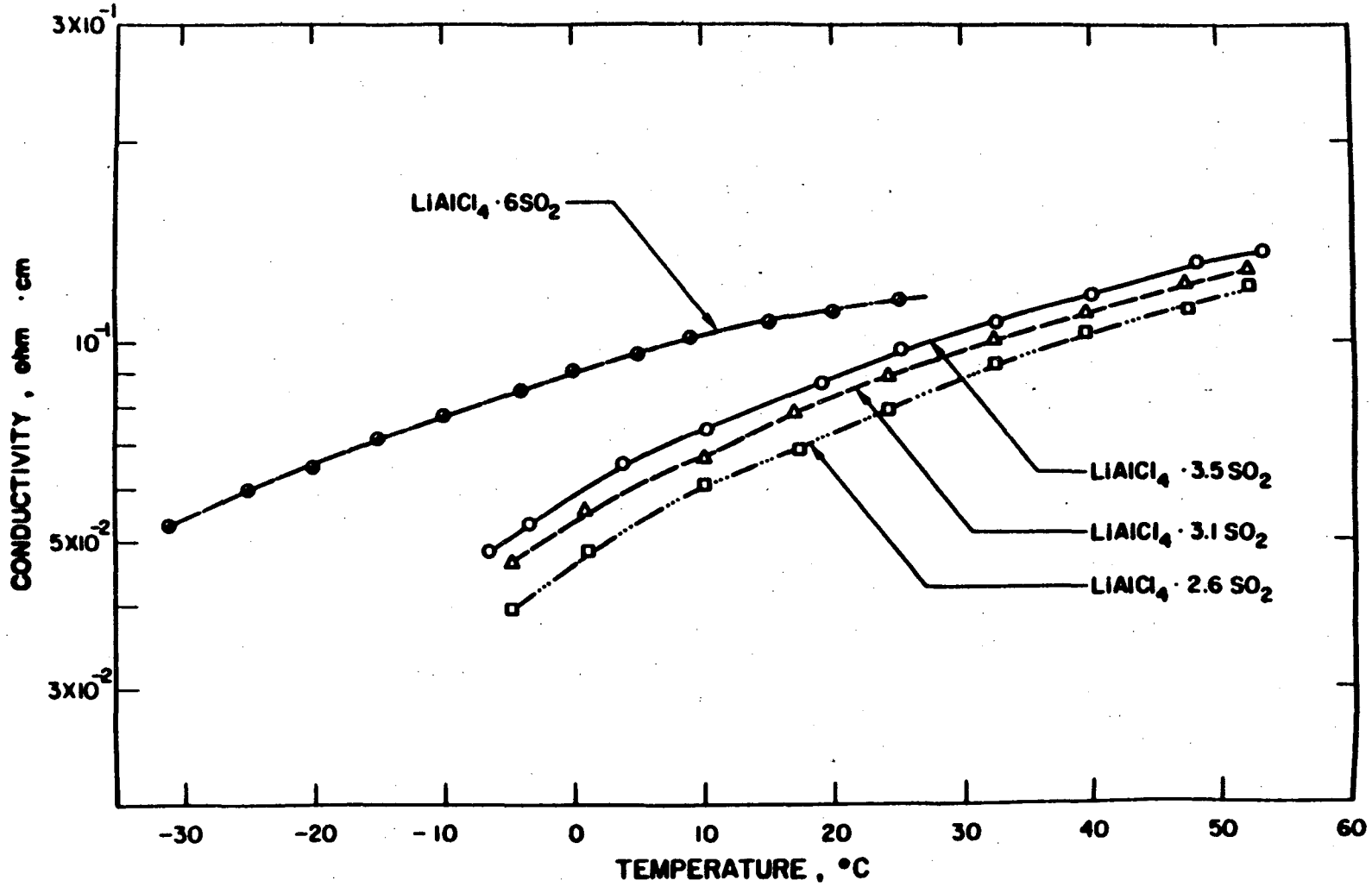

FIGURE 6. Conductivity of $LiAlCl_4SO_2$ Electrolytes Measured at Various Temperatures.

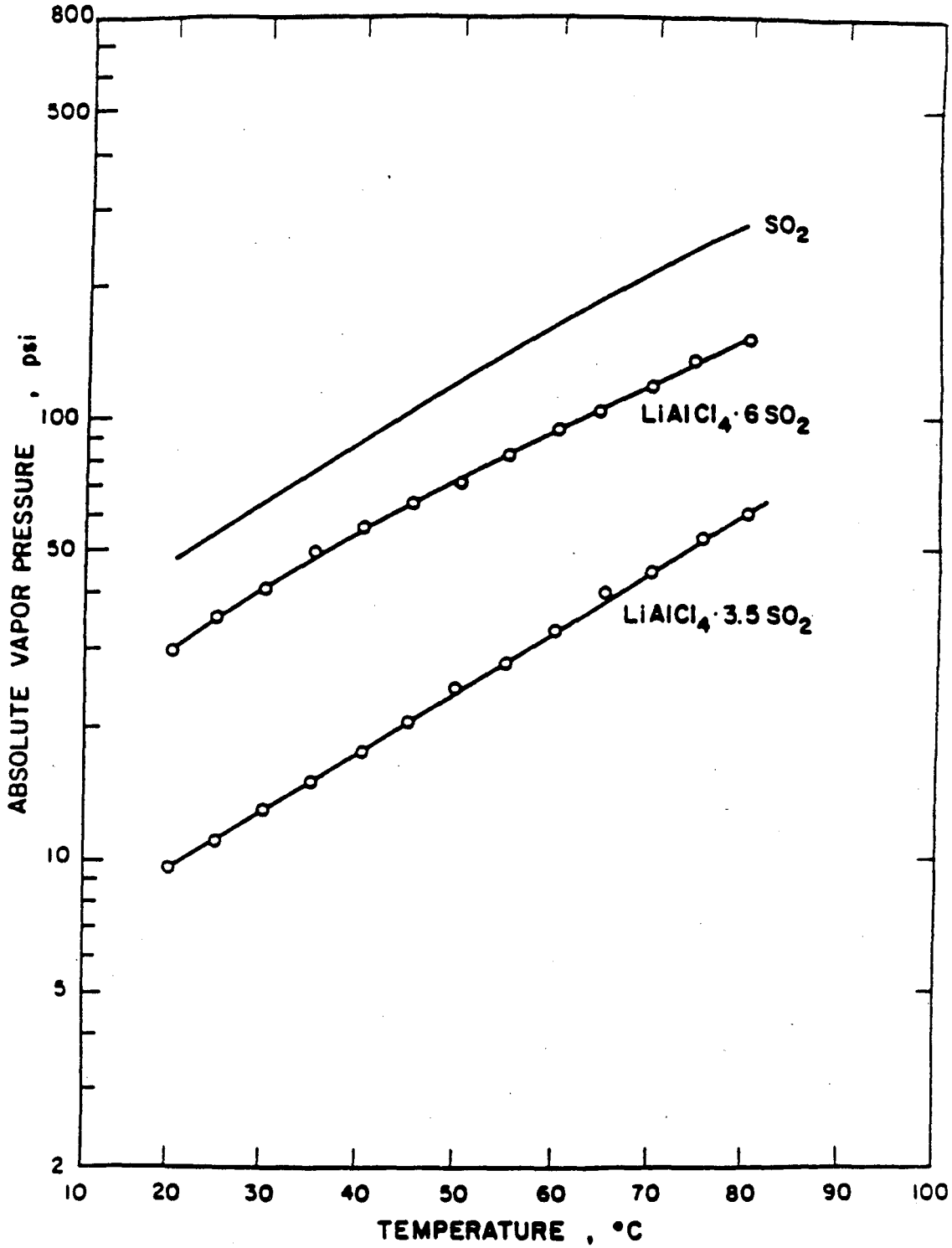

Figure 7. The Vapor Pressures of $LiAlCl_4$-$3SO_2$ and $LiAlCl_4$-$6SO_2$ Measured at Various Temperatures

The equilibrium pressure of SO_2 is also shown in the figure for comparison.

The density of the $LiAlCl_4$-$3SO_2$ solvated electrolyte was measured to be 1.65 g/cc. Figure 8 shows the thermal expansion of the electrolyte vs. temperature which gives a coefficient of about $1\%/10^{o}C$.

Metallic lithium can be plated out from the $LiAlCl_4$-xSO_2 electrolyte when it is cathodically polarized to below lithium potential. On oxidation, the electrolyte salt $LiAlCl_4$ decomposes to generate $AlCl_3$ and Cl_2. Both reaction products are highly soluble in the electrolyte. Figure 9 shows the polarization of the electrolyte on a platinum electrode with a scan rate of 10 mv/sec. The evolution of Cl_2 starts at about 3.9 volt vs. Li. The overpotential for electrolyte decomposition on nickel surface is significantly higher than that on a platinum electrode as shown in Figure 10. Chlorine is generated at above 5.0 V. vs Li.

Other Alkali or Alkaline-earth Metal Tetrachloroaluminates/SO_2 Electrolytes.

In addition to $LiAlCl_4$, other alkali or alkaline-earth metal tetrachloroaluminates were found to be readily soluble in SO_2 or to form solvates with SO_2. $NaAlCl_4$-$3SO_2$ has physical

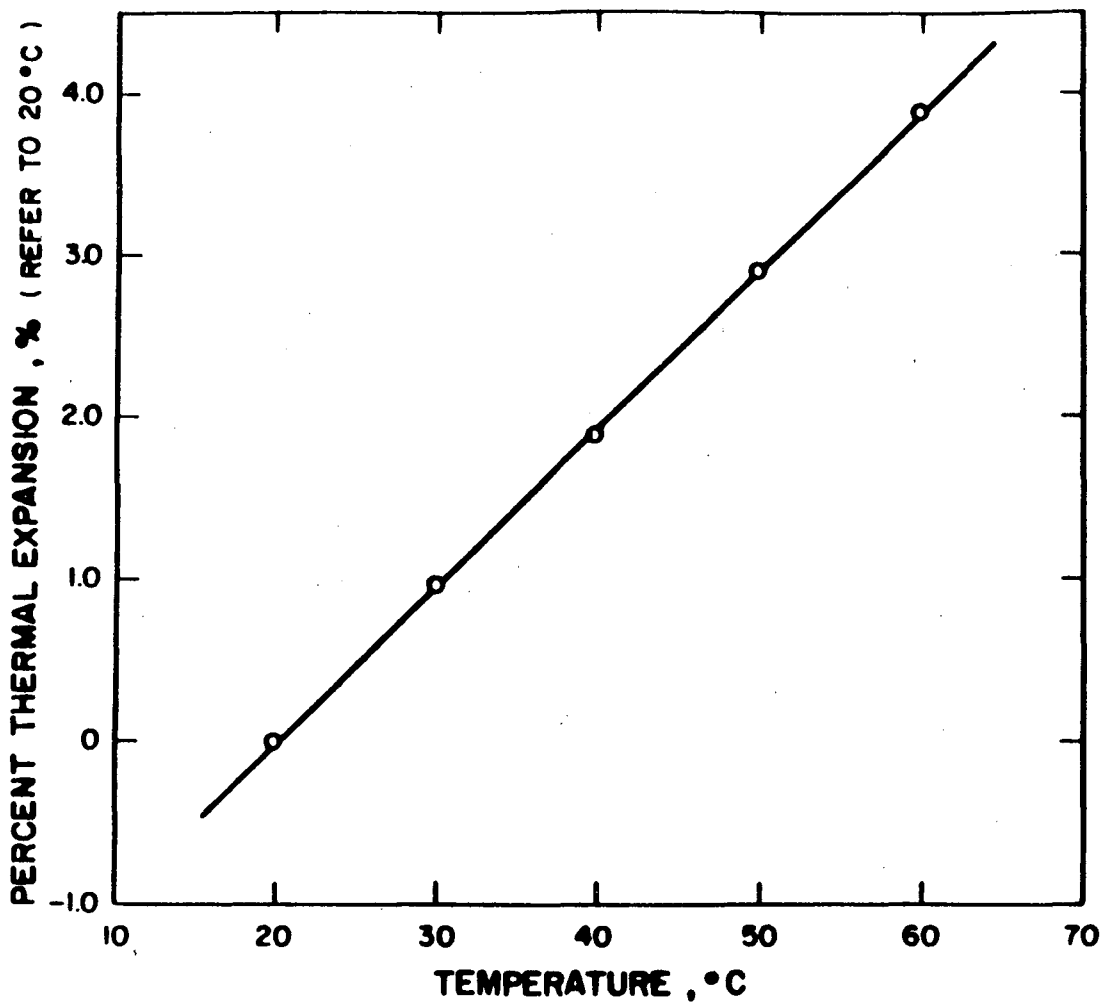

FIGURE 8. The Thermal Expansion of the $LiAlCl_4$-$3SO_2$ Electrolyte vs. Temperature.

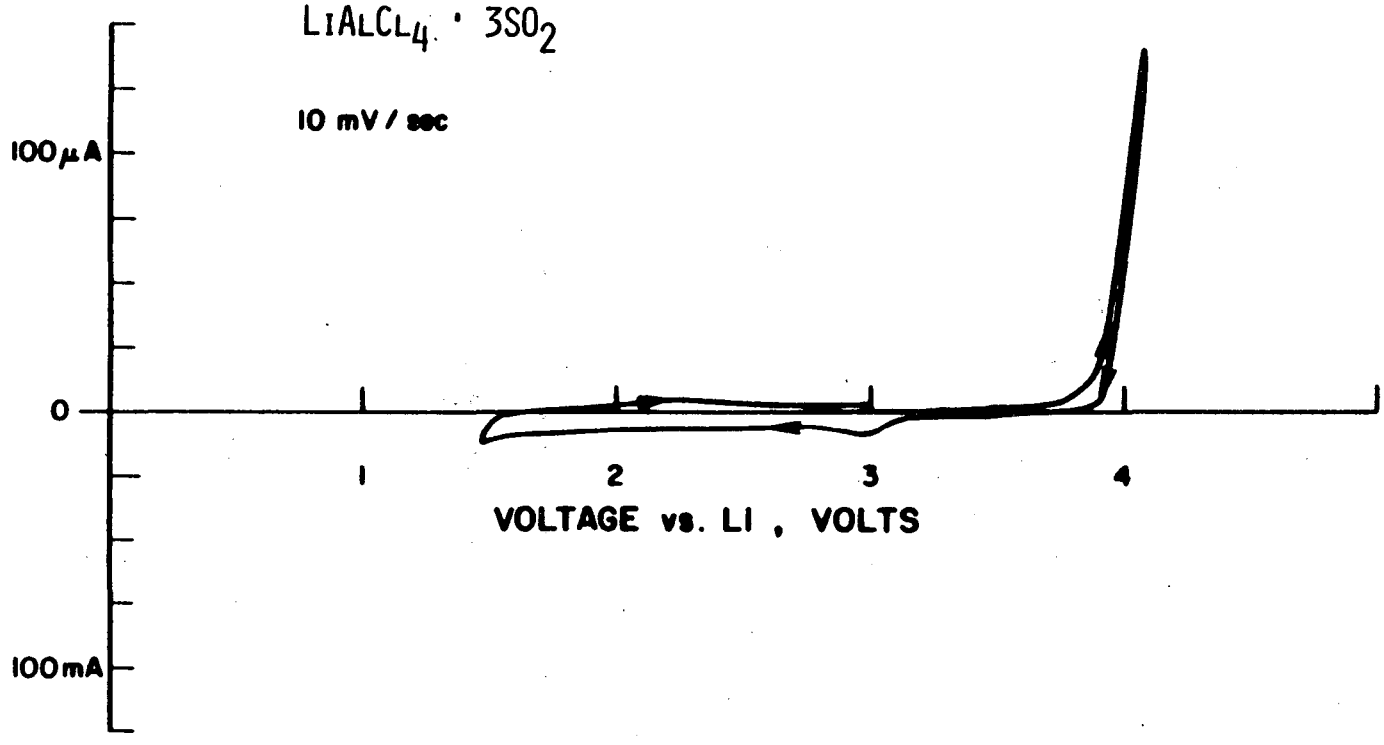

FIGURE 9. The Electrochemical Characteristic of the $LiAlCl_4$-$3SO_2$ Electrolyte on a Platinum Electrode.

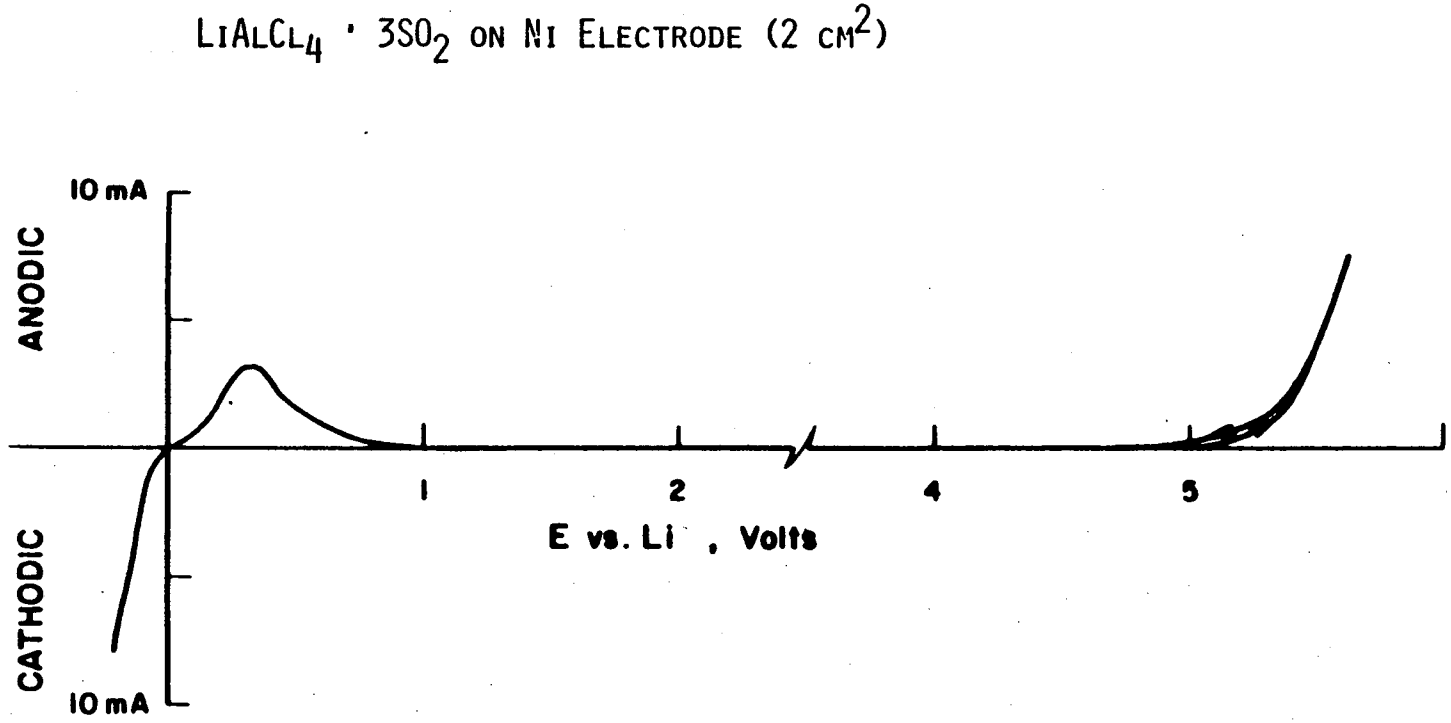

FIGURE 10. The Electrochemical Characteristic of the $LiAlCl_4$-$3SO_2$ Electrolyte on a Nickel Electrode (Sweep Rate: 10 mV/sec).

properties similar to those of $LiAlCl_4$-$3SO_2$[9,10]. Although the orthorhombic crystals of $NaAlCl_4$-$3SO_2$ have a melting point of -13°C, the liquid state can be super cooled to -40°C without freezing. Figure 11 shows the conductivity of the electrolyte measured at temperatures from -35°C to 50°C before and after freezing. The conductivity is about the same as that of the $LiAlCl_4$-$3SO_2$ electrolyte. Similar to the $LiAlCl_4$-$3SO_2$ electrolyte, the sodium electrolyte decomposes to generate chlorine when it is anodized to above 5.0 v. vs Li on a nickel electrode as shown in Figure 12. Sodium can be plated out during cathodic reduction. The overpotential for sodium plating in the sodium electrolyte is higher than that of lithium plating from the lithium electrolyte as shown in Figure 10 and 12.

Since $LiAlCl_4$-$3SO_2$ electrolyte can only be super-cooled to about -10°C, a study of the effects of mixing $NaAlCl_4$-$3SO_2$ with $LiAlCl_4$-$3SO_2$ on conductivity and freezing point was carried out. Figure 13 shows the conductivity of the mixed electrolyte of composition, $0.5LiAlCl_4$-$0.5NaAlCl_4$-$3SO_2$. The electrolyte can certainly be super-cooled to below -10°C and is partially frozen at -30°C. The conductivity measurements after freezing also show a partially melted region. Figure 14 shows the conductivity of the mixed electrolyte of composition $0.2LiAlCl_4$-$0.8NaAlCl_4$-$3SO_2$. With high $NaAlCl_4$ content, the conductivity characteristic is similar

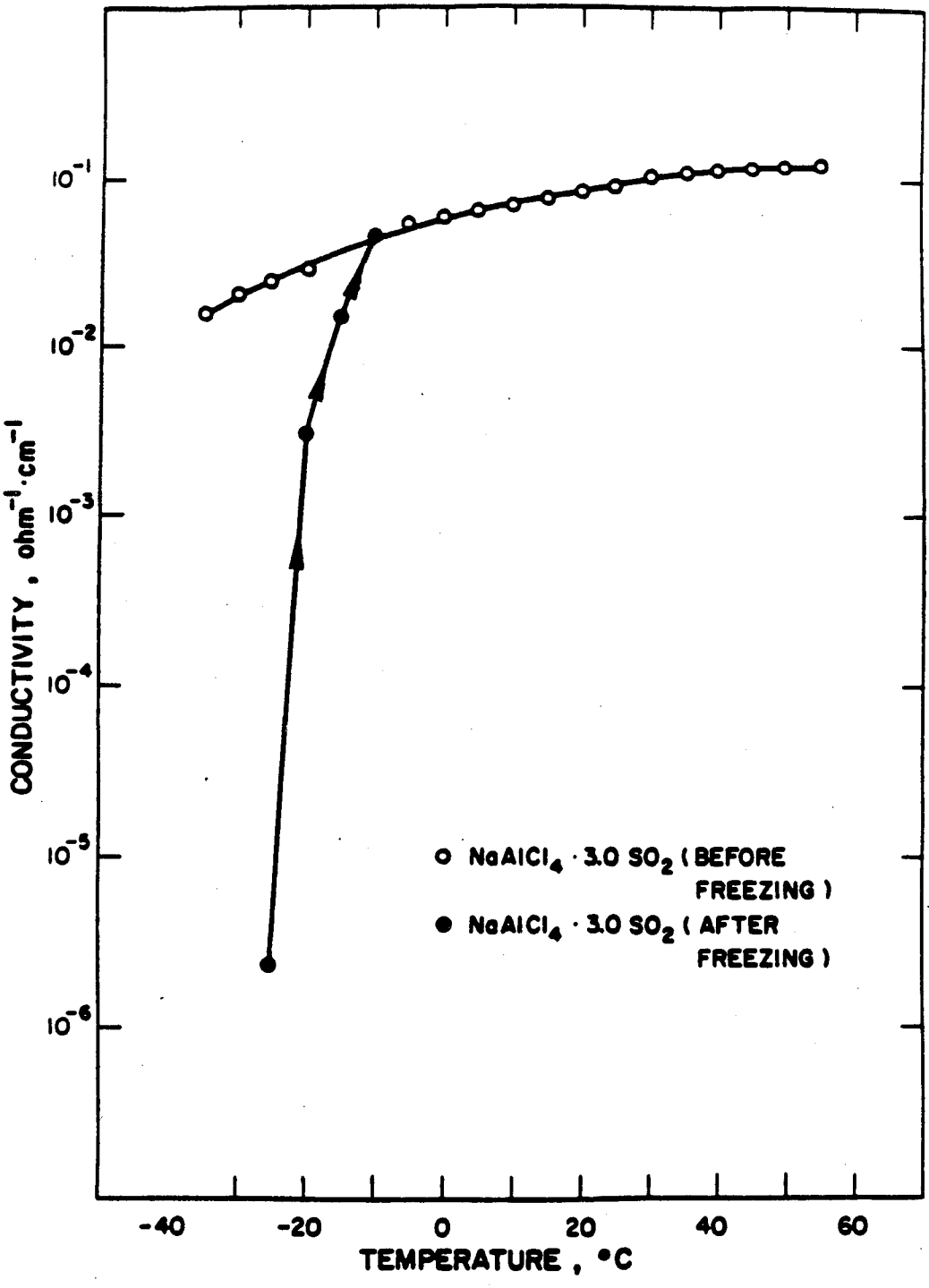

Figure 11. The Conductivity of the $NaAlCl_4$-$3SO_2$ Electrolyte Measured at Various Temperatures

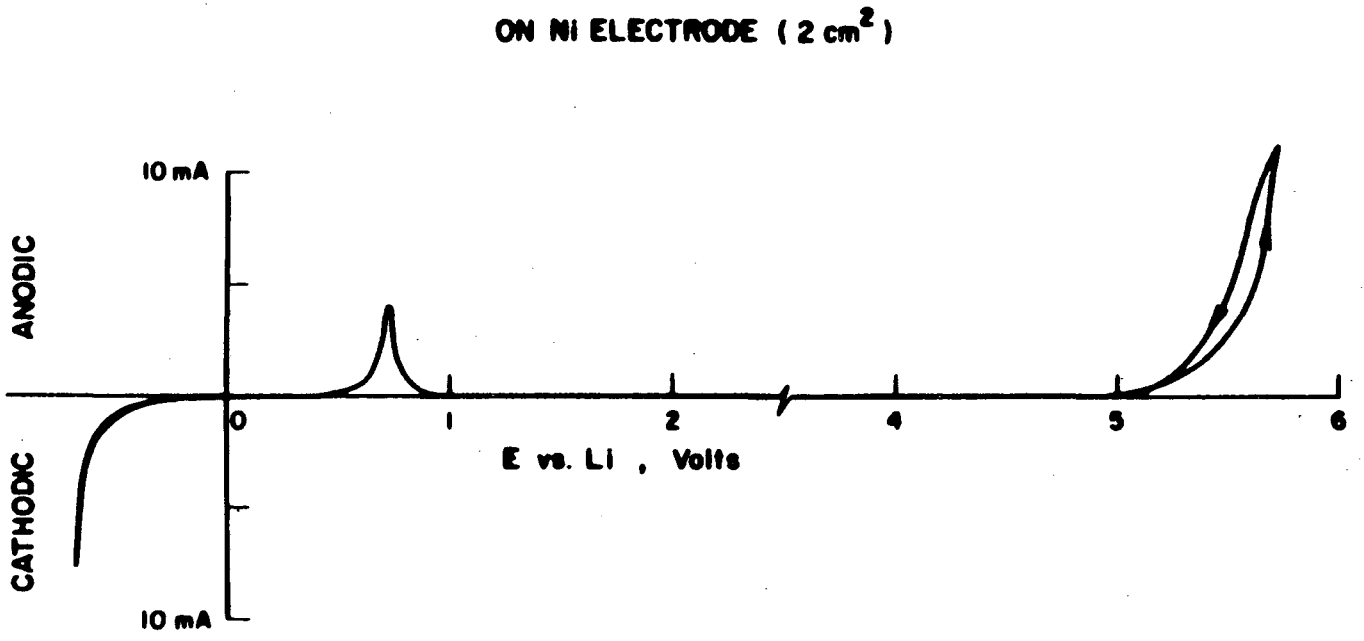

FIGURE 12. The Electrochemical Characteristic of the $NaAlCl_4$-$3SO_2$ Electrolyte on a Nickel Electrode (Sweep Rate: 10 mV/sec).

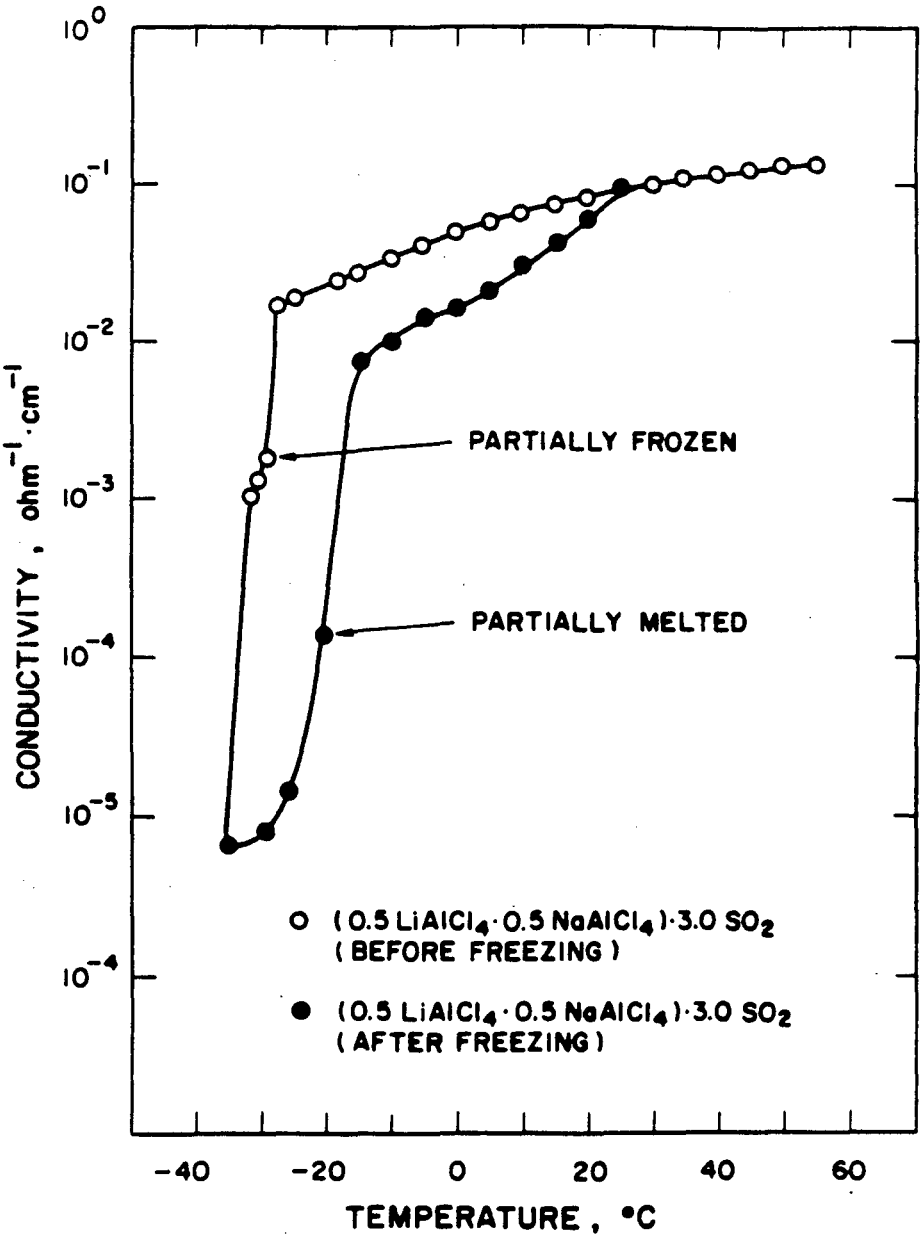

FIGURE 13. The Conductivity of (0.5 $LiAlCl_4$-0.5 $NaAlCl_4$)-3SO_2 Electrolyte Measured Before and After Freezing.

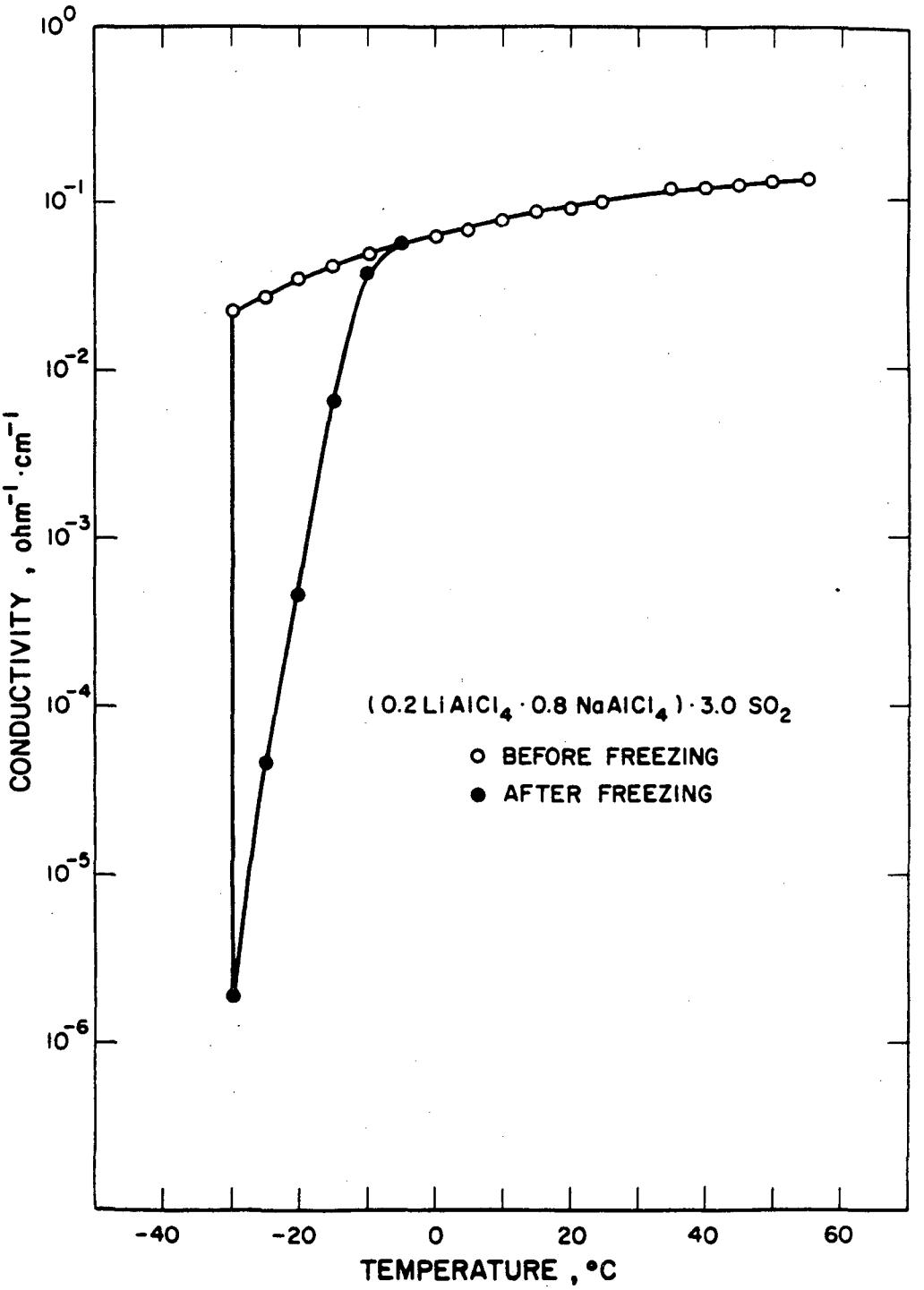

FIGURE 14. The Conductivity of $(0.2\ LiAlCl_4\text{-}0.8\ NaAlCl_4)\text{-}3SO_2$ Electrolyte Measured Before and After Freezing.

to that of the pure $NaAlCl_4$ electrolyte.

$KAlCl_4$, $RbAlCl_4$ and $CsAlCl_4$ (mixtures of KCl, RbCl or CsCl with $AlCl_3$) have been found unable to form solvates with SO_2.

Alkaline-earth metal tetrachloroaluminates such as $Ca(AlCl_4)_2$ and $Sr(AlCl_4)_2$ can form liquid SO_2 solvates with SO_2 having vapor pressure less than an atmosphere. Electrolytes of compositions $Ca(AlCl_4)_2$-$5.5SO_2$ and $Sr(AlCl_4)_2$-$5.6SO_2$ were prepared for evaluation. Figures 15 and 16 show the conductivities of the electrolytes measured at various temperatures. The conductivities of both electrolytes are about a factor of 5 less than those of the lithium or sodium counterparts. Also, the conductivity declines more rapidly with temperature and is less than 1×10^{-3} $ohm^{-1}cm^{-1}$ at $-35^{o}C$. Both electrolytes were not found to crystallize even at extremely low temperatures. However, the viscosity increased dramatically and the electrolyte became gummy at temperatures below about $-50^{o}C$. At $-78^{o}C$ both electrolytes looked clear and were immobile. Tests of the electrolyte with a freezing point apparatus did not show any latent heat associated with the liquid/solid transition. The conductivity curves measured as shown in Figures 15 and 16 are completely reversible.

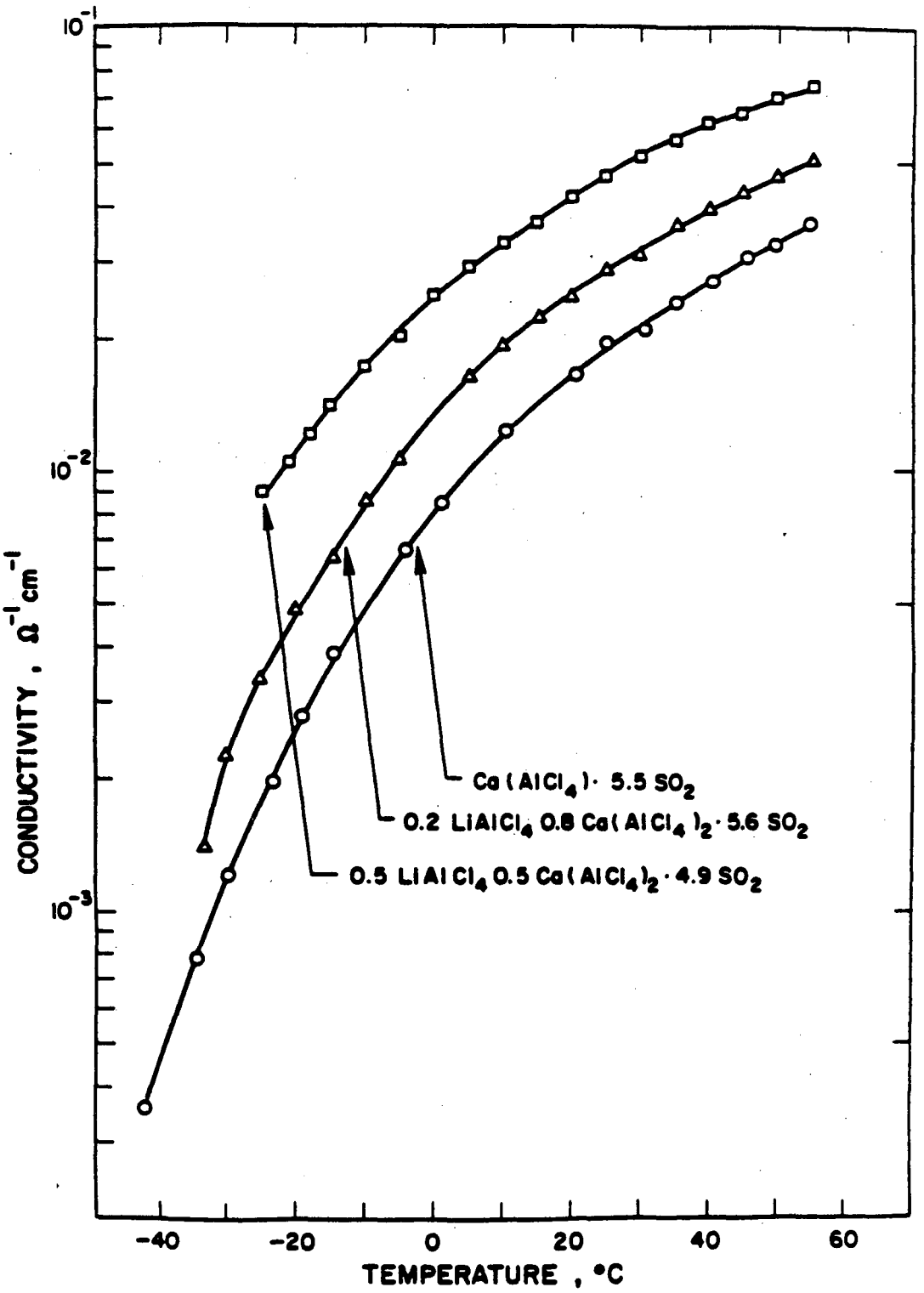

FIGURE 15. The Conductivity of the $Ca(AlCl_4)_2$-5.5 SO_2 Electrolyte and the Electrolyte with the Addition of $LiAlCl_4$.

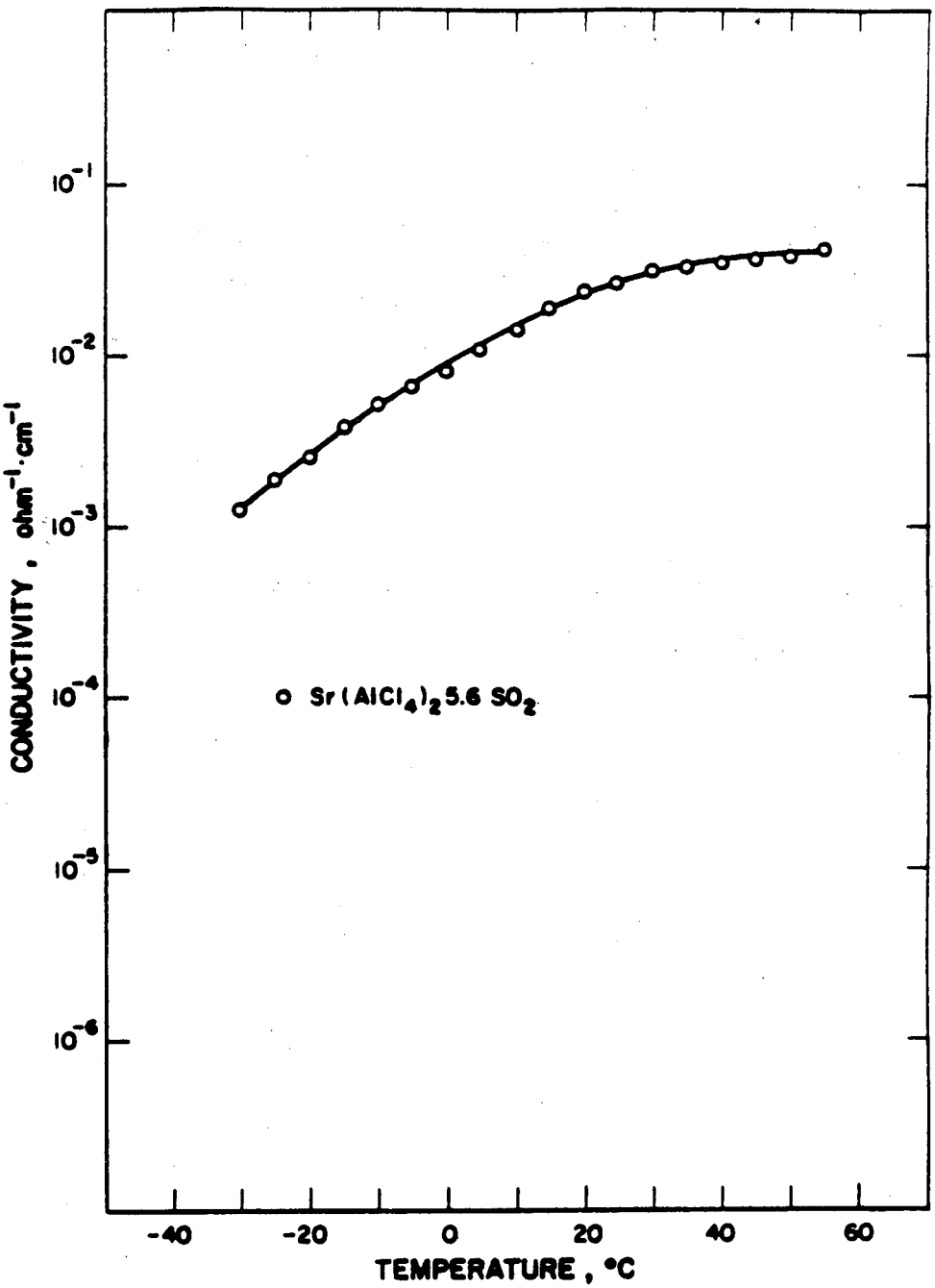

FIGURE 16. The Conductivity of the $Sr(AlCl_4)_2$-5.6 SO_2 Electrolyte.

Although the electrolyte oxidizes on a nickel electrode to generate chlorine at potential above 5 v. vs Li as shown in Figure 17, calcium metal can not be plated out during cathodic polarization even to a potential of about -2.0 v vs. Li.

Addition of small amounts of lithium tetrachloroaluminate to the calcium or strontium electrolytes did not change the freezing characteristics but did improve somewhat the conductivity as shown in the curve for $0.2LiAlCl_4$-$0.8Ca(AlCl_4)_2$-$5.6SO_2$ in Figure 15. The addition of higher concentrations of the lithium electrolyte, such as the 1:1 stoichiometric mixture shown in Figure 15, caused part of the electrolyte to freeze at -20°C with the rest remaining in liquid state.

No SO_2 solvated electrolyte could be made for $Mg(AlCl_4)_2$ or $Ba(AlCl_4)_2$.

B. LITHIUM ELECTRODE STUDIES

1. Stability of Lithium in SO_2 Electrolytes

Accelerated corrosion tests were carried out at 71°C to investigate the stability of lithium in tetrachlorogallate and various tetrachloroaluminate electrolytes.

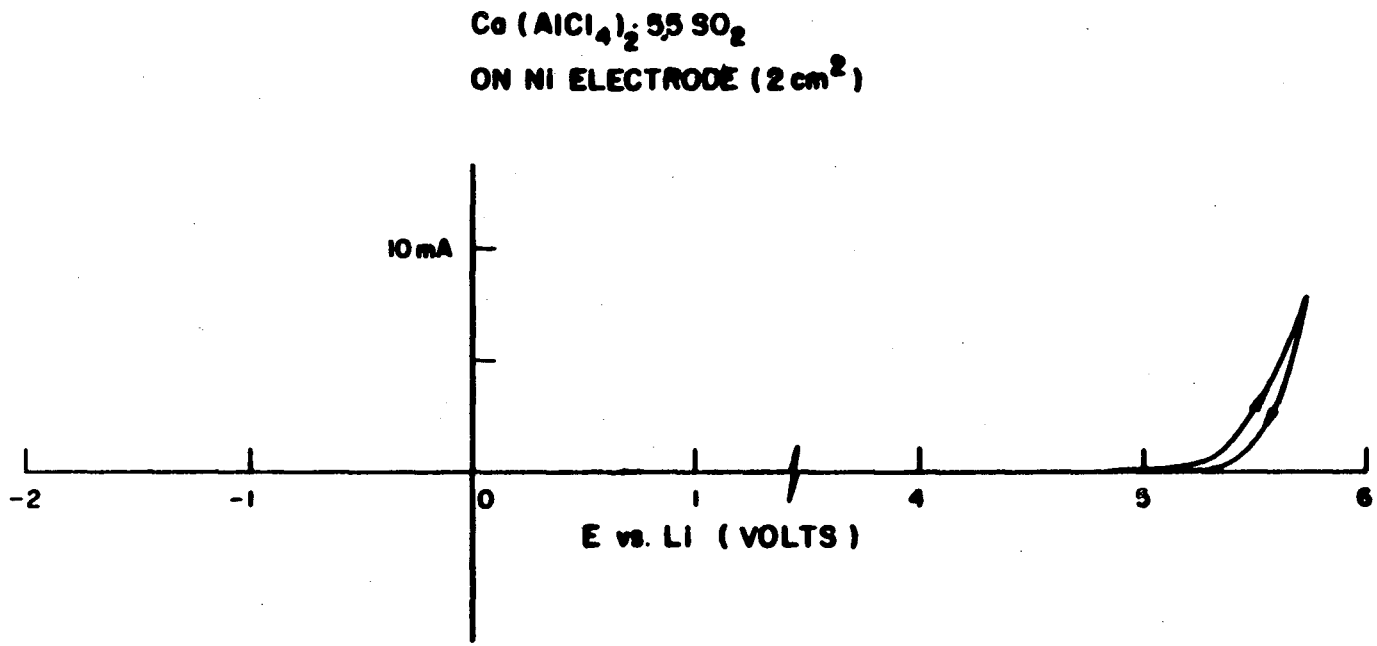

FIGURE 17. The Electrochemical Characteristic of the $Ca(AlCl_4)_2 5.5\ SO_2$ Electrolyte.

a. Experimental

The corrosion rates of various electrolytes at 71°C were determined using hermetically sealed cells (D size cans) containing a pre-weighed lithium working electrode sandwiched between two lithium counter electrodes as shown in Figure 18. The lithium working electrodes of size 2.5cm x 4 cm were made by pressing 5 mil lithium foil on each side of copper foil substrate. After being filled with electrolytes, the cells were stored at 71°C for fixed periods of time. The remaining active lithium was determined by stripping electrochemically from the working electrode at ambient temperature, first at 1 mA/cm^2 and then at 0.1 mA/cm^2 until potential excursion indicating polarization of the working electrode. Finally the electrode was removed from the cell and any remaining lithium was determined by chemical titration. This method provided quantitative information concerning the loss of active lithium during high temperature storage as well as the loss of rate capability which may have resulted from high temperature storage.

b. Results and Discussion

Table 2 and Figure 19 summarize the test results. The $NaAlCl_4$-$2.8SO_2$ and the mixed lithium and sodium tetrachloroaluminate electrolyte showed the best lithium stability at 71°C among the electrolytes evaluated. Almost all the active lithium was

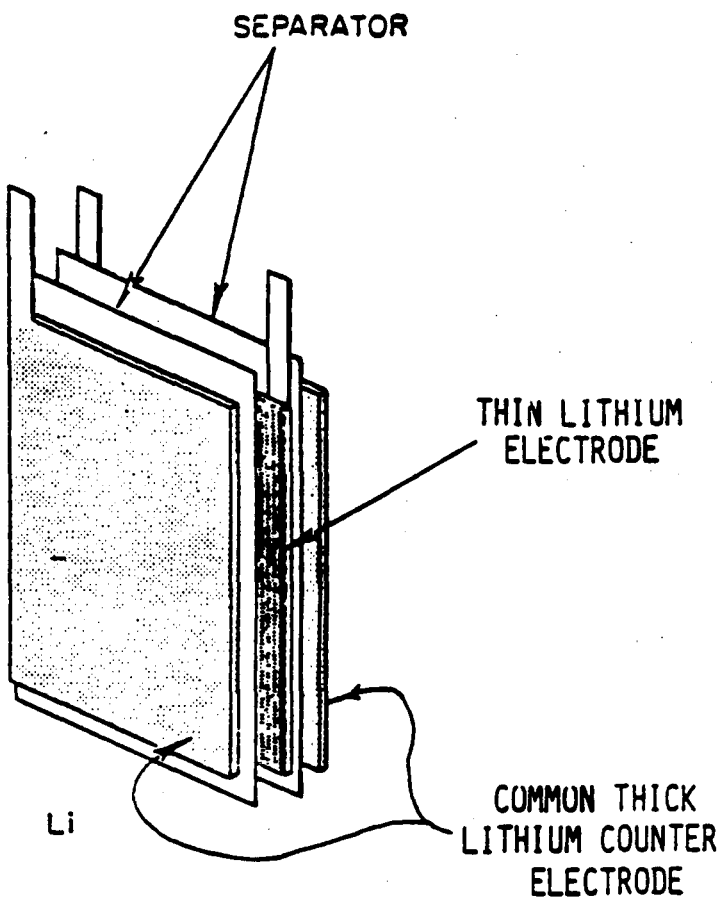

FLAT ELECTRODE CELL FOR MEASURING LITHIUM CORROSION AFTER STORAGE

FIGURE 18. The Experimental Cell with Flat Electrodes for Lithium Corrosion Study.

TABLE 2. LITHIUM CORROSION IN VARIOUS ELECTROLYTES AFTER STORAGE AT 71oC
AS MEASURED BY THE ELECTROCHEMICAL STRIPPING TECHNIQUE

Electrolyte	Theoretical Capacity (mAh)	Capacity Delivered at 1 mA/cm2 (mAh)	Additional Capacity at 0.1 mA/cm2 (mAh)	Determined by Titration (mAh)	Lithium Lost by Corrosion (mAh)	(mg/cm2)	(mils)
A. LiAlCl4-3SO2							
Fresh #1	579.2	553	0	0	26.2	0.34	0.25
Fresh #2	594.7	586	0	0	8.7	0.113	0.084
1 week @ 71C	606	510	26.6	0	69.4	0.898	0.67
2 weeks @ 71C	598.6	440	78.8	0	79.8	1.033	0.77
3 weeks @ 71C	598.6	402	78	0	118.6	1.53	1.14
B. 0.8NaAlCl4-0.2LiAlCl4-2.8SO2							
Fresh	594.7	586	0	0	8.7	0.113	0.084
1 week @ 71C	597.2	555.9	0	0	23.3	0.302	0.224
2 weeks @ 71C	544	520	3.8	0	20.2	0.262	0.194
3 weeks @ 71	583	572	4	0	7.0	0.091	0.067
C. Ca(AlCl4)2-5.6SO2							
1 week @ 71C	560	0	0	405	155	2.01	1.48
2 weeks @ 71C	560	0	0	232	328	4.25	3.13
3 weeks @ 71C	548	0	0	200	348	4.5	3.31
D. 1M LiAlCl4/SO2							
Fresh	560	480	2	58	20	0.269	0.192
1 week @ 71C	545	525	4	8	11	0.142	0.106
2 weeks @ 71C	594	545	4	5	40	0.518	0.384
E. NaAlCl4-2.8SO2							
Fresh	669	590	31	10.5	37.5	0.487	0.36
1 week @ 71C	727	-	-	689	38	0.492	0.36
2 weeks @ 71C	634	-	-	606	28	0.362	0.27
4 weeks @ 71C	-	-	-	622	51	0.66	0.48
F. 0.2LiAlCl4-0.8Ca(AlCl4)2-5SO2							
Fresh	684	0	0	602	82	1.061	0.78
1 week @ 71C	702	0	0	622	80	1036	0.76

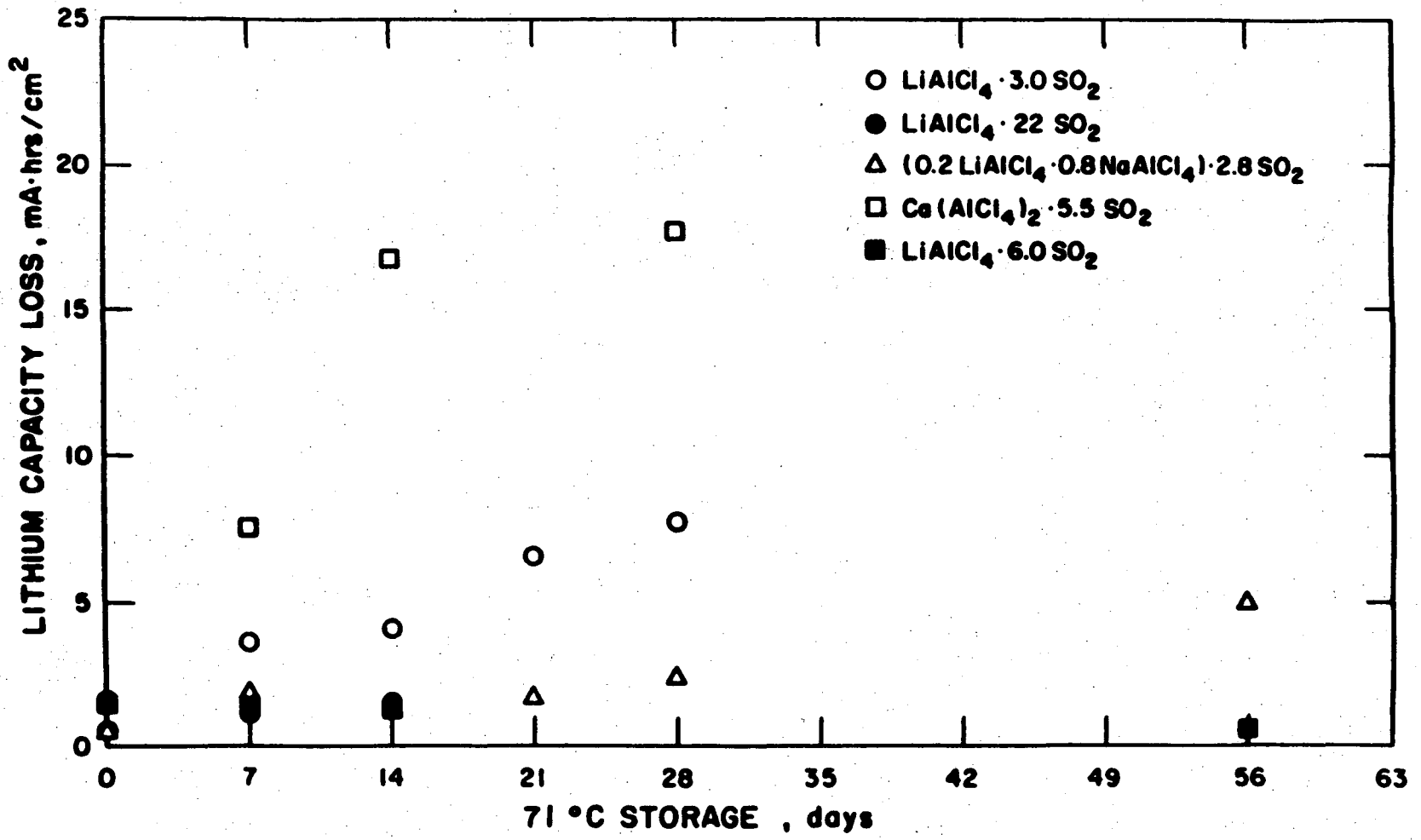

FIGURE 19. Corrosion of Lithium in Various Electrolytes After Storage at 71°C.

stripped off electrochemically at the 1 mA/cm^2 rate. The corrosion rate of lithium in $LiAlCl_4$-$3SO_2$ electrolyte was significantly higher than that in the sodium containing electrolytes. Although all active lithium could be stripped off electrochemically in the $LiAlCl_4$-$3SO_2$ electrolyte after storage similar to that in the sodium containing electrolytes, some active lithium could only be stripped at low rates (0.1 mA/cm^2). However, increasing the SO_2 content of the lithium tetrachloroaluminate electrolyte decreased the corrosion rate of lithium on 71°C storage. The $LiAlCl_4$-$6SO_2$ and $LiAlCl_4$-$22SO_2$ (1M $LiAlCl_4$) electrolytes gave superior stability for lithium. The loss of lithium after 8 weeks of storage at 71°C was less than 0.3 mils. Much more lithium capacity was delivered at 1 mA/cm^2 rate in the SO_2-rich electrolytes after high temperature storage than in the $LiAlCl_4$-$3SO_2$ electrolyte. The calcium containing electrolyte showed a high corrosion rate for lithium at 71°C. The loss of lithium was more than 3 mils after 2 weeks of storage. The amount of active lithium in calcium containing electrolyte after storage could only be determined by titration since the cells tended to short when lithium was stripped electrochemically from the working electrode to plate on the counter electrodes. It indicated that the plating morphology was very poor in calcium containing electrolytes.

Lithium immersed in $LiAlCl_4$-$3SO_2$ electrolyte and stored at elevated temperature (70^oC) for a week usually showed darkening or tarnish of the lithium surface. SEM/Kevex x-rayanalyses were carried out to evaluate the surface morphology and chemistry of the lithium electrode in the SO_2 solvated lithium and sodium tetrachloroaluminates after a fixed period of high temperature storage. Figure 20 exhibits the SEM photomicrograph of lithium surface after 1 week storage at 70^oC in $LiAlCl_4$-$3.0SO_2$ electrolyte. The surface of lithium was covered with crystals of a cubic structure. Kevex x-ray spectra showed that chlorine is the predominant element detected. Other elements of trace amount are sulfur and aluminum. The cubic crystals are presumed to be lithium chloride. Figure 21 shows the photomicrograph of the lithium surface after storing in $NaAlCl_4$-$2.8SO_2$ at 70^oC for the same amount of time. Similar cubic crystals were observed on the lithium surface while the size of the crystals was considerably smaller than that observed with $LiAlCl_4$-$3.0SO_2$ electrolyte. The rather dense coating on the lithium surface with the sodium electrolyte might be the reason that the lithium has better stability with low corrosion rate on high temperature storage.

LITHIUM SURFACE: STORED IN $LiAlCl_4 \cdot 3.0\ SO_2$

TYPICAL AREA SEM PHOTOMICROGRAPHS

#1

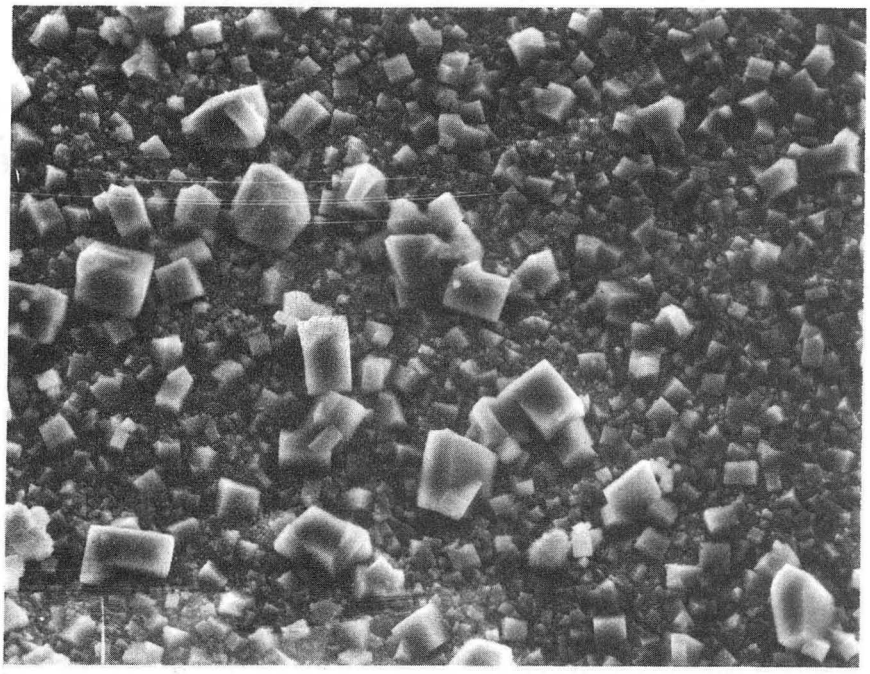

500X

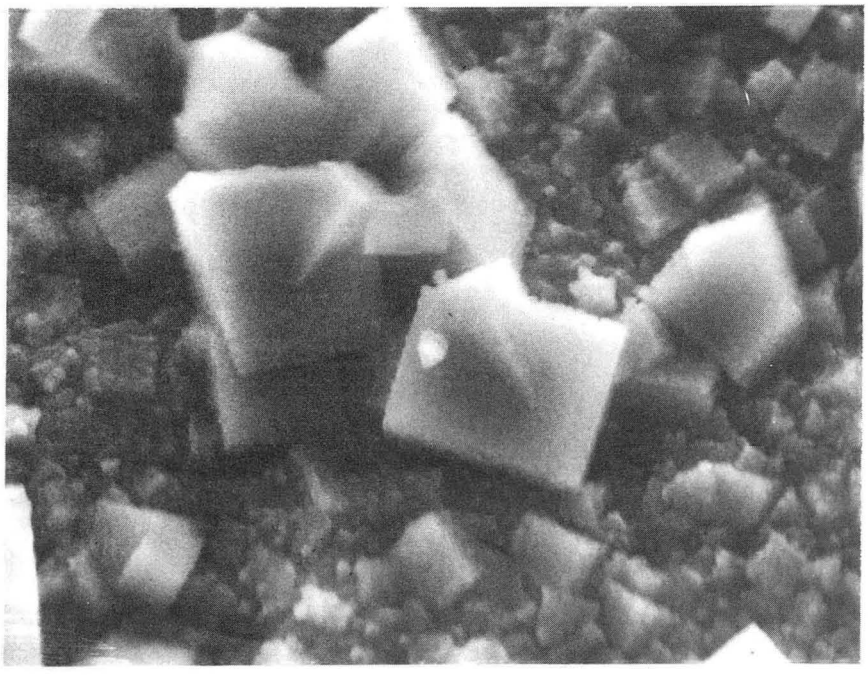

2,000X

FIGURE 20. SEM Photographs of Lithium Surface after 1 Week Storage at 70°C in $LiAlCl_4$-$3SO_2$ Electrolyte.

LITHIUM FOIL STORED IN $NaAlCl_4 \cdot 2.8\ SO_2$

CLEAR AREA ON #1.

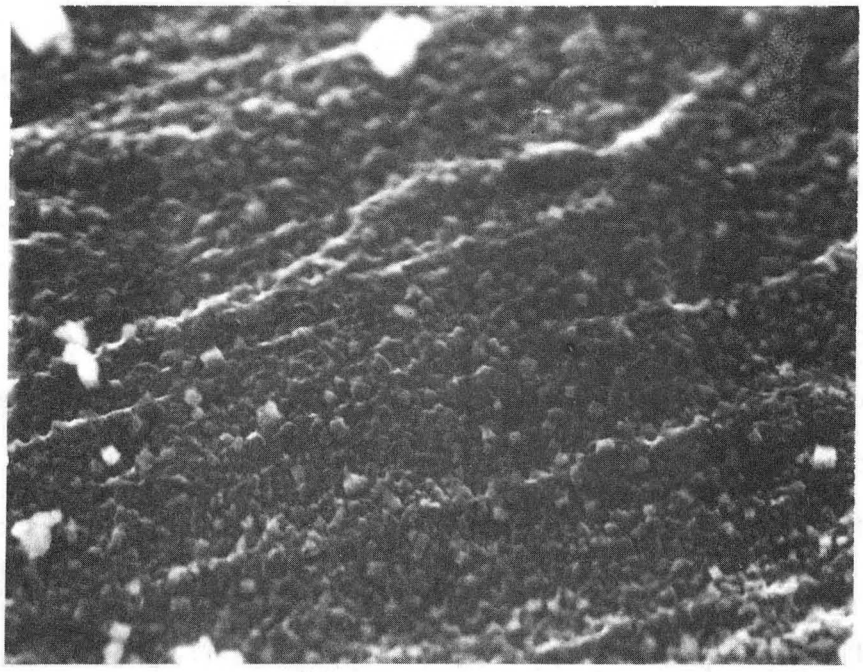

2,000X

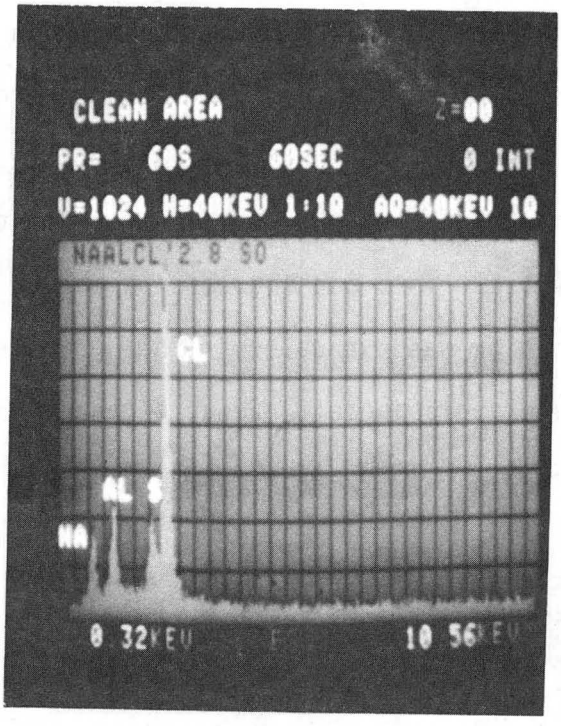

Kevex X-Ray Spectra

FIGURE 21. SEM Photograph and Kevex X-ray Spectrum of the Lithium Surface after 1 Week Storage at 70°C in $NaAlCl_4$-$2.8SO_2$ Electrolyte.

2. Cycling Efficiency of Lithium

a. Experimental

The cycling performances of the lithium electrode in various inorganic SO_2 electrolytes were evaluated using small flat electrode cells of size 2.5 cm x 4 cm with one lithium electrode sandwiched between two positive electrodes. The lithium working electrode was made by pressing a layer of preweighed lithium foil on both sides of a 1 mil copper foil substrate. Either porous carbon or $CuCl_2$ electrodes were used for this study. Figure 22 exhibits the cell assembly. The cells were cycled at different rates and depths of discharge and charge. The cycle life of the lithium working electrode was determined when it failed to deliver the preset depth of discharge due to exhaustion of the active lithium and showed a rapid drop in cell voltage as shown in the schematic diagram in Figure 23. Since the plating/stripping efficiency of the lithium was less than 100%, in each discharge cycle the freshly deposited lithium would be discharged first. Then the original lithium reserve was cut into and showed an apparent efficiency of 100% until all lithium was exhausted in the last discharge cycle. The average plating/stripping efficiency of the lithium was calculated as follows:

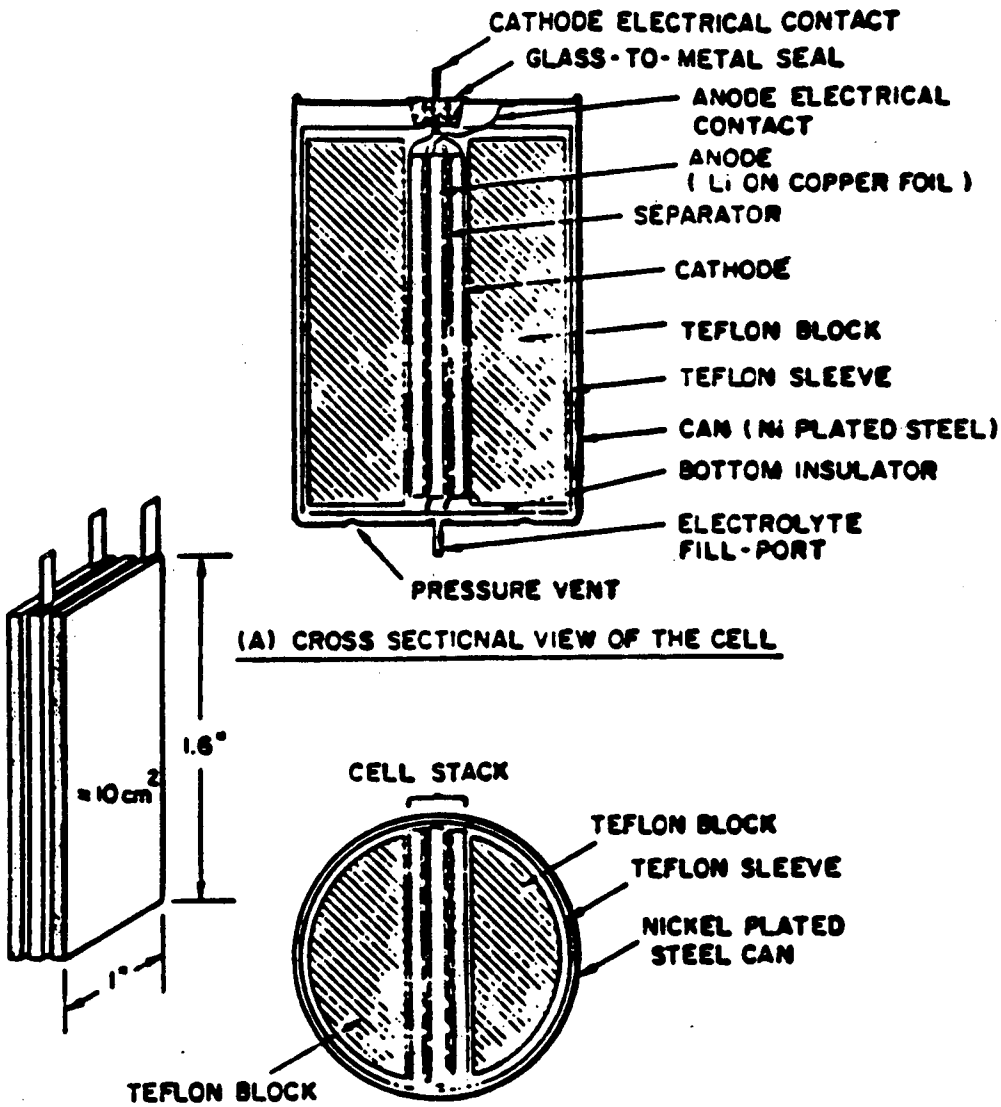

CELL ASSEMBLY

FIGURE 22. Cell Assembly for Lithium Cycling Study.

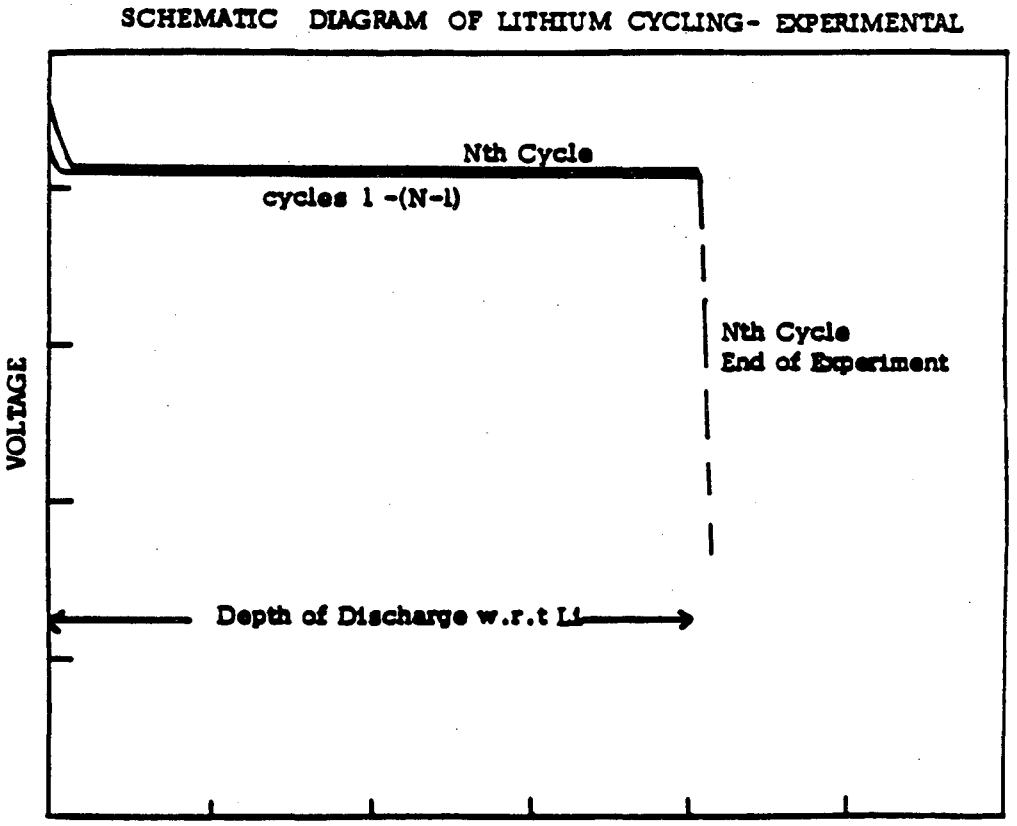

FIGURE 23. Schematic Diagram of the Voltage Profile of the Lithium Electrode on Cycling Study.

$$E_{ave} = 1 - (C_T - C_d)/(N \times C_d) \qquad [II-1]$$

where C_T is the total capacity of the lithium electrode

C_d is the capacity discharged each cycle

E_{ave} is the average efficiency of stripping/plating

N is number of cycles at anode failure

The lithium turnover was defined as

$$\text{Li Turn-over} = \frac{Cd \times N}{C_T} \qquad [II-2]$$

b. Results and Discussion

Table 3 shows the cycling efficiency of lithium in 0.25 M $Li_2B_{10}Cl_{10}/SO_2$ electrolyte obtained at 20% depth with 10 mil lithium as well as at various depths with 3 mil lithium. The average cycling efficiency of lithium ranged from 85% to 93% at a discharge rate of 1-2 mA/cm^2 and charge rate of 1 to 3 mA/cm^2. The data with 10 mil lithium showed that the cycle life of lithium decreased with increasing the charging rate.

TABLE 3. LITHIUM CYCLING DATA IN 0.25M $Li_2B_{10}Cl_{10}$ ELECTROLYTE

Cell#	Positive Electrode	Rate of Discharge/ Charge, (mA/cm^2)	Lithium Thickness	Depth	No. of Cycles	Average Cycling Efficiency	Lithium Turnover
582-146	Carbon	2 / 2	10 mil	20%	32	88%	6.4
582-147	Carbon	2 / 1	10 mil	20%	52	92%	10
582-148	Carbon	2 / 3	10 mil	20%	27	85%	5.4
A-5	$CuCl_2$	1 / 1	3 mil	12.8%	55	88%	7.0
A-6	$CuCl_2$	1 / 1	3 mil	25.6%	25	88%	6.4
A-7	$CuCl_2$	1 / 1	3 mil	51.2%	15	93%	7.7

Table 4 shows the cycling performance of lithium in 1M $LiGaCl_4/SO_2$ electrolyte. The cycling efficiency obtained with 10 mil lithium and carbon counter electrode ranged from 85% to 87%. The efficiencies obtained with 3 mil lithium and $CuCl_2$ counter electrodes were somewhat higher in the range of 85% to 94%.

Table 5 summarizes the test results of lithium cycling in $LiAlCl_4$-$3SO_2$ electrolyte. Tests with 3 mil lithium at various depths at 0.5 mA/cm^2 and 1 mA/cm^2 rates showed cycling efficiencies ranged from 92 to 98.8%. A lithium turnover of over 40 times was observed for cells with shallow cycling (12.8% depth). Tests with 5 mil lithium at 20 and 40% depths and higher discharge rates, 5 mA/cm^2 and 10 mA/cm^2, showed that the efficiency decreased to 85-86%. The cycling efficiency of lithium in this SO_2 solvated electrolyte was significantly better than that in either $Li_2B_{10}Cl_{10}/SO_2$ or $LiGaCl_4/SO_2$ electrolyte.

Table 6 shows the results of lithium cycling tests in $LiAlCl_4$-$6SO_2$ electrolyte with 5 mil lithium. Cycling efficiencies ranged from 92 to 96 was obtained. Although the tests were carried out with various charge and discharge rates, the data were quite scattered and no conclusive effect of rate on the cycling efficiency was obtained.

TABLE 4. LITHIUM CYCLING DATA IN 1 M $LiGaCl_4/SO_2$ ELECTROLYTE

Cell#	Positive Electrode	Rate of Discharge/ Charge, (mA/cm^2)	Lithium Thickness	Depth	No. of Cycles	Average Cycling Efficiency	Lithium Turnover
482-18	Carbon	2 / 2	10 mil	20% (2 mil) *	26	85%	5.2
481-29	Carbon	2 / 2	10 mil	20% (2 mil)	32	87%	6.4
582-14	Carbon	2 / 1	10 mil	20% (2 mil)	28	86%	5.6
582-142	Carbon	2 / 2	10 mil	20% (2 mil)	30	87%	6.0
582-144	Carbon	2 / 3	10 mil	20% (2 mil)	28	86%	5.6
A-1	$CuCl_2$	1 / 1	3 mil	12.8% (0.38 mil)	102	93%	13.1
A-2	$CuCl_2$	1 / 1	3 mil	25.6% (0.77 mil)	50	94%	12.8
A-4	$CuCl_2$	1 / 1	3 mil	51.2% (1.54 mil)	13	93%	6.7
A-3	$CuCl_2$	2 / 2	3 mil	12.8% (0.38 mil)	108	94%	13.8
A-14	$CuCl_2$	0.5/0.5	3 mil	12.8% (0.38 mil)	43	85%	5.5
A-15	$CuCl_2$	0.5/0.5	3 mil	25.6% (0.77 mil)	19	85%	4.9
A-16	$CuCl_2$	0.5/0.5	3 mil	51.2% (1.54 mil)	13	93%	6.7

* Equivalent thickness of lithium stipped/plated each cycle

TABLE 5. LITHIUM CYCLING DATA IN $LiAlCl_4$-$3SO_2$ ELECTROLYTE

Cell#	Positive Electrode	Rate of Discharge/ Charge (mA/cm^2)	Lithium Depth Thickness	No. of Cycles	Average Cycling Efficiency	Lithium Turnover
A-8	$CuCl_2$	0.5/0.5	3 mil 12.8% * (0.38 mil)	150	95.5%	19.2
A-11	$CuCl_2$	"	3 mil 25.6% (0.77 mil)	35	91.7%	8.96
A-21	$CuCl_2$	"	3 mil 51.2% (1.54 mil)	28	96.6%	14.3
A-22	$CuCl_2$	"	3 mil 76.8% (2.3 mil)	20	98.5%	15.4
A-12	$CuCl_2$	"	3 mil 25.6% (0.77 mil)	70	95.8%	17.9
A-24	$CuCl_2$	"	3 mil 51.2% (1.54 mil)	37	97.4%	18.9
A-11	$CuCl_2$	"	3 mil 12.8% (0.38 mil)	349	98.0%	44.7
A-13	$CuCl_2$	"	3 mil 25.6% (0.77 mil)	103	97.1%	26.4
A-27	$CuCl_2$	"	3 mil 51.2% (1.54 mil)	77	98.8%	39.4
B-8	$CuCl_2$	5 / 1	5 mil 10% (0.5 mil)	105	91%	10.5
B-3	$CuCl_2$	5 / 1	5 mil 20% (1 mil)	57	93%	11.4
B-12	$CuCl_2$	5 / 1	5 mil 40% (2 mil)	18	92%	7.2
B-4	$CuCl_2$	10/ 1	5 mil 20% (1 mil)	88	95%	17.6
B-5	$CuCl_2$	10/ 1	5 mil 40% (2 mil)	10	85%	4
B-6	$CuCl_2$	10/ 1	5 mil 40% (2 mil)	11	86%	4.4

* Equivalent thickness of lithium stipped/plated each cycle

TABLE 6. LITHIUM CYCLING DATA IN $LiAlCl_4$-$6SO_2$ ELECTROLYTE

Cell#	Positive Electrode	Rate of Discharge/ Charge (mA/cm^2)	Lithium Thickness	Depth	No. of Cycles	Average Cycling Efficiency	Lithium Turnover
C-1	$CuCl_2$	1/1	5 mil	50% (2.5 mil)	13	92%	6.5
C-6	Carbon	2/1	5 mil	20% (1.0 mil)	100	96%	20
C-7	Carbon	2/2	5 mil	20% (1.0 mil)	113	96%	22.6
C-8	Carbon	2/5	5 mil	20% (1.0 mil)	60	93%	12
C-9	Carbon	2/10	5 mil	20% (1.0 mil)	103	96%	20.6
C-11	Carbon	5/2	5 mil	20% (1.0 mil)	96	96%	19.2
C-12	Carbon	10/2	5 mil	20% (1.0 mil)	53	92%	10.6

* Equivalent thickness of lithium stipped/plated each cycle

The cycling efficiencies of lithium in the mixed electrolyte $Li_{0.2}Na_{0.8}AlCl_4$-$3SO_2$ are summarized in Table 7. The tests were carried out at discharge rates of 2 and 4 mA/cm^2 and charge rates of 1 and 2 mA/cm^2. Efficiencies ranging from 84 to 88% were observed. Although the sodium containing electrolyte had been found to provide better stability towards lithium, theplating efficiency is somewhat worse than that in pure $LiAlCl_4$-xSO_2 electrolytes.

TABLE 7. LITHIUM CYCLING DATA IN $Li_{.2}Na_{.8}AlCl_4$-$3SO_2$ ELECTROLYTE

Cell#	Positive Electrode	Rate of Discharge/ Charge (mA/cm^2)	Lithium Thickness	Depth	No. of Cycles	Average Cycling Efficiency	Lithium Turnover
D-1	$CuCl_2$	2 / 2	5 mil	5% (1.25 mil) *	21	86%	5.25
D-2	$CuCl_2$	4 / 1	5 mil	25% (1.25 mil)	19	84%	4.75
D-3	$CuCl_2$	4 / 1	5 mil	25% (1.25 mil)	21	86%	5.25
D-4	$CuCl_2$	2 / 1	5 mil	25% (1.25 mil)	20	85%	5
D-5	$CuCl_2$	2 / 1	5 mil	25% (1.25 mil)	25	88%	6.25
D-7	$CuCl_2$	2 / 1	5 mil	25% (1.25 mil)	22	86%	5.5

* Equivalent thickness of lithium stipped/plated each cycle

III. Li/SO_2 SYSTEM

A. CELL CHEMISTRY

The Li/SO_2 rechargeable system consists of a Li negative electrode and a porous carbon-PTFE catalytic positive electrode similar to a primary Li/SO_2 system [11, 12]. The totally inorganic electrolyte comprises liquid SO_2 and the electrolyte salts $Li_2B_{10}Cl_{10}$ or $LiGaCl_4$. Liquid SO_2 is the solvent as well as the liquid depolarizer. The Li/SO_2 system has an open circuit voltage of 2.92V with a theoretical energy density of about 1100 Wh/Kg. On discharge, sulfur dioxide is reduced on the carbon electrode and lithium dithionite, $Li_2S_2O_4$, is generated which is insoluble in the SO_2 electrolyte and stays within the pores of the carbon electrode [13,14]. On charging, the solid $Li_2S_2O_4$ is oxidized and liquid SO_2 is regenerated on the carbon electrode.

Discharge:

Negative Electrode

$$Li \text{ ----------> } Li^+ + e \qquad \text{(III-1)}$$

Positive Electrode

$$2SO_2 + 2\ Li^+ + 2e\text{----->}Li_2S_2O_4 \qquad \text{(III-2)}$$

Charge:

Negative Electrode

$$Li^+ + e \text{ --------> } Li \qquad \text{(III-3)}$$

Positive Electrode

$$Li_2S_2O_4\text{---->}2\ Li^+ + 2SO_2 + 2e \qquad \text{(III-4)}$$

The system with either $Li_2B_{10}Cl_{10}/SO_2$ electrolyte or $LiGaCl_4/SO_2$ electrolyte is able to take overcharge. On overcharge, the electrolyte salt oxides. The soluble oxidation products can either be reduced during discharge or recombined chemically with un-recovered discharge product in the positive electrode. The

overcharge products can also diffuse through the separator and recombine with the excess lithium plated during overcharge to regenerate the electrolyte salt. The recombination reaction is useful for scavenging the inactive lithium dendrites or the unoxidized lithium dithionite particles in the positive electrode following the following postulated reactions.

With $Li_2B_{10}Cl_{10}$ Electrolyte:

On overcharge:

Negative Electrode $Li^+ + e \text{ -----> } Li$ (III-5)

Positive Electrode $B_{10}Cl_{10}^{2-} \text{ -----> } B_{10}Cl_{10}^{-} + e$

3.6V vs Li (III-6)

On discharge :

Negative Electrode $Li \text{ -----> } Li^+ + e$ (III-7)

Positive Electrode $B_{10}Cl_{10}^{-} + e \text{ -------> } B_{10}Cl_{10}^{2-}$ (III-8)

Scavenging Reactions:

$$Li_2S_2O_4 + 2\ B_{10}Cl_{10}^- \text{---------->}\ 2\ Li^+ + 2B_{10}Cl_{10}^{2-} + 2SO_2 \quad \text{(III-9)}$$

$$Li + B_{10}Cl_{10}^- \text{-------->}\ Li^+ + B_{10}Cl_{10}^{2-} \quad \text{(III-10)}$$

With $LiGaCl_4/SO_2$ Electrolyte:

On Overcharge:

Negative Electrode $\quad Li^+ + e \text{--------->}\ Li \quad \text{(III-11)}$

Positive Electrode $\quad GaCl_4^- \text{----->}\ GaCl_3 + 1/2\ Cl_2 + e$ (soluble) $\quad \text{(III-12)}$

On discharge:

Negative Electrode $\quad Li \text{-------->}\ Li^+ + e \quad \text{(III-13)}$

Positive Electrode $\quad 1/2Cl_2 + GaCl_3 + e \text{----->}\ GaCl_4^- \quad \text{(III-14)}$

Scavenging Reactions:

$$Li_2S_2O_4 + Cl_2 + 2GaCl_3 \text{ ------> } 2LiGaCl_4 + 2\ SO_2 \qquad \text{(III-15)}$$

$$Li + 1/2\ Cl_2 + GaCl_3 \text{ -----> } LiGaCl_4 \qquad \text{(III-16)}$$

The capability for overcharge is one of the advantages of inorganic rechargeable systems. This is an important characteristic for it provides overcharge protection for individual cells to balance other cells in multi-cell battery. None of the rechargeable lithium systems with organic electrolytes currently under development have the capability to take overcharge.

B. EXPERIMENTAL

The lithium electrodes used in cell studies were made by pressing lithium foils on both sides of a copper foil substrate of 1 mil thickness. The copper foil substrate was employed to prevent the perforation of lithium foil after numerous cycles.

The porous carbon positive electrodes were prepared by mixing Shawinigan carbon with an appropriate amount of Teflon dispersion and pressing the mix on expanded aluminum or other metal substrate

using rollers. It was then cut into the proper size, dried and stored in oven at 140°C before cell assembly.

Prototype D cells with a wound electrode design were made using the hardware of the Duracell L026S primary Li/SO_2 cell having overall dimensions of : 60.2mm height, and 33.8mm OD. The hardware consisted of a nickel plated cold rolled steel can having a convoluted safety vent, a fill port at the bottom and a nickel plated cold rolled steel cover having a G/M seal feed through as shown in Figure 24. The cell was made by winding the Li electrode, carbon electrode and separator into a spool and then inserting the spool in the can. The cathode was electrically connected to the center post of the G/M seal and the negative electrode was connected to the can by means of a tab. The cell cover was welded to the can by a laser welder or Tig welder. The cell was then evacuated and filled with electrolyte and the fill port was closed by crimping and welding.

Experimental cells with a flat electrode design were also used to carry out some preliminary studies of the electrodes, separators and electrolytes, and to diagnose the problems of the system. The cell structure was basically the same as that used in lithium cycling study as shown in Figure 22. The working electrode, such as porous carbon electrode was sandwiched between two counter electrodes with 2 or 3 layers of Celgard #2400 separator. The cell

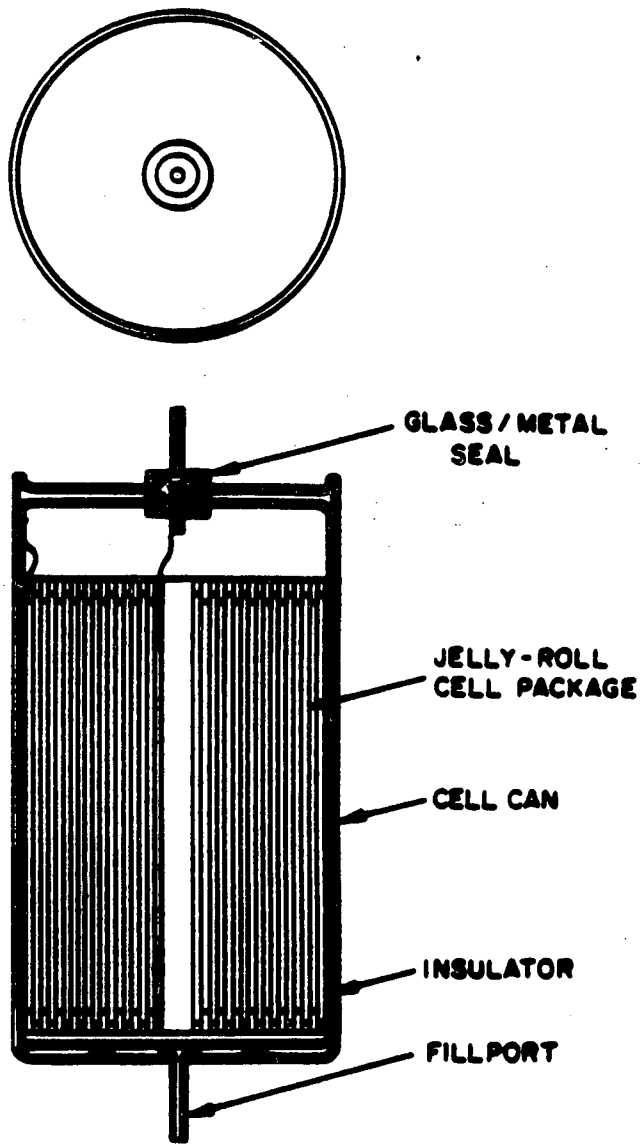

FIGURE 24. D Cell Assembly.

stack was placed between two half cylindrical teflon shims and inserted in D size can. The positive electrode was connected to the center post in the cover with the glass-to-metal seal and the negative electrode was connected to the can. The cell was then sealed and filled with electrolyte for evaluation.

C. CELL PERFORMANCE AND DISCUSSION

1. Performance of D Size Cells

Figure 25 shows the typical voltage profiles of D cells with 0.25M $Li_2B_{10}Cl_{10}/SO_2$ electrolyte discharged at rates from 0.1 to 1 A. The cells had 22 inch electrodes that were 1.5 inch in width. The thickness of the carbon electrode was 23-25 mils and the thickness of the lithium electrode was 20 mils. The cells showed a flat discharge voltage and delivered capacity similar to that of the primary Li/SO_2 cells with LiBr/acetonitrile/SO_2 electrolyte. Figure 26 shows the voltage profiles of the D cells of the same structure with 1M $LiGaCl_4/SO_2$ electrolyte. Although the cells showed the same discharge voltages, the capacities delivered were significantly lower than that with the boron electrolyte at the corresponding rates.

Table 8 compares the cell capacity, carbon utilization and the primary energy density of the D cell with $Li_2B_{10}Cl_{10}/SO_2$ to

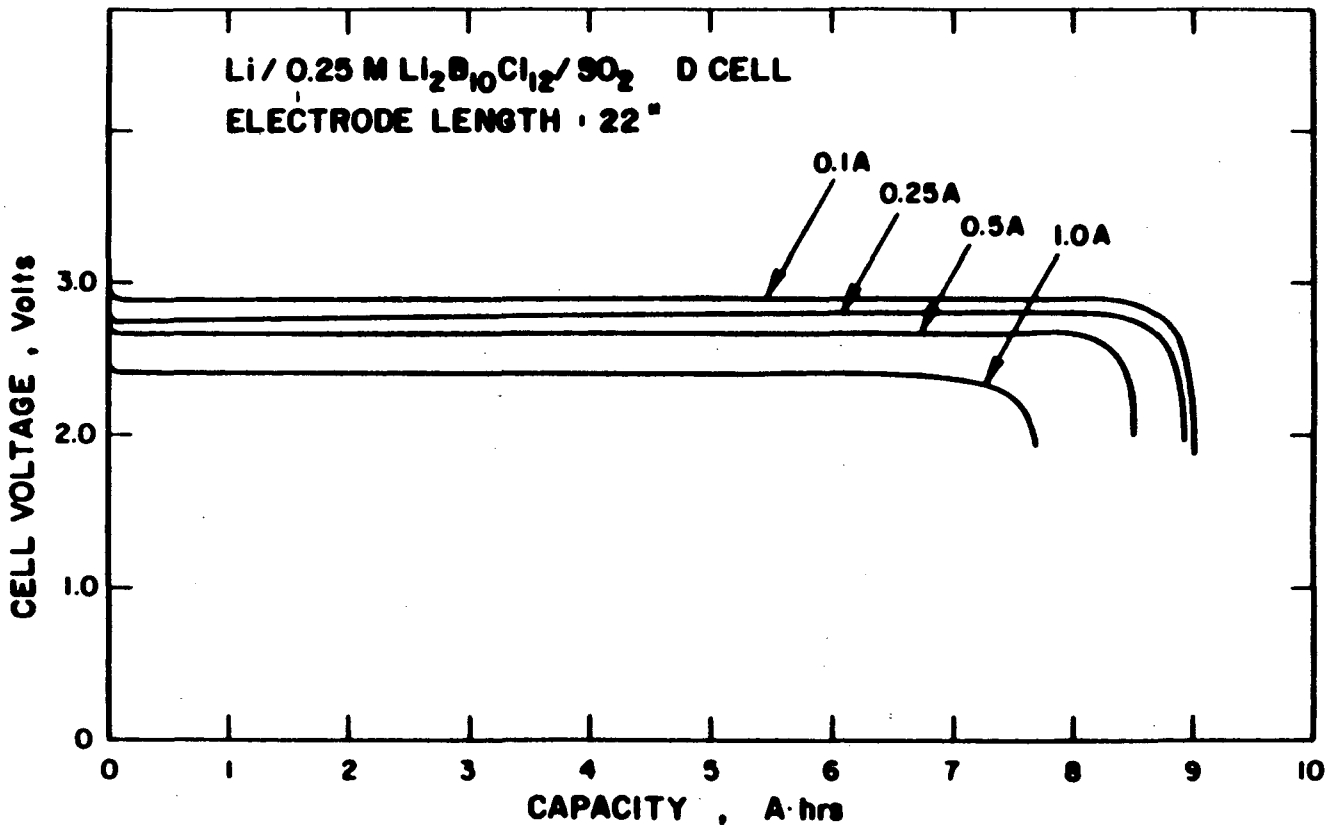

FIGURE 25. The Voltage Profiles of the Li/SO_2 D Cells With 0.25M $Li_2B_{10}Cl_{10}/SO_2$ Electrolyte Discharged at Various Rates.

TABLE 8. PERFORMANCE COMPARISON OF Li/SO_2 CELLS WITH 0.25M $Li_2B_{10}Cl_{10}/SO_2$ AND 1M $LiGaCl_4/SO_2$ ELECTROLYTES

	$Li_2B_{10}Cl_{10}$	$LiGaCl_4$
Ah/gm of Carbon	2-3 Ah/g	1.3-2.0 Ah/g
Ah/in^2 of Cathode (27 Mils)	0.29-0.35 Ah/in^2	0.16-0.25 Ah/in^2
D Cell Capacity	8-9 Ahs	5-7 Ahs
Energy Density (D Cell)	260-290 Wh/kg	175-240 Wh/kg

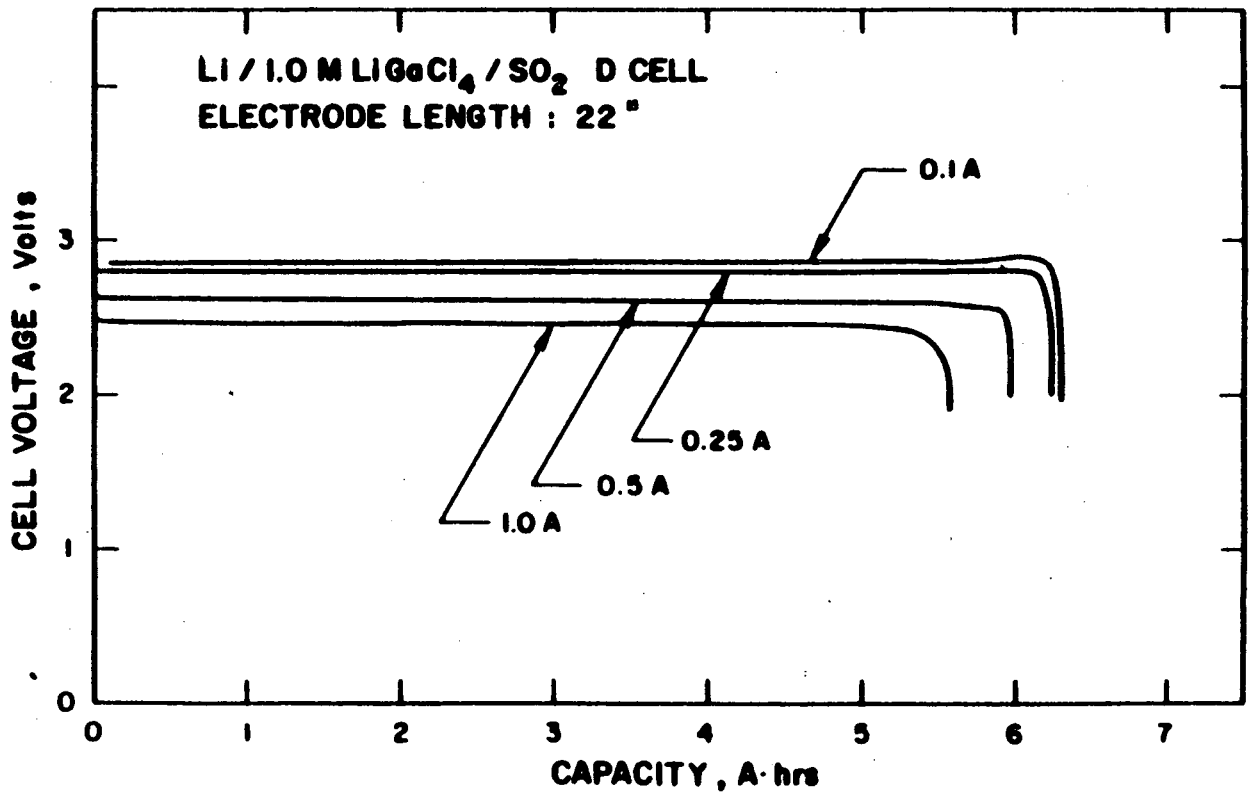

FIGURE 26. The Voltage Profiles of the Li/SO_2 D Cells with 1M $LiGaCl_4/SO_2$ Electrolyte Discharged at Various Rates.

those with $LiGaCl_4/SO_2$. Cells with the boron electrolyte have better carbon utilization and significantly higher energy density than cells with the gallium electrolyte.

Cycling tests of D cells with the boron electrolyte between 2.5 and 3.5 v (100% depth) indicated the cycle life was very poor. Although a previous study [14] showed that the discharge product, $Li_2S_2O_4$, in the porous carbon electrode could be fully recharged back to SO_2, there was a significant loss of discharge capacity on next discharge cycle. Figure 27 shows the typical discharge/charge voltage profiles at the first and the 7th cycles at 0.5 Amp discharge and charge rates.

Cells filled with 1M $LiGaCl_4/SO_2$ electrolyte showed somewhat better cycle life on deep discharge. The loss of capacity in consecutive cycles was not as drastic as that with boron electrolyte as compared in Figures 28 and 29. However, the capacity decreased to less than 50% of the original capacity after about 10 cycles.

Several D size cells with implanted Li reference electrodes were made for evaluation. The test results indicated that the cell capacity was primarily limited by the positive carbon electrode. Normally cells were built with 200%-300% excess of lithium.

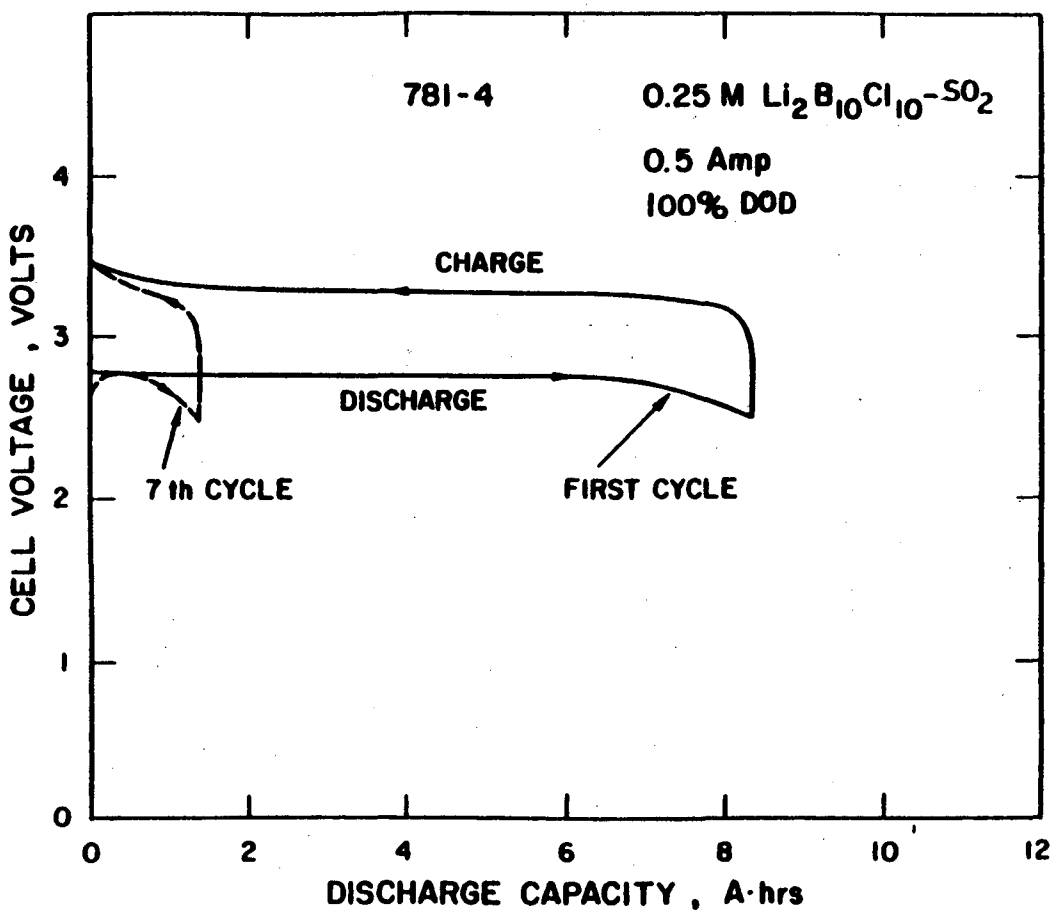

FIGURE 27. The Voltage Profiles of a Li/SO_2 D Cell with 0.25M $Li_2B_{10}Cl_{10}/SO_2$ Electrolyte Charged at 0.5A.

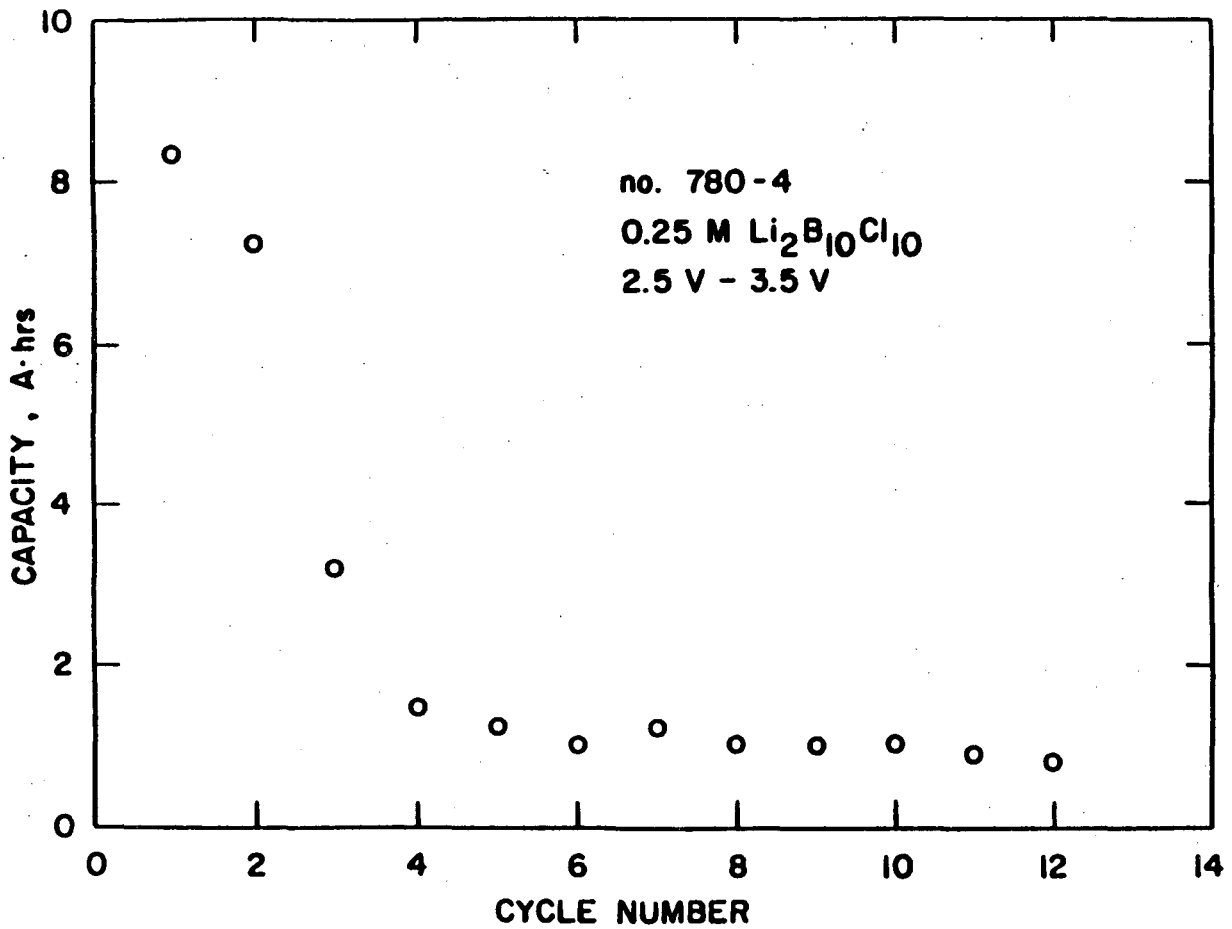

FIGURE 28. The Cycling Performance of a Li/SO_2 Cell with 0.25M $Li_2B_{10}Cl_{10}$/SO_2 Electrolyte Discharged and Charged at 0.5 A to]00% Depth.

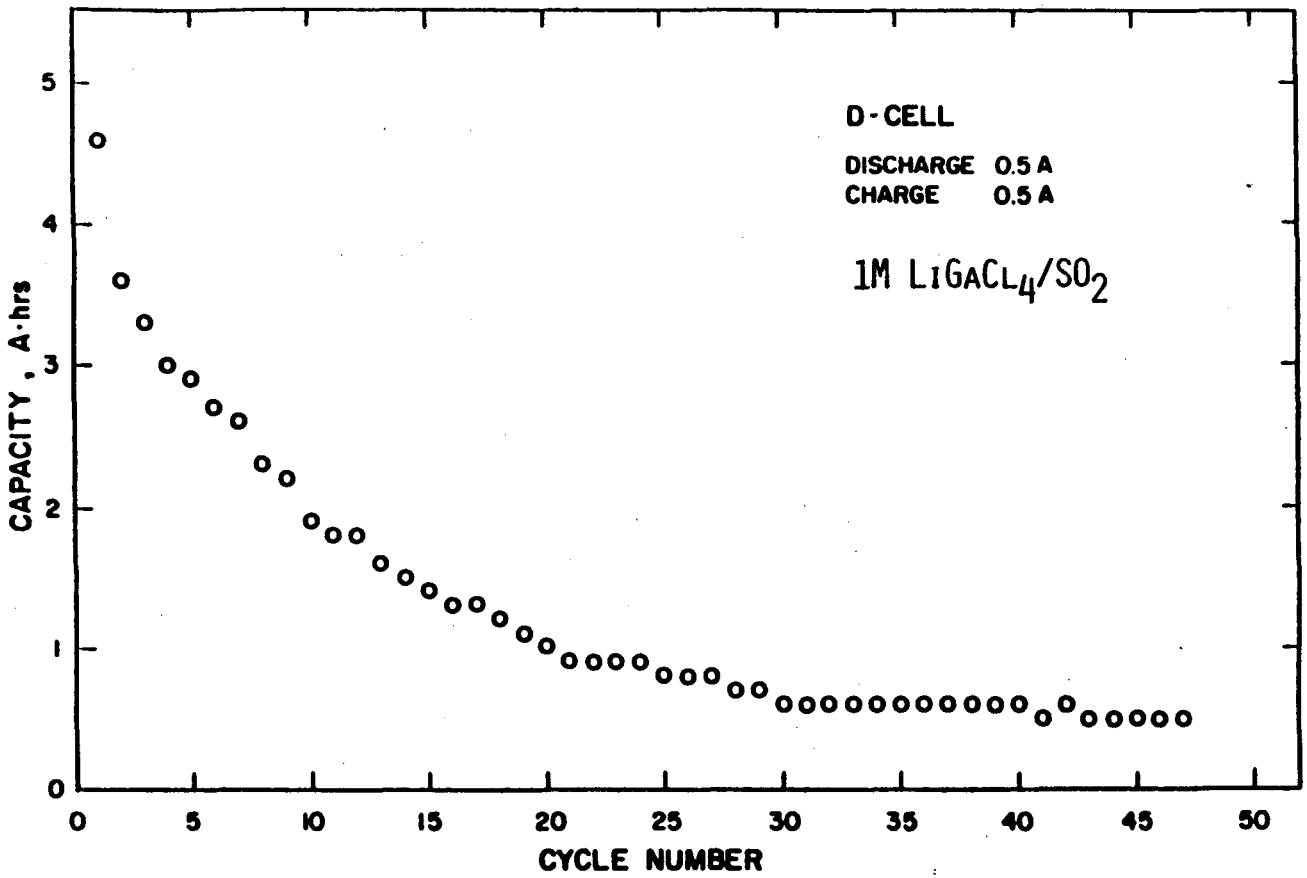

FIGURE 29. The Cycling Performance of a Li/SO_2 D Cell with 1M $LiGaCl_4$ Electrolyte Discharged and Charged at 0.5A to 100% Depth.

Figure 30 shows the typical polarization of the electrodes in a D cell filled with $LiGaCl_4/SO_2$ electrolyte at the 1st and the 10th cycles.

Numerous D size cells filled with both electrolytes were made for evaluation on continuous charge/discharge cycling at currents of 0.1A, 0.25A , 0.5A and 1 A at 10-20% depth of discharge (1 Ah cycling). On shallow discharge, the cells with boron electrolyte were able to deliver over 100 cycles depending on the rate of discharge and charge. Some cells had been subjected limited overcharge (less than 50% of their original capacity) and did not showed adverse effect. Most cells failed due to internal shorts after numerous cycles. A large amount of cells (over 1/3) vented violently after the development of internal shorts. Figure 31 shows the voltage profiles at the first, the 54th and the 100th cycles of a D cell cycled at 0.5 A to a depth of 1Ah.

Cells filled with 1 M $LiGaCl_4$ electrolyte delivered less cycles on shallow discharge as shown in Table 9 in comparison with the performance of cells filled with boron electrolyte. Cells with gallium electrolyte failed mostly due to loss of capacity after numerous cycles. Considerably less amount of cells failed due to internal shorts or vented violently. However, cells with gallium electrolyte had a high tendency to vent violently on overcharge. This might have been due to $GaCl_3$ generated during overcharge

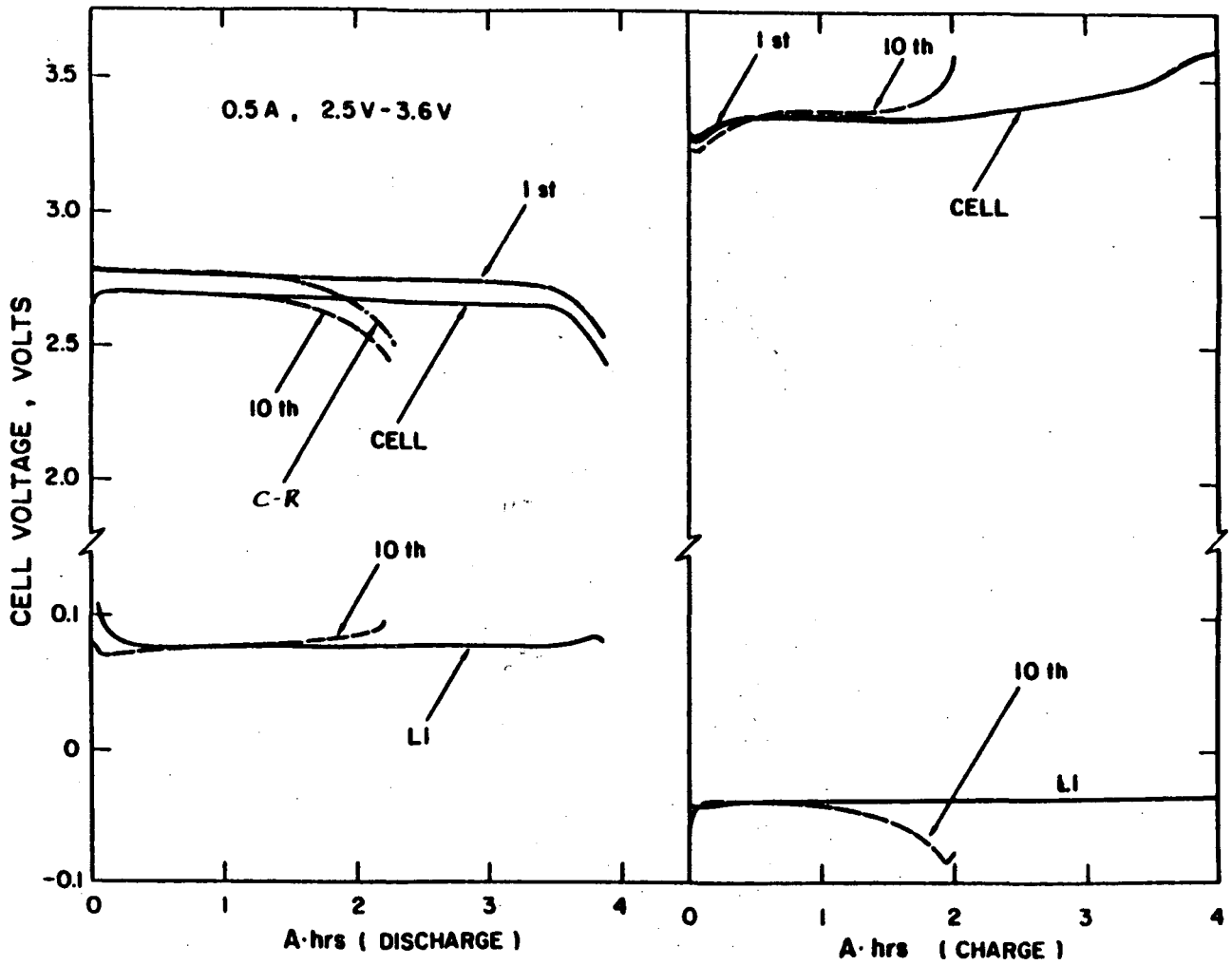

FIGURE 30. The Voltage Profiles of the Electrodes vs. a Li Reference Electrode in a D Cell with 1M $LiGaCl_4/SO_2$ Electrolyte.

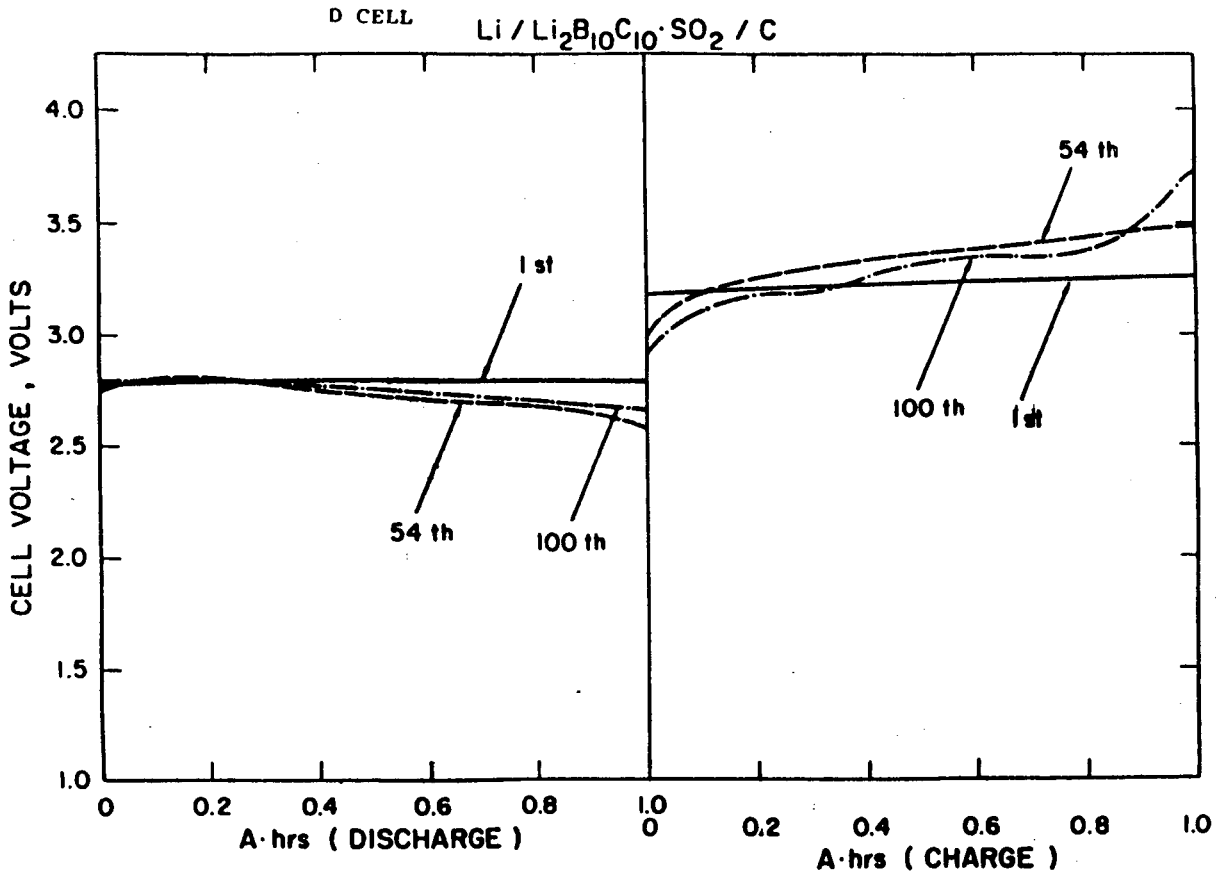

FIGURE 31. The Voltage Profiles of a Li/SO_2 D Cell with 0.25M $Li_2B_{10}Cl_{10}/SO_2$ Electrolyte at 0.5 A Discharge/Charge Rates to Depth of 1 Ahr at Selected Cycles.

TABLE 9. CYCLING PERFORMANCE OF D SIZE Li/SO_2 CELLS

RATE	$Li_2B_{10}Cl_{10}$	$LiGaCl_4$
0.5 Amp	40-75 cycles	40-70 cycles
0.25 Amp	70-130 cycles	50-85 cycles
0.1 Amp	70-130 cycles	60-80 cycles
1 Amp	--	30-60 cycles
	100% DEPTH	
0.5 AMP	3-7 cycles (Capacity to less than 1 AH)	10-20 cycles

being highly corrosive and attacking the Celgard separator to cause cell shorting.

2. Postmortem Examination

Postmortem examination of some cells which had failed after cycling showed that the carbon electrode became relatively brittle with numerous small cracks observed on the surface. The resistivity of the carbon layer was also found significantly higher than that of a fresh carbon electrode. The lithium electrode obtained from the cell with boron electrolyte had converted to a mat of powdery lithium after numerous cycles. The powdery lithium recovered from cells after cycling was highly active and could ignite spontaneously when disturbed by scratching even in argon filled dry box.

The lithium electrode recovered from cells filled with gallium electrolyte showed that a thick light purple color deposit was formed on the lithium surface. A thickness of coatings as high as 60 mils had been observed on a lithium electrode having 10 mil original thickness after 40-50 cycles of charge and discharge. The deposit was soluble in water and gave a basic solution. Emission spectrographic analysis and Kevex analysis of the deposit detected large amounts of S, Li and smaller amounts of Ga and Cl. Debye-Scherer powder diffraction analysis was not able to identify any simple composition of the deposit. However, IR spectrum analysis

detected the presence of larger amount of dithionite. It was not clear how the dithionite was formed on the lithium surface.

3. Diagnostic Studies

Experimental cells with prismatic electrode design were made to diagnose the problems of the system. The cells were normally made with the positive electrode sandwiched between two lithium electrodes having electrode dimension of 4 cm x 2.5 cm.

Figure 32 shows the performance of an experimental cell filled with excess gallium electrolyte. The cell showed a loss of capacity similar to the performance of a wound cell even though it contained excess electrolyte. Since the electrode stack was confined between two Teflon inserts(shims), the expansion of the electrode stack was limited. The electrode stack was compressed under high pressure during discharge due to expansion of the carbon electrode with the formation of dithionite. Another experimental cell was made with a spring on the back of the shims which allowed the electrode to expand and shrink under constant stack pressure. The performance of this cell is shown in Figure 33. The loss of cell capacity on cycling was much lower than that of the cell with confined electrode stack. It seems that the performance of the carbon electrode is affected significantly by the stack pressure. Due to the nature of the wound cell design, it is impossible to

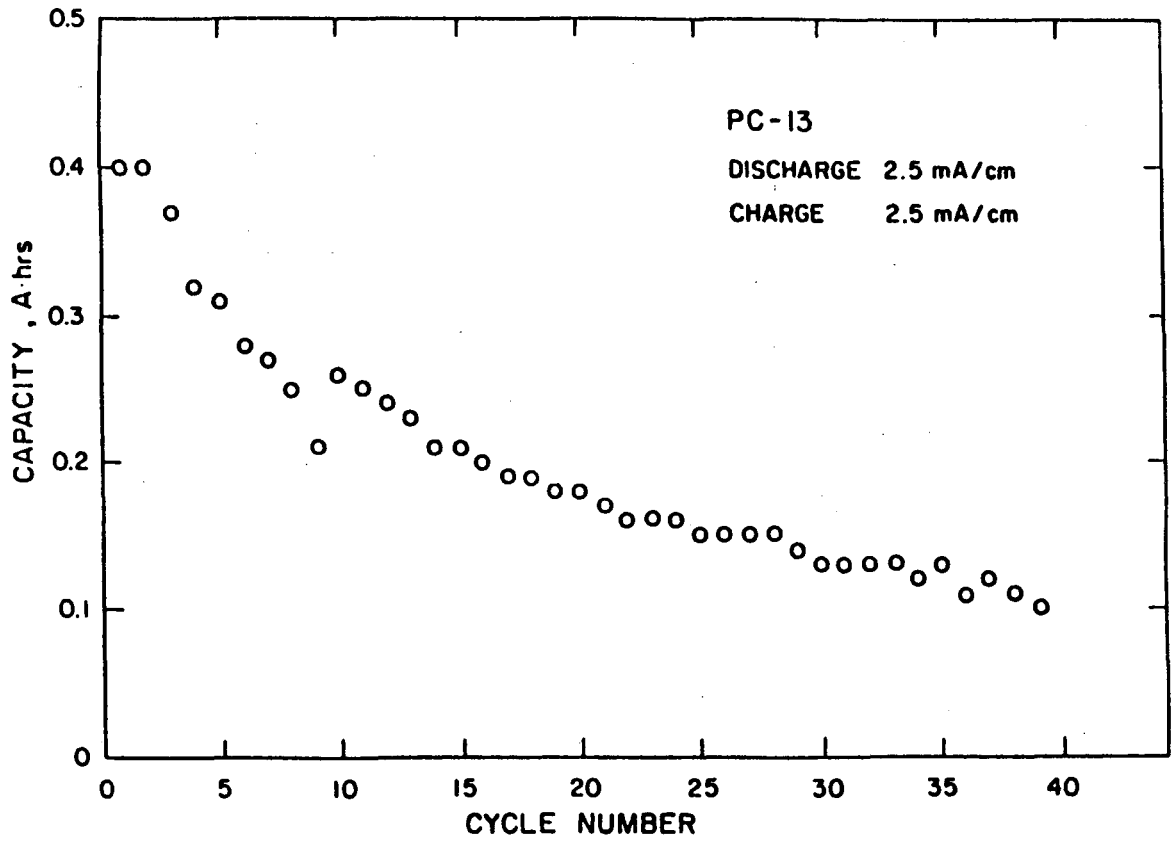

FIGURE 32. The Performance of a Li/SO_2 Experimental Flat Electrode Cell with 1M $LiGaCl_4/SO_2$ Electrolyte.

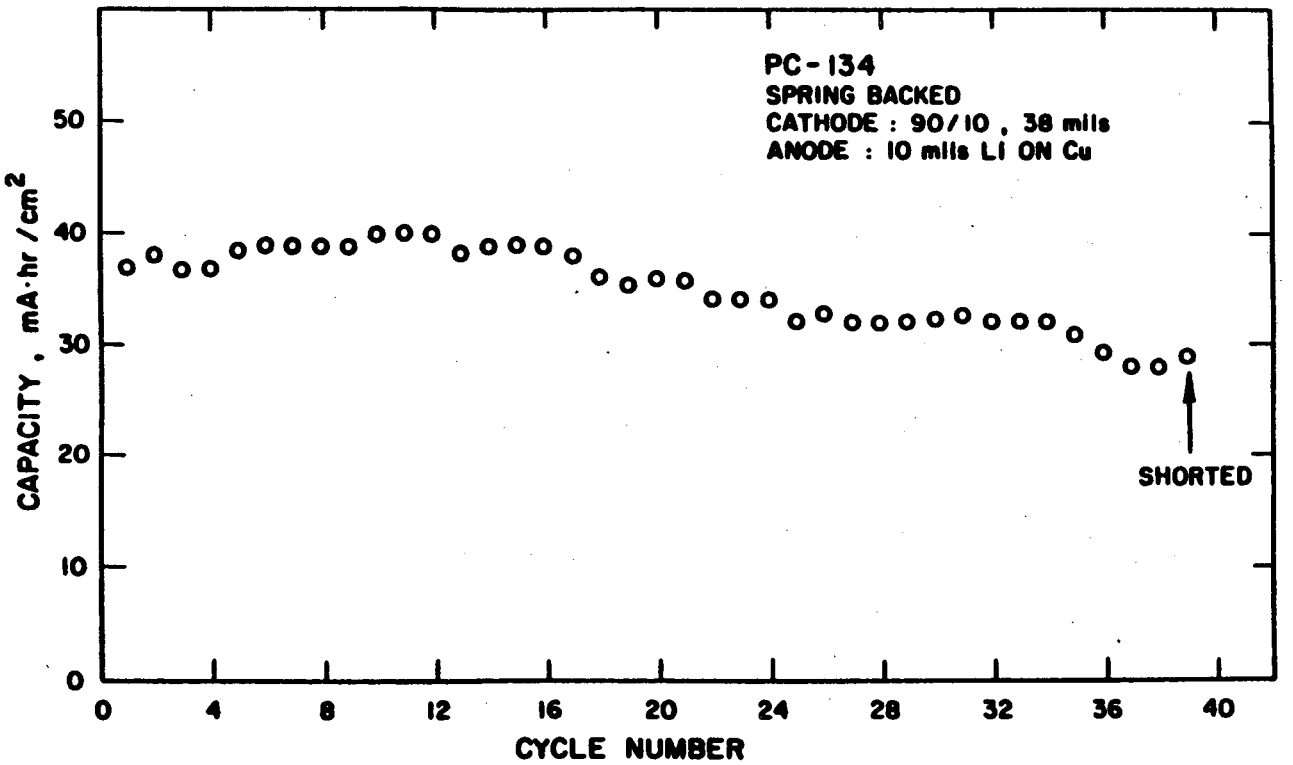

FIGURE 33. The Performance of a Li/SO_2 Experimental Flat Electrode Cell with 1M $LiGaCl_4/SO_2$ Electrolyte Having the Electrode Stack Compressed by a Spring.

maintain a constant stack pressure. Other approaches had to be taken for improving the cell performance.

4. Improvement of the Carbon Positive Electrode

Since postmortem examination of the cell indicated that the carbon electrode became brittle and some carbon material had flaked away from the substrate, several attempts to improve the integrity of the carbon electrode were carried out. Following approaches were evaluated :

a. Increase of the Teflon content in the cathode for improving the elasticity of the electrode.

b. Using alternate materials and designs of the current collector for improving the integrity as well as the current distribution of the electrode. Materials such as nickel, aluminum and titanium etc. were evaluated.

c. Addition of conductive filler in the carbon cathode which included aluminum fiber, graphite fiber, graphite powder, nickel powder, copper powder etc.

None of the above approaches showed effective improvement of the performance of the carbon electrode. Other carbon materials of different physical properties such as Vulcan 72, Cabot CSX 179, Ketjenblack EC etc. were also evaluated for the positive electrode and none of them was able to provide better performance in cycle life or cell capacity than the Shawinigan Carbon.

Impregnating foam nickel (80% porosity) with carbon was also evaluated. The loss of capacity was significantly less than that of a standard pasted carbon electrode on expanded metal as shown in Figure 34. However the cell still showed a 50% loss of capacity after nearly 50 cycles. Since a large amount of volume was wasted with the use of the carbon impregnated foam metal, a D size cell made with foam metal could only deliver about 2 Ahs.

The poor cycling performance of the system is believed to be due to the poor elastic structure of the carbon electrode. A large internal stress is generated during discharge with the formation of solid lithium dithionite within the pores of the carbon electrode which might cause irreversible structural damage with the formation of isolated carbon particles and the reduction of the flexibility and the microscopic porosity of the electrode.

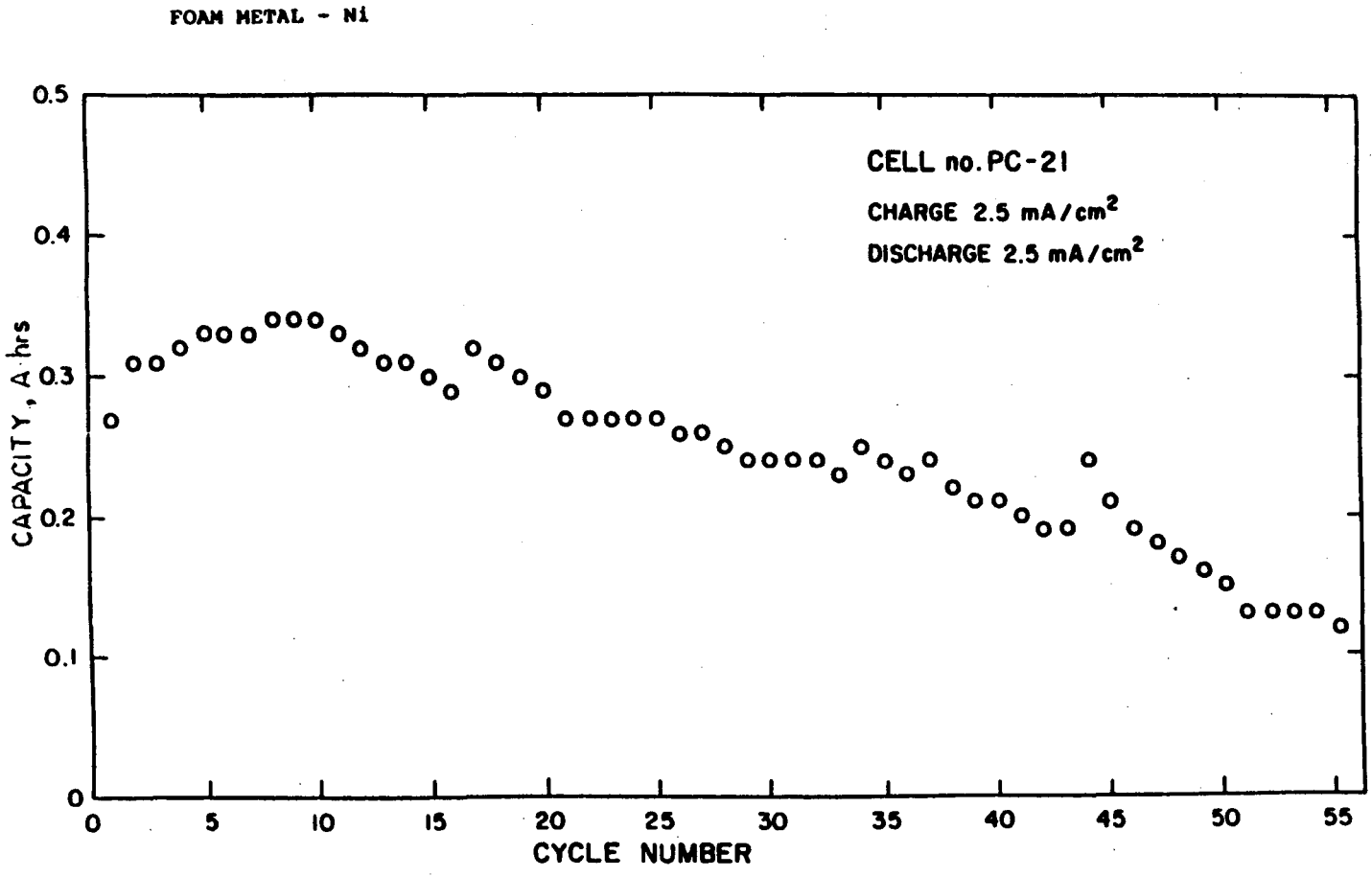

FIGURE 34. The Performance of a Li/SO_2 Experimental Flat Electrode Cell with 1M $LiGaCl_4/SO_2$ Electrolyte Having Foam Nickel as Substrate for the Carbon Electrode.

IV. $Li/LiAlCl_4-xSO_2$/CARBON SYSTEM

A. INTRODUCTION

Cells with a lithium negative electrode, carbon positive electrode and filled with $LiAlCl_4-SO_2$ electrolyte show an OCV of about 3.26 V. This voltage is significantly higher than the reduction potential of $SO_2/S_2O_4^{=}$ on carbon. Previous screening tests using glass cells with Shawinigan carbon electrodes showed a high short circuit current but very poor capacity utilization as indicated in Table 1. A D size cell with a Shawinigan carbon electrode filled with 1M $LiAlCl_4/SO_2$ electrolyte delivered only 0.4 Ah at 0.25 Amp discharge rate, which was far less than the capacities delivered with the $Li_2B_{10}Cl_{10}/SO_2$ and the $LiGaCl_4/SO_2$ electrolytes. The carbon utilization was about 0.13 Ah/g. However, using experimental cells, we found that the capacity utilization depended strongly on the type of carbon and the composition of the electrolyte. A preliminary cycling study of lithium using experimental cells filled with the complexed $LiAlCl_4-3SO_2$ or $LiAlCl_4-6SO_2$ electrolytes showed significantly better cycle life and lithium plating efficiency than cells with the $Li_2B_{10}Cl_{10}/SO_2$ and the $LiGaCl_4/SO_2$ electrolytes (Tables 5 and 6).

Since the material cost of the $LiAlCl_4$ is far less than that of the $Li_2B_{10}Cl_{10}$ or $LiGaCl_4$ salt, substantial efforts were carried out to investigate the performance and cell chemistry of this system.

B. EXPERIMENTAL

Experimental cells with a flat electrode design were used to study the cell chemistry and the performance of various carbons. The structure of the cell was similar to that used for lithium cycling as described previously and shown in Figure 22 except that the positive carbon electrode was positioned in the center and sandwiched between two lithium electrodes. Both rolled or dry pressed positive electrodes were used in experimental cell. The dry pressed electrode was made by mixing proper amounts of carbon with Teflon and then pressed on expanded nickel screen in a die of dimension 4 cm x 2.4 cm within an argon filled dry box.

The rolled carbon electrode was made by mixing proper amounts of carbon, Teflon, alcohol and water to form a dough. The dough was then rolled on an expanded metal substrate to a thickness of about 15 to 25 mils and dried in oven at 140°C.

2/3A size prototype cells with a spirally wound electrode design were made for evaluation using the hardware of Duracell L032S

primary Li/SO_2 cells. The cell can had dimensions of 34.5 mm in height and 16.3 mm in diameter. The cover had an electrical feed through with M/G seal. The bottom of the can had a convoluted safety vent and a fill port for electrolyte similar to the L026S cans used for D cells as described previously.

C. CELL CHEMISTRY

Figure 35 shows the typical voltage profile of an experimental cell with a lithium negative electrode and a pressed carbon positive electrode (Ketjenblack EC 90%, PTFE 10%) filled with $LiAlCl_4$-$3SO_2$ and discharged/charged at 1 mA/cm^2. The cell delivered 480 mAh per gram of carbon to 2.6 V cutoff. Although the flat voltage profile is similar to Li/SO_2 cells, the discharge voltage near 3.2 V is significantly higher than the 2.9 V for the reduction of SO_2 having $Li_2S_2O_4$ as discharge product in the regular Li/SO_2 cell. The charge voltage of 3.6 V is also significantly higher than the value of 3.4 V for the rechargeable Li/SO_2 cells with $Li_2B_{10}Cl_{10}/SO_2$ or $LiGaCl_4/SO_2$ electrolytes. Various studies were carried out to investigate the discharge chemistry as described in following.

1. Instrumental and Chemical Analyses

Infrared spectra study of the discharged cathode did not show

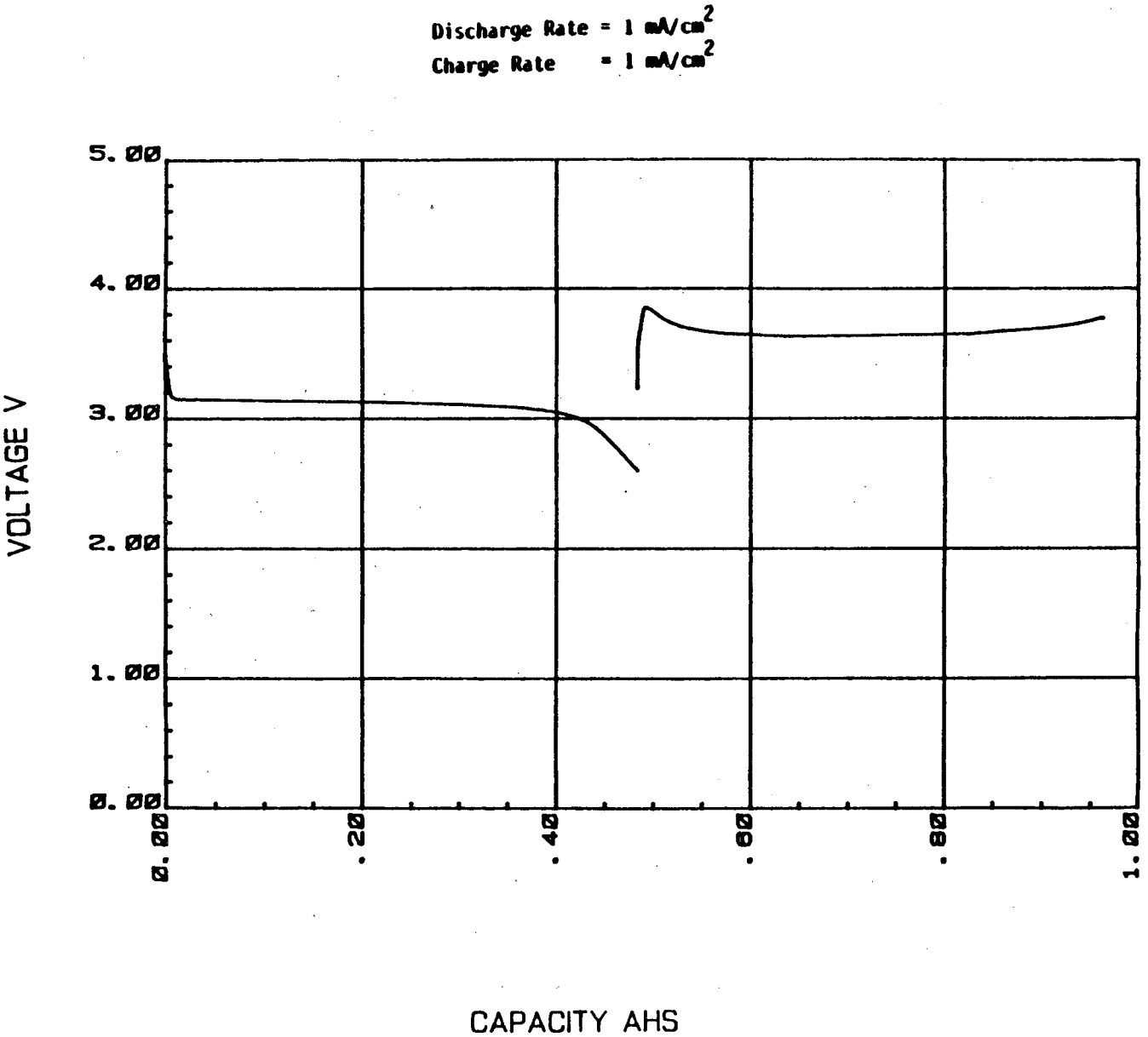

FIGURE 35. Typical Discharge/Charge Voltage of an Experimental $Li/LiAlCl_4$-$3SO_2$ Carbon Cell Having 1 Gm Carbon Positive Electrode (Ketjen Black EC 90%, PTFE 10%), Discharged/Charged at 1 mA/cm^2.

the presence of lithium dithionite. It indicated that the discharge reaction could not be the $SO_2/S_2O_4^=$ reaction. Thorough instrumental and chemical analyses were performed to identify the reaction product and to characterize the discharge mechanism. The detailed experiments and results are listed as follows:

a. Measurement of the Weight Gain of The Carbon Electrode

Significant weight gain was observed after the carbon electrode was immersed in the electrolyte. The material adsorbed in the carbon could not be washed off with SO_2. Measurements of weight gain were made for fresh electrodes after immersing in electrolyte and for electrodes after various depths of discharge as well as fully recharged. The weight of each positive electrode was measured after washing with liquid SO_2 to remove the residual electrolyte and vacuum dried to remove SO_2. The measured weight gains are listed in Table 10.

XRD analysis identified $LiAlCl_4$ as the only detectable component in the undischarged positive electrode. Additional weight was gained during discharge proportional to the amount of discharge as shown in Table 10. About 44% of this weight gain was lost after the charge cycle. XRD analysis confirmed that LiCl is the only species detectable in the discharged positive electrode.

TABLE 10. MEASUREMENTS OF WEIGHT GAIN OF THE POSITIVE ELECTRODE

		Dry Weight g	Wt. After Soaking In Electrolyte, g	Wt. Gain/g Dry Wt. g
Undischarged Carbon Electrode	1	1.11	2.40	1.16
	2	1.04	2.28	1.19

		Dry Weight g	Cell #	mAh of Discharge	Wt. After Discharge	Wt. Gain/ 100 mAh
Discharged Carbon Electrode	1	0.97	650	406	3.54	0.63
	2	0.96	652	390	3.45	0.64
	3	0.52	720	300	2.40	0.63
	4	0.49	721	300	2.37	0.63
	5	0.51	722	300	2.21	0.57

		Dry Weight g	Cell #	mAh of Discharge	mAh of Charge	Wt. After Charge g	Wt. Gain/ g Dry Wt.
Discharged-Charged Electrode	1	0.90	649	480	480	2.42	1.69

b. Chemical Analysis

Table 11 lists the elemental analyses of a discharged and an undischarged carbon positive electrode. Attempts to derive an exact formula from the chemical analyses would not be realistic because the analytical results were the combination of at least three components: LiCl, residual electrolyte and the discharge products. In addition, washing the sample with SO_2 did not guarantee the integrity of the discharged products even though they were believed to have very low solubilities.

Since $LiAlCl_4$ has been identified by XRD to be the only detectable component in the undischarged cathode, Table 12 shows the calculated elemental weight distribution of the weight gain assuming $LiAlCl_4$ is the only compound causing weight gain (0.04 g is detected from the weight gain for the residual SO_2 found). It shows good agreement with the chemical analyses data of the undischarged electrode.

c. Infrared Spectra Study

Figure 36 shows the IR spectra of the fresh and discharged electrolyte samples indicating that the cathodic discharge does not involve the formation of soluble species. Figure 37 shows the IR spectrum of a discharged electrode taken by pulverizing the sample

TABLE 11. ELEMENTAL ANALYSIS OF DISCHARGED AND UNDISCHARGED CARBON POSITIVE ELECTRODES

Sample	Li, g	Al, g**	Cl, g**	S, g	Weight Gain, g
Undischarged Carbon Electrode	0.045	0.16	0.90	0.020	1.24
Discharged* Carbon Electrode	0.15	0.25	1.25	0.36	2.49

* = Cell #652, 390 mAh discharge

** = The results shown are the averages of XRF and AA analyses

TABLE 12. CALCULATED WEIGHT DISTRIBUTION OF THE UNDISCHARGED CARBON POSITIVE ELECTRODE

Sample	Li, g	Al, g	Cl, g	S, g
Undischarged Carbon with 1.24g weight gain	0.047	0.18	0.97	--

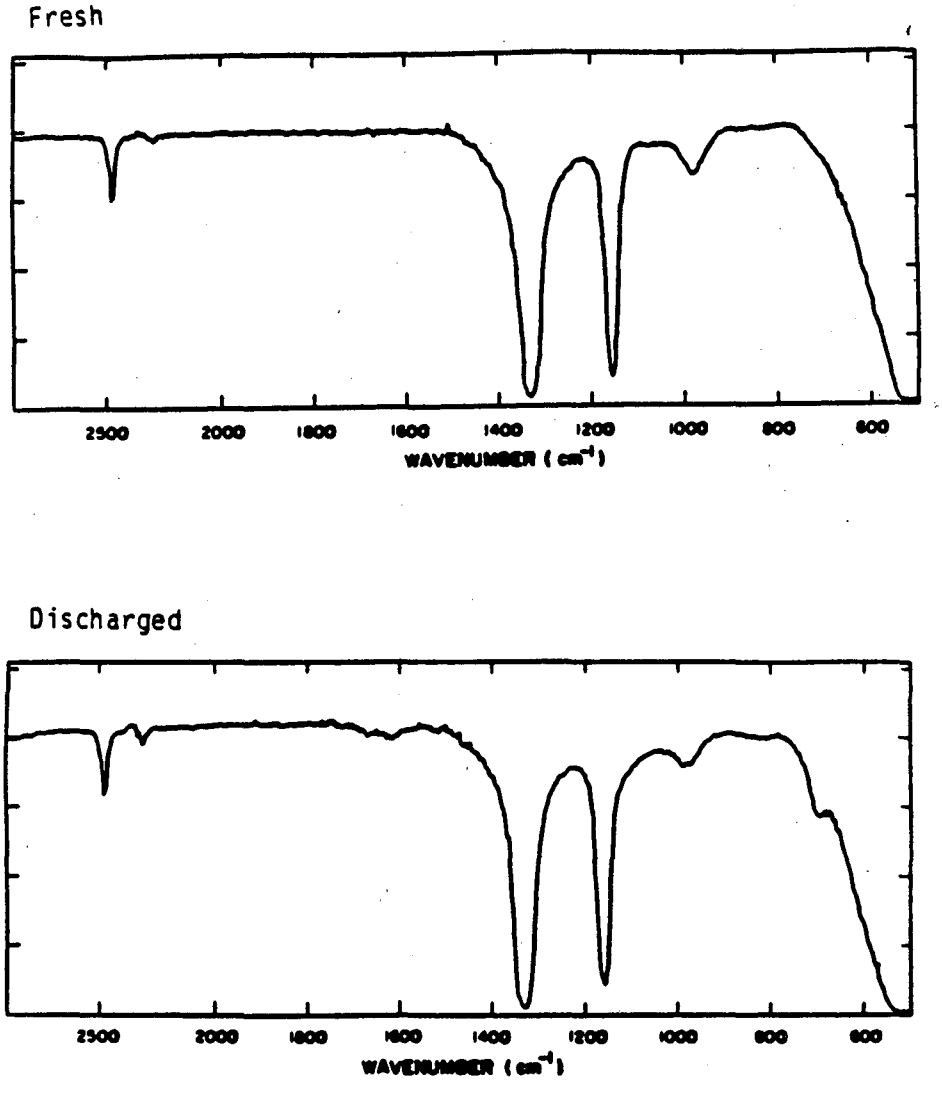

FIGURE 36. IR Spectra of Fresh and Discharged $LiAlCl_4$-$3SO_2$ Electrolyte Samples.

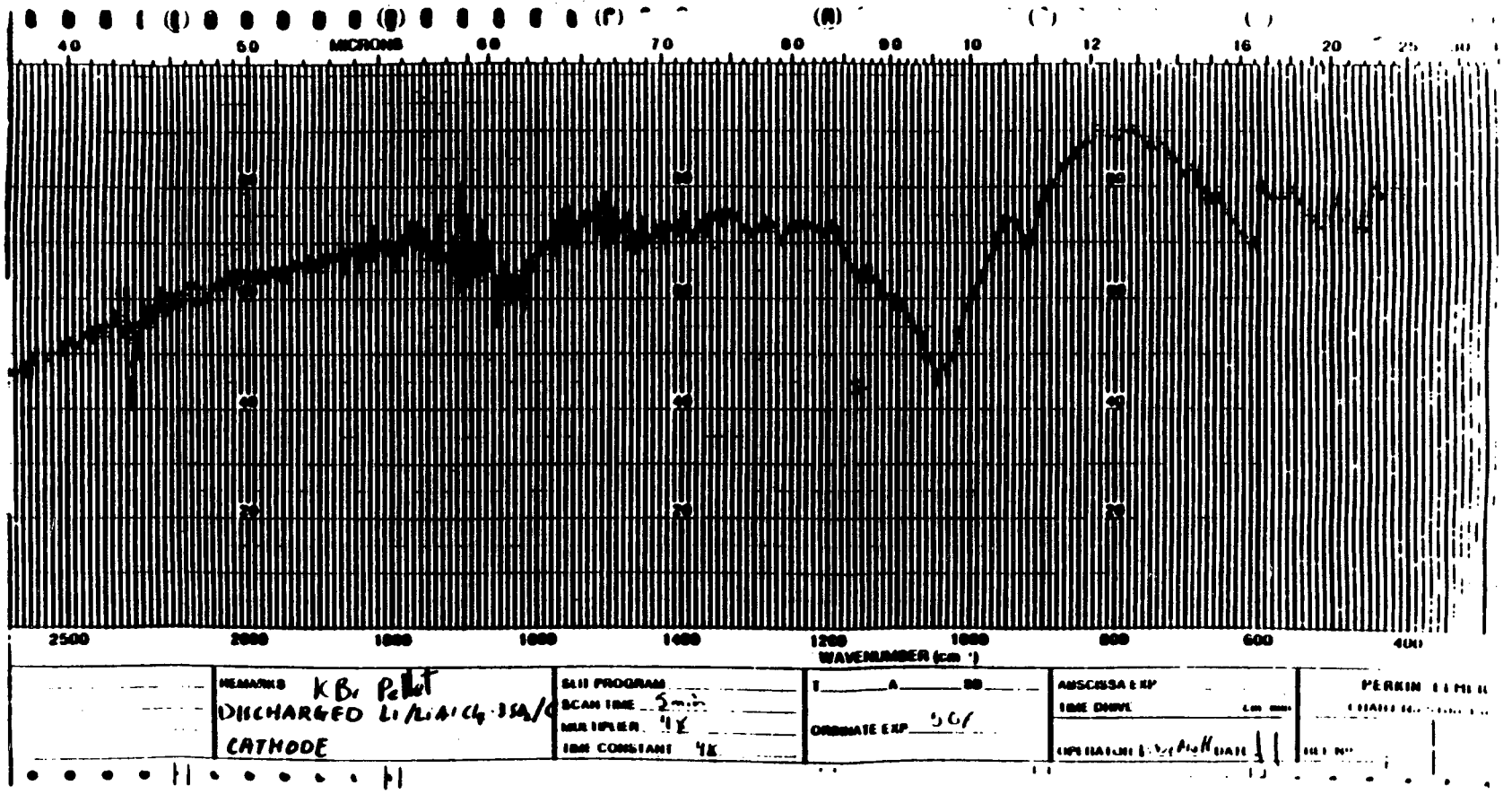

FIGURE 37. IR Spectrum of a Carbon Electrode After Discharge in $LiAlCl_4$-$3SO_2$ Electrolyte.

with KBr powder. Two peaks, 1040 cm^{-1} and 920 cm^{-1}, are located in the sulfur-oxygen vibration region. IR spectra of inorganic anions are strongly affected by the coupling cations and the crystal structures. Figure 38 shows the spectra of $Li_2S_2O_4$ and $Na_2S_2O_4$. Note that $Li_2S_2O_4$ spectrum displays an extra peak at 1070 cm^{-1}. These results indicate that the sulfur oxygen species in the positive electrode has vibration energy very similar to those of dithionites, but not $Li_2S_2O_4$.

d. ESCA Analysis

X-ray Photoelectron Spectroscopic Analysis was carried out on a positive electrode discharged to a 3.0 V cutoff. Figure 39 shows the complete scan and Figure 40 shows the expanded spectrum of the sulfur 2p electron region. The sulfur 2p electron binding energy references are listed in Table 13. The sulfur binding energy, -167.2 EV, of the sample does not belong to either sulfide or elemental sulfur which is confined to an area between -160 to -165 EV. It actually falls into the region between +2 and +4 oxidation states, of sulfur indicating that the oxidation state of sulfur may be +3. Unfortunately the exact identification of the oxidation state of sulfur is not possible because the binding energies of the these three oxidations are somewhat mixed together.

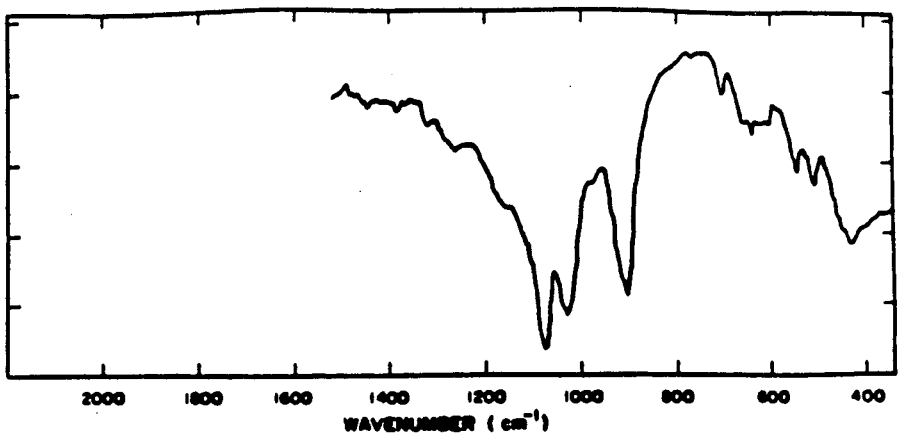

Infrared spectrum of $Li_2S_2O_4$.

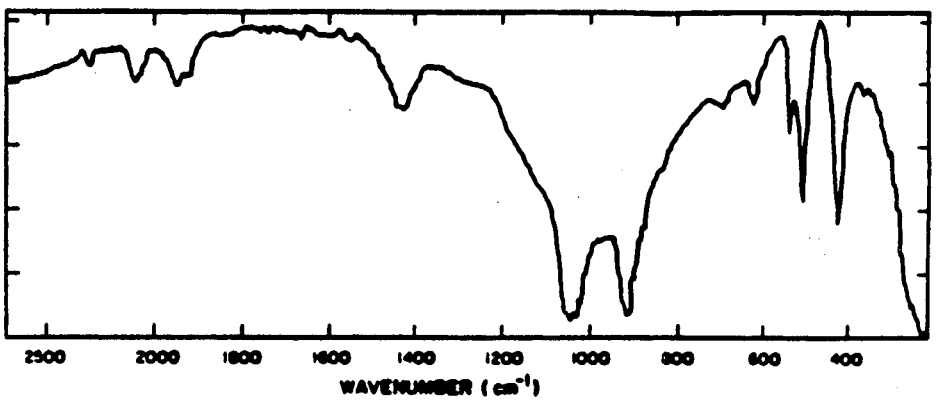

Infrared spectrum of $Na_2S_2O_4$.

FIGURE 38. IR Spectra of $Li_2S_2O_4$ and $Na_2S_2O_4$.

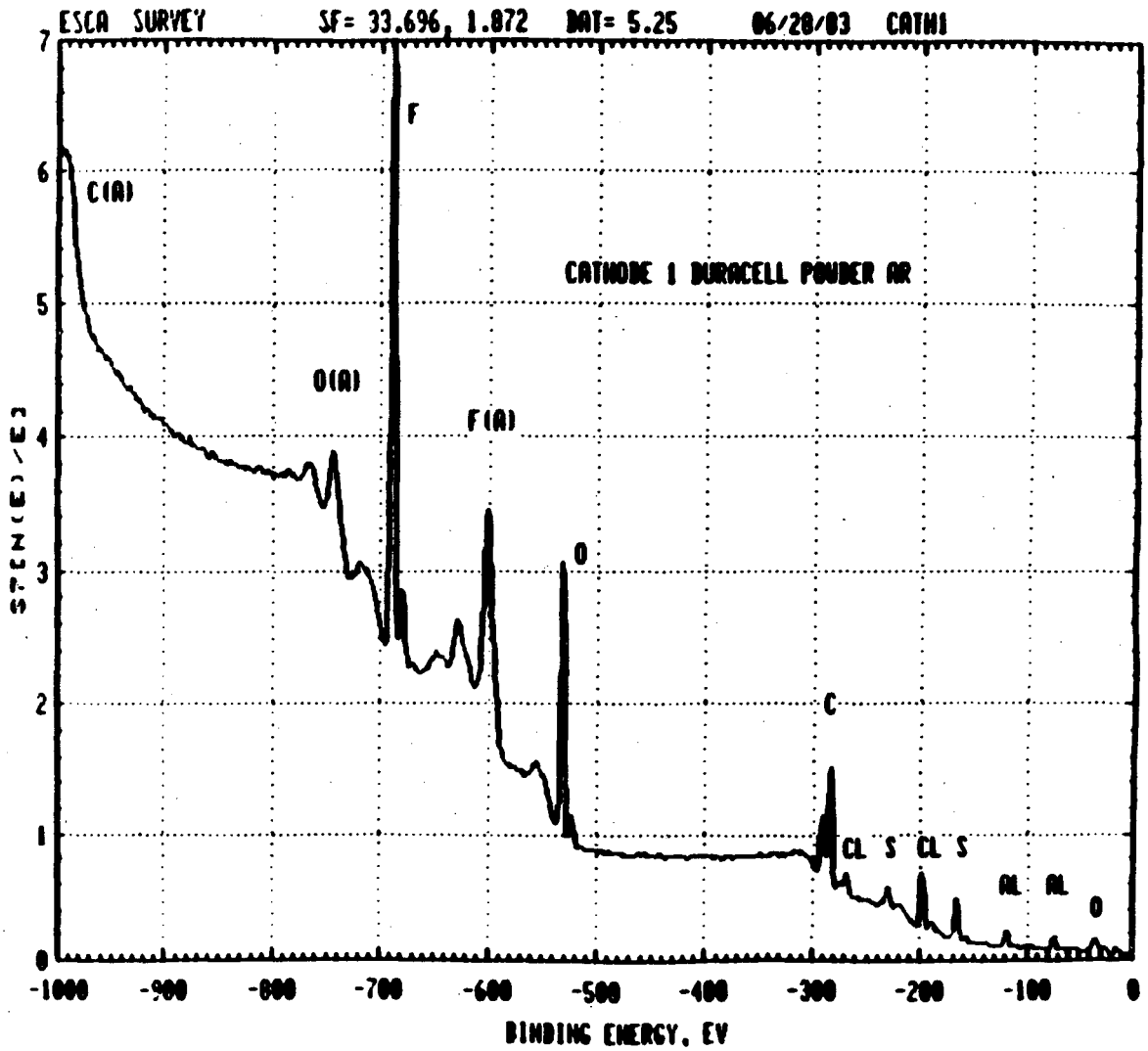

Figure 39. X-Ray Photoelectron Spectroscopic Scan of a Carbon Electrode After Being Discharged to 3.0V in $LiAlCl_4$-$3SO_2$ Electrolyte

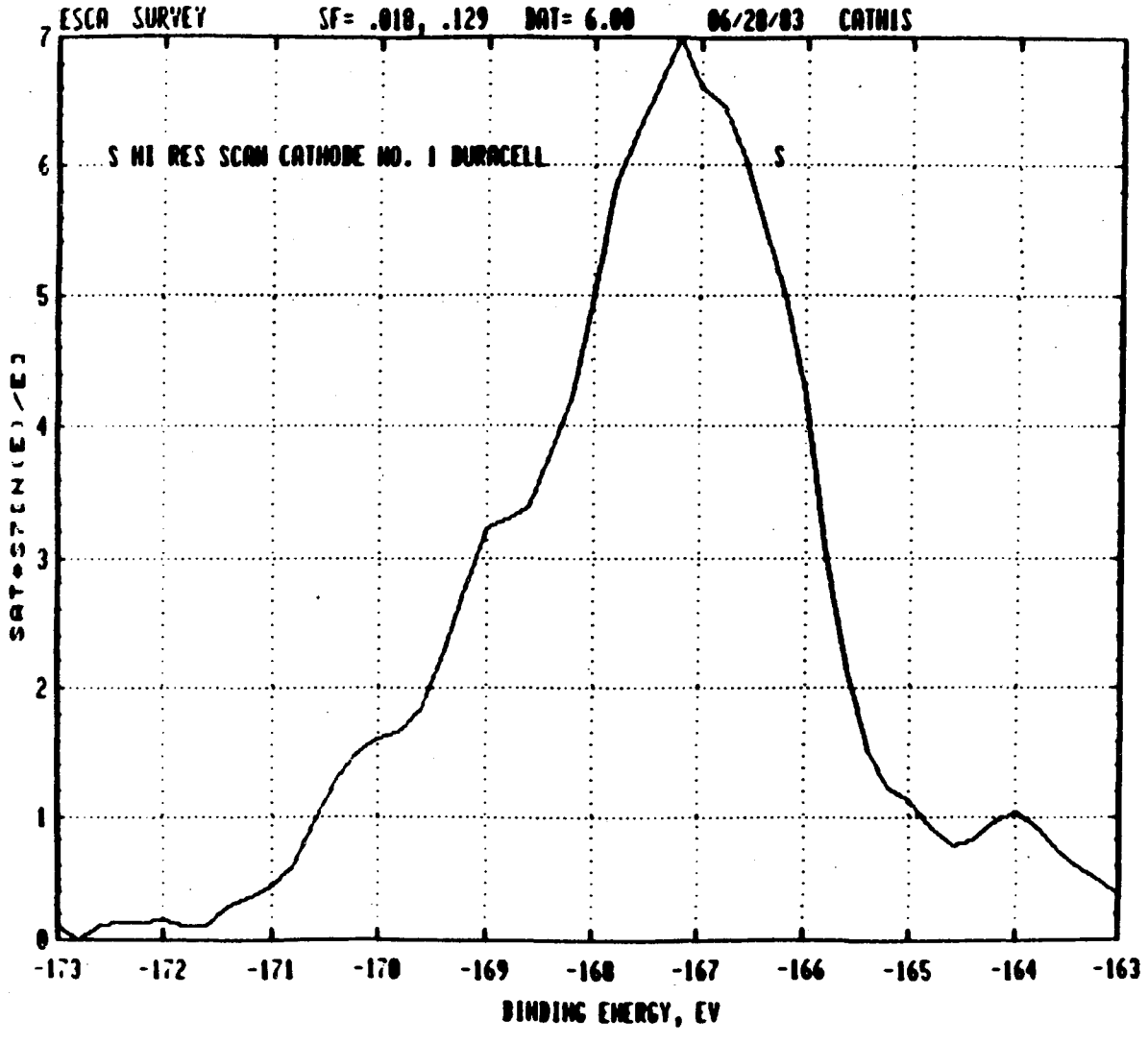

FIGURE 40. Expanded X-ray Photoelectron Spectrum of the Sulfur 2p Electron Region.

Sulfur, S Atomic Number 16

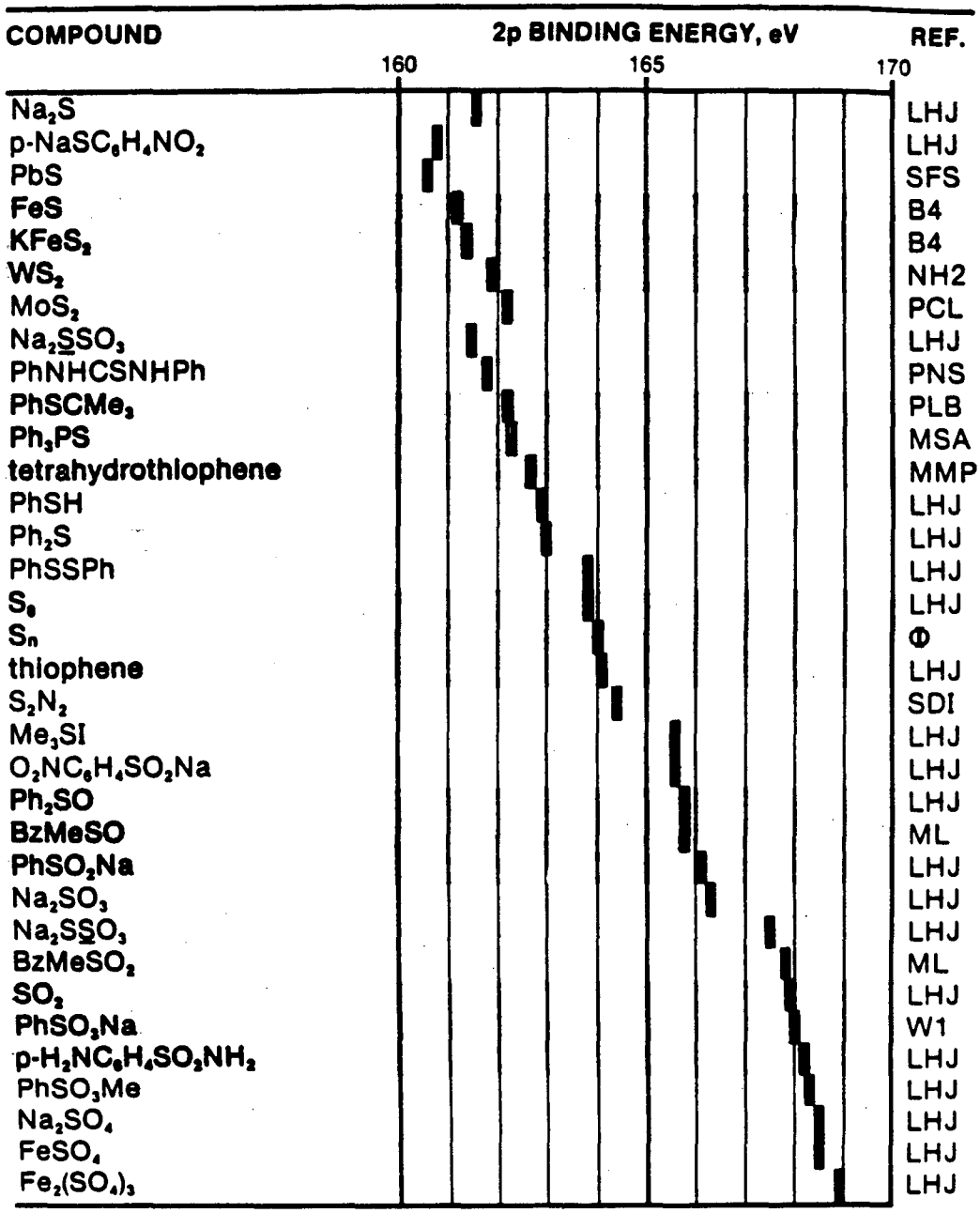

TABLE 13. Sulfur 2P Binding Energy Reference Table

e. Aqueous Wet Chemical Analysis :

Additional experiments were carried out to identify the decomposition products derived from the discharged positive electrode.

Experiment 1.- Leaching the Positive Electrode in Aqueous Ammonium Buffer Solution

Bleaching of $Cu(NH_3)_4^{+2}$ complex in pH=10 buffer is a selective indicator for dithionites (S^{-2} may interfere by precipitating black CuS). Direct reaction of a positive electrode discharged to 2.6V with this indicator for 4 hrs under argon atmosphere did not bleach the blue complex. However it is possible that the species may be buried inside the carbon and the aqueous buffer may not wet the carbon electrode well enough to leach the species.

Experiment 2. - Leaching in Aqueous Ammonium Buffer Solution after Pulverizing

A positive electrode discharged to 3.0 V was immediately pulverized at liquid nitrogen temperature under argon to prevent sample decomposition. The resultant powder was then leached in pH = 10 buffer. The leachate bleached $Cu(NH_3)_4^{+2}$ complex with large

amount of black precipitation (suspected to be CuS). Quantitative analyses for both S^{-2} and $S_2O_4^{-2}$ were performed by precipitating S^{-2} from the leachate with Cd^{+2}. The precipitate was filtered and collected for sulfide determination by oxidizing it with peroxide to sulfate and weighing it in the form of $BaSO_4$. The dithionite content in the filtrate was determined by reaction with $Ag(NH_3)_2^+$ complex (selective oxidizing agent for dithionites). The results are shown in Table 14. The recovery is 54% of the theoretical values. The 46% loss may be due to the difficulty in leaching those trapped deeply inside the carbon black.

Experiment 3. - Leaching in Water Followed by Hot 2N HCl.

Two positive electrode discharged to 2.6 V were leached with water followed by hot 2N HCl. Elemental sulfur precipitated as anticipated. Quantitative results are listed in Table 15. Since it was not possible to determine the S^{-2} quantitatively in this experiment, the recovery could not be calculated.

Experiment 4. - Conformation of Dithionite Using Differential Pulse polarographic Technique.

In addition to Experiment 2, a differential pulse polarographic technique was developed to identify and determine

TABLE 14. CHEMICAL ANALYSES OF S^{-2} AND $S_2O_4^{-2}$ IN DISCHARGED CARBON POSITIVE ELECTRODE

Sample Cell #	mAh Discharge	S^{-2} Found mg	$S_2O_4^{-2}$ mg	Theoretical* S^{-2}, mg	Theoretical* $S_2O_4^{-2}$, mg
747	385	24	210	76	910

* = Theoretical values are calculated by assuming the entire discharge product is converted into either S^{-2} or $S_2O_4^{-2}$ respectively.

TABLE 15. ELEMENTAL SULFUR ANALYSIS OF THE ACID LEACHED DISCHARGED CARBON POSITIVE ELECTRODE

Cell #	mAh Discharge	Elemental Sulfur Found, mg	Theoretical Amount of Sulfur, mg
1	392	28	114
2	408	32	119

quantitatively the amounts of sulfide and dithionite simultaneously. A positive electrode discharged to 2.6 V with 440 mAh capacity was pulverized at liquid nitrogen temperature under argon. The pH=10 buffer extract of the powder was analyzed polarographically and found to contain 215 mg dithionite and 12 mg sulfide, which are much less than the expected values based on the reaction to be discussed later.

2. Discharge Reaction and Discussion.

Koslowski [10] found that the presence of aromatics in $LiAlCl_4$-$3SO_2$ increased the conductivity of the solution and proposed the following species to be responsible for the above:

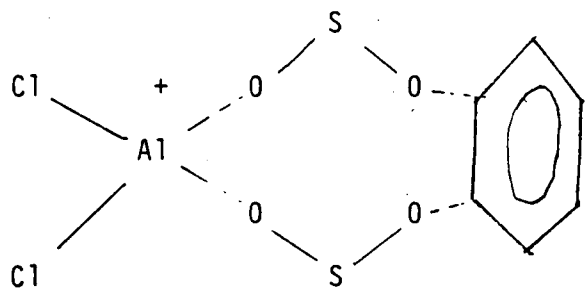

Since carbon black has a conjugated double bond structure similar to that of the aromatics, we propose the following reactions to account for all the experimental results obtained.

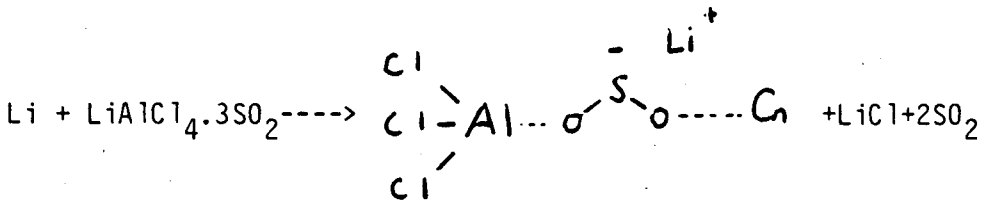

(IV-1)

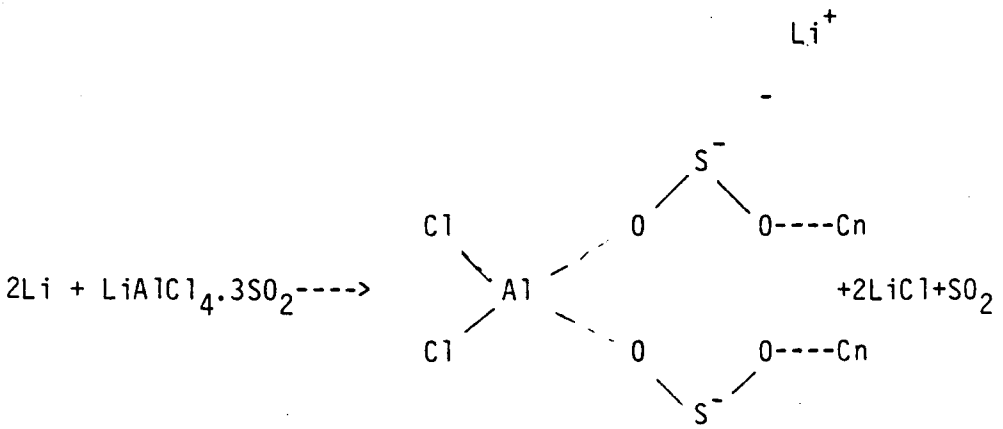

(IV-2)

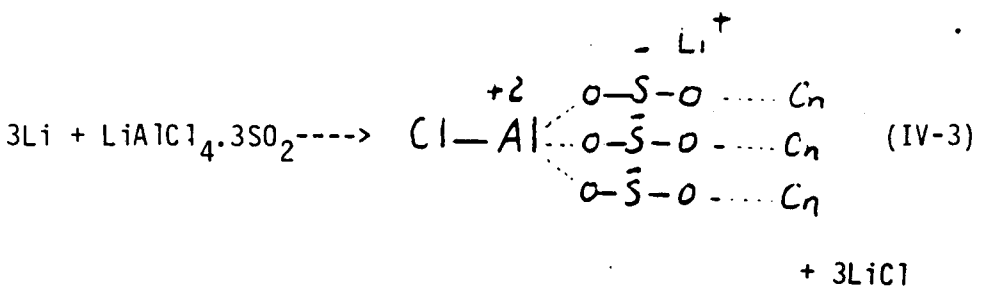

(IV-3)

where Cn = Carbon Structure

An important implication behind these proposed cell reactions is that large molecules are fixed and LiCl is precipitated in the positive electrode during discharge. This means the cathode should gain substantial weight during discharge as was found to be the case.

The weight of LiCl obtained from chemical analysis is enough to account for only a fraction of the total weight gain. The fact that large amounts of Al, S, Cl and possibly Li containing molecules are not detected by XRD indicates that the products must be present in totally amorphous forms. This is reasonable if the the proposed reaction products are actually formed on the carbon structure which is amorphous to begin with.

The electrolyte salt, $LiAlCl_4$ is detected in the undischarged carbon electrode but not in the discharged electrode. The discharged products must occupy most of the pore volumes and do not allow much electrolyte to be adsorbed. This implies that the carbon volume should be one of the capacity limiting factors. Additional tests with experimental cells with excess electrolyte has confirmed this. As shown in Figure 41, the capacity delivered is proportional to the amount of carbon.

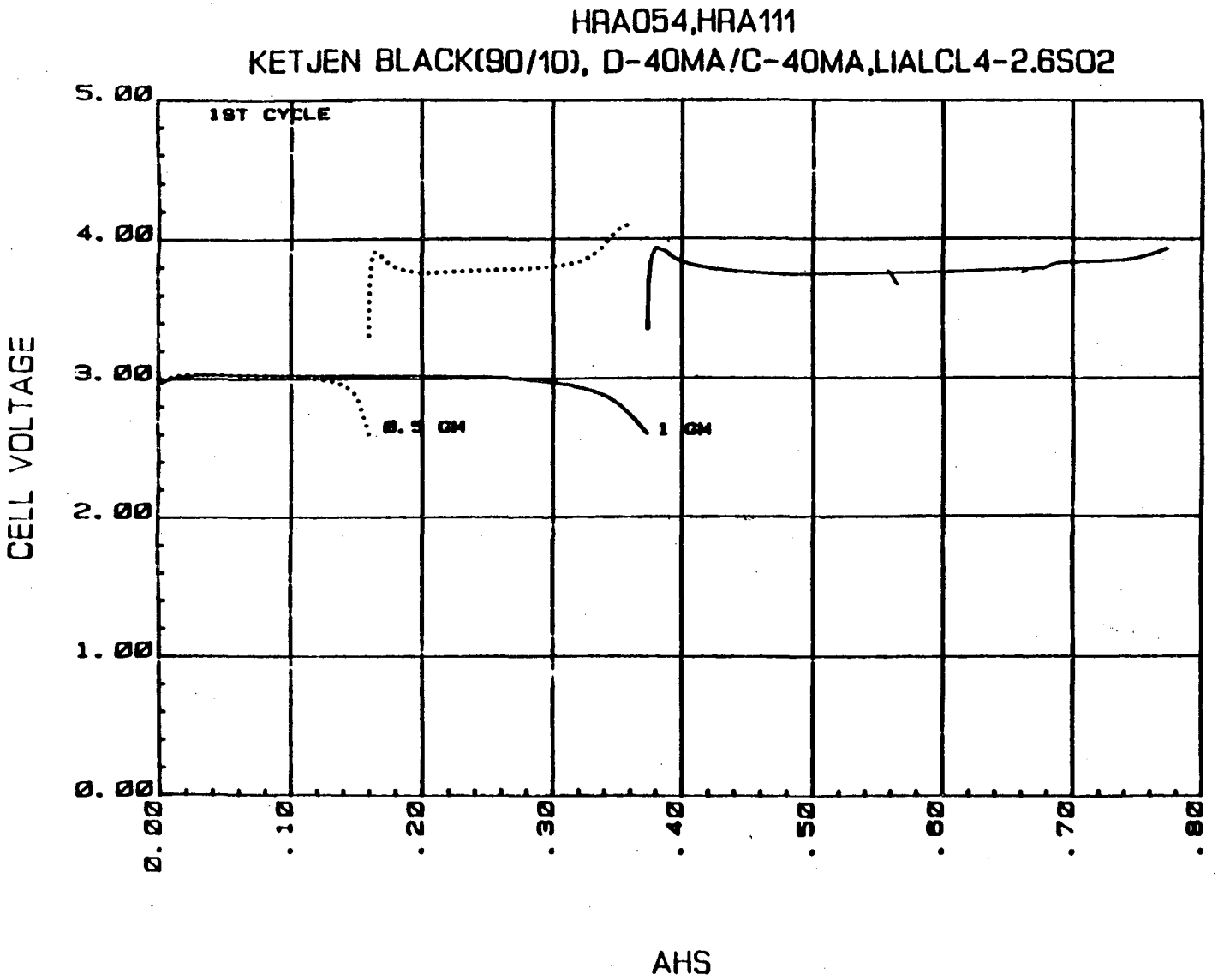

FIGURE 41. Effect of the Amount of Carbon on the Capacity Delivered in $LiAlCl_4$-$3SO_2$ Electrolyte.

The fact that the IR spectrum of the discharged carbon electrode is not identical to that of $Li_2S_2O_4$ is because the species proposed, Al---O-S-O---Cn, may have the same +3 sulfur oxidation state as dithionite, but is totally different from it structurally.

Carbon black is a good IR light scatterer. If an IR active species is buried inside the carbon structure, it will not be detected. The facts that the electrode spectrum had to be taken with pulverization (peaks were not detectable when the spectrum was taken directly) and that the absorption peaks were observed only at a large scale expansion imply that the compounds are buried inside the carbon structure.

Table 16 shows the theoretical elemental weight distribution and the total weight gain for all three proposed positive electrode reactions based on 390 mAh discharge as well as the experimental results of the above parameters. Comparison of the theoretical calculations with the experimental results indicates Reaction [IV-2] as being the most likely reaction occurring. Reaction (IV-3) is very unlikely since it would be sterically difficult to have the carbons in the right position for one Al atom. Slightly higher Al and Cl analytical results may be caused by residual electrolyte and the same is also true for the total weight gain results. However, the possibility of a mixed discharge between all three reactions should not be eliminated.

TABLE 16. ELEMENTAL WEIGHT DISTRIBUTION AND THE WEIGHT GAIN OF THE DISCHARGED CATHODE*

Theoretical based on	Li, g	Al, g	Cl, g	S, g	Theoretical Weight Gain g
Reaction [IV-1]	.20	.39	2.02	.46	3.52
Reaction [IV-2]	.15	.195	1.02	0.46	2.28
Reaction [IV-3]	.13	.13	.68	.46	1.85
Experimental	0.15	0.25	1.25	0.36	2.49

* = The calculation is based on 390 mAh discharge

Dithionites have very interesting aqueous chemistry [15]. $S_2O_4^{-2}$ is stable at pH=10. In alkaline medium the following reaction is expected to occur

$$3S_2O_4^{-2} + 6OH^- \text{-----} S^{-2} + 5SO_3^{-2} + 3H_2O \quad [IV\text{-}4]$$

In acidic medium the following reactions are expected to occur:

$$S_2O_4^{2-} + H_2O \text{--------} > S_2O_3^{-2} + 2HSO_3^- \quad [IV\text{-}5]$$

or $$2S_2O_4^{2-} \text{------} > S_2O_3^{-2} + SO_3^{-2} + SO_2 \quad [IV\text{-}6]$$

$$2H^+ + S_2O_3^{2-} \text{------} > S + SO_2 + H_2O \quad [IV\text{-}7]$$

Similar chemistry is expected to occur from the proposed reaction product:

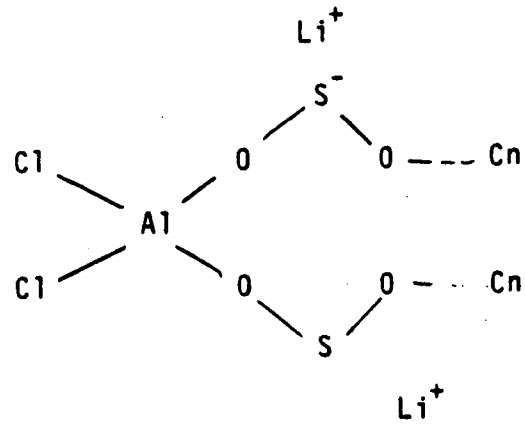

Because of the high affinity of Al toward oxygen, SO_2^- is probably not stable without attaching to the carbon. Under certain circumstances, one of the SO_2^- with Li^+ adjacent to it may be removed as $LiSO_2$. and the other may have to give up the oxygen and leave. In pH=10 buffer, part of the SO_2^- may be released as $LiSO_2$ followed by dimerization :

$$2LiSO_2 \text{--------} Li_2S_2O_4 \qquad [IV\text{-}8]$$

and part of it may be released and disproportionate into sulfide. In acidic medium, $S_2O_4^{-2}$ formed is not stable and should decompose according to Reactions [IV-4] to [IV-6] and generate elemental sulfur. In alkaline medium, the product should be sulfide according to Reaction [IV-4]. All of these agree qualitatively with the results of the Wet Chemical Analysis.

The proposed mechanism suggests that the discharge capacity is probably limited by the combination of the surface area and pore volume of the carbon electrode. The former is needed for the attachment of the discharge product and the latter is needed to contain the bulky products.

D. CELL PERFORMANCE AND DISCUSSION

1. Experimental Cells

a. Effect of Carbon Material

The primary capacity of the Li/Carbon system with $LiAlCl_4$-SO_2 electrolyte depends strongly on the type of carbon employed for the positive electrode. Early work with positive electrode made with Shawinigan carbon showed very poor capacity utilization. Several different carbon materials were evaluated using experimental cells. Although all carbon positive electrodes showed a flat discharge voltage near 3.1-3.2V as exhibited in Figure 35 for the cell made with a Ketjenblack positive electrode, the capacities delivered were significantly different. Table 17 compares the capacity utilization of the positive electrodes made from different carbon materials. Electrodes made with Ketjen black EC, carbon B and carbon C delivered significantly more capacity both gravimetrically and volumetrically than the cells made with other carbon materials. These carbon materials have considerably higher values of both BET surface area and pore volume(DBP adsorption) comparing with the values of other carbons as shown in Table 18. Cells made with graphitized Shawinigan Black and Ketjen black, which should have significant lower surface area and pore volume due to recrystallization of the structure, showed considerable reduction of

TABLE 17. CAPACITY UTILIZATION OF POSITIVE ELECTRODES MADE FROM VARIOUS CARBON MATERIALS (discharged at 1 mA/cm^2 to 2.6V cutoff)

Carbon Material	Composition Wt%(carbon/PTFE)	Capacity Utilization Ah/g	Ah/cc
Shawinigan Black	90/10	0.35	0.146
Graphitized Shawinigan Black	90/10	0.10	0.096
Graphite(KS-2)	90/10	0.13	0.200
Coconut Charcoal	90/10	0.06	0.039
Ketjenblack EC	90/10	0.48	0.289
Graphitized Ketjenblack EC	90/10	0.21	0.146
Carbon A	90/10	0.14	0.183
Carbon B	90/10	0.434	0.247
Carbon C	90/10	0.473	0.254

TABLE 18. SURFACE AREA AND DBP ADSORPTION (PORE VOLUME) OF VARIOUS CARBON

CARBON	BET SURFACE AREA (M^2/G)	DBP ADSORPTION (CC/100GM)
Ketjenblack EC (Noury)	950	360
Carbon C	1060	335
Carbon B	1125	--
Carbon A	250	180
Shawinigan Black (Shawinigan)	60	250
KS-2 Graphite (Lonza)	22	--

the capacity utilization (Table 18) compared with cells made from corresponding un-graphitized carbon. It is likely that high surface area and high pore volume are necessary for good electrode utilization. The result is consistent with our proposed reaction mechanism for the positive electrode.

b. Cycling Performance

The cycling performances of carbon positive electrodes made from both Lonza KS-2 graphite and Ketjenblack EC were evaluated in the experimental cells. Figure 42 shows the typical voltage profiles at selected cycles of a pressed graphite positive electrode (90wt% KS-2 graphite, 10wt% PTFE) discharged at 2 mA/cm^2 and charged at 1 mA/cm^2. The cell was filled with $LiAlCl_4$-$3SO_2$ electrolyte. Figure 43 shows the capacity delivered to 2.6 V cutoff vs cycles. The cell operated for 130 cycles and failed due to the development of internal shorts. The positive electrode was able to hold its original capacity without fading.

Figures 44 and 45 show the typical voltage profiles and the capacity delivered on cycling of a cell with a 0.5 gm Ketjenblack positive electrode discharged at 3 mA/cm^2 and charged at 1.5 mA/cm^2. The cell operated for 120 cycles without showing any capacity loss and failed due to developing internal shorts.

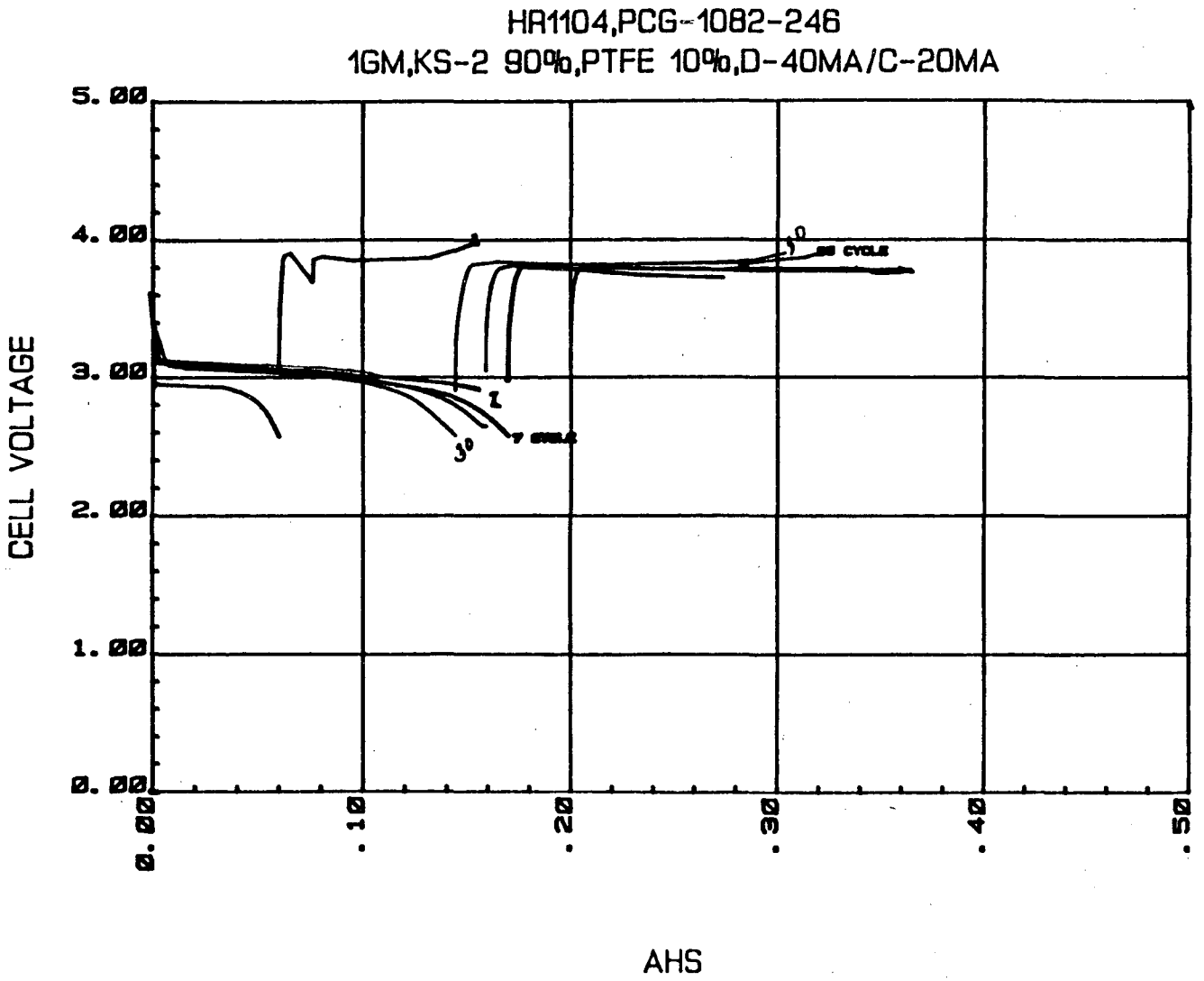

FIGURE 42. Voltage Profile of the KS-2 Graphite Positive Electrode in $LiAlCl_4$-$3SO_2$ Electrolyte at the Selected Cycles.

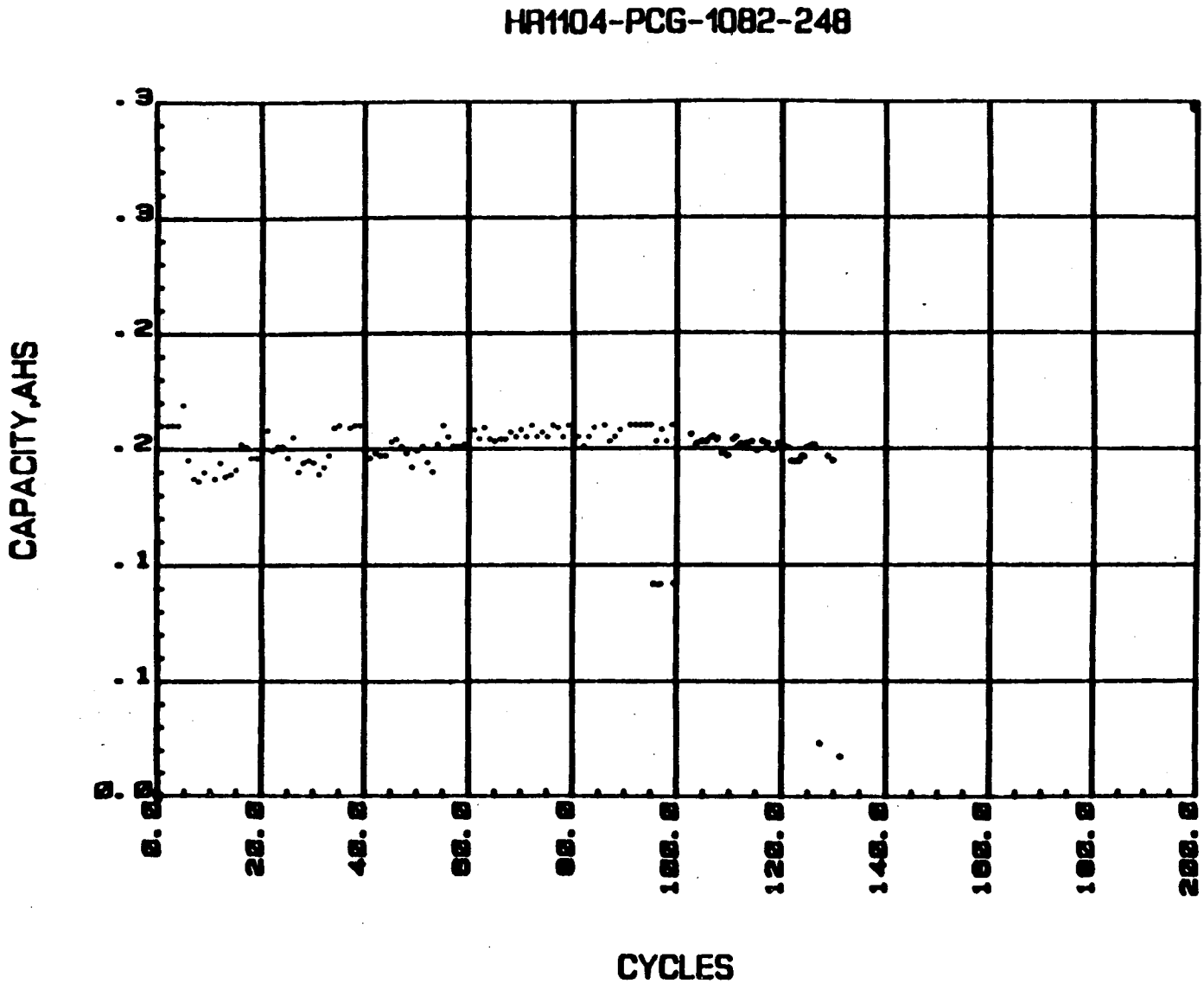

FIGURE 43. Cycling Performance of an Experimental Cell with Graphite Positive Electrode (KS-2 90%, PTFE 10%) and $LiAlCl_4$-$3SO_2$ Electrolyte, Discharged at 2 mA/cm^2 and Charged at 1 mA/cm^2.

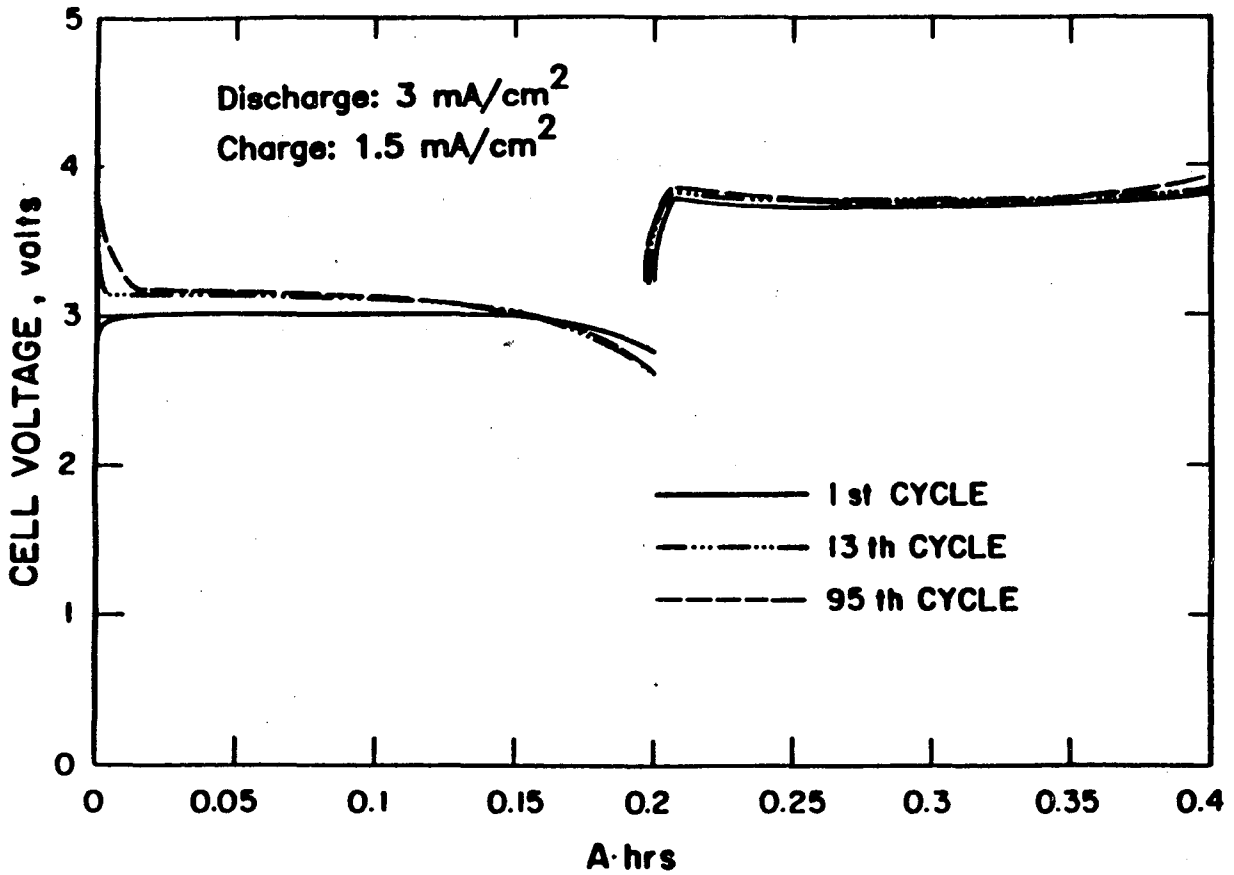

FIGURE 44. Discharge / Charge Voltages of an Experimental Cell having Ketjen Black EC Carbon Positive Electrode (10% PTFE) and $LiAlCl_4$-$3SO_2$ Electrolyte Discharged at 3 mA/cm^2 and Charged at 1.5 mA/cm^2.

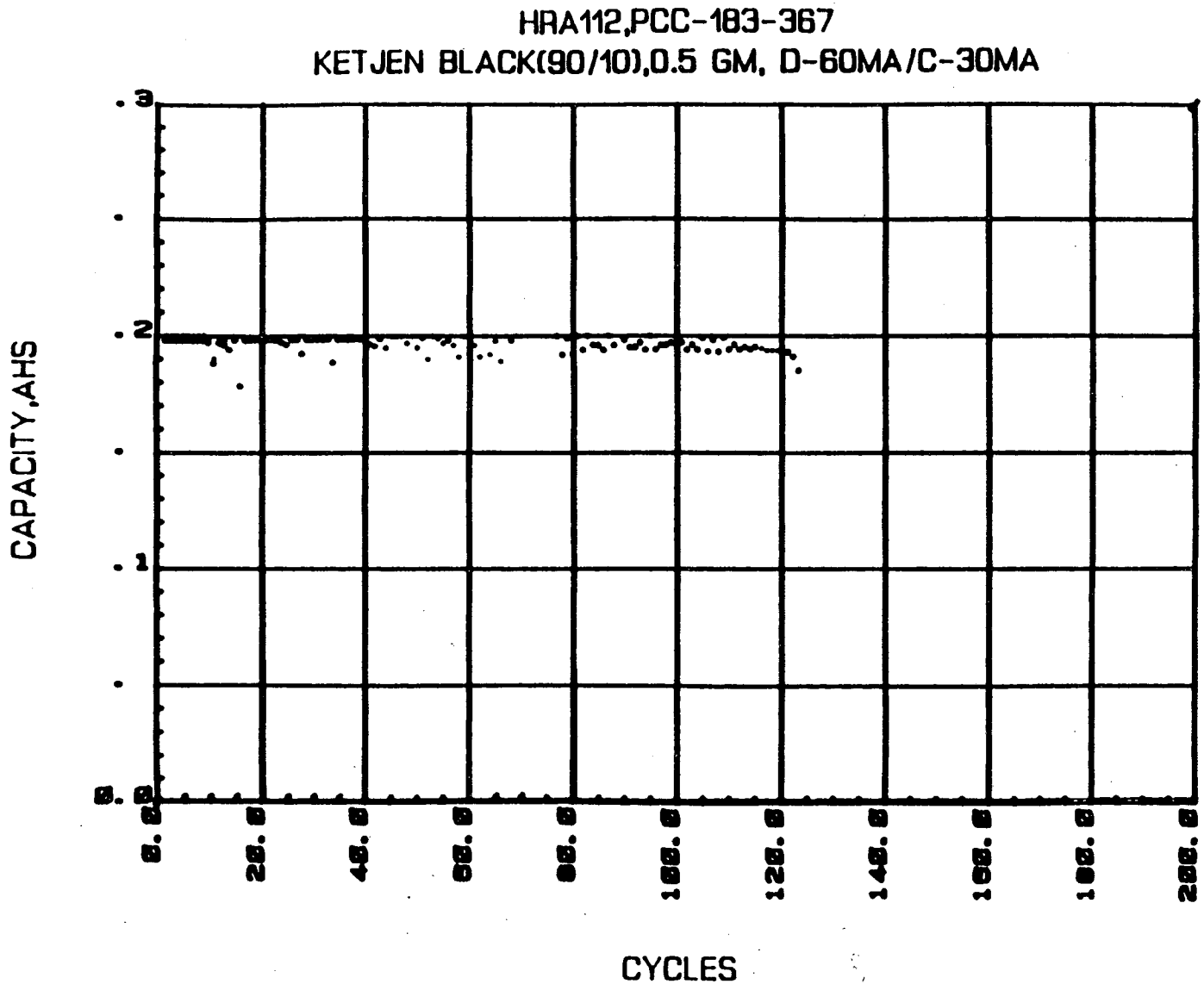

Figure 45. Cycling Performance of an Experimental Cell having Ketjen Black EC Carbon Positive Electrode (10% PTFE) and $LiAlCl_4$-$3SO_2$ Electrolyte Discharged at 2 mA/cm^2 to Various Depths and Charged at 1 mA/cm^2. (Positive Electrode Thickness: 15 mils)

Many additional experimental cells with Ketjenblack positive electrodes were made and evaluated at rates from 0.5 mA/cm^2 to 4 mA/cm^2. Most cells were able to operate for 100-200 cycles without showing capacity fading. However, none of the cells had been cycled for over 200 cycles on deep discharge to 2.6 V. due to either development of internal shorts or malfunction of the computer controlled testing system. Some cells cycled at 25% and 50% depths have been operated for 300-400 cycles as exhibited in Figure 46. The cells were made with rolled Ketjenblack EC positive electrode of 15 mil thickness and filled with $LiAlCl_4$-$6SO_2$ electrolyte.

c. Shelf Life

Figure 47 shows the discharge performance of 2 experimental cells containing positive electrodes made from Ketjenblack carbon (80wt%) and filled with $LiAlCl_4$-$3SO_2$ electrolyte after 7 months storage at ambient temperature. The discharge/charge voltage profiles of a fresh cell from the same batch is also shown in the figure for comparison. No capacity loss is observed after the storage and the system has very good charge retention.

2. Prototype Wound Cells

2/3 A size prototype cells with a wound electrode design were made for evaluation. The cell normally consists of a roll pressed

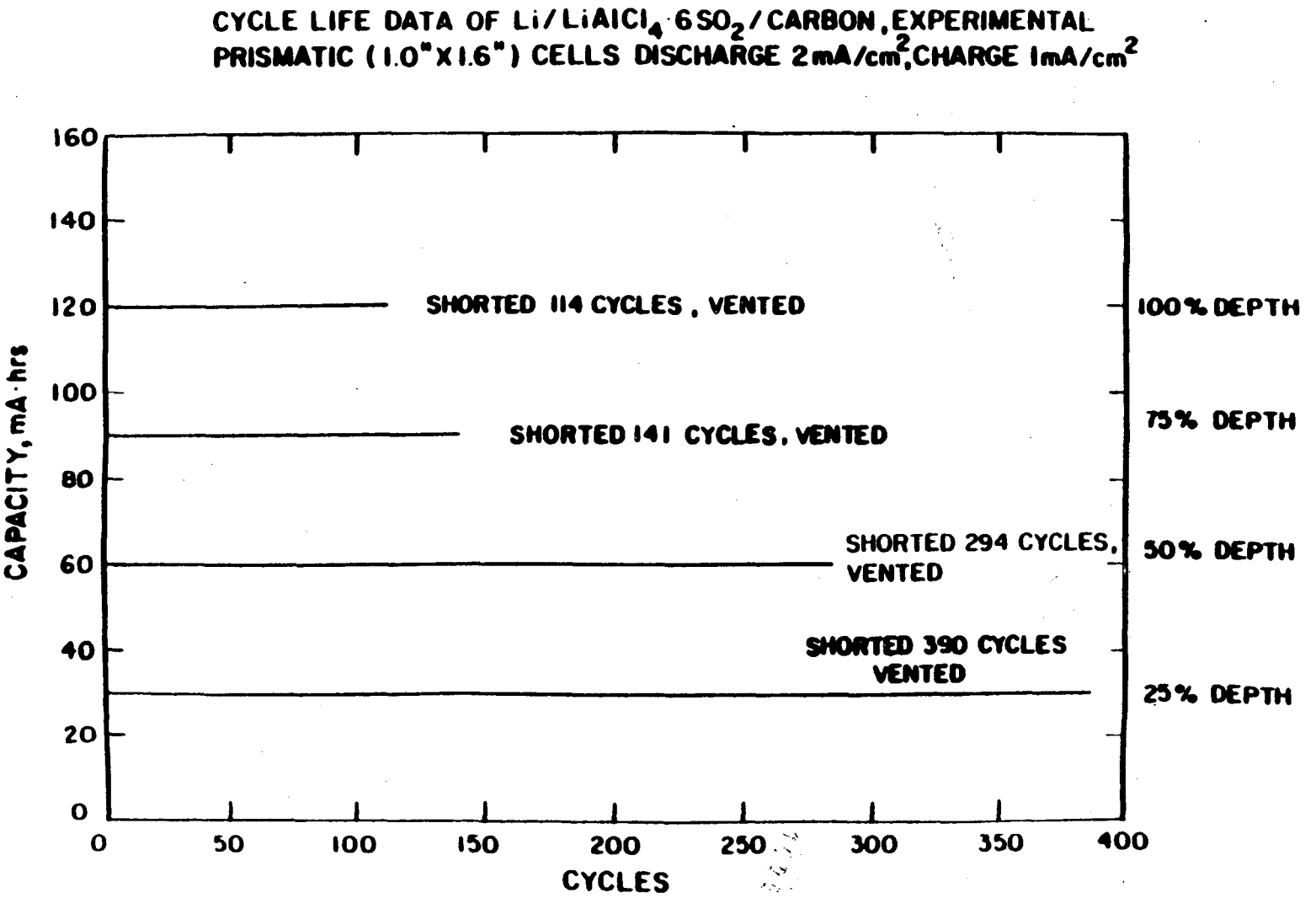

Figure 46. Cycling Performance of Experimental Cells Having Rolled Ketjen Black EC Carbon Positive Electrode (10% PTFE) and $LiAlCl_4$-$3SO_2$ Electrolyte Discharged at 2 mA/cm^2 to Various Depths and Charged at 1 mA/cm^2. (Positive Electrode Thickness: 15 mils)

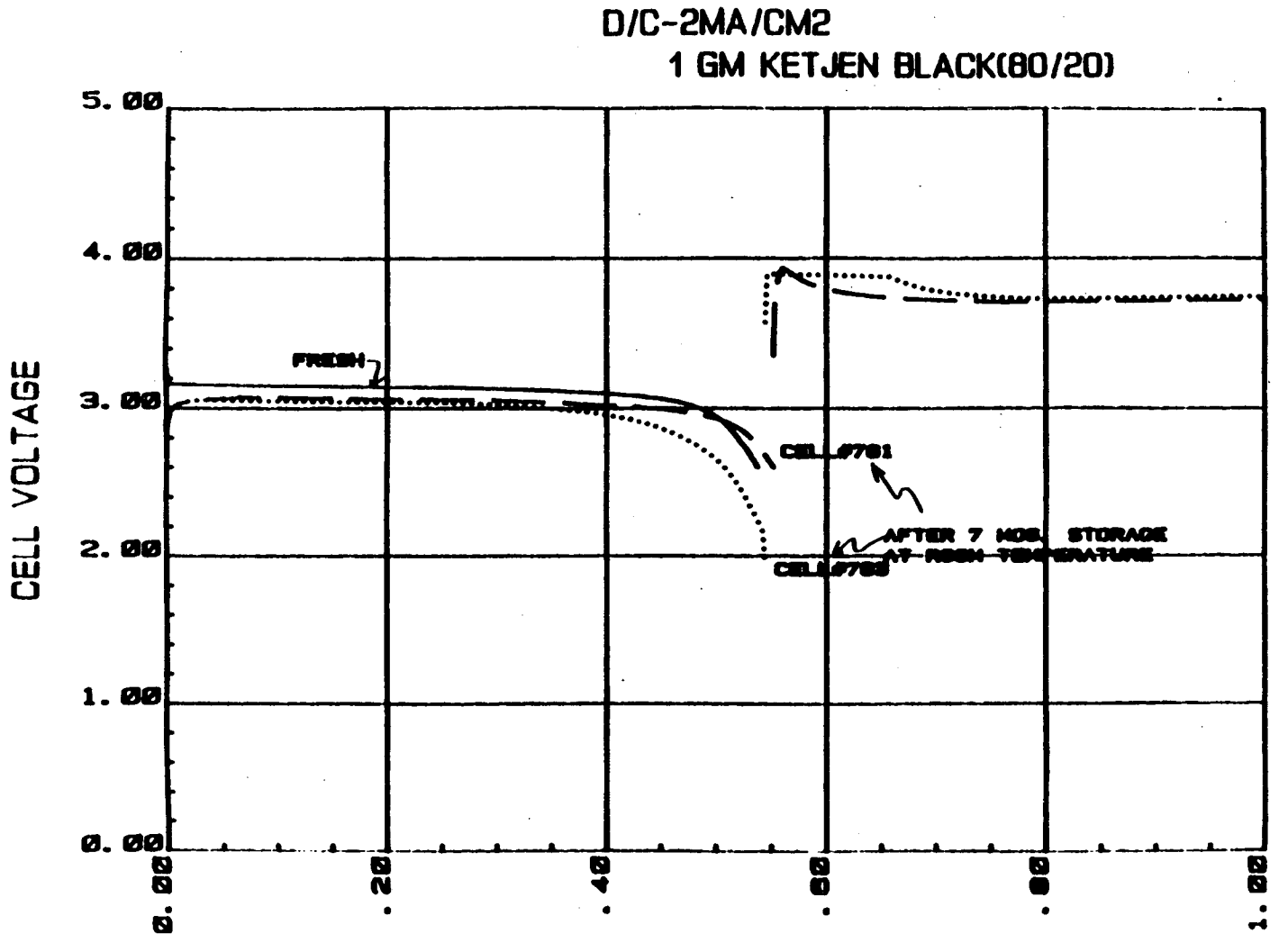

FIGURE 47. Discharge Performance of Experimental Cells Having Ketjen Black Carbon Electrodes after Seven Months Storage at Ambient Temperature.

carbon electrode and a lithium electrode. Ketjenblack EC carbon was used in making the prototype wound cells since it provided the best volumetric capacity among the carbon materials being evaluated. The positive electrode had a composition of 90wt% carbon and 10wt% PTFE with dimensions of 15 mil in thickness, 6 inches in length and 0.75 inch in width. The lithium electrode was made by pressing 5 mil lithium foil on both sides of a copper foil. The dimensions of the lithium electrode were 6.5 inches in length and 0.65 or 0.7 inch in width. Celgard 3401 or K-857 was used as the separator. Cells with other separator materials were also made for evaluation. Most cells were filled with $LiAlCl_4$-$6SO_2$ electrolyte since it provided better low temperature performance.

a. Capacity and Rate Capability

Figure 48 shows the primary discharge voltage profiles at various rates of a batch of cells made with K-857 separator. The cell delivered about 0.36 Ah to 2.0V cut off at 50 mA rate (C/8 rate). The energy density is only about 90 Wh/kg. Since the 2/3A size cell package is not very efficient volumetrically or gravimetrically, the energy density can be improved significantly when scaled-up to larger size cells. Figure 49 shows the polarization of a cell measured at various rates. The cell is able to provide a voltage above 2.0 V even at 2 Amp rate (4C rate). Figure 50 shows a cell discharged at -30°C at 200 mA rate (C/2).

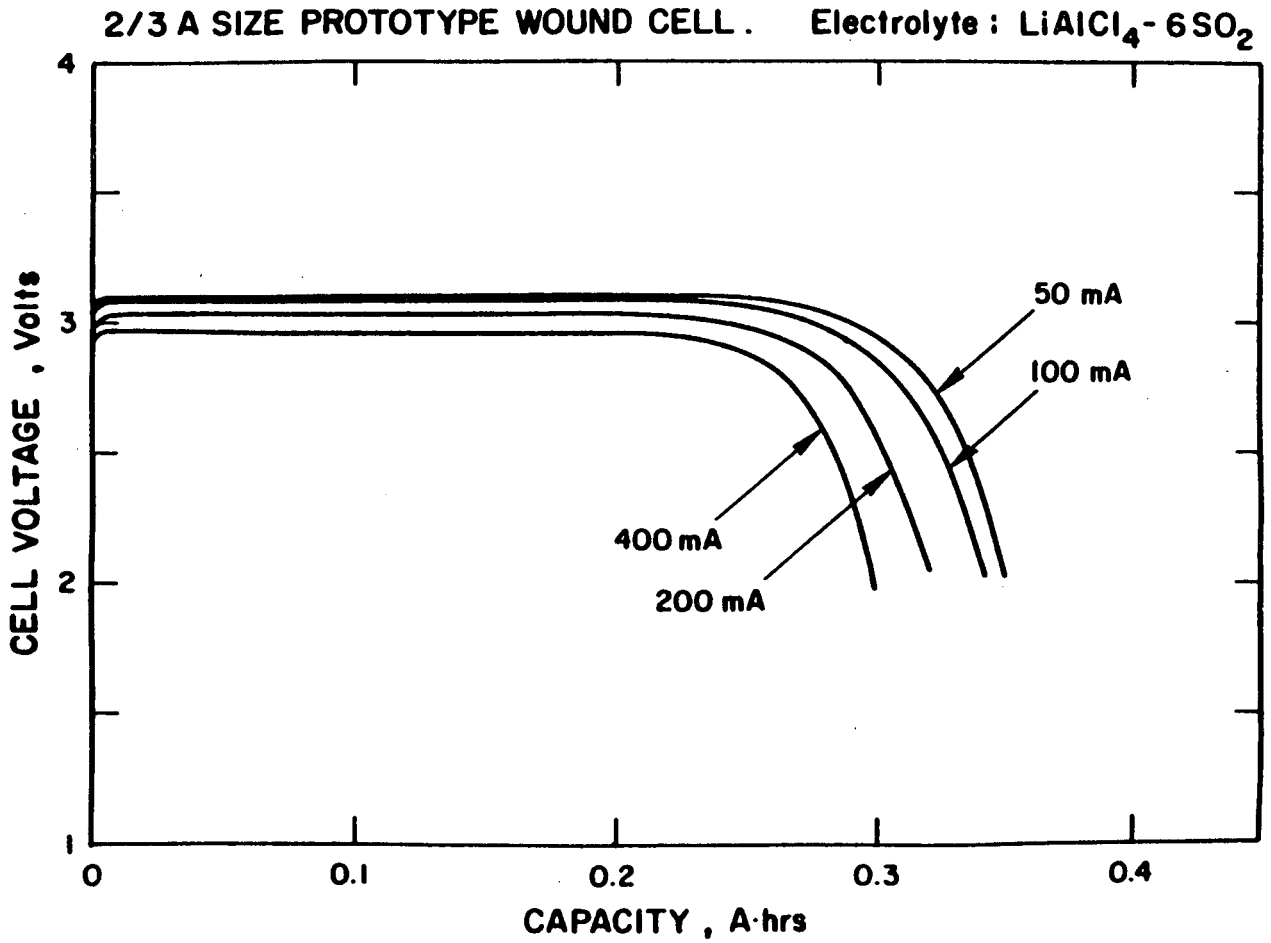

FIGURE 48. Discharge Voltage Profiles of the 2/3A Size Prototype $Li/LiAlCl_4$-$6SO_2$/Carbon Wound Cells at Various Rates.

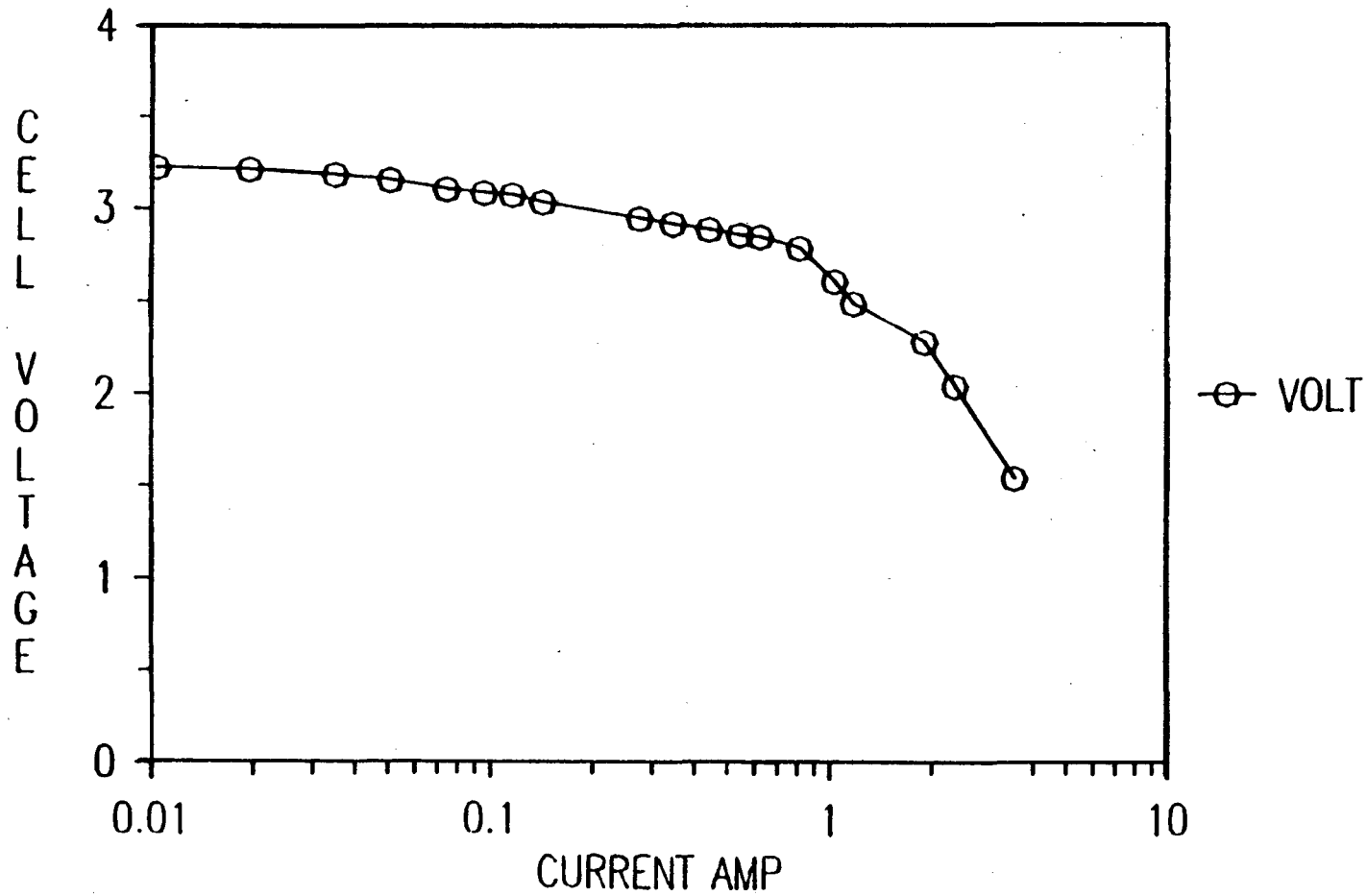

FIGURE 49. Polarization of a 2/3A Size Prototype Li/$LiAlCl_4$-$6SO_2$ Carbon Wound Cell.

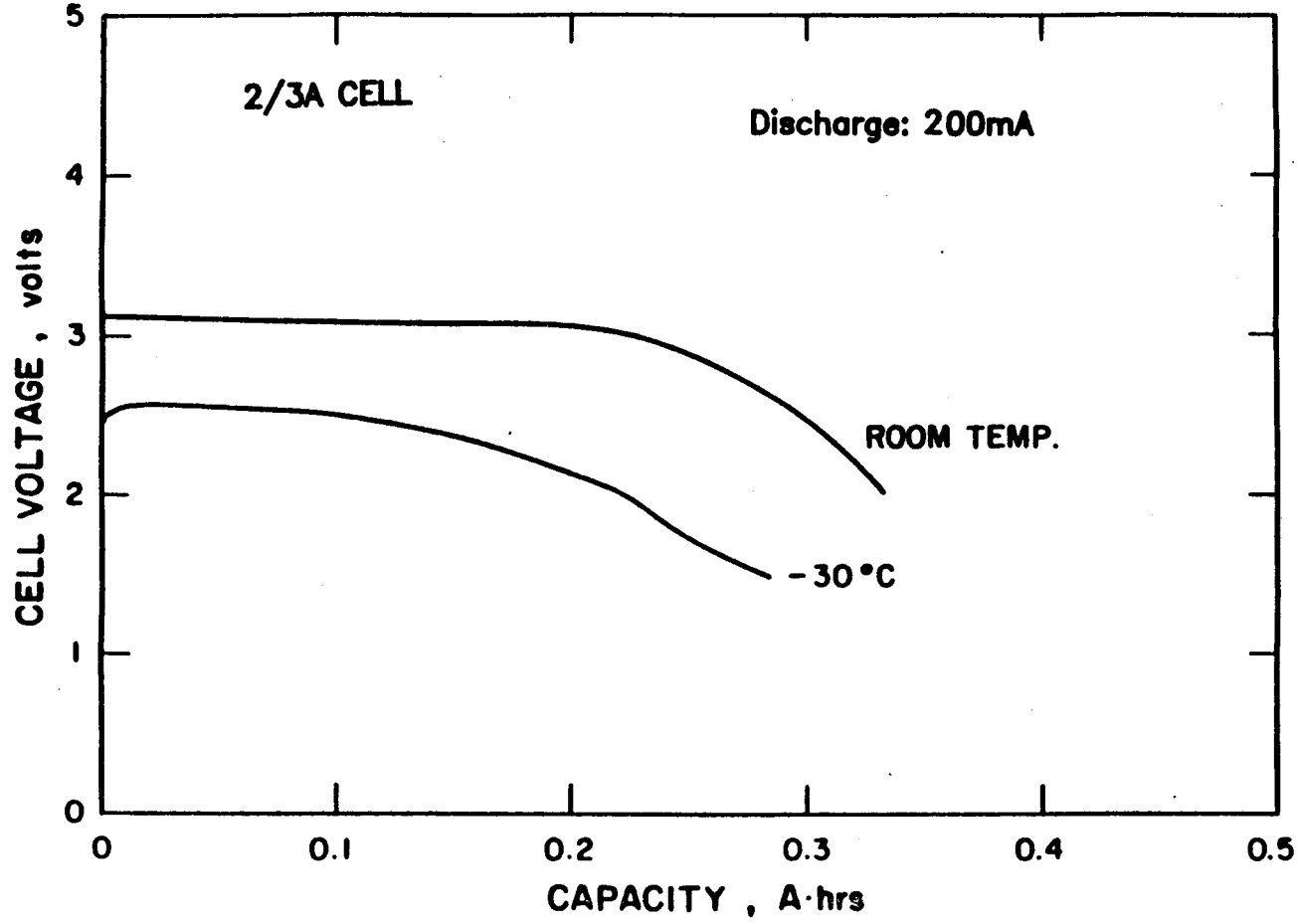

FIGURE 50. PERFORMANCE OF A 2/3A Size Prototype $Li/LiAlCl_4-6SO_2$/Carbon Wound Cell at -30°C.

Although the discharge voltage is lower than that at room temperature, it delivers over 60% of its original capacity above 2.0 V.

b. Electrolyte Composition

2/3A size wound cells were made and filled with $LiAlCl_4$-xSO_2 electrolytes with x varying from 3 to 22 to evaluate the effect of electrolyte composition on discharge performance. Table 19 summarizes the test results and Figure 51 shows the discharge curves of several cells having electrolytes as indicated. The cell capacity increased with decreasing SO_2 content and increasing amount of $LiAlCl_4$. The results are consistent with the proposed reaction mechanism with the reduction of the complex $LiAlCl_4$-xSO_2 on the carbon surface. Figure 52 shows the comparison of the discharged capacities of cells filled with electrolyte of different SO_2 content with the theoretical capacities based on Equation (IV-3) for 3 equivalents per mole of $LiAlCl_4$ and Equation (IV-2) for 2 equivalents per mole of $LiAlCl_4$. All experimental data are within the two theoretical lines as shown in Figure 52 except the cell with $LiAlCl_4$-$3SO_2$ electrolyte. The cell with $LiAlCl_4$-$3SO_2$ electrolyte delivered less capacity than expected. It was likely that the capacity was limited by the amount of carbon.

TABLE 19. CAPACITIES DELIVERED OF 2/3A SIZE CELLS HAVING ELECTROLYTES OF VARIOUS COMPOSITION.

ELECTROLYTE COMPOSITION	WT. OF ELECTROLYTE (g)	WT. OF SO_2 (g)	WT. OF $LiAlCl_4$ (g)	CAPACITY DELIVERED. (Ah)
$LiAlCl_4$-22SO_2	3.34	2.97	0.37	0.120
$LiAlCl_4$-18SO_2	4.10	3.56	0.54	0.138
	3.04	2.64	0.40	0.122
$LiAlCl_4$-15SO_2	4.05	3.42	0.63	0.155
	3.04	2.57	0.47	0.122
$LiAlCl_4$-12SO_2	4.03	3.28	0.75	0.320
	3.65	2.97	0.68	0.315
$LiAlCl_4$-9SO_2	4.10	3.14	0.96	0.352
	4.17	3.20	0.97	0.360
$LiAlCl_4$-6SO_2	3.60	2.47	1.13	0.355
$LiAlCl_4$-3SO_2	3.77	1.97	1.80	0.390

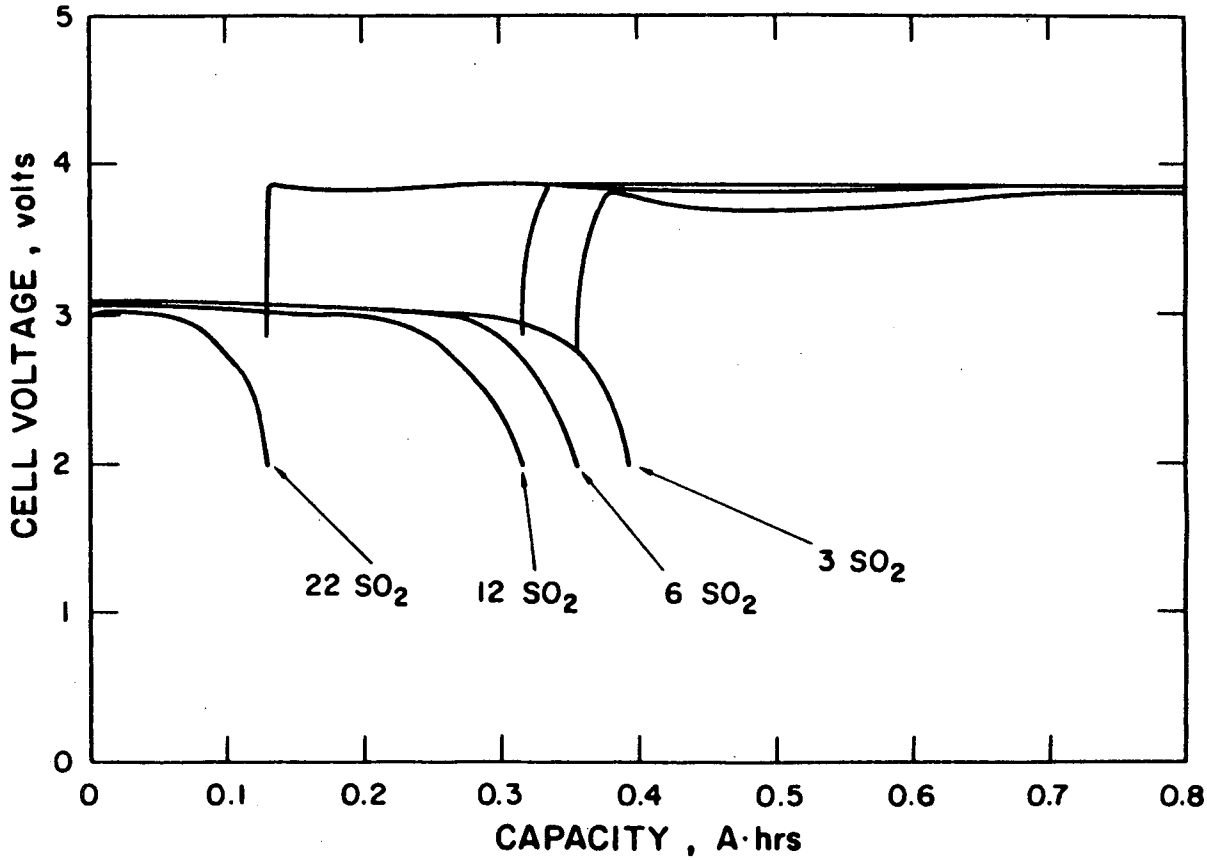

CAPACITY AHS

FIGURE 51. Discharge Performance of 2/3A Size Prototype Li/Carbon Wound Cells Filled with $LiAlCl_4$-xSO_2 Electrolytes of Various SO_2 Content.

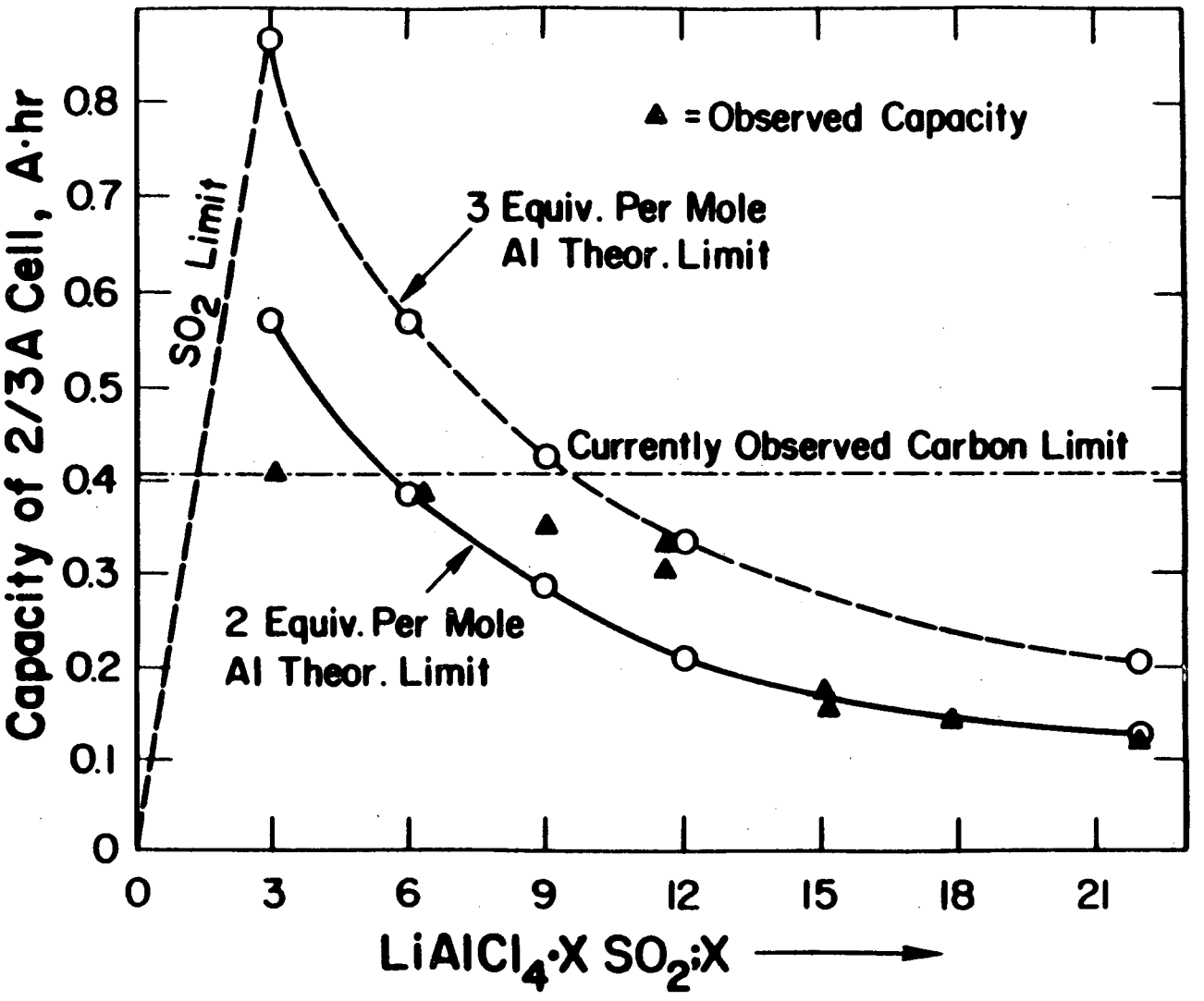

FIGURE 52. Comparison of the Capacity Delivered by 2/3A Size $Li/LiAlCl_4$-xSO_2/Carbon Wound Cells and the Calculated Capacities Based on the Amount of $LiAlCl_4$ in the Cell.

c. Cycling Performance

Figures 53 and 54 show the typical cycling performance of the 2/3A size cells filled with $LiAlCl_4$-$3SO_2$ and $LiAlCl_4$-$6SO_2$ electrolytes. The cells were discharged at 50 mA to 2 V cutoff and recharged at 25 mA to 3.9 V. Both cells showed capacity fading on cycling. The capacity of the cells dropped to 50% of their original capacity after about 40 cycles. Figure 55 exhibits the typical voltage profile of the cell with $LiAlCl_4$-$3SO^2$ electrolyte. The end of the cycling life was probably caused by starvation of the electrolyte since both the salt and the solvent, SO_2, of the electrolyte were consumed during discharge which might have resulted in inefficiency of charge.

Cells delivered better cycle life on partial discharge. The small 2/3 A size wound cells delivered about 250-300 cycles at 25% depth and about 150-200 cycles at about 50% depth. Figures 56 and 57 show the voltage profiles of cells dicharged at 50 mA and recharged at 25 mA at selected cycles with depths of 50% and 25% respectively. Cells on shallow discharge usually failed due to development of internal shorts.

Cells were capable of discharge to near 0 volt. However the cycle life was significantly poor. Figure 58 shows the voltage

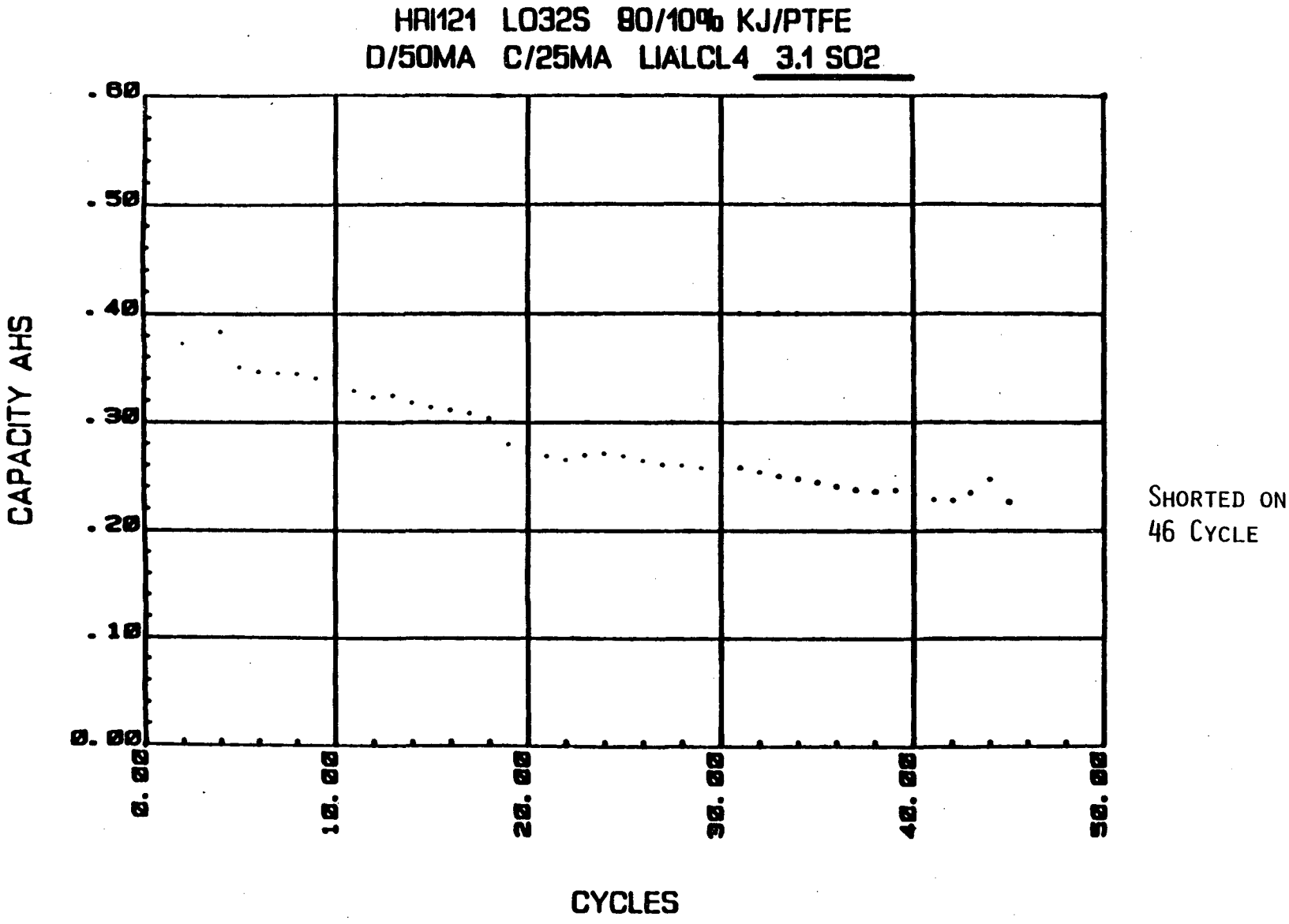

FIGURE 53. Cycling Performance of a 2/3A Prototype Li/$LiAlCl_4$-$3SO_2$/Carbon Wound Cell Discharged at 50 mA and Charged at 25.

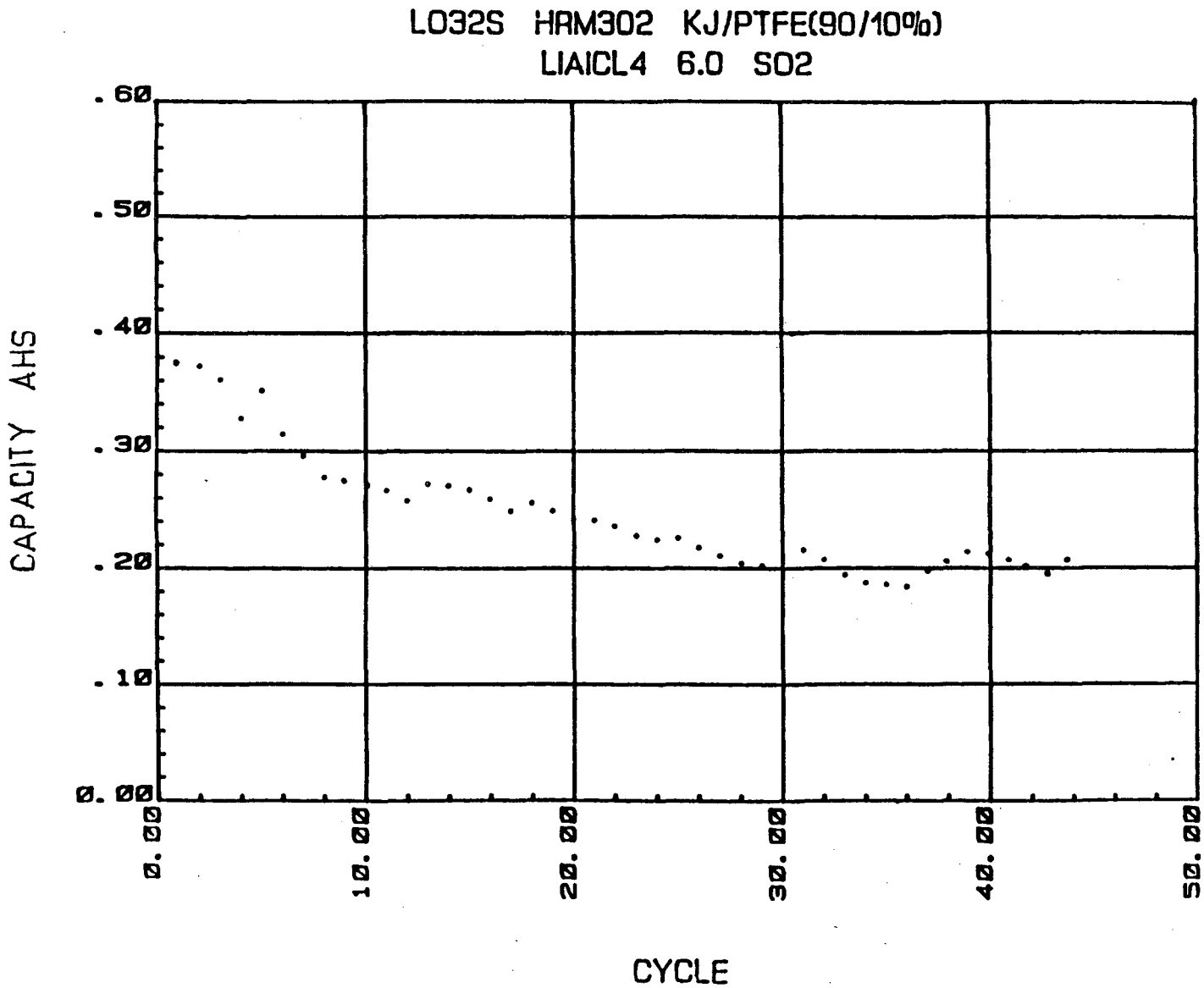

FIGURE 54. Cycling Performance of 2/3A Size Prototype $Li/LiAlCl_4$-$6SO_2$/Carbon Wound Cell Discharged at 50 mA and Charged at 25 mA.

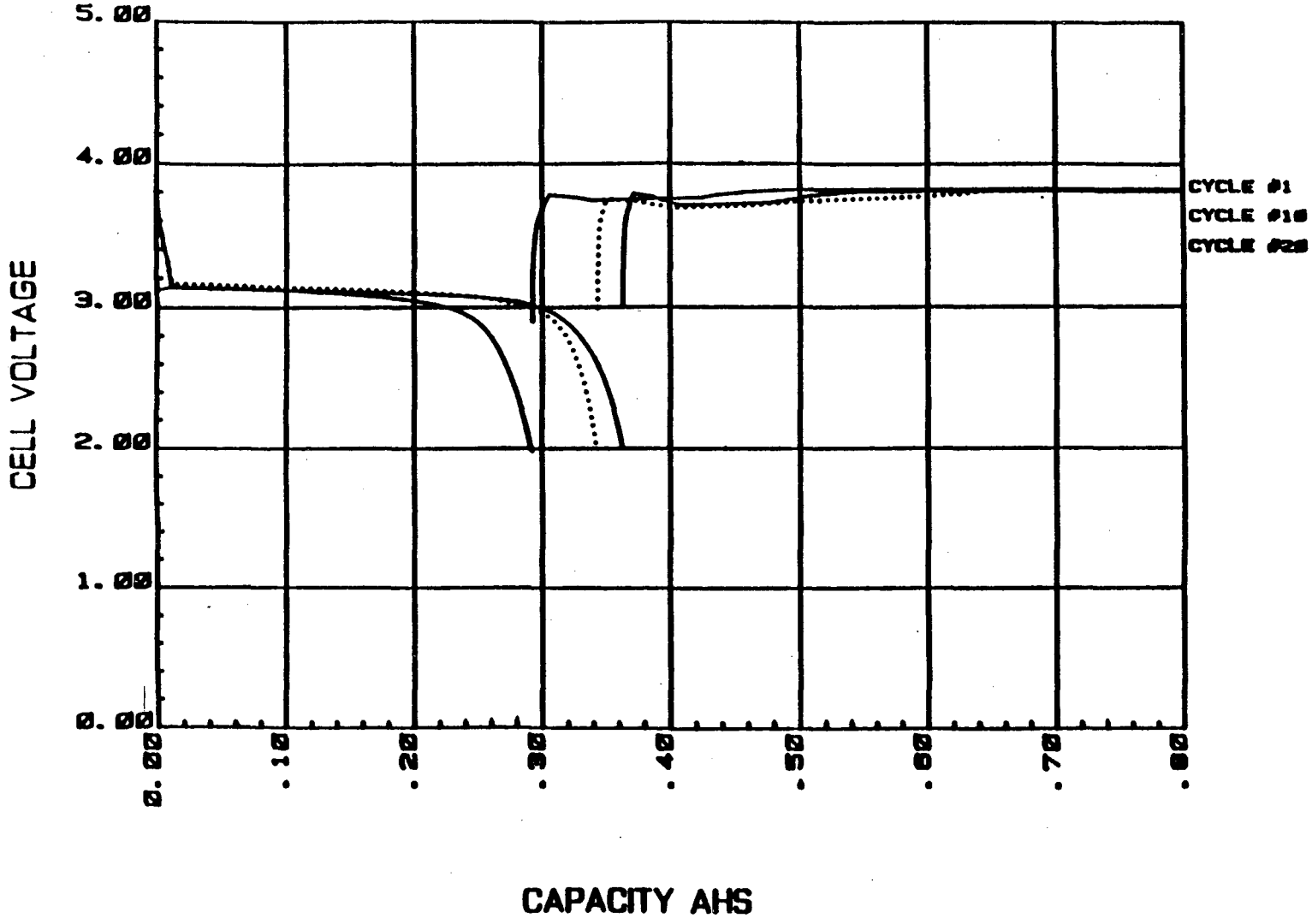

FIGURE 55. Voltage Profiles of a 2/3A Size Prototype $Li/LiAlCl_4$-$6SO_2$/Carbon Wound Cell at Selected Cycles, Discharged at 50 mA and Charged at 25 mA.

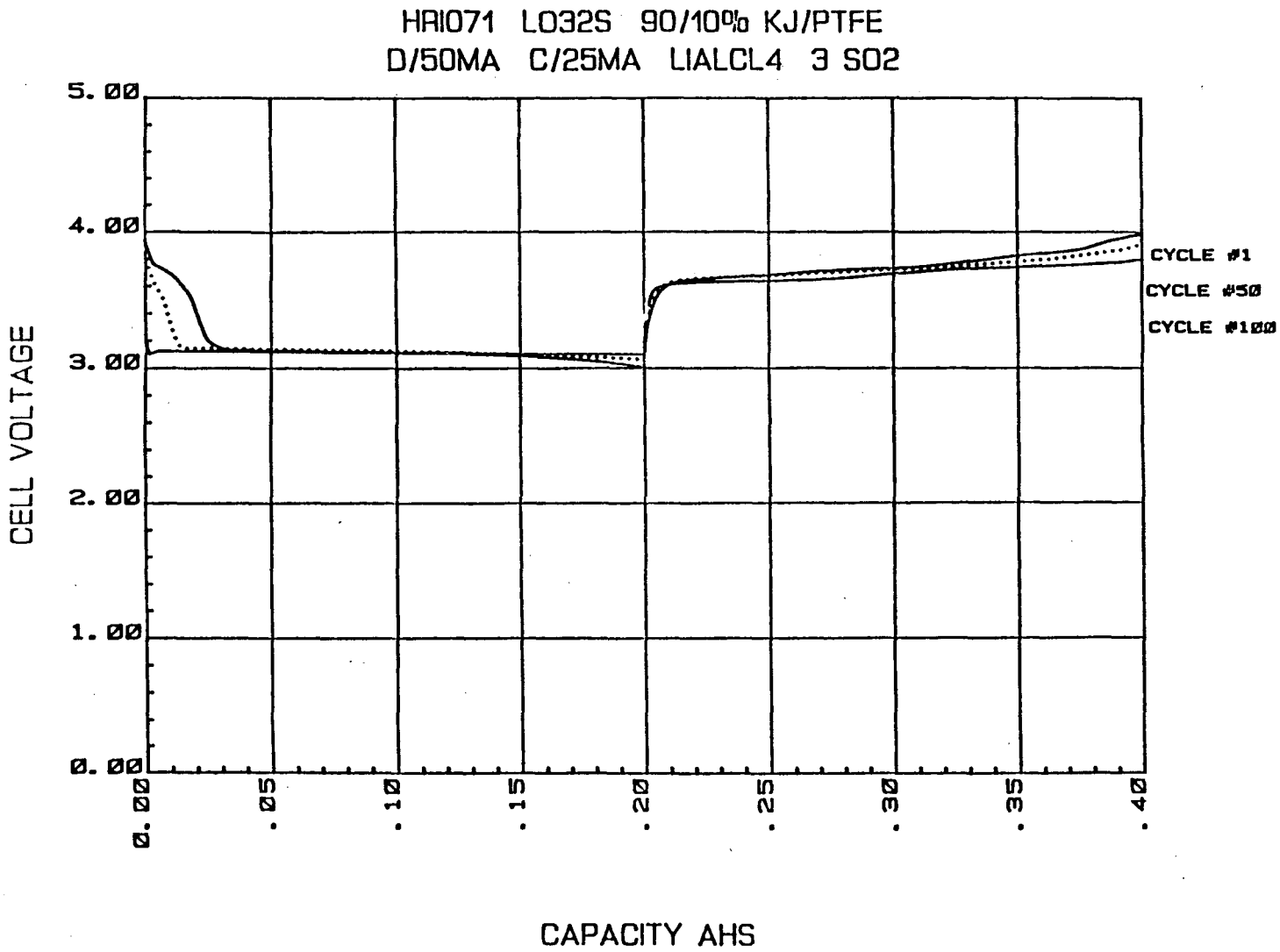

FIGURE 56. Voltage Profiles of a 2/3A Size Prototype $Li/LiAlCl_4\text{-}3SO_2$/Carbon Wound Cell at Selected Cycles, Discharged at 50 mA to 50% Depth and Charged at 25 mA.

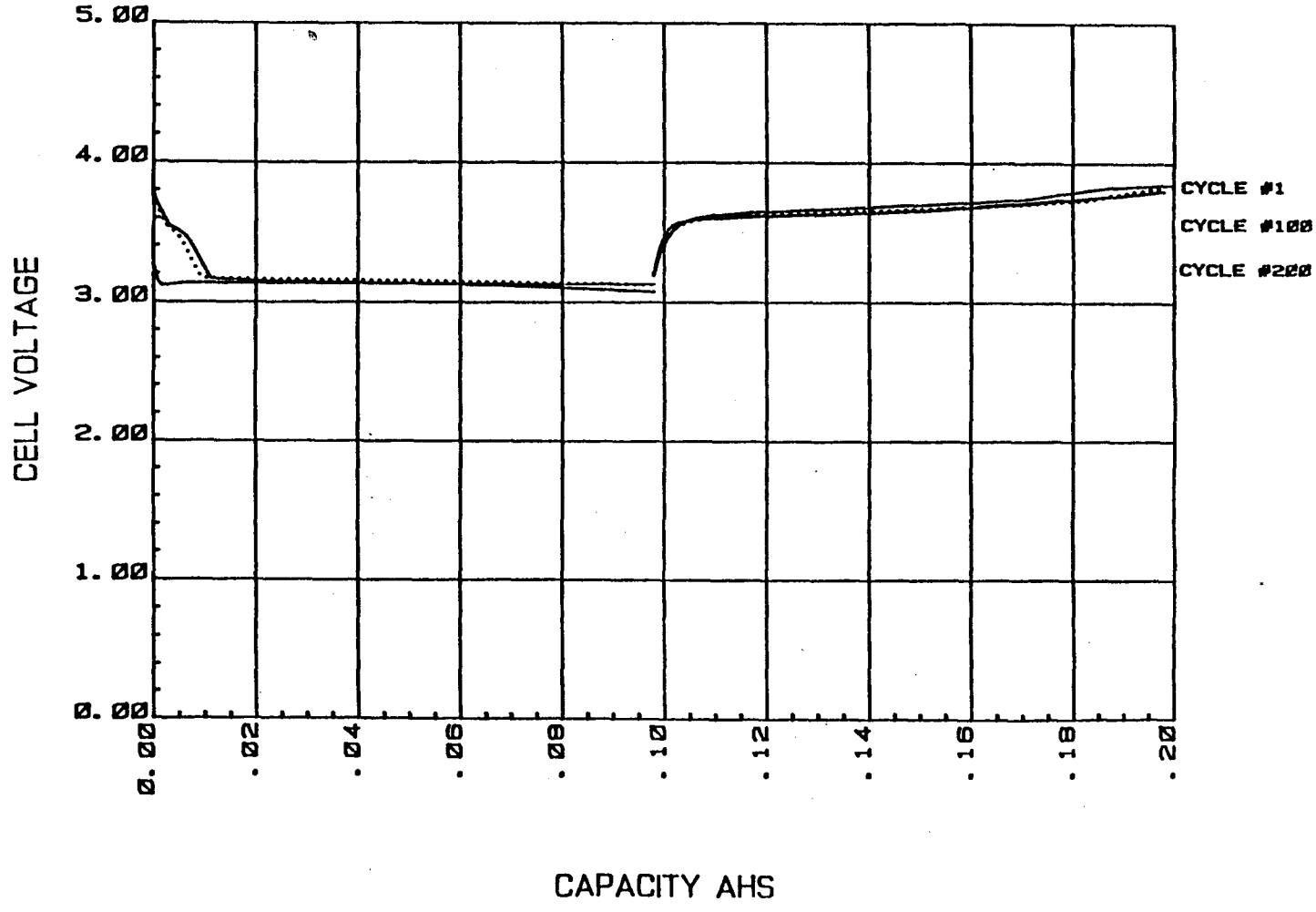

FIGURE 57. Voltage Profiles of a 2/3A Size Prototype $Li/LiAlCl_4$-$3SO_2$Carbon Wound Cell at Selected Cycles, Discharged at 50 mA to 25% Depth and Charged at 25 mA.

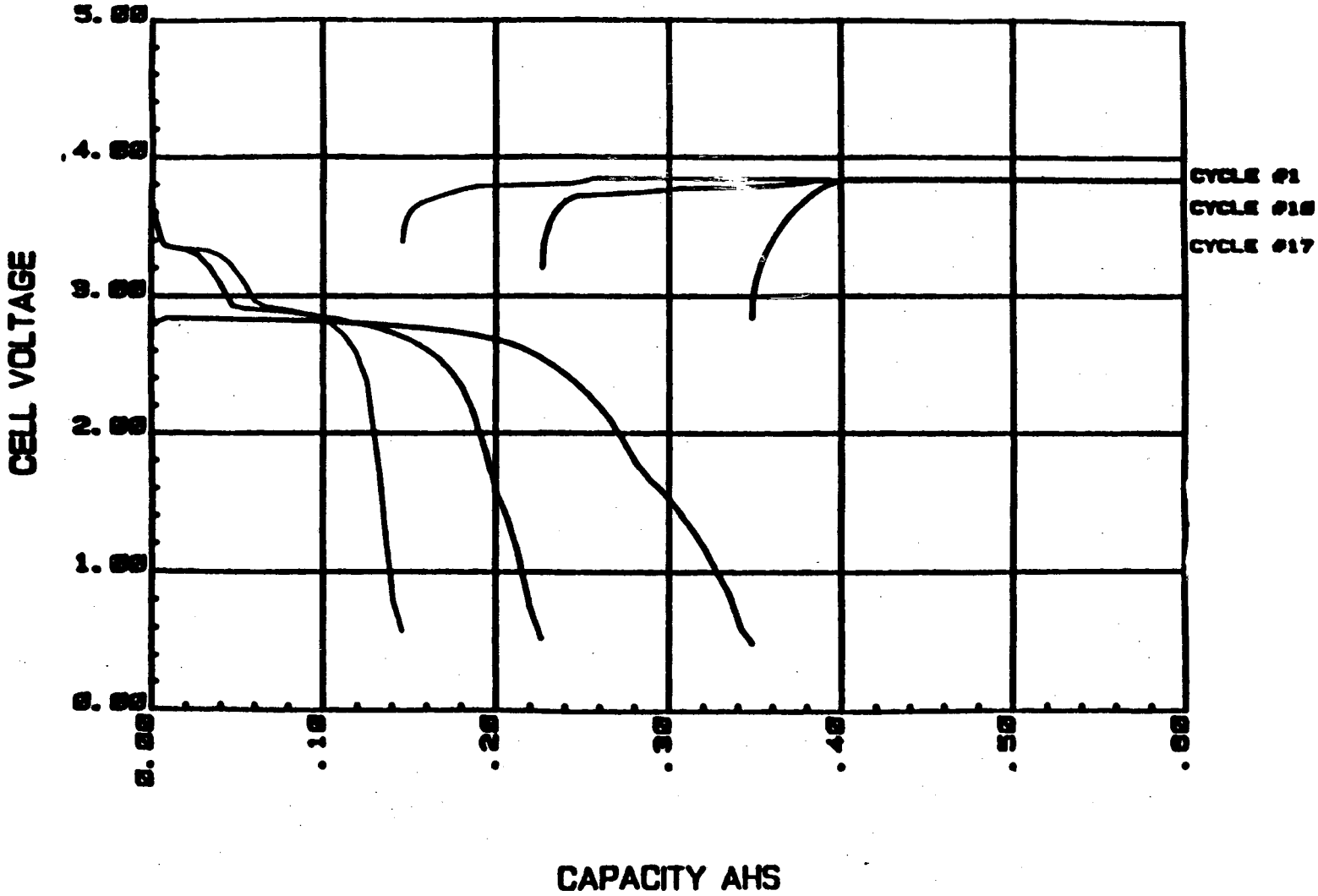

FIGURE 58. Performance of a 2/3A Size Prototype $Li/LiAlCl_4$-$6SO_2$/Carbon Wound Cell on Deep Discharge to 0.5V at 50 mA and charge at 25 mA.

profiles of a cells discharged at 400 mA to 0.5 volt. The cell showed a rapid loss of cell capacity and had operated for 17 cycles before termination.

d. Effect of the Amounts of Electrolyte and Lithium

Since the cycle life on deep discharge was significantly less than for cells on partial discharge, a study was carried out to investigate if the amounts of electrolyte and lithium affected the performance on deep discharge.

Two batches of cells were made with a regular 2/3 A size wound electrode stack and packed in D size cans filled with excess electrolyte. The electrode stacks were confined tightly with a cylindrical Teflon insert, which had inside diameter the same as the L032S(2/3A) cans. One batch of cells had the lithium electrode made by pressing 5 mil lithium on both side of a copper foil similar to the lithium electrodes used in the regular 2/3A size cells. The cells had normally 200% excess lithium based on the cell capacity delivered. The other batch of cells had lithium electrode made with 10 mil lithium pressed on both sides of the copper foil, which provided about 500% excess lithium.

Figure 59 compares the typical performance of the cell having excess electrolyte and 5 mil lithium with that of the regular 2/3 A

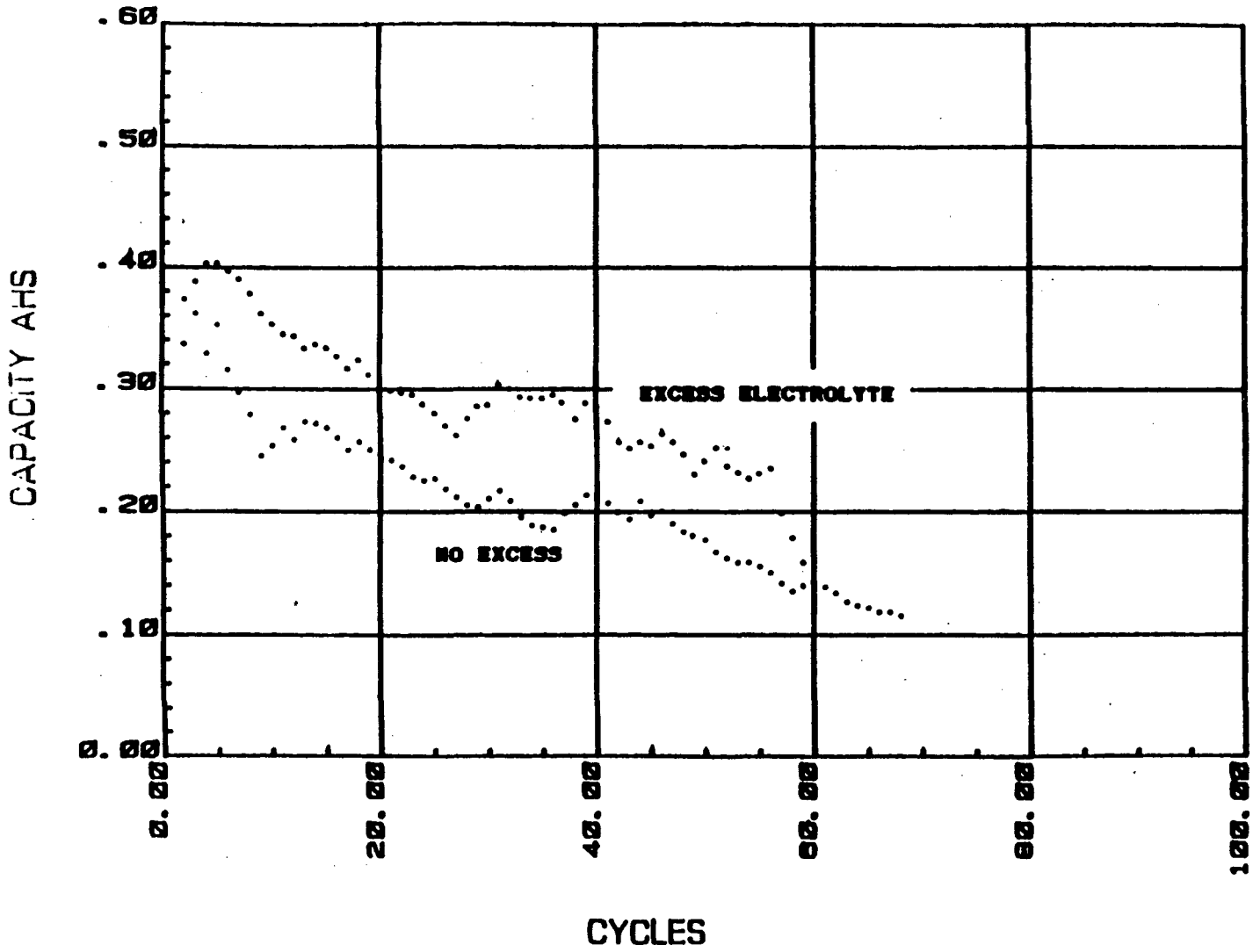

FIGURE 59. Comparison of the Cycling Performance of 2/3A Size Cell with and without Excess Electrolyte.

cell containing limited electrolyte. Although the cell with excess electrolyte delivered more capacity on each cycle, the fading of the capacity on cycling was similar to the cell without excess electrolyte.

However, the cell with excess lithium (10 mil lithium) and filled with excess electrolyte showed significantly better cycle life as exhibited in Figure 60. Significant capacity fading occurred only in the initial 20 cycles.

Figure 61 compares the voltage profiles at the 70th cycles of a regular 2/3A size cell made with 5 mil lithium and of the cells with excess electrolyte. The cells with 5 mil lithium showed a sharp drop in cell voltage at the end of discharge indicating the exhaustion of the lithium electrode due to inefficiency in recharging of the lithium electrode. Cells made with 10 mil lithium showed a normal discharge in the 70th cycle without exhaustion of lithium.

The high voltage plateaus near 3.6 V shown in Figure 61 are attributed to the discharge of dissolved Cl_2 which is generated near the end of the charging cycle or on overcharge according the reaction :

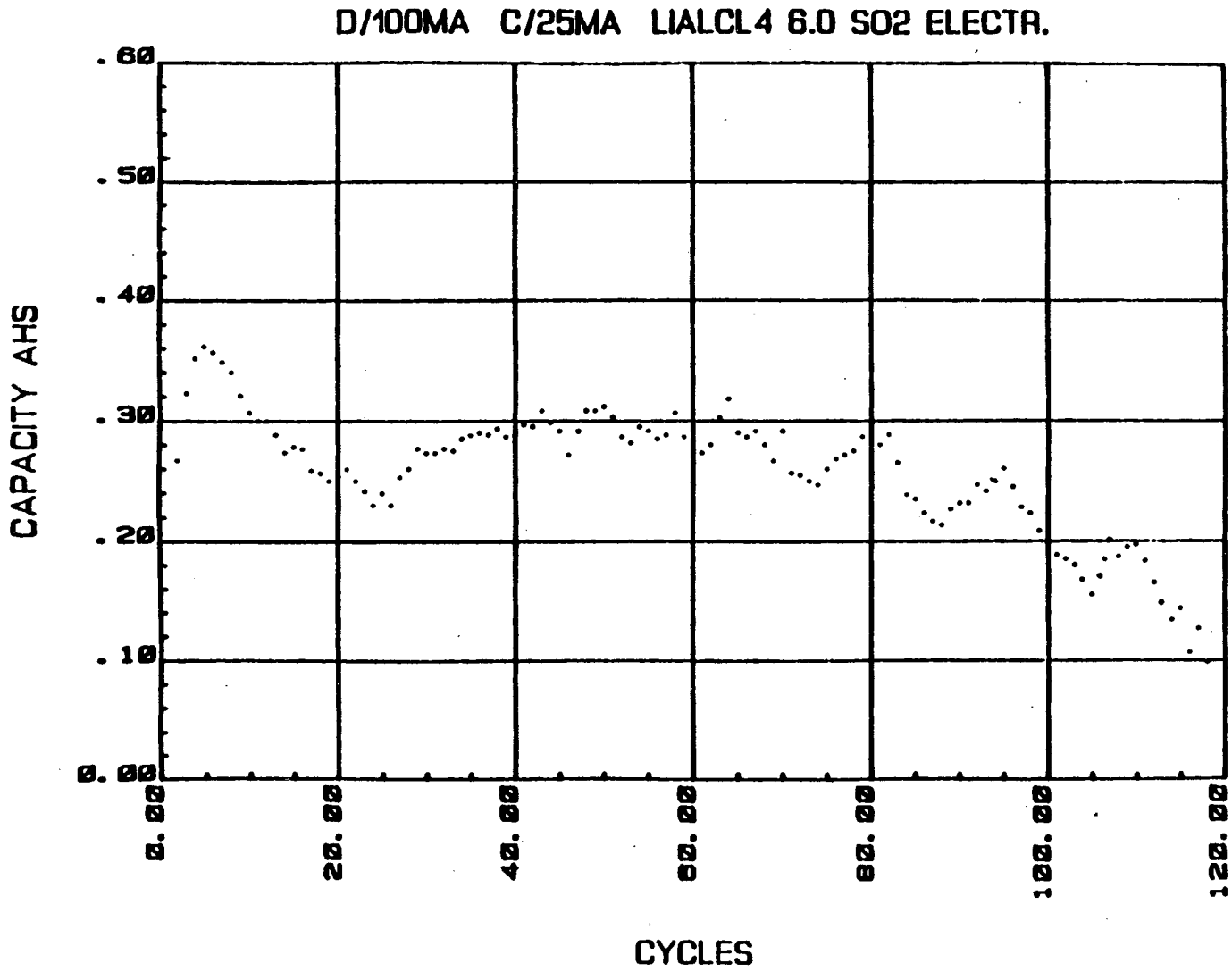

FIGURE 60. Performance of 2/3A Size Cell Made with 10 Mil Li and Tested in D can with Excess $LiAlCl_4$-$6SO_2$ Electrolyte.

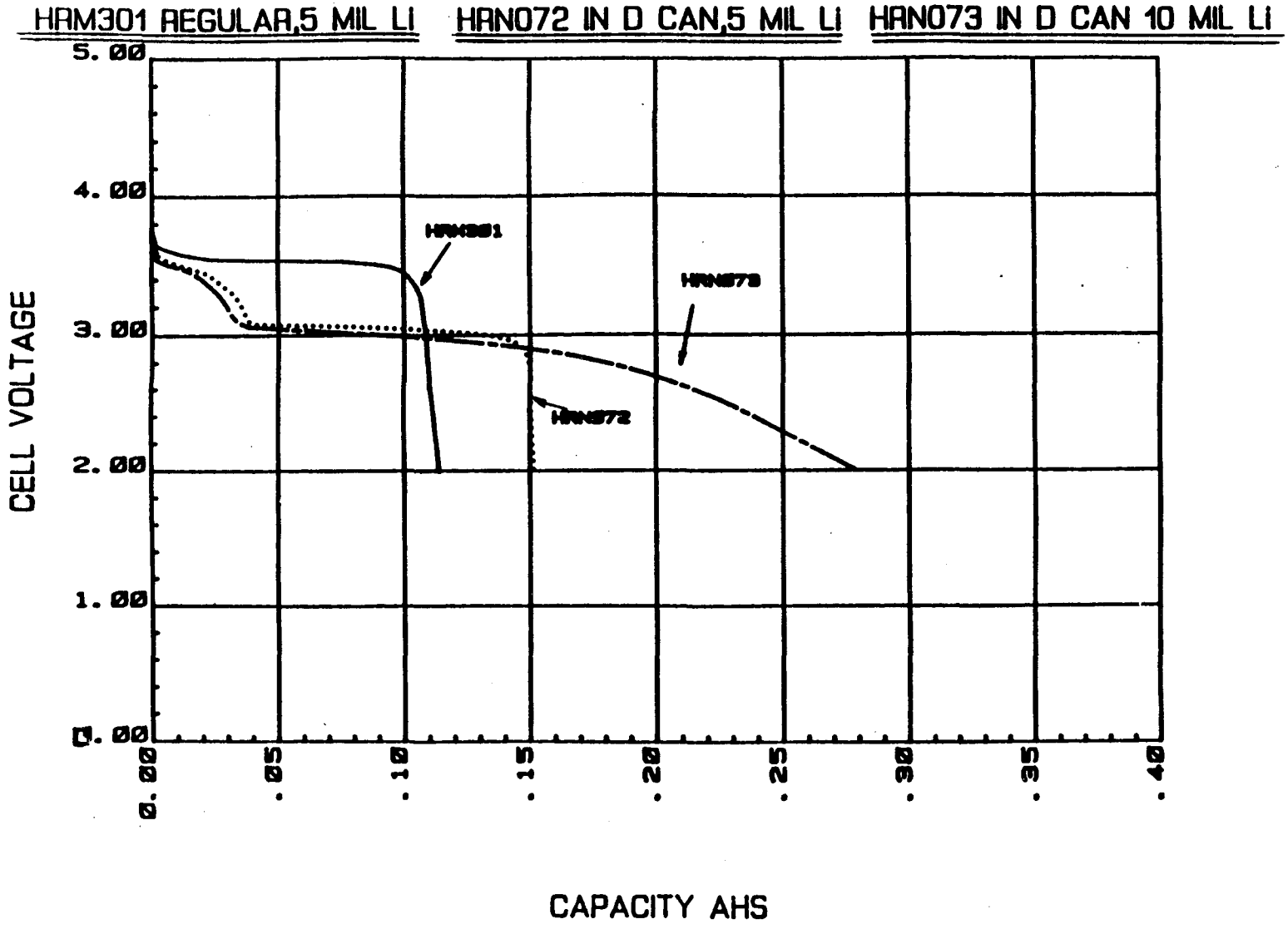

FIGURE 61. Comparison of the Voltage Profiles at the 70th Cycle of the Regular 2/3A Size Cell and Cells Tested in D Cans with Excess $LiAlCl_4$-$6SO_2$ Electrolytes.

$$AlCl_4^- \text{ ---------> } AlCl_3 + 1/2\ Cl_2 + e$$

On discharge,

$$1/2Cl_2 + Li^+ + e \text{ -------> } LiCl$$

$$LiCl + AlCl_3 \text{ -------> } Li^+ + AlCl_4^-$$

The $AlCl_3$ and Cl_2 generated are highly soluble in the electrolyte and may chemically react with the insufficiently charged discharge products on the positive electrode or may diffuse through the separator and react with the excess lithium to reform the electrolyte salt following the reaction,

$$Li + 1/2\ Cl_2 + AlCl_3 \text{ --------> } LiAlCl_4$$

Normal 2/3A cells contain only limited electrolyte. In addition to showing fading of capacity on deep cycling, they also show an increase in the discharge portion of the high voltage plateau near 3.6 V as exhibited in Figure 62 due to accumulation of the dissolved chlorine. This is caused by inefficiency of recombination of the reaction products after cycling.

Cells packed in D can with excess electrolyte showed less

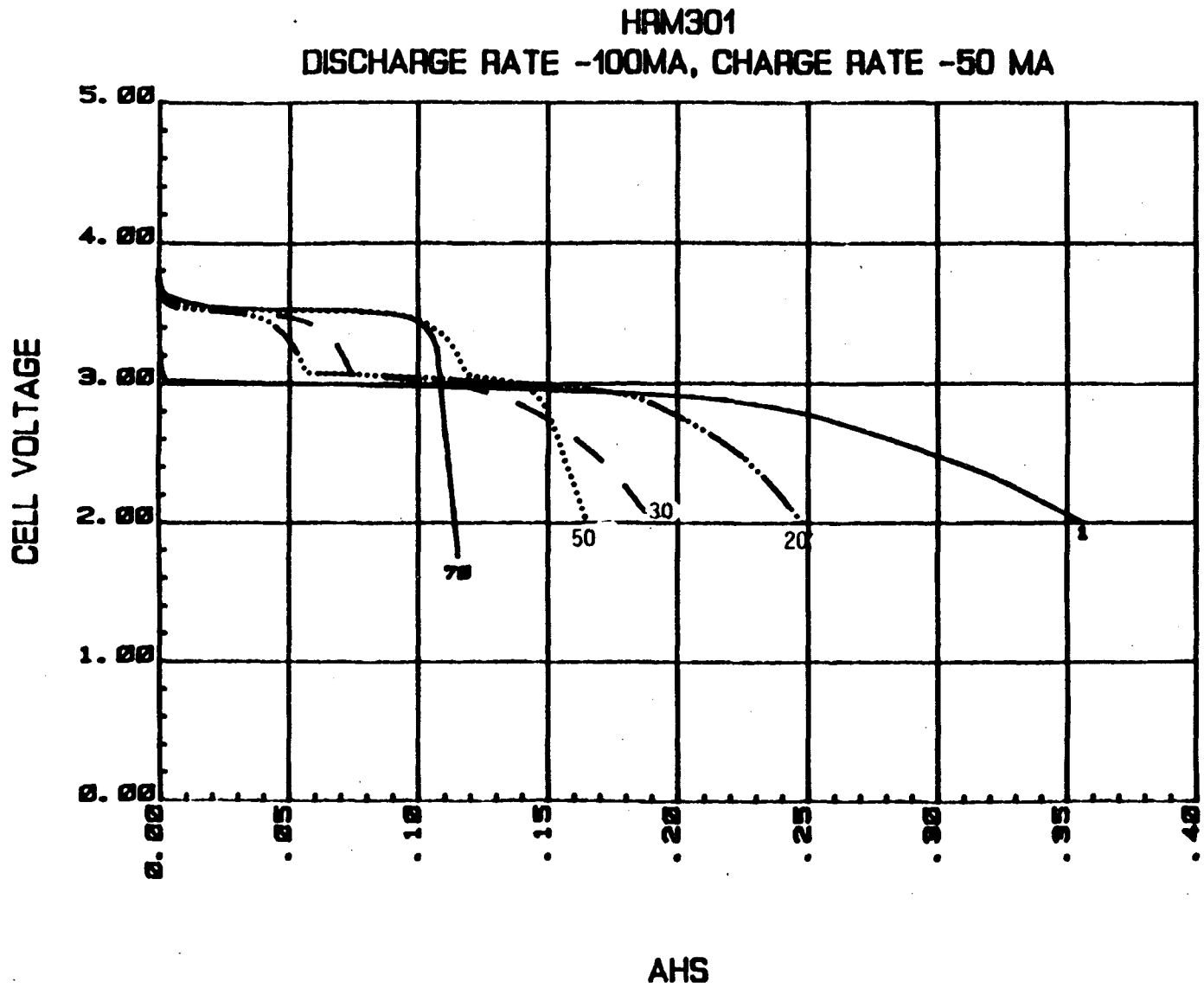

FIGURE 62. Voltage Characteristics of a 2/3A Size Prototype $Li/LiAlCl_4$-$6SO_2$/Carbon Wound Cell at Selected Cycles.

accumulation of the overcharge products as indicated in Figure 61 which exhibits a smaller portion of the high voltage plateau comparing to that of a real 2/3A size cell with limited electrolyte.

e. Shelf Life

Similar to the test results of the experimental prismatic cells, 2/3A size prototype wound cells also showed excellent shelf life (charge retention) as exhibited in Figure 63. The cell was stored at ambient temperature for 9 months and delivered almost the same amount of capacity as a fresh cell.

f. Safety Characteristics

Only limited safety characteristics of the cell were evaluated. Figure 64 shows the temperature and current of a fresh cell when shorted externally. The cell was covered with 6 inches of insulator. The cell gave a maximum short circuit current of about 11 Amp with a maximum temperature near 80°C. The cell was safe without venting under such condition. However, shorting cells after numerous cycles(over 20 cycles) caused explosion or venting with flame. Occasional venting or explosion was also observed when cell shorted internally due to developing dendritic lithium after numerous cycles.

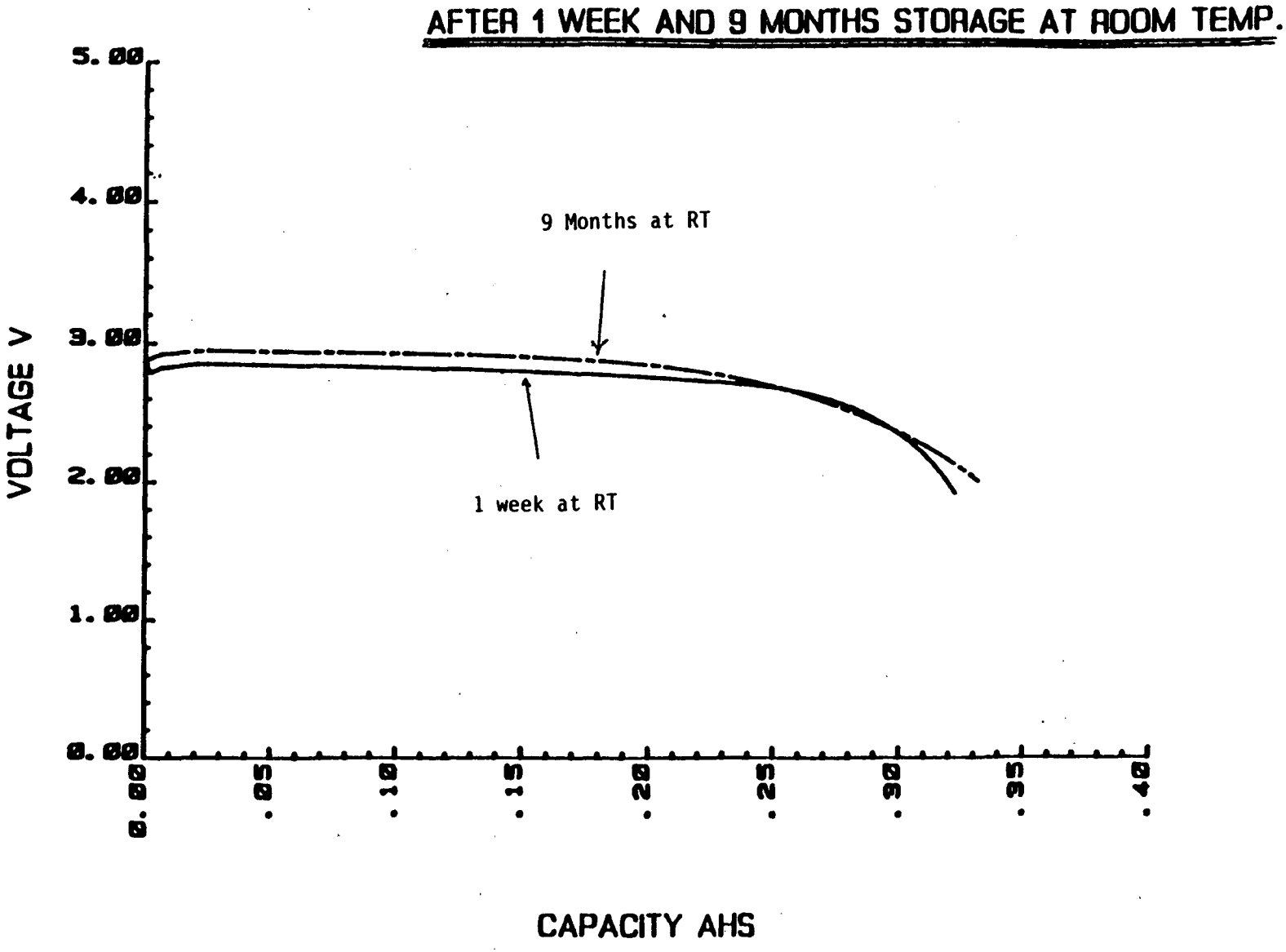

FIGURE 63. Comparison of the Discharge Voltage Profiles of a 2/3A Size Prototype Li/$LiAlCl_4$-$6SO_2$/Carbon Wound Cell Before and After Storage.

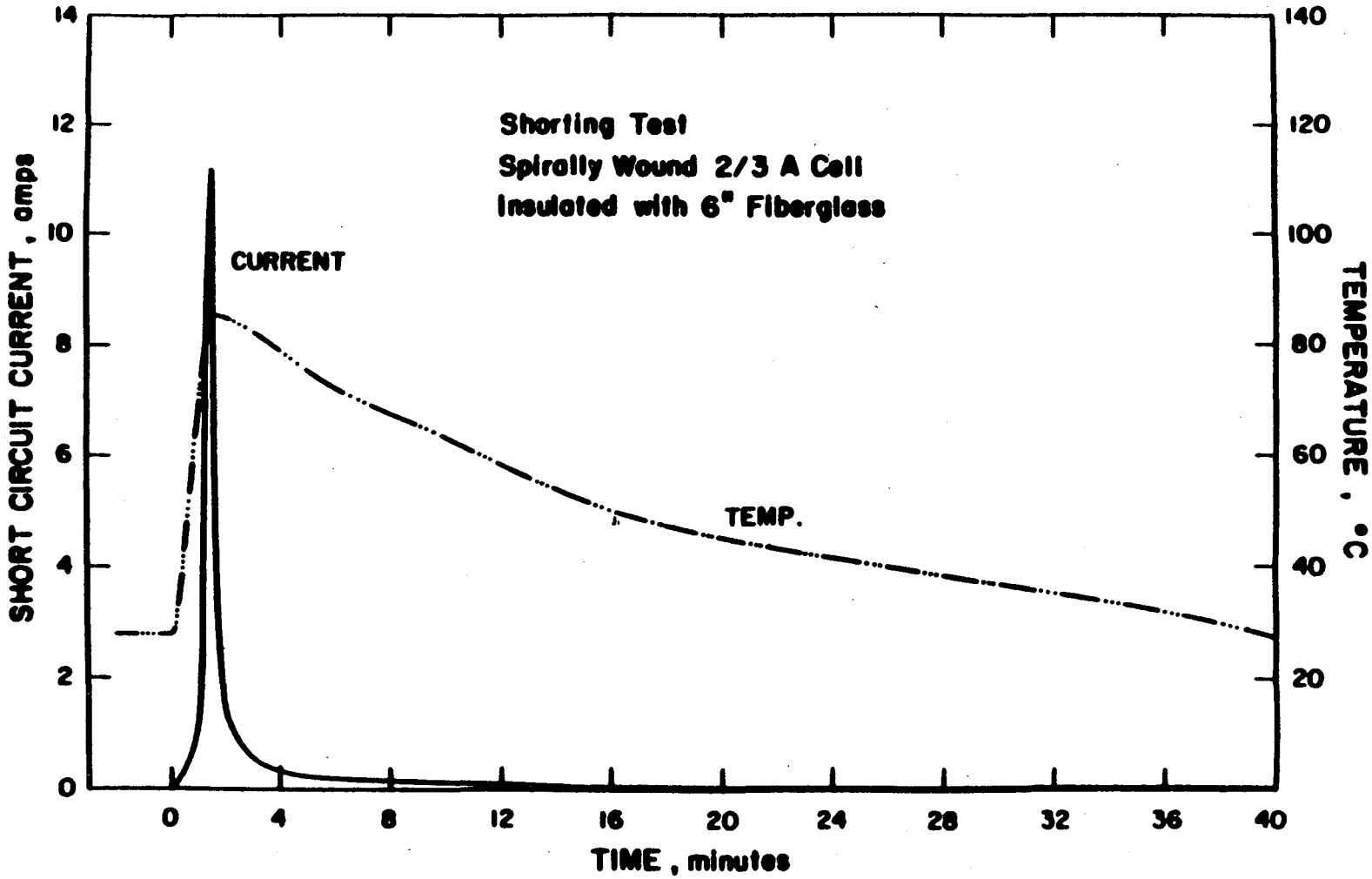

FIGURE 64. The Temperature and Current of a 2/3A Size Prototype $Li/LiAlCl_4$-$6SO_2$/Carbon Wound Cell on External Shorting.

3. Overcharge Studies

The Li/$LiAlCl_4$-xSO_2/carbon system is capable of accepting overcharge by virtue of the recombination of the Cl_2 and $AlCl_3$ generated on the positive electrode with the lithium plated on the negative electrode during overcharge according to the following reactions:

On overcharge:

at the positive electrode,

$$AlCl_4^- \dashrightarrow AlCl_3 + 1/2\ Cl_2 + e$$

at the negative electrode,

$$Li^+ + e \dashrightarrow Li$$

Recombination reaction:

$$1/2\ Cl_2\ (\text{dissolved}) + Li \dashrightarrow LiCl$$

$$LiCl + AlCl_3 \dashrightarrow LiAlCl_4$$

Thus there is no net consumption of the chemicals as a result of overcharge. Although the Cl_2 and $AlCl_3$ generated on overcharge are highly soluble in the electrolyte, they have to diffuse to the lithium electrode through the separator in order to react with the excess lithium or dendritic lithium deposits. The efficacy of the recombination process is affected strongly by the structure and stability of the separator employed.

In addition to the recombination reaction, the $AlCl_3$ and Cl_2 generated can also react chemically with the unoxidized discharge products on the positive electrode material. An experiment was carried out to demonstrate the mentioned capability. A 1 cm^2 piece of carbon electrode was discharged at 2 mA against a lithium electrode in a glass cell to 2.0V cutoff and then removed from the cell and stored overnight in electrolyte containing the overcharge products, $AlCl_3$ and Cl_2. The carbon electrode was then put back in the glass cell with a Li negative electrode and discharged again. It delivered about the same capacity as the first discharge as shown in Figure 65. this indicated clearly that the discharged positive electrode had been recharged chemically.

Several experiments were carried out using prismatic cells and the 2/3A size prototype wound cells to demonstrate the capability of overcharge and to study the effect of separators.

a. Effect of Separator on Rate of Recombination

The rate of recombination was studied using prismatic cells with one brass center electrode as the negative electrode sandwiched between two carbon positive electrodes of size 2.5 cm x 4 cm shown in Figure 66. A layer of separator was used between the brass electrode and the carbon electrode. The cells were charged at 20 mA (1 mA/cm^2) and allowed to overcharge for various durations. On

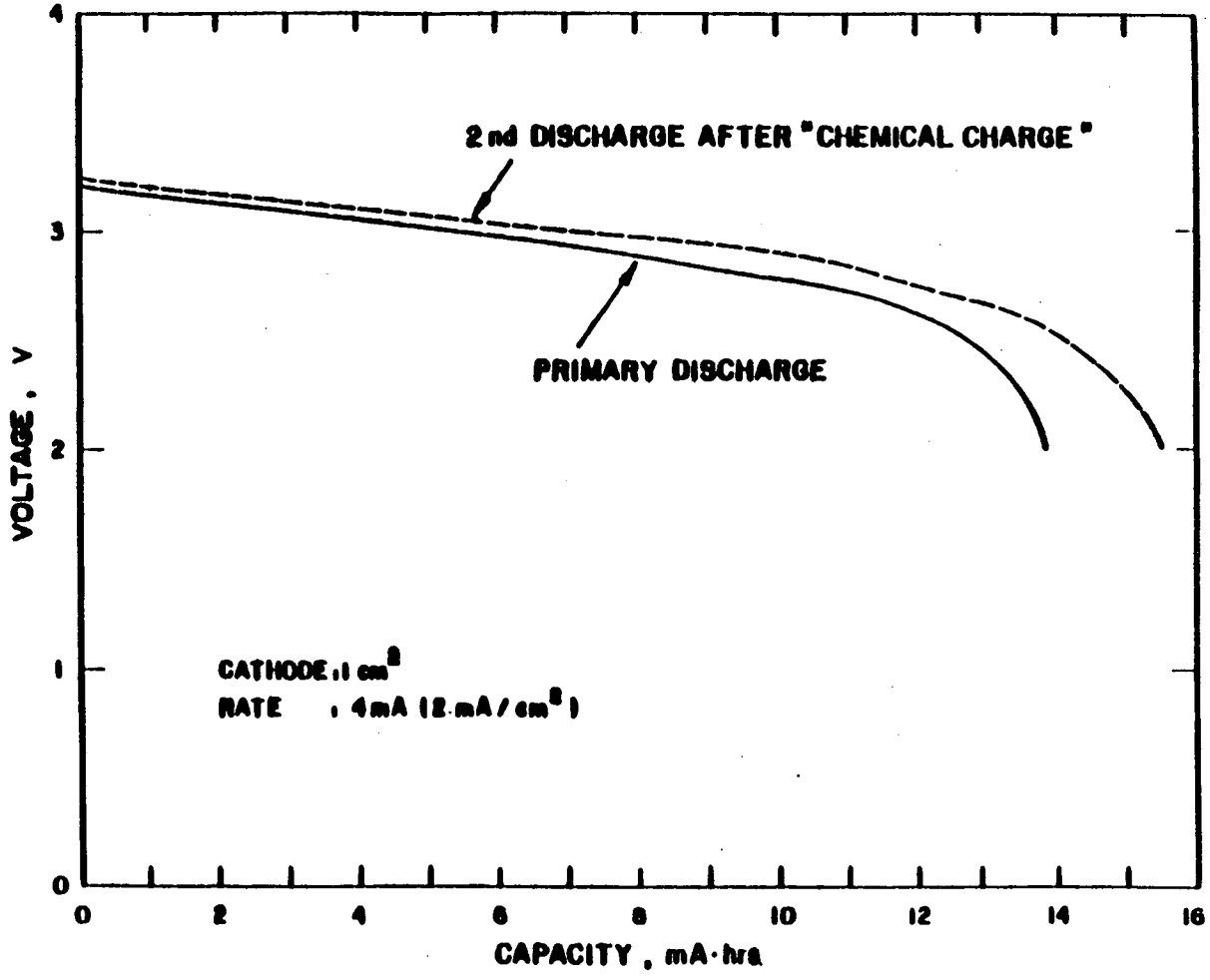

FIGURE 65. Performance of the Carbon Positive Electrode After Being Charged Chemically.

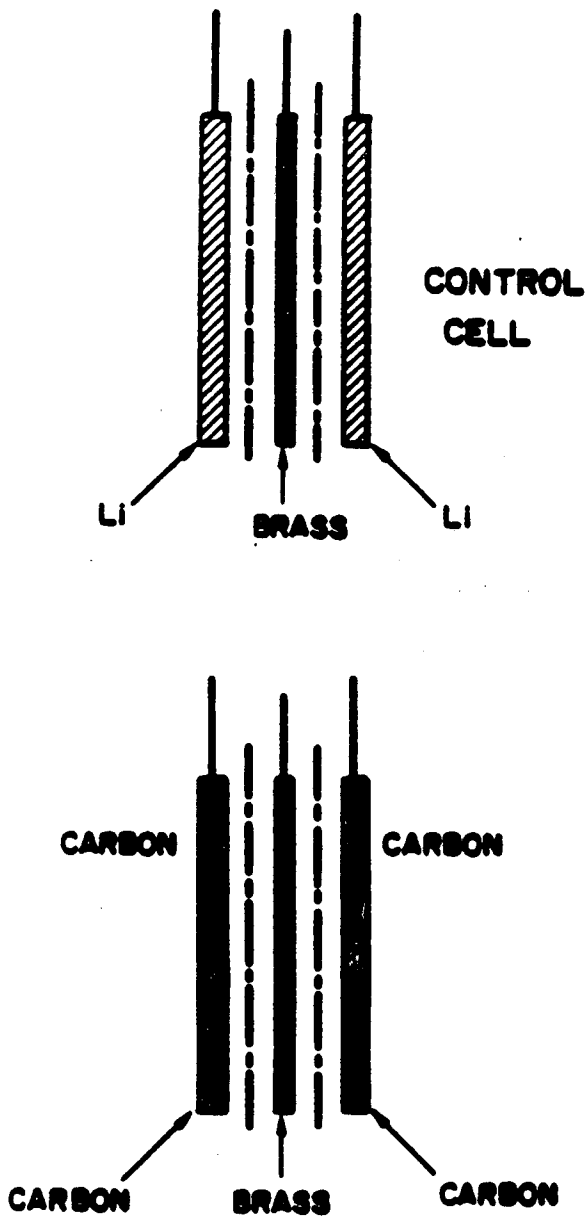

FIGURE 66. Experimental Cell for Overcharge Study.

charge Li is plated on brass negative and Cl_2 and $AlCl_3$ are generated on the carbon electrode. The cells were then stored at room temperature for a period of time to allow the plated lithium on brass to recombine with the overcharge products. The amount of lithium which had not been reacted with the overcharge products after the rest period was then determined by stripping electrochemically. The average rate of recombination during plating and the rest period was calculated from the amount of lithium remaining. However, since the efficiency of lithium deposition/dissolution is not 100%, control cells of brass versus lithium electrodes were used to determine the efficiency of lithium plating/stripping in the same electrolyte, $LiAlCl_4$-$6SO_2$, for the same amount of "overcharge" and rest period as the cells containing the carbon electrodes. The data obtained with the control cells was used for making necessary corrections in determining the average recombination rates.

Figure 67 shows the amount of the deposited lithium which has been reacted with the overcharge products after being "overcharged" for 60 mAhs and rested for various periods. The cells were made with Celgard separator. The average rate of recombination within the first 20 hours of the rest period is about 0.028 mA/cm^2, which can be calculated from the initial slope of the curve. Experiments were carried out to various extents of overcharge. In these experiments the deposited lithium was stripped immediately after

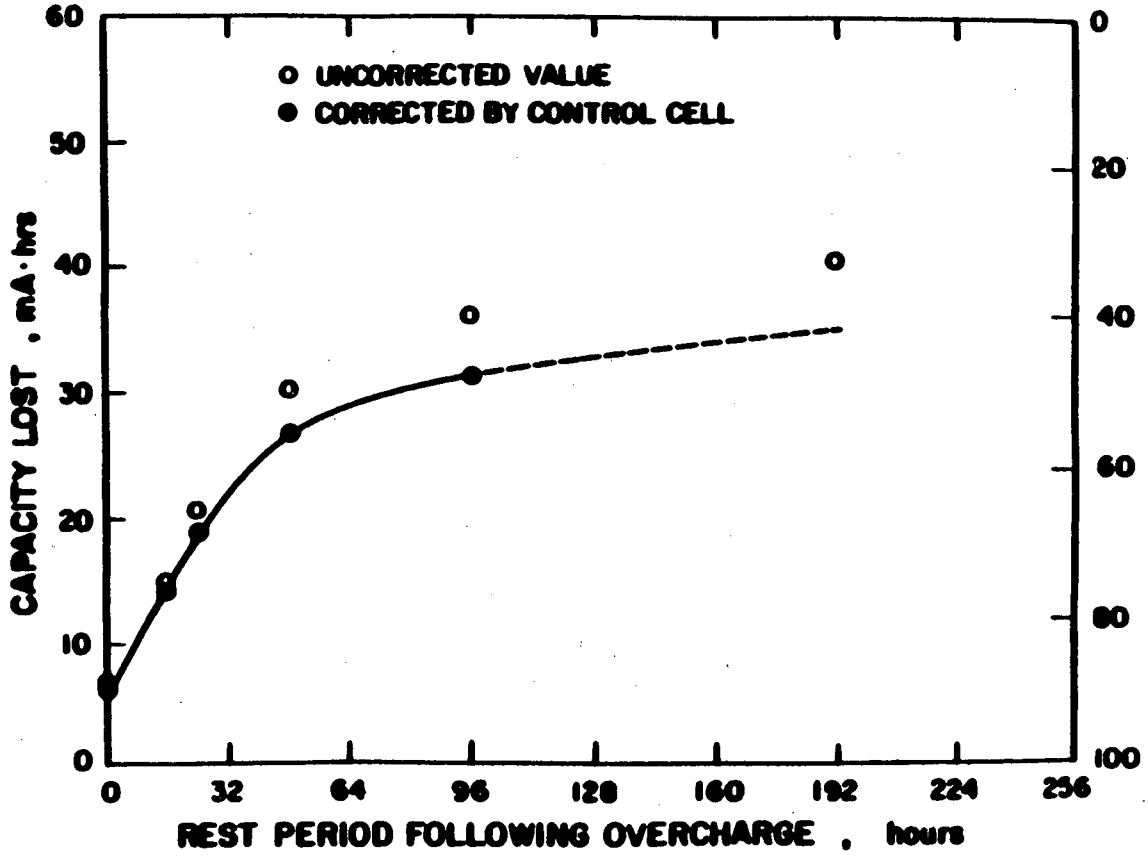

FIGURE 67. Capacity Loss of the Plated Lithium Electrode on Rest After Charge.

overcharge without rest. Figure 68 shows the average recombination rate as a function of the amount of overcharge for two types of separators. The results indicated that the rate of recombination of the overcharge products increases with increasing the amount of overcharge or the concentration of the overcharge products. Furthermore, the rate of recombination depends also on the type of separator. Asahi Hipor 3000 separator has higher porosity with larger pore size than the Celgard separator as compared in Figure 69. The recombination rate of the cell with Asahi separator, as shown in Figure 68 is also considerably higher than that of the cell with Celgard separtor. The recombination rate of 0.4 mA/cm^2, shown in Figure 68 is equivalent to approximately C/16 for a real 2/3A wound cell.

b. Overcharge of 2/3A Wound Cells

According to the data shown in Figure 68 a 2/3A wound cell should be able to take overcharge continuously at C/20 rate with either K-857 or Asahi 3000 separator. Experiments were carried out to investigate the capability of the 2/3A cells to take extensive overcharge. Figure 70 shows the result for cells with 2 layers Asahi 300 separator at various overcharge rates. Each cell contained about 4 grams of electrolyte which was equivalent to about 200 mAh of charge for lithium ions or $AlCl_4^-$ anions. Theoretically,

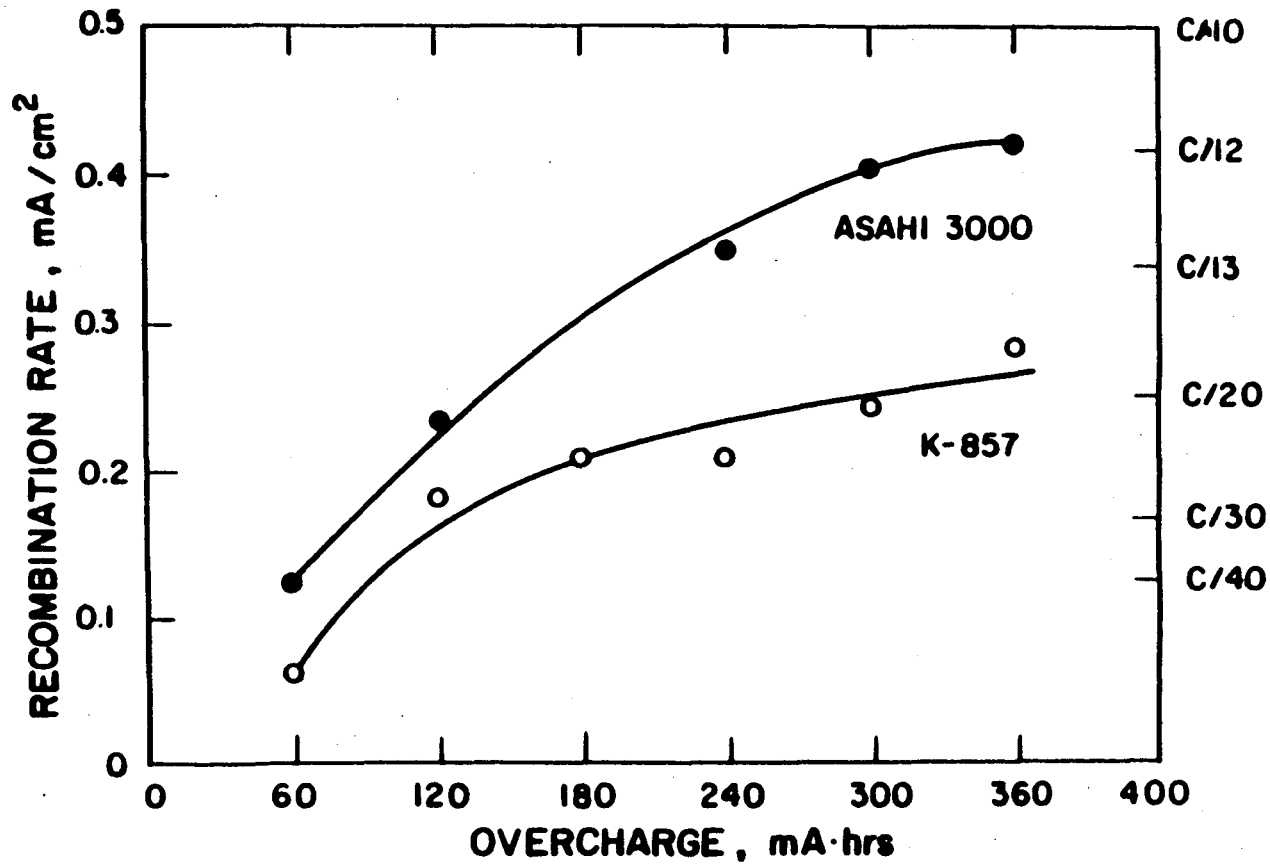

FIGURE 68. Recombination Rate as a Function of the Amount of Overcharge for Two Types of Separator.

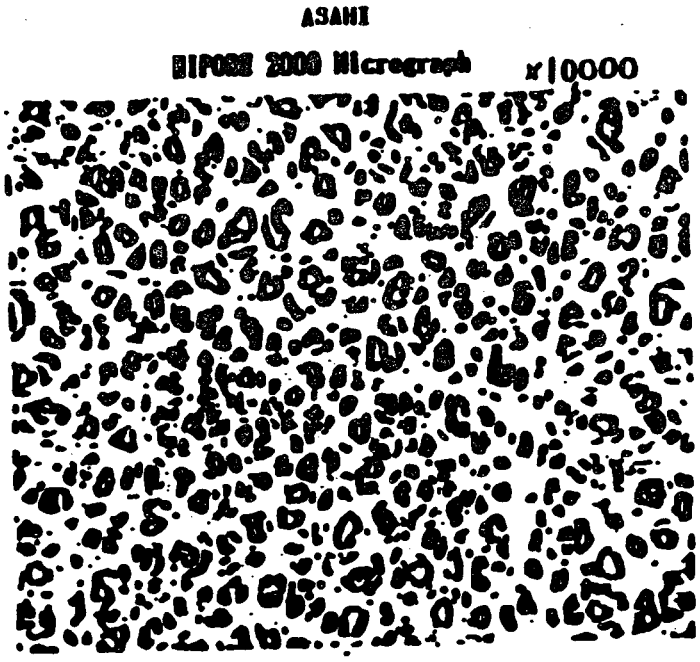

	ASAHI HIPORE #3000	Celgard 2500
Porosity	90%	45%
Thickness	50 micron	25 micron
Pore Size	0.5 micron	0.04 micron

FIGURE 69. Comparison of the Structure of the Asahi Hipore Separator and that of the Celgard Separator.

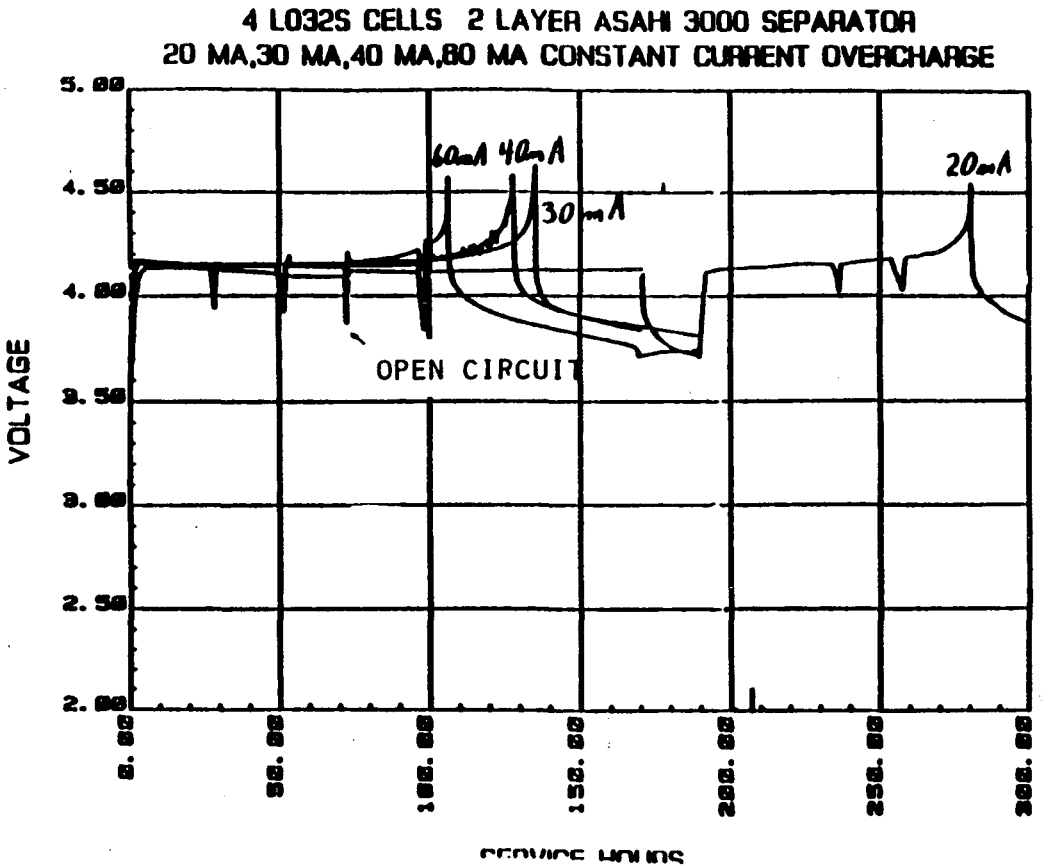

FIGURE 70. Voltage Characteristics of the 2/3A Size $Li/LiAlCl_4$-$6SO_2$/Carbon Wound Cells With Asahi Hipore 3000 Separator Overcharged at Various Rates.

if the recombination rate could not keep up with the charging rate, the cell should fail due to depletion of the charge carriers in the electrolyte. The sharp rise of the cell voltage before failure as shown in Figure 70 seemed to be caused by this process. However, all cells with a sharp rise in cell voltage after prolonged overcharge were also found to have vented. The rise in cell voltage could be due to exhaustion of electrolyte after venting. Figure 70 indicated also that the cells overcharged at higher rates failed earlier than cells overcharged at lower rates. Tests of wound cells made with Celgard K-857 separator showed that the cells failed significantly sooner than cells with Ashai 3000 separator as exhibited in Figure 71. K-857 separator is similar to Celgard 2500 and has much smaller pore size and less porosity compared with Asahi 3000 separator as shown in Figure 69. A less open separator gave a lower recombination rate due to poor transport of the overcharge products. The results is consistent with that obtained with experimental prismatic cells as exhibited in Figure 68.

Table 20 summarizes the test results of the wound cells with various separators on prolonged overcharge. Cells with K-857 separator could take an amount of overcharge equivalent to about 3 times its primary cell capacity and cells with Asahi separator can take an amount of overcharge equivalent to over 10 times its primary capacity. Table 20 also shows that cells made with only one layer of separator (cell #8,9,10) are more prone to developing internal

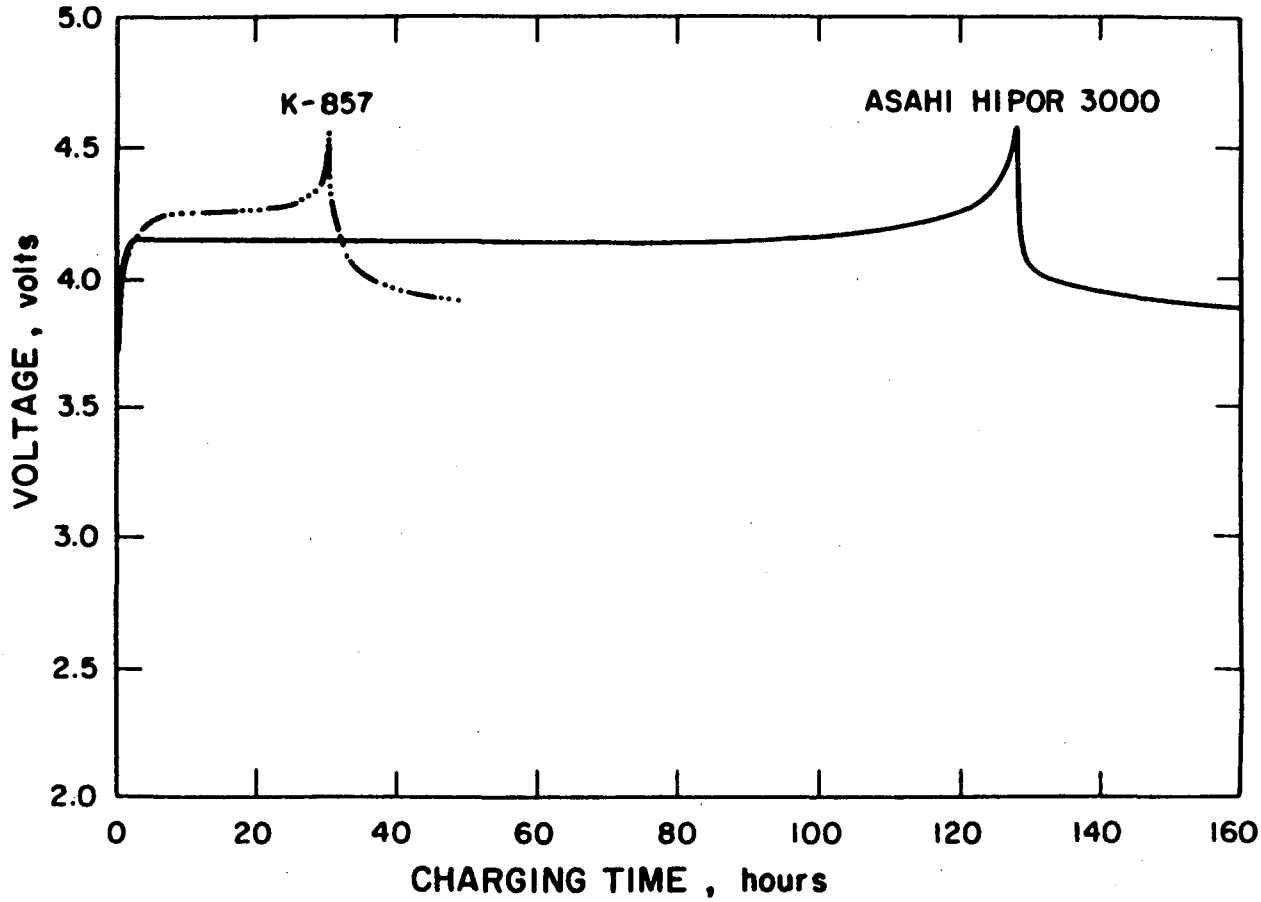

FIGURE 71. Comparison of the Voltage Characteristics of 2/3A Size $Li/LiAlCl_4$-$6SO_2$/Carbon Wound Cell Having Different Separators on Overcharge at 40 mA Rate.

TABLE 20. OVERCHARGE DATA OF 2/3A SIZE WOUND CELLS MADE WITH VARIOUS SEPARATORS

Separator	Cell #	Rate	Service Hours	Amount of Overcharge
K-852 (2 Layers)	1	40 mA	30 Hr.	1.2 Ah
	2	20 mA	30 Hr.	1.2 Ah
ASAHI 3000 2 Layers	3	60 mA	100 Hr	6 Ah
	4	40 mA	130 Hr	5 Ah
	5	30 mA	135 Hr	4 Ah
	6	20 mA	250 Hr	5 Ah
		Cycle 5 times then overcharge		
	7	20 mA	300 Hr	6 Ah
ASAHI 3000 1 Layer	8	40 mA	200 Hr	8 HH (Short)
	9	20 mA	350 Hr	7 Ah (Short)
		Discharge 2V then Overcharge		
	10	40 mA	110 Hr	4 Ah (Short
ALUMINA	11	20 mA	720 Hr	14 Ah
	12	40 mA	200 Hr	8 Ah (Short)
	13	20 mA	600 Hr	12 Ah (Short)
	14	10 mA	720 Hr	7 Ah

shorts on overcharge compared to cells made with 2 layers of separator (cell #4,6,7) tested at the same rates. However, cells made with one layer of separator could be overcharged significantly longer than cells made with 2 layers of separator. This indicates that the separator is actually limiting the rate of recombination of the overcharge products.

Alumina separator (F-K Fiber Products, Inc., Al-2) is inert chemically to the electrolyte and Cl_2. Since it is brittle, flexible pieces of separator with thickness less than 10 mils were not available. Although it is impractical to use a thick separator in wound cells, cells were made to demonstrate the overcharge capability. As shown in Table 20, cells with alumina separator were able to charge continuously at 20 mA for 600 Hrs or 200 Hrs at 40 mA without showing shorting or depletion of the electrolyte.

According to the data for Cell no. 3 shown in Table 20, which was charged at 60 mA and lasted for 100 Hrs. With about 4 grams of electrolyte, the recombination rate was estimated to be about 58 mA. With such a high value of recombination rate, cells overcharged at 40, 30 or 20 mA should last indefinitely without showing the type of failure as depicted in Figure 70. One of the cells with 2 layers of Ashahi Hipore 3000 separator was opened for examination after failure. The separator was adhering to the lithium electrode and had turned completely black and brittle. Degradation of the

polyethylene separator due to reaction with Cl_2 and $AlCl_3$ might have closed the pores and impeded the recombination.

Figure 72 shows the discharge performance of a 2/3A size cell with Asahi Hipor 3000 separator after being overcharged at 60 mA for 40 Hrs (6 times of the primary cell capacity) and rested for one week. The voltage curve showed only a very little portion of chlorine discharge since most of the dissolved overcharge products. Cl_2 and $AlCl_3$, were recombined during the rest period. The delivered capacity after overcharge was essentially the same as a fresh cell.

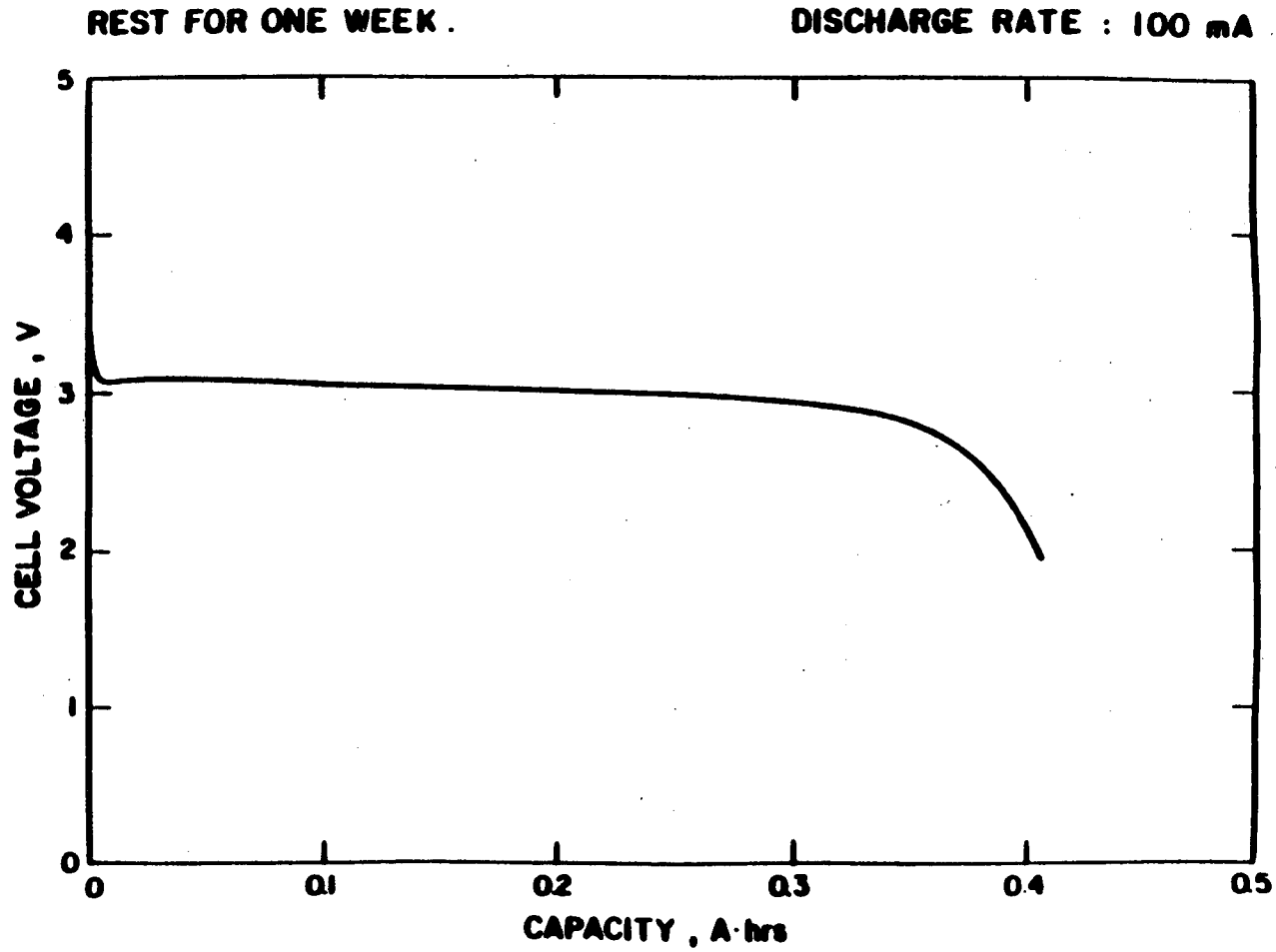

FIGURE 72. Discharge Characteristics of a 2/3A Size $Li/LiAlCl_4$-$6SO_2$/Carbon Wound Cell After Being Overcharged at 60 mA for 40 Hours and Rest for One Week.

V Li/$CuCl_2$ SYSTEM

A. INTRODUCTION

Since the totally inorganic SO_2 electrolytes with proper lithium salts can provide high conductivity and good lithium plating efficiency. They are certainly suitable to operate with solid active positive materials. With active solid positive electrodes, the solvent, SO_2, and the lithium salt are not the main active reactants and should not be consumed during discharge. Therefore, it will not have the problem of electrolyte starvation or accumulation of discharge products in the porous electrode as in the case with carbon positive electrode. The cell capacity will not be limited by the amount of electrolyte either.

Studies were carried out to explore new solid positive electrode materials for use with the inorganic SO_2 electrolytes. Experimental prismatical cells similar to that shown in Figure 22 were employed for the evaluation. The positive electrodes were prepared by mixing the active material with proper amounts of the electrode mixtures were then pressed on a expanded nickel screen using a steel die. The positive electrode of size, 2.5 cm x 4 cm, was then sandwiched between two lithium electrodes (10 mil in thickness) and installed in the D size can with Teflon shims and spacers. The positive electrode materials were evaluated with both

the $LiAlCl_4$-$3SO_2$ and the pressurized 1 M $liGaCl_4/SO_2$ electrolytes. All cells were discharged at 1 mA/cm^2 to a 1.0 V cut off to determine the capacity utilization and specific energy.

Table 21 lists the positive materials evaluated and the test results in both the $LiAlCl_4$-SO_2 and the 1M $LiGaCl_4/SO_2$ electrolytes. Some typical discharge voltage profiles are shown in Figures 73 to 75. Since the active materials were mixed with Ketjen Black EC carbon for providing electronic conductivity, most electrodes showed OCV reflecting the equilibrium potential of SO_2 or $LiAlCl_4$-$3SO_2$ on carbon and the voltage profiles are also exhibited the portion contributed by the electrolyte or SO_2 reduction in addition to the discharge of the solid positive material. Many positive electrodes showed the synergetic effect and delivered more than 100% of their theoretical capacities. However, some electrode materials showed only the discharge of the electrolyte similar to a pure carbon electrode.

Among the solid positive electrodes tested, $CuCl_2$ has shown the best rechargeability with reasonable energy density. Other transition metal halides such as $NiCl_2$, $CoCl_2$, AgCl, $CuBr_2$ $CrCl_3$ etc., have also shown reasonable capacity utilization and rechargeability.

Table 20. Discharge Performance of Various Solid Positive Electrode Materials

(Positive Electrode Mix : Active Material 80%, Carbon 12% PTFE 8%)

Discharged at 20 mA (1 mA/cm^2) to 1.0 V Cut-off.

Material	Capacity Delivered			
	$LiAlCl_4$-$3SO_2$		1M $LiGaCl_4/SO_2$	
	OCV	mAh/g	OCV	mAh/g
AgBr	3.16	263	2.89	100
$CuBr_2$	3.45	168	2.59	119
CuF_2	3.47	79.4	3.49	91.8
$NiCl_2$	3.15	500	2.90	167
$CoCl_2$	3.18	207	2.91	176
NiF_2	3.16	188.2	2.96	167
AgI_2	3.15	105	2.88	110
CuI	3.43	100	3.19	116
$CrCl_3$	3.15	215	3.00	163
AgCl	3.15	400	2.88	112
MnCl2	3.19	135	3.07	28
$MoCl_3$	3.77	220	3.81	93.3
$ZnCl_2$	3.14	38.9	3.13	72.2
$MoCl_5$	4.01	221	4.09	116
FeF_3	-	53.8	-	258
ZrF_4	3.16	21.4	3.05	164
$PbCl_2$	3.96	212	3.00	118
CoF_3	3.96	16.7	-	163.9
V_2O_5	3.45	191	3.25	200
$Mo(OCl)_2$	3.78	121	3.64	110
$HgCl_2$	3.17	116	3.26	131
$FeBr_3$	3.86	287	3.78	146
$ZnBr_2$	-	154	-	-
$ZrCl_4$	-	-	3.82	147
$MoCl_4$	-	-	3.98	168
MnF_2	-	-	3.19	115
$SnCl_2$	-	-	3.01	54
BiOCl	3.10	70	3.06	258
Hg_2Cl_2	-	-	2.95	242
$FeCl_3$	3.90	63	3.79	57
CuCl	-	-	3.34	74
$CuCl_2$	3.42	760	3.44	225
FeS_2	3.20	219	-	-
NiS	-	-	2.90	530

Discharge at 1 mA/cm^2 to 1.0 V
(Active Material 80%, Carbon 12%, PTFE 8%)

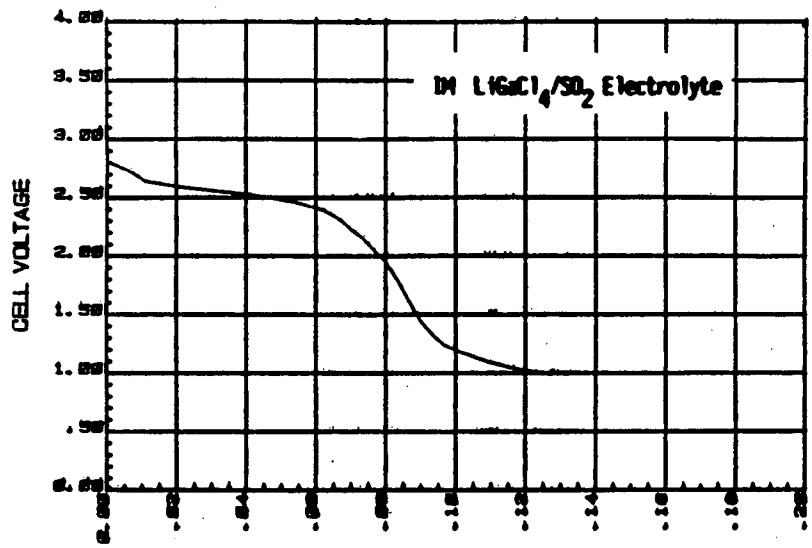

FIGURE 73. Discharge Characteristics of Solid Positive Electrodes

(I) $FeCl_3$

Discharge at 1 mA/cm^2 to 1.0 V
(Active Material 80%, Carbon 12%, PTFE 8%)

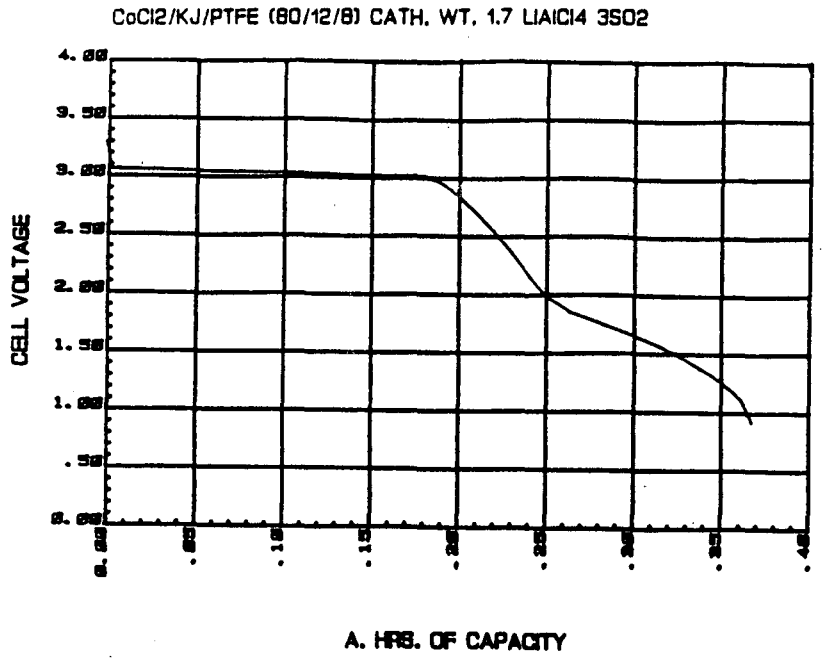

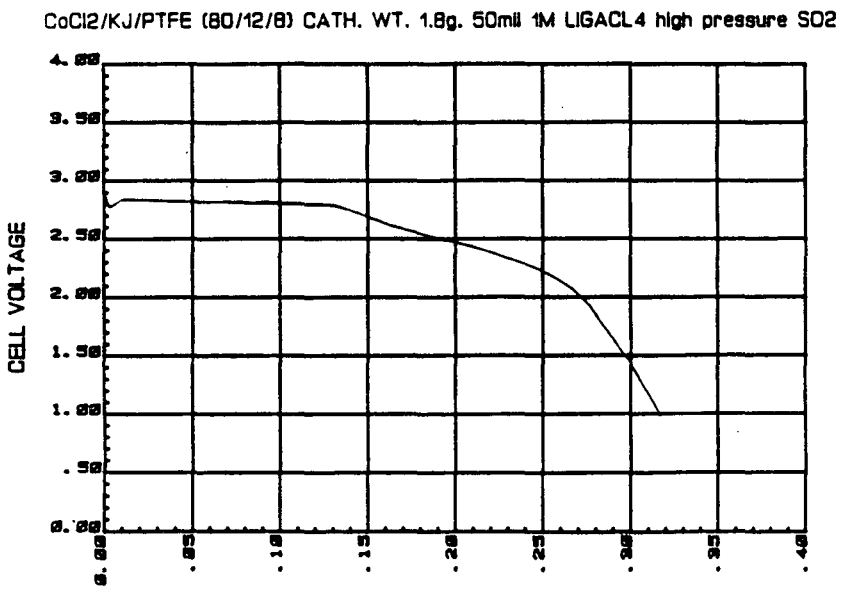

FIGURE 73. Discharge Characteristics of Solid Positive Electrodes (II) $CoCl_2$,

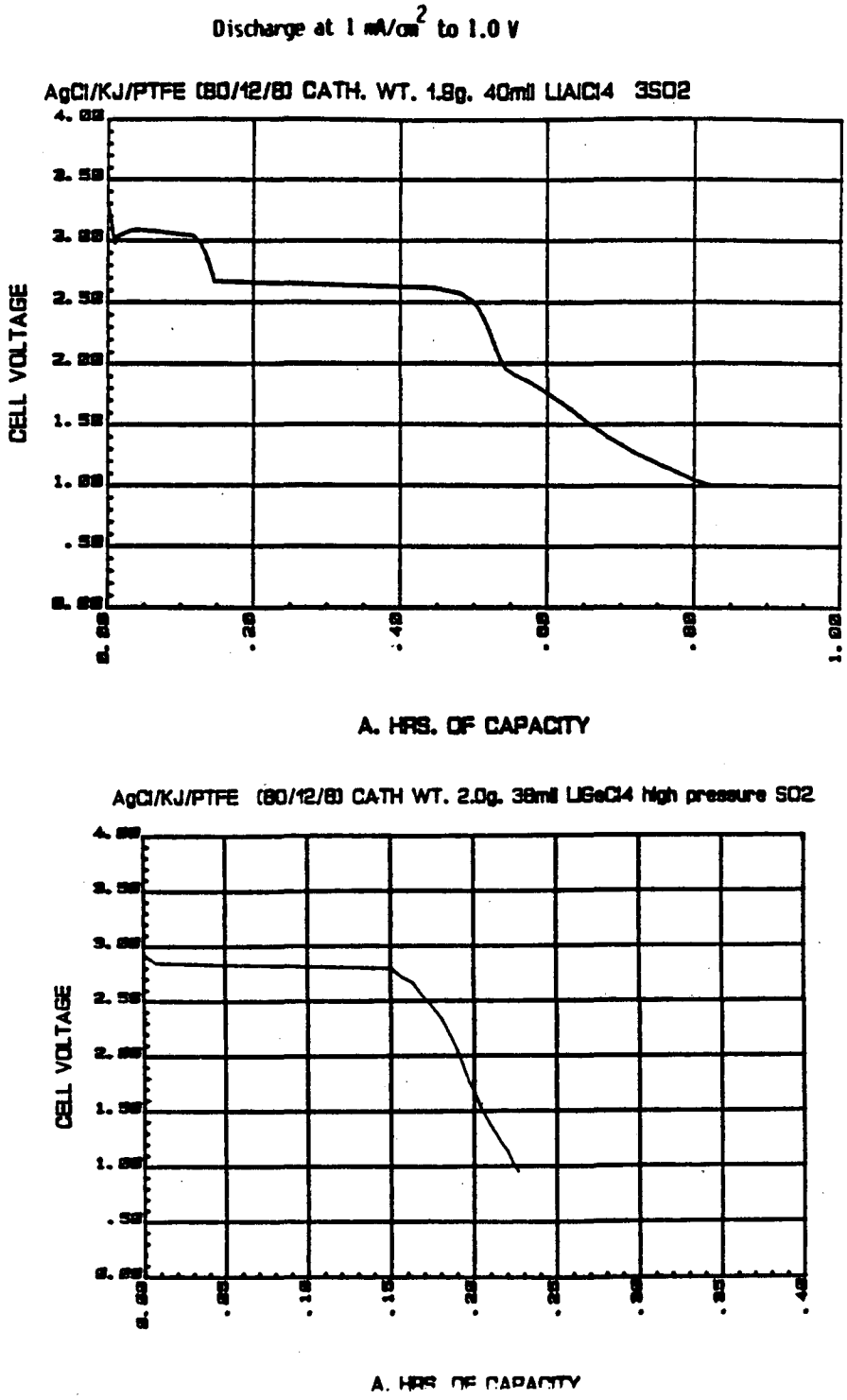

FIGURE 73. Discharge Characteristics of Solid Positive Electrodes (III) AgCl,

1 mA/cm^2

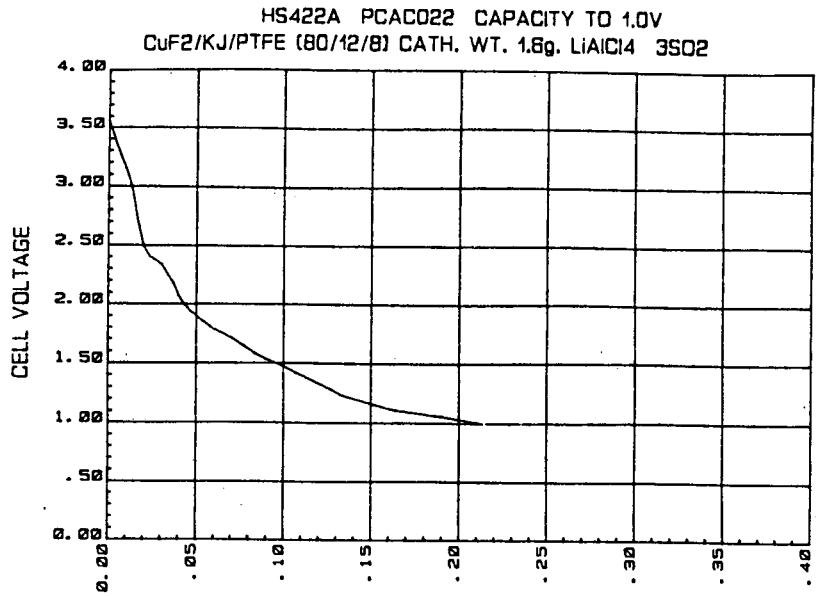

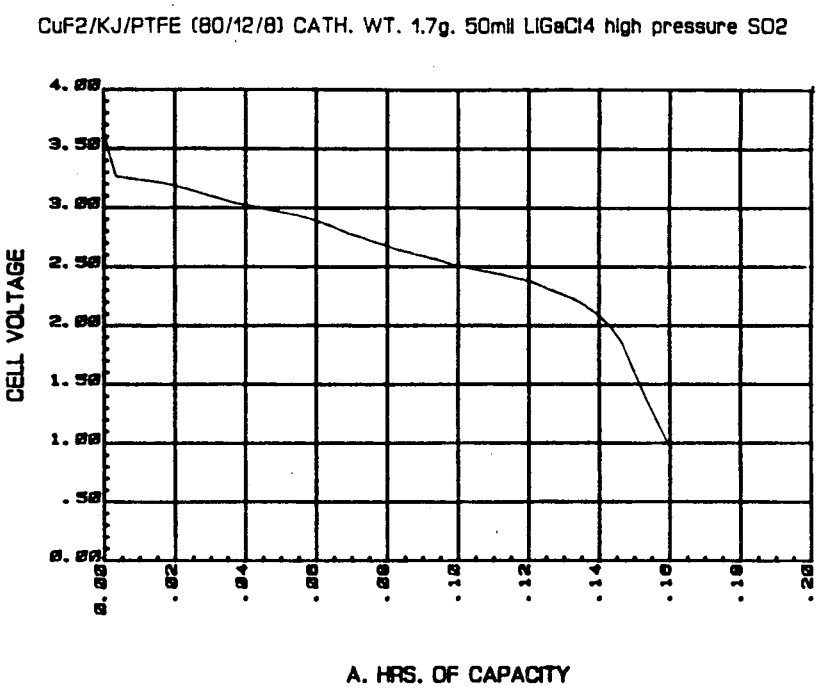

FIGURE 73. Discharge Characteristics of Solid Positive Electrodes (IV) CuF_2.

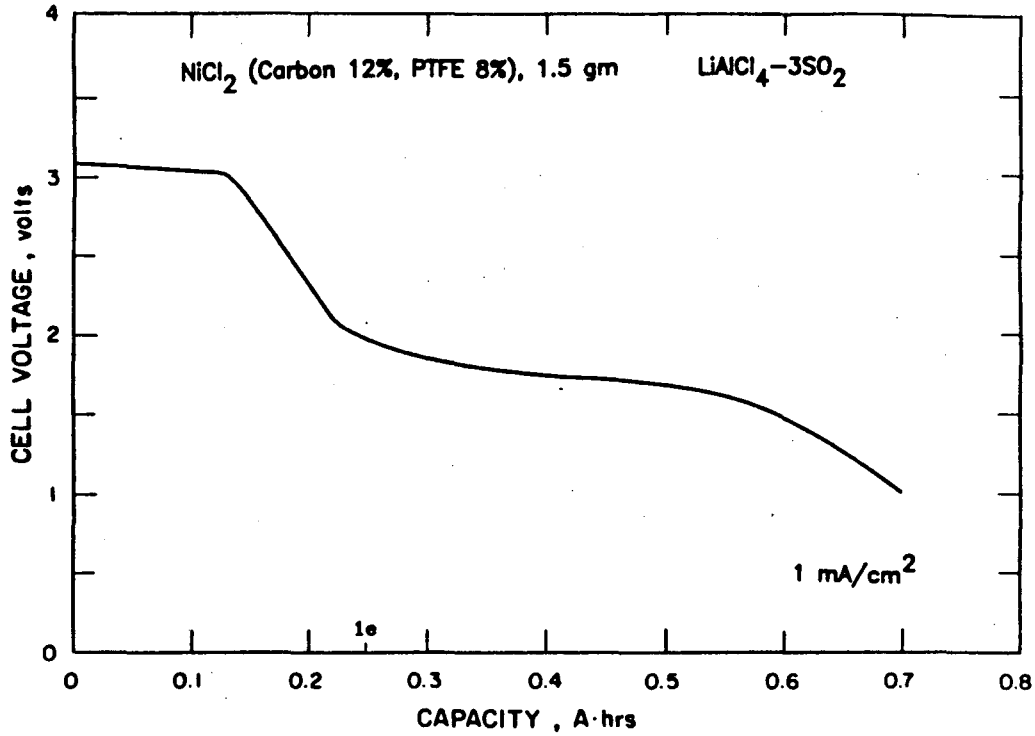

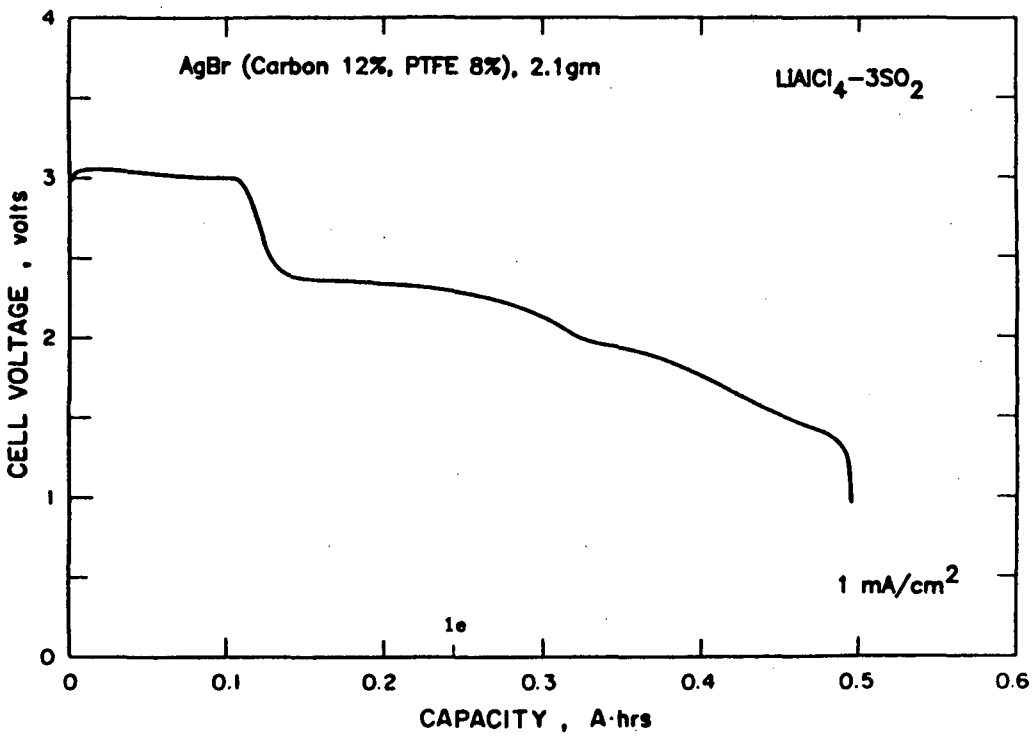

FIGURE 73. Discharge Characteristics of Solid Positive Electrodes (V) $NiCl_2$, (VI) AgBr.

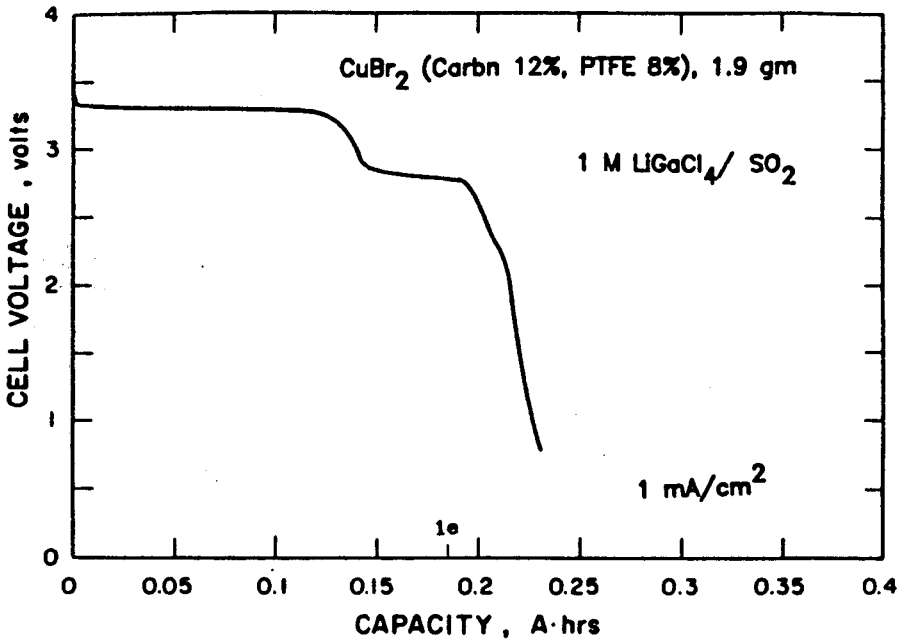

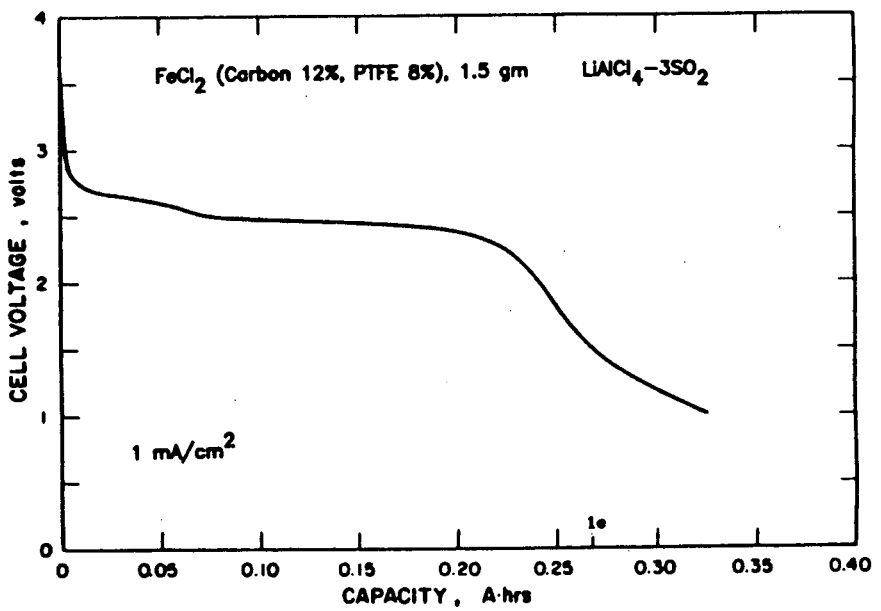

FIGURE 73. Discharge Characteristics of Solid Positive Electrodes (VII) $CuBr_2$ (VIII) $FeCl_2$

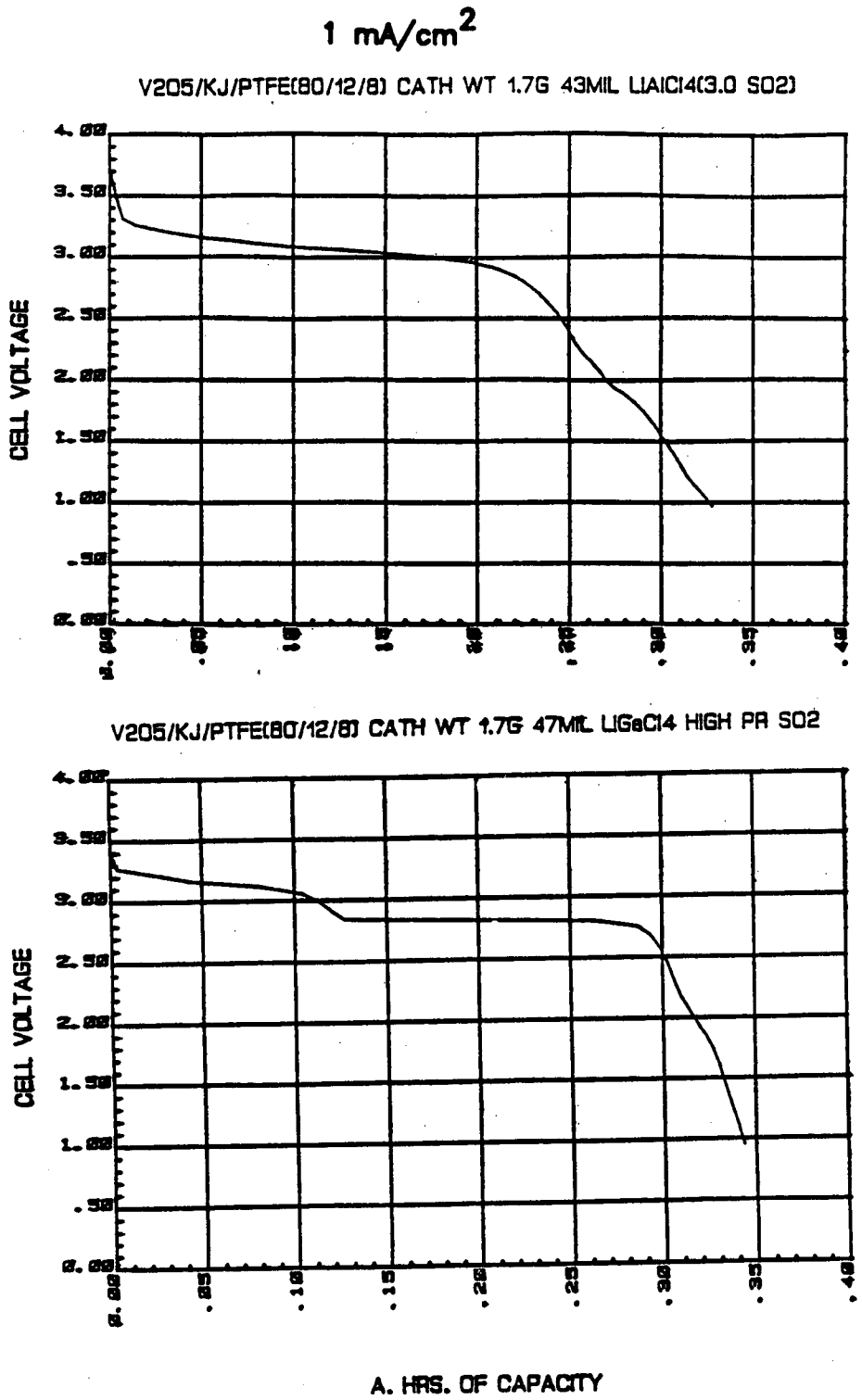

FIGURE 74. Discharge Characteristics of Solid Positive Electrodes (I) V_2O_5,

1 mA/cm^2

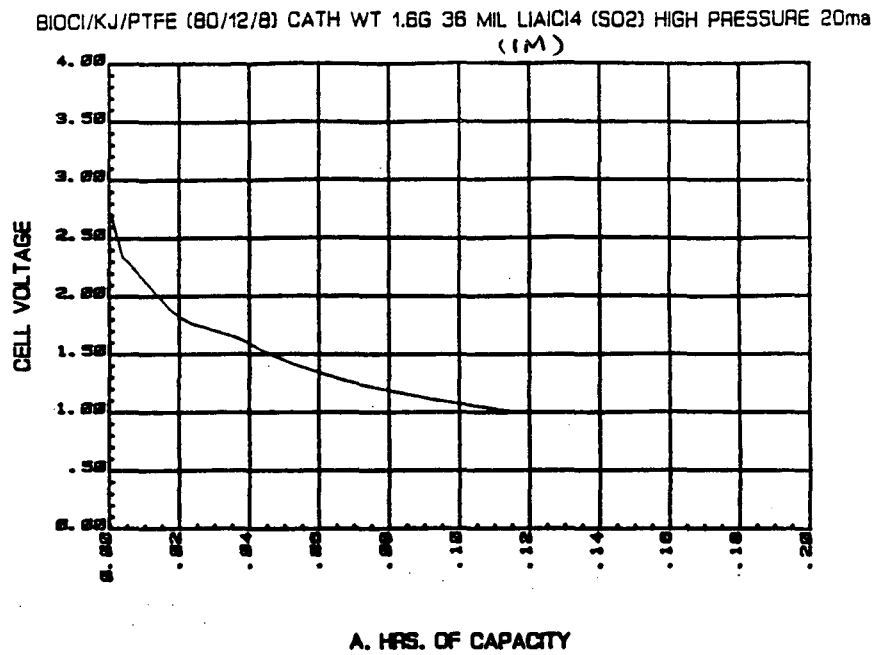

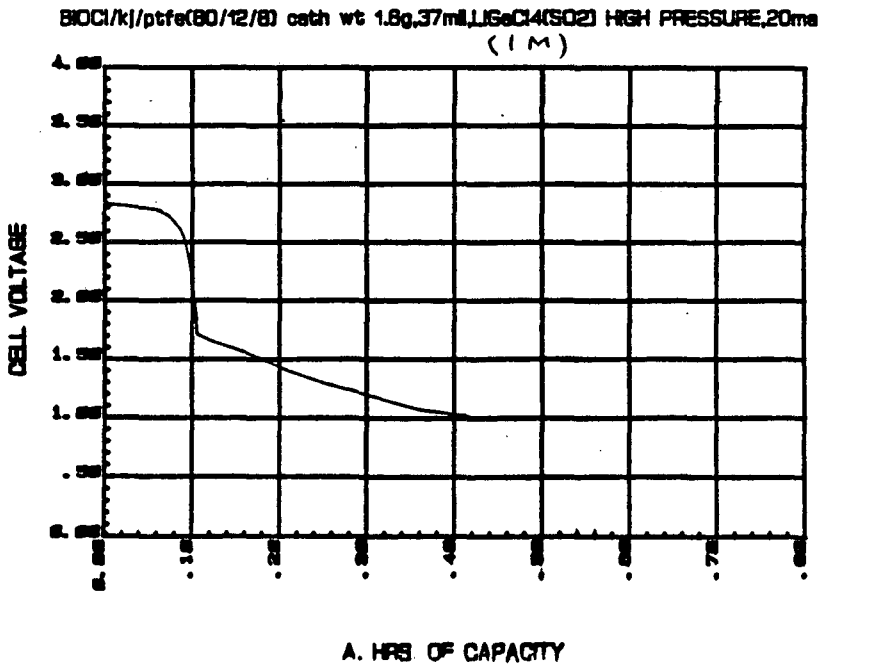

FIGURE 74. Discharge Characteristics of Solid Positive Electrodes (II) BiOCl.

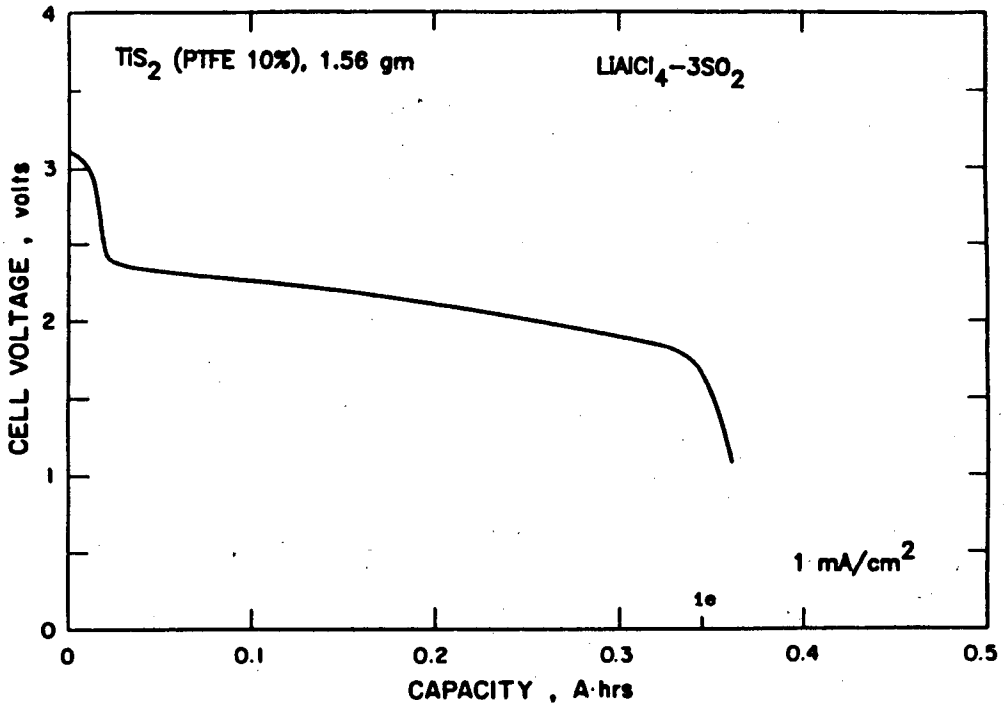

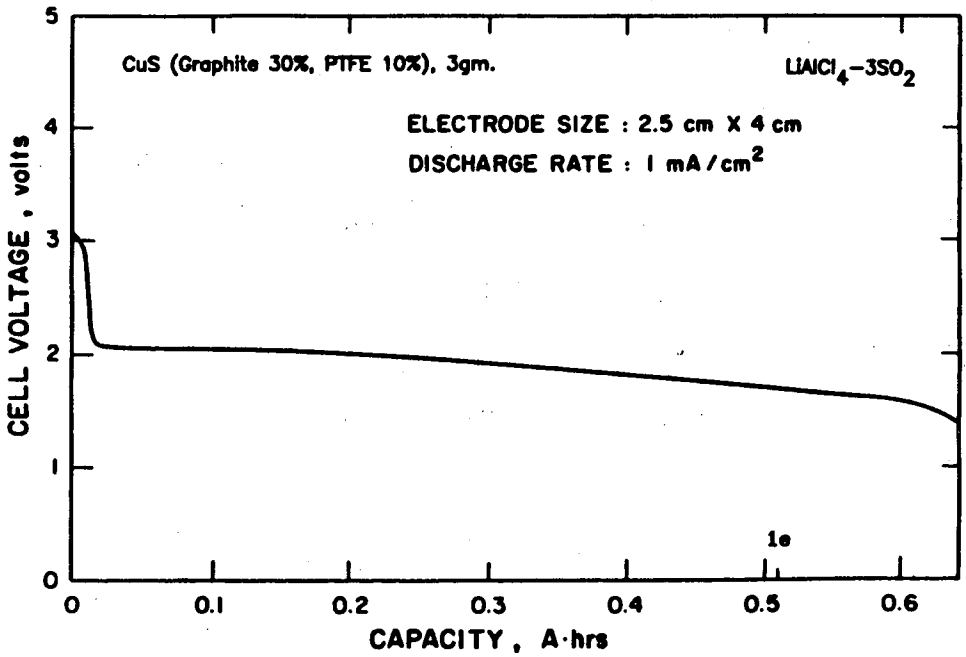

FIGURE 75. Discharge Characteristics of Solid Positive Electrodes (I)TiS_2, (II) CuS.

Since $CuCl_2$ showed the most promising performance in preliminary studies, extensive efforts were focused on the development and evaluation of this system. The details are described in following.

B. EXPERIMENTAL

The same prismatic cells as shown in Figure 22 were used to evaluate ther performance of the $CuCl_2$ positive material in various electrolytes. 2/3A size wound cells were also made for some evaluations.

C. CELL CHEMISTRY

Figures 76 and 77 show the typical discharge voltage profiles of $CuCl_2$ positive electrode in 1 M $LiGaCl_4/SO_2$ and in $LiAlCl_4$-$3SO_2$ electrolytes. The $Li/CuCl_2$ system has an OCV of 3.42 V and discharges in two major voltage steps. The first voltage plateau at near 3.3-3.4 V corresponds to the reduction of $CuCl_2$ to CuCl or $LiCuCl_2$.

$$CuCl_2 + Li^+ e \dashrightarrow LiCl + CuCl \text{ or } LiCuCl_2$$

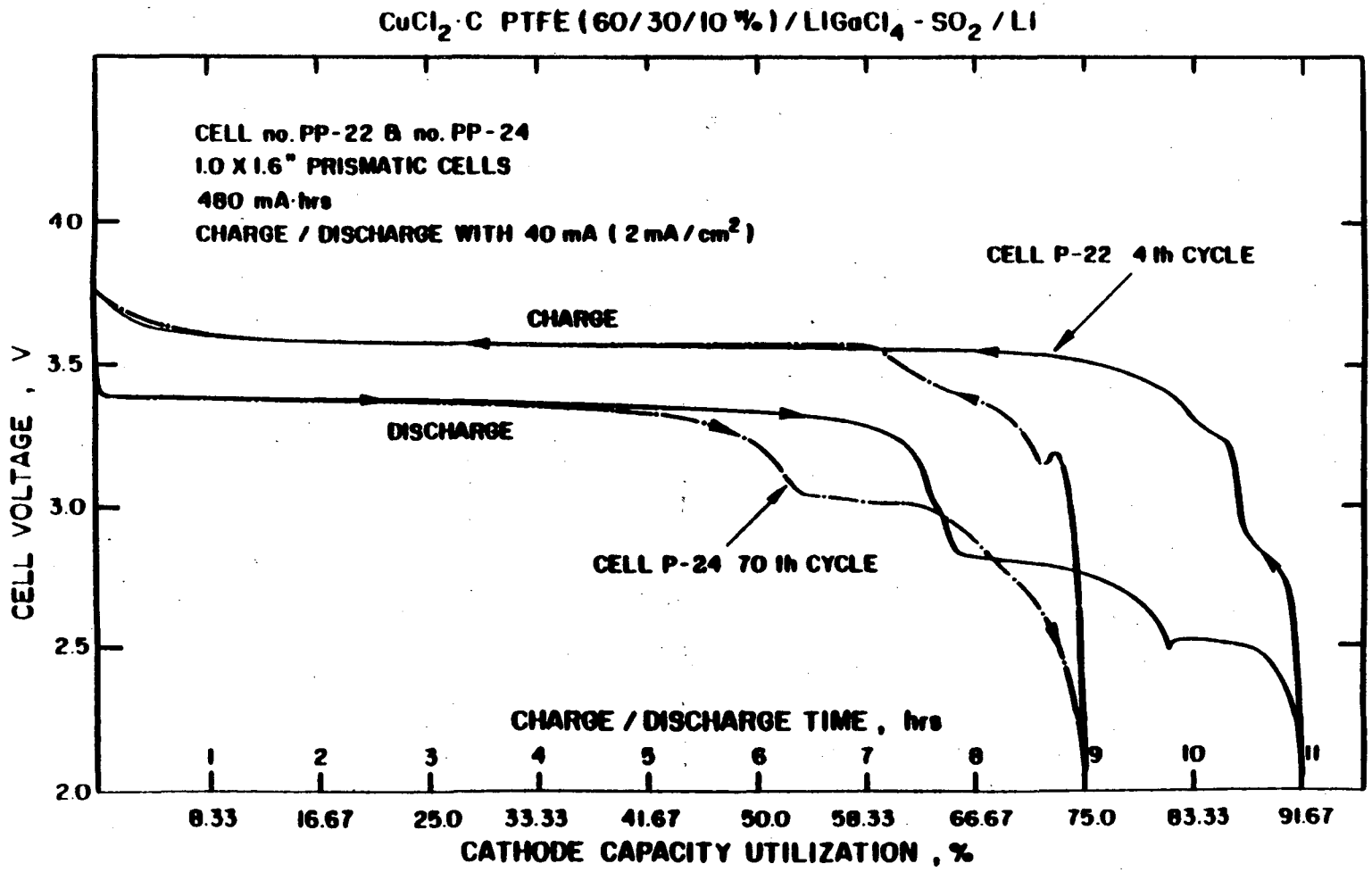

FIGURE 76. Voltage Characteristics of an Experimental $Li/CuCl_2$ Cell with 1M $LiGaCl_4/SO_2$ Electrolyte.

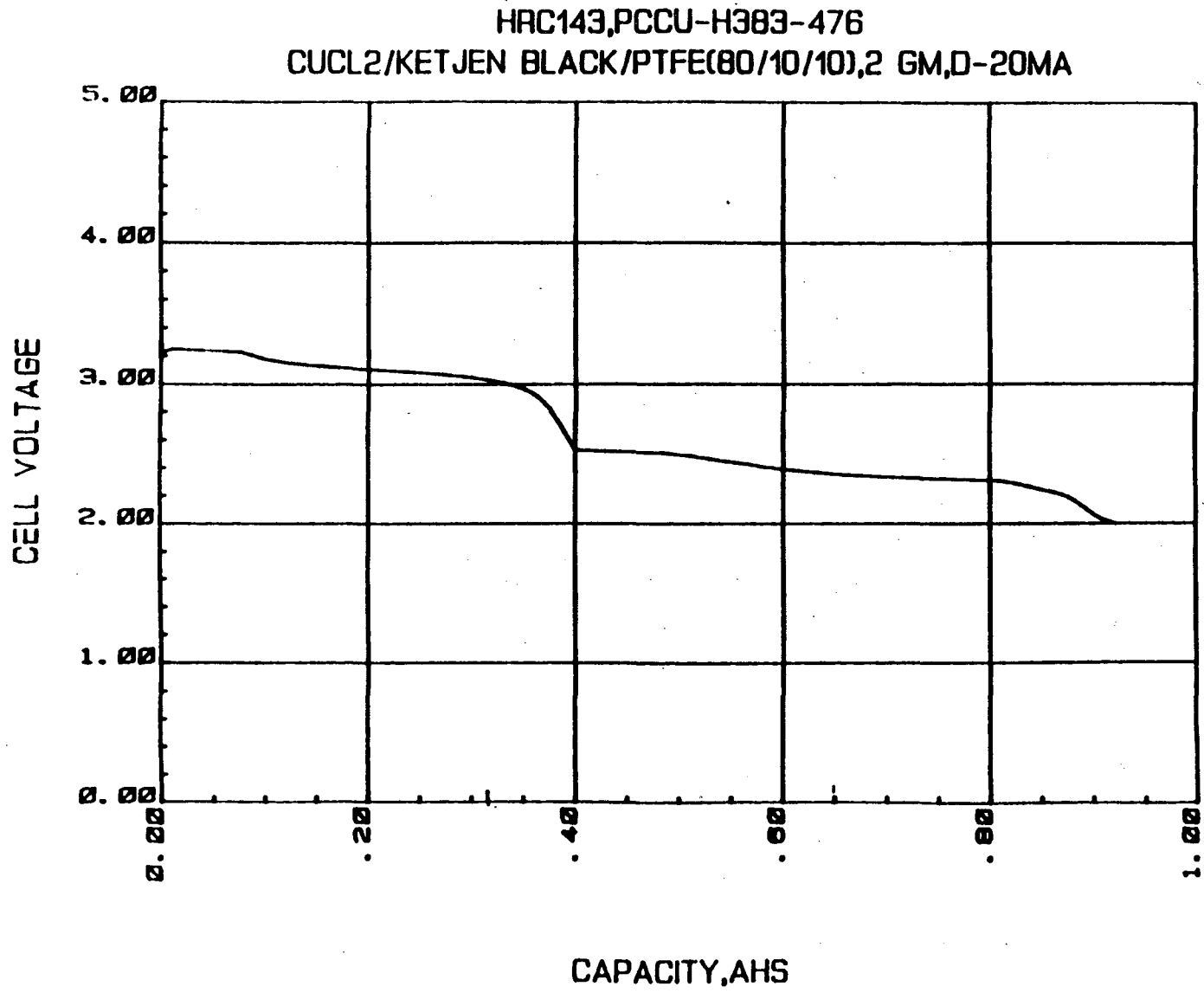

FIGURE 77. Voltage Characteristics of an Experimental Li/$CuCl_2$ Cell with $LiAlCl_4$-$3SO_2$ Electrolyte.

On further discharge to near 2.5V, another voltage plateau appears, which corresponds to the discharge of $LiCuCl_2$ to form LiCl and Cu.

$$LiCuCl_2 + Li^+ + e \text{ ------- } 2\ LiCl + Cu$$

The system has an energy density of about 1200 Whr/kg for 2 electron discharge and about 600 Whr/kg for one electron discharge. Since $CuCl_2$ is not conductive, the addition of carbon to obtain the electron conductivity is necessary. The utilization of the electrode material depends strongly on proper mixing of the active material and the carbon. It depends also on the type of electrolyte employed.

D. PERFORMANCE AND DISCUSSION

1. With $LiGaCl_4/SO_2$ Electrolyte.

As shown in Figure 76, the discharge voltage profile of a $CuCl_2$ positive electrode of composition, $CuCl_2$ 60 w%, graphite 30 w% and PTFE 10 w% in 1 M $LiGaCl_4/SO_2$ electrolyte exhibits three voltage plateaus. The first plateau near 3.4 V is the first electron discharge of $CuCl_2$. The second plateau at 2.8 V corresponds to the discharge of SO_2 on carbon while the third plateau at near 2.5 V is the discharge of the second electron of $CuCl_2$, from $LiCuCl_2$ to Cu

and LiCl. The utilization of the first electron discharge is near 100% while the that of the second electron discharge is rather poor, probably due to the interference of the SO_2 discharge.

Cells with $LiGaCl_4/SO_2$ electrolyte usually delivered about 100 cycles and failed with a gradual loss of capacity. Figure 78 shows the performance of a cell which had been discharged at various rates. It indicates that the cell capacity declines faster when operated at higher rates of discharge.

2. With 1M $LiAlCl_4/SO_2$ Electrolyte.

Figure 79 shows the typical first discharge/charge voltage profiles of a $CuCl_2$ electrode ($CuCl_2$ 60 w%, graphite 30 w%, PTFE 10 w%) in 1M $LiAlCl_4/SO_2$ electrolyte at 2 mA/cm^2 discharge rate. The voltage plateau near 2.8 V for SO_2 reduction as that shown in $LiGaCl_4/SO_2$ electrolyte was not observed. An electrode utilization of about 95% based on two electron discharge was obtained. The first electron discharge of $CuCl_2$ was rather poor while a long voltage plateau of the second electron discharge was observed. The capacity delivered with a flat voltage plateau of about 2.5 V was more than 100% of the theortical capacity of the second electron reduction for cuprous to copper. It was likely that the $LiCuCl_2$ or CuCl formed initially on the surface of the active particle

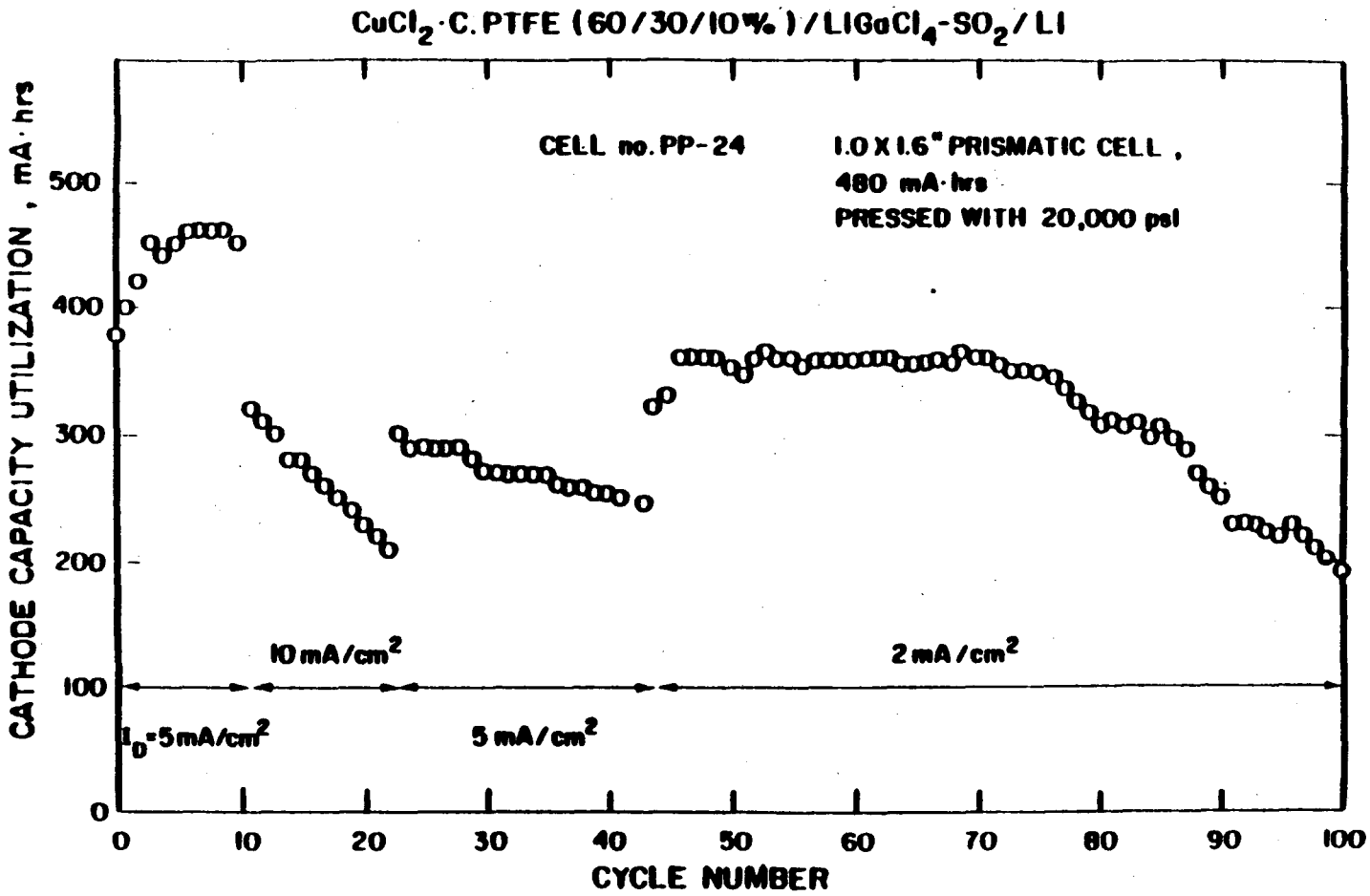

CELL PERFORMANCE ON CHARGE/DISCHARGE TESTING
CHARGE 2 mA/cm², DISCHARGE 2,5 AND 10 mA/cm² RATE

FIGURE 78. Cycling Performance of an Experimental Li/$CuCl_2$ Cell With 1M $LiGaCl_4/SO_2$ Electrolyte, Discharged at 2, 5 and 10 mA/cm^2 and Charged at 2 mA/cm^2.

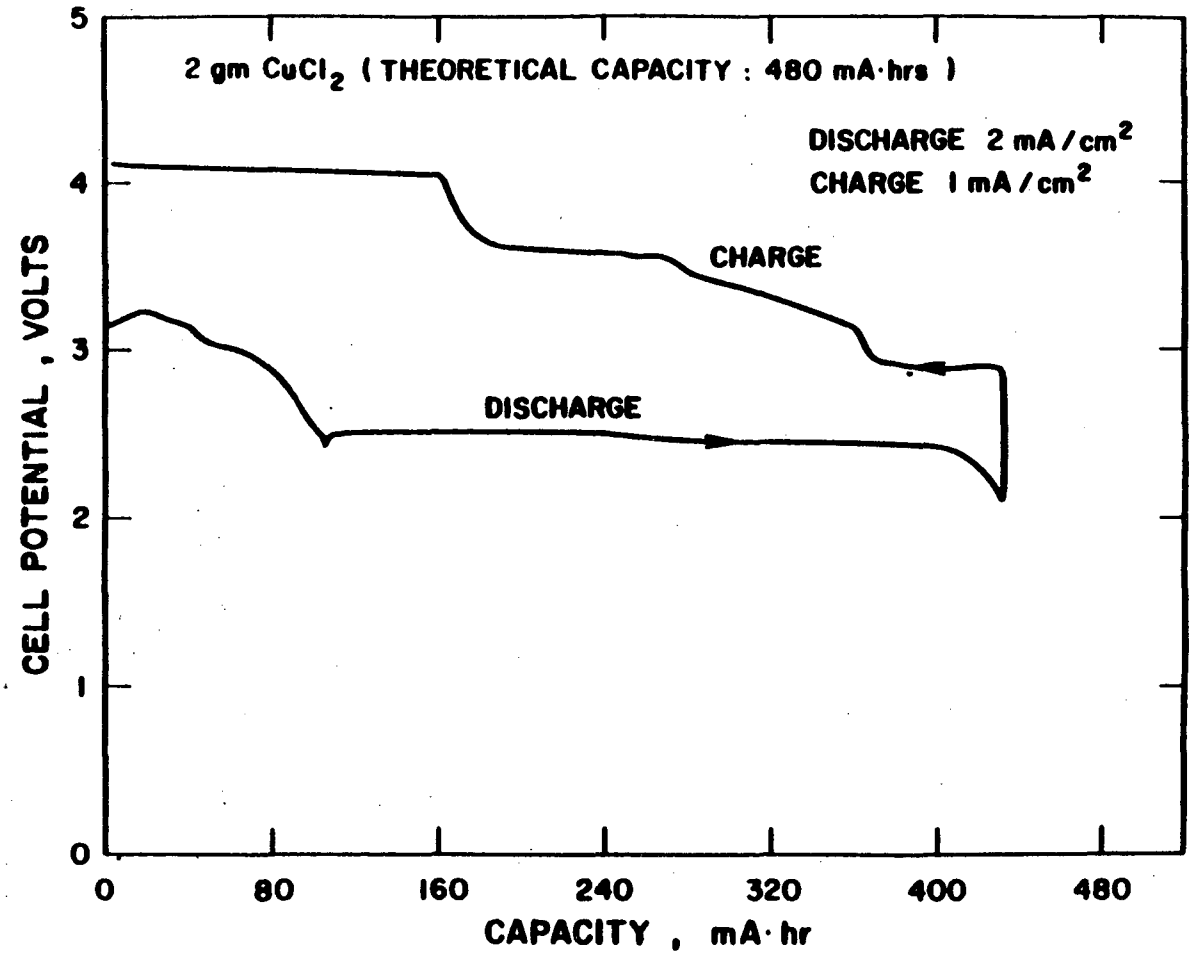

FIGURE 79. Voltage Profile of the First Cycle of an Experimental $Li/CuCl_2$ Cell with 1M $LiAlCl_4/SO_2$ Electrolyte, Discharged at 2 mA/cm^2 and Charged at 1 mA/cm^2.

during discharge was further discharged to Cu and LiCl. The freshly formed Cu might react rapidly with the undischarged $CuCl_2$ to reform the cuprous chloride. Therefore the electrochemical reduction of the cuprous chloride predominated and a long voltage plateau at about 2.5 V appeared.

Continuously cycling the cell to 2.0 V showed a rapid loss of capacity. However, the discharge of the first electron could be improved gradually when the cell was cycled to a cutoff of 2.6 V as shown in Figure 80. The cell was discharged at 2 mA/cm^2 and charged at 1 mA/cm^2. Lowering the discharge cutoff to 2.2 V at the 49th cycle showed good utilization on both electron utilization as exhibited in Figure 81-a. Further cycling of the cell to a 2.2 V cut-off caused a gradual loss of the second electron utilization as shown if Figure 81-b for the voltage profile at the 62nd cycle. The cell retained an overall electrode utilization of about 70% for the next 70-80 cycles and failed finally with a rapid loss of capacity after that.

3. With $LiAlCl_4$-$3SO_2$ Solvated Electrolyte.

a. General Performance

Discharge of $CuCl_2$ electrodes containing 10 w% carbon as conductive filler and 10 w% PTFE as binder in $LiAlCl_4$-$3SO_2$

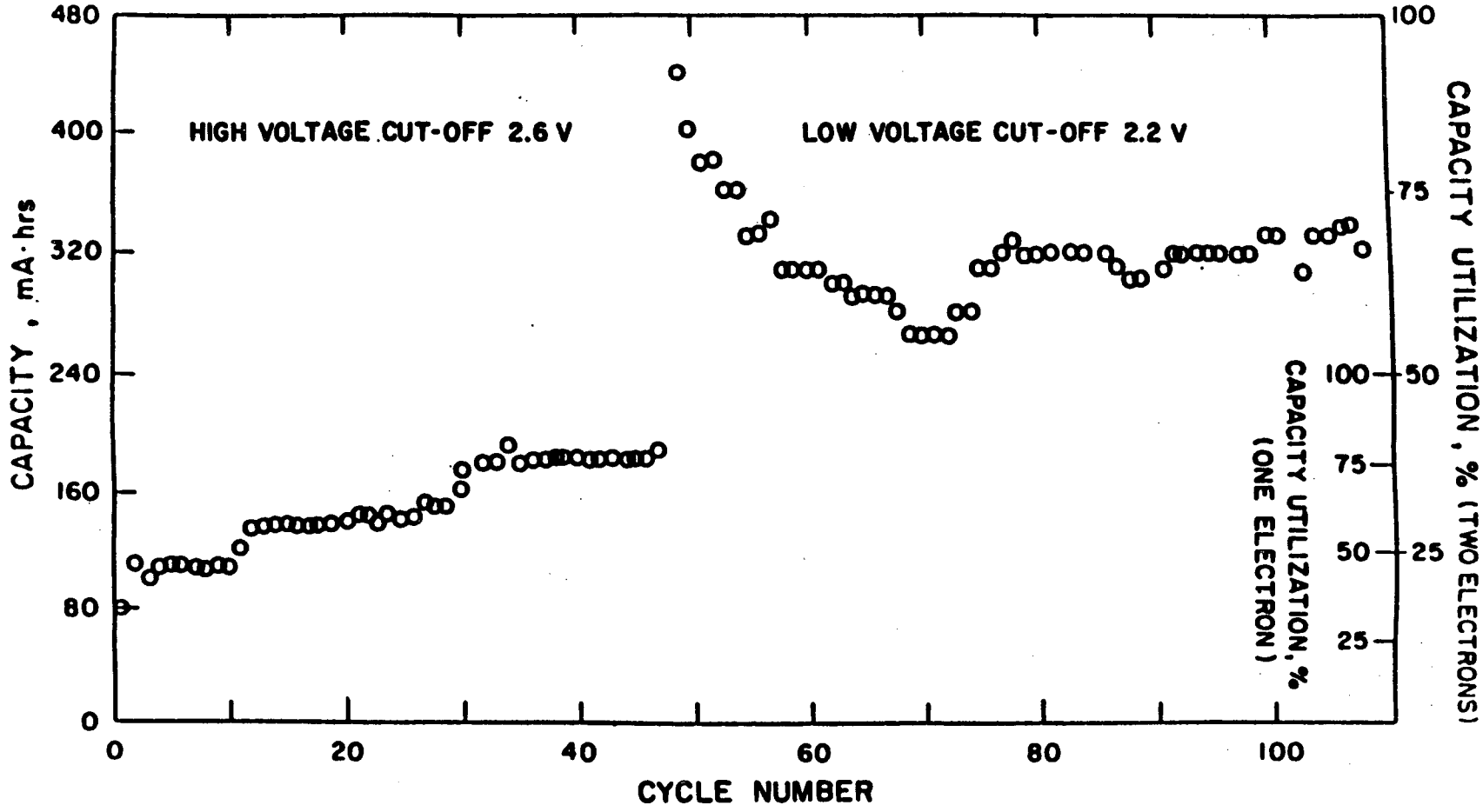

FIGURE 80. Cycling Performance of an Experimental $Li/CuCl_2$ Cell With 1M $LiAlCl_4/SO_2$ Electrolyte, Discharged at 2 mA/cm^2 and Charged at 1 mA/cm^2.

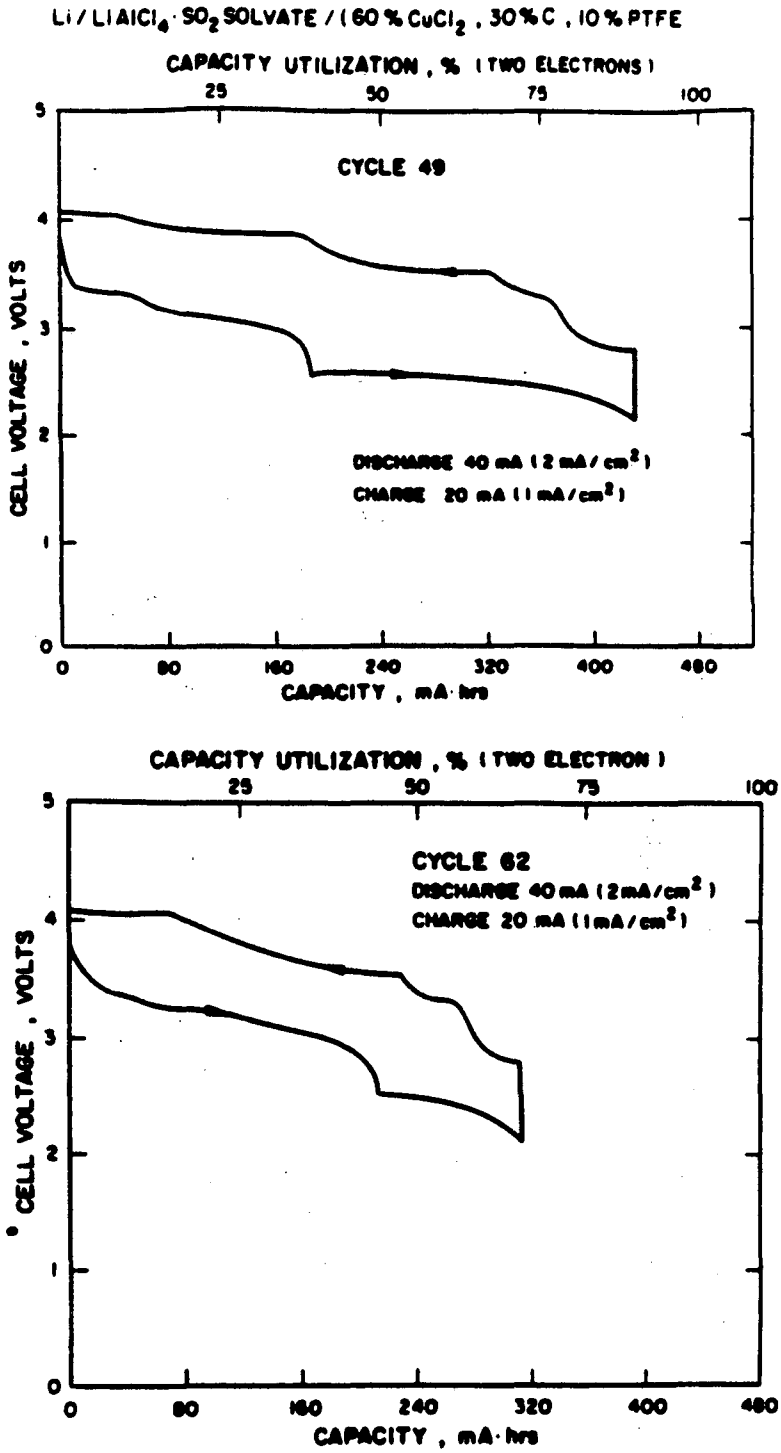

FIGURE 81. Voltage Profile of the 49th and the 62nd Cycles of an Experimental $Li/CuCl_2$ Cell with 1M $LiAlCl_4/SO_2$ Electrolyte, Discharged at 2 mA/cm^2 and Charged at 1 mA/cm^2.

electrolyte exhibited two major voltage plateaus, one near 3.2 V and the other at about 2.5 V, as shown in Figure 77. The capacity delivered was found significantly higher than the theoretical capacity based on the amount of $CuCl_2$ for 2 electron discharge. It was obvious that the additional capacity was contributed by the discharge of $LiAlCl_4$-SO_2 solvate on the carbon surface which had a load voltage very close to the reduction of $CuCl_2$ to CuCl.

Although a fresh positive electrode showed excellent utilization of the second electron of the $CuCl_2$ electrode, repeatedly operating the cell to 2.0 V cut off showed a rapid decrease of cell capacity as illustrated in Figure 82 for a 2 gram $CuCl_2$ electrode of composition 60 w% $CuCl_2$, 30 w% carbon and 10 w% PTFE discharged at 2 mA/cm^2 and recharged at 1 mA/cm^2. The cell was initially operated with 2.2 V cutoff and showed rapid loss of cell capacity. Raising the discharge cut-off to 2.6 V, the capacity recovered to the amount corresponding to 100% utilization of the first electron discharge of the $CuCl_2$ and remained at this level for more than 100 cycles.

Figure 83 shows the performance of another cell cycled at 2 mA/cm^2 discharge rate to 2.6 V cutoff and charged at 1 mA/cm^2 to a 4.0 V cut off. The cell delivered a total of 400 cycles. The voltage profiles of a few selected cycles are shown in Figure 84.

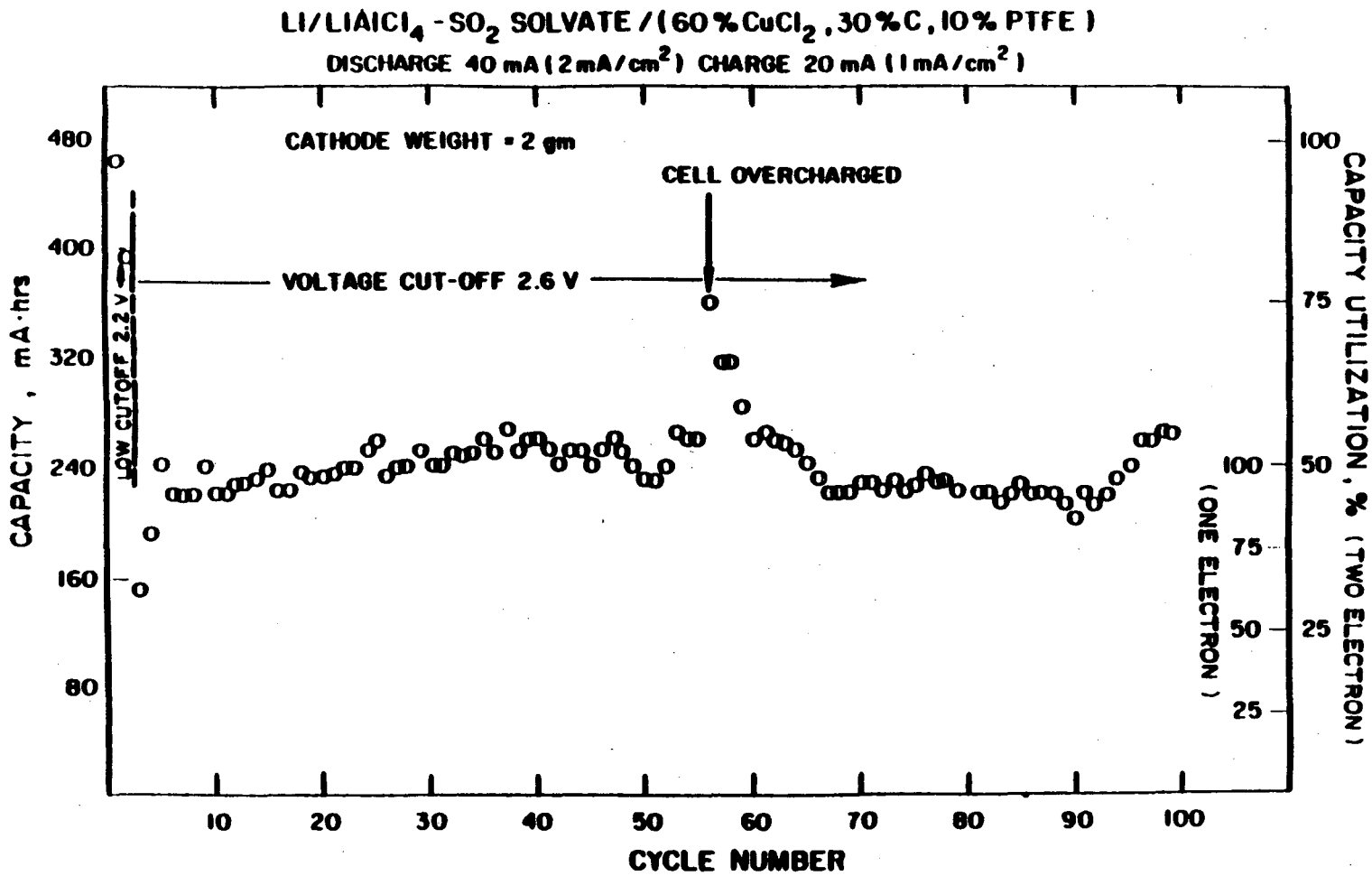

FIGURE 82 Cycling Performance of an Experimental $Li/CuCl_2$ Cell with $LiAlCl_4$-$3SO_2$ Electrolyte, Discharged at 2 mA/cm^2 and Charged at 1 mA/cm^2 - Effect of Cutoff Voltage.

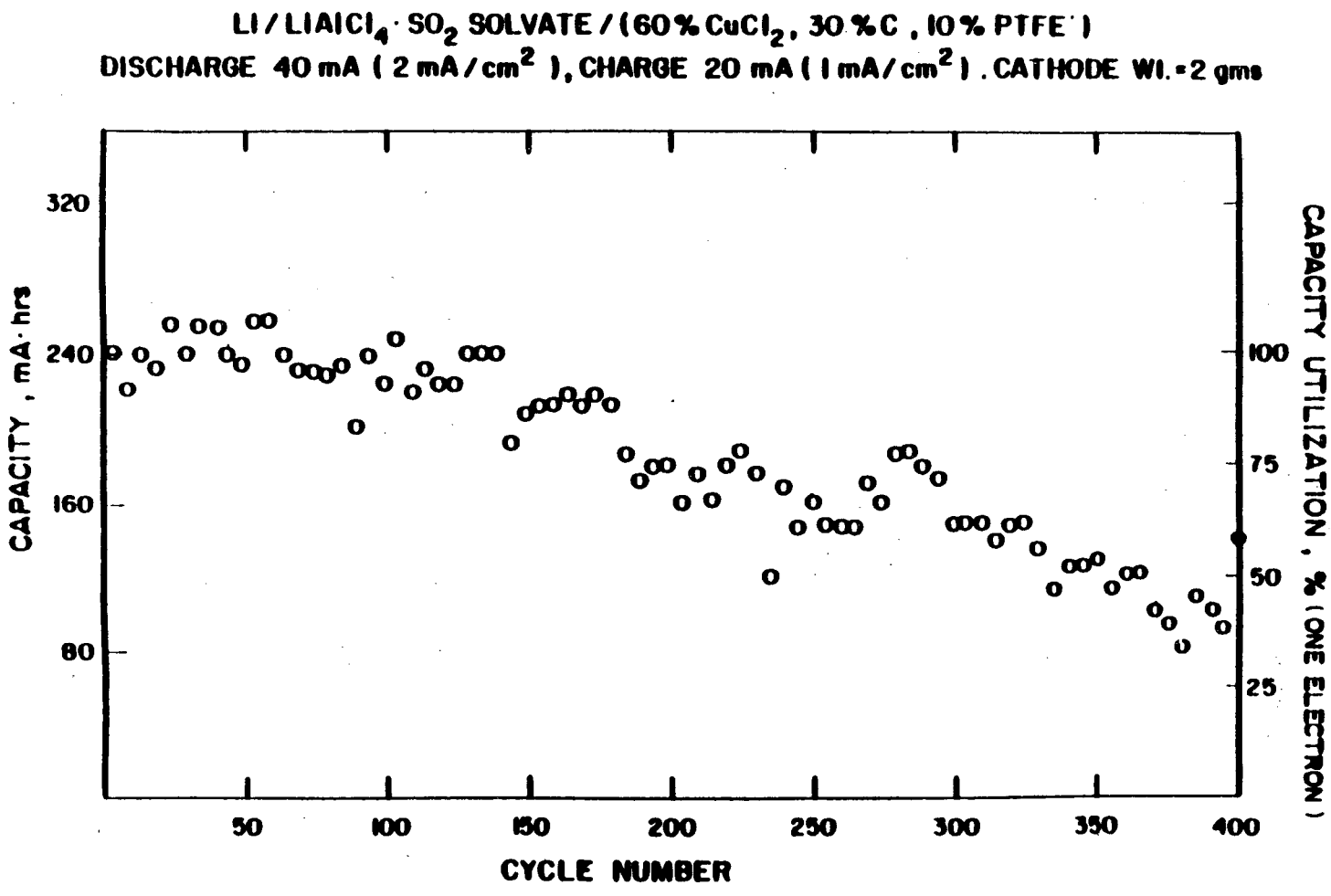

FIGURE 83. Cycling Performance of an Experimental $Li/CuCl_2$ Cell with $LiAlCl_4$-$3SO_2$ Electrolyte, Discharged at 2 mA/cm^2 to 2.6V Cut-off and Charged at 1 mA/cm^2.

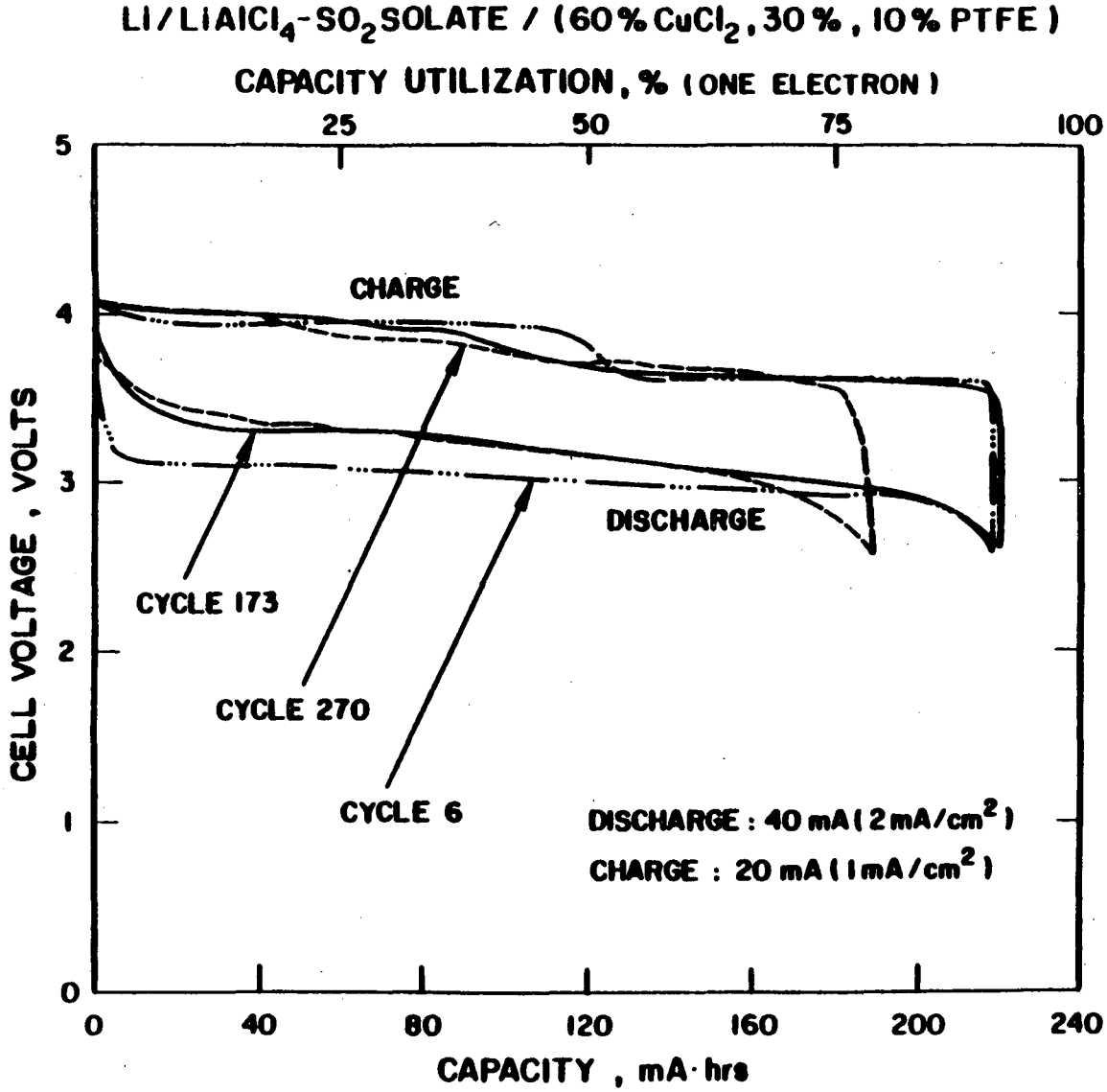

FIGURE 84. The Voltage Profiles of an Experimental $Li/CuCl_2$ Cell with $LiAlCl_4$-$3SO_2$ Electrolyte at Selected Cycles, Discharged at 2 mA/cm^2 to 2.6V Cut-off and Charged at 1 mA/cm^2.

Figure 85 shows a cell with a 1 gm electrode containing 80% $CuCl_2$ discharged at 2 mA/cm^2 to 25% depth (based on 2 electron utilization) and recharged at 1 mA/cm^2. The cell delivered over 1000 cycles. The cell had the positive electrode sandwiched between two 10 mil lithium electrodes (4 cm x 2.5 cm). A total capacity of about 80 turnovers of lithium was achieved in this cell.

b. Storage Characteristics

An experimental cell having a positive electrode of composition, $CuCl_2$ 80%, carbon 10% and PTFE 10%, was stored at 71°C for 2 weeks. The cell showed a voltage loss of about 0.2 V in the first discharge after the storage and the voltage recovered to normal in the sequential cycles as exhibited in Figure 86. The cell cycled for about 50 cycles and failed due to development of internal shorts.

Another experimental cell having $CuCl_2$ positive electrode ($CuCl_2$ 80%, carbon 10%, PTFE 10%) was stored for 100 days and then tested at 75% depth with 2 mA/cm^2 discharge and charge rates. The first discharge cycle showed a loss of capacity as shown in Figure 87. However, after recharge the cell recovered to show its normal voltage characteristics as exhibited in the figure. The cell operated for about 80 cycles and failed due to development of internal shorts.

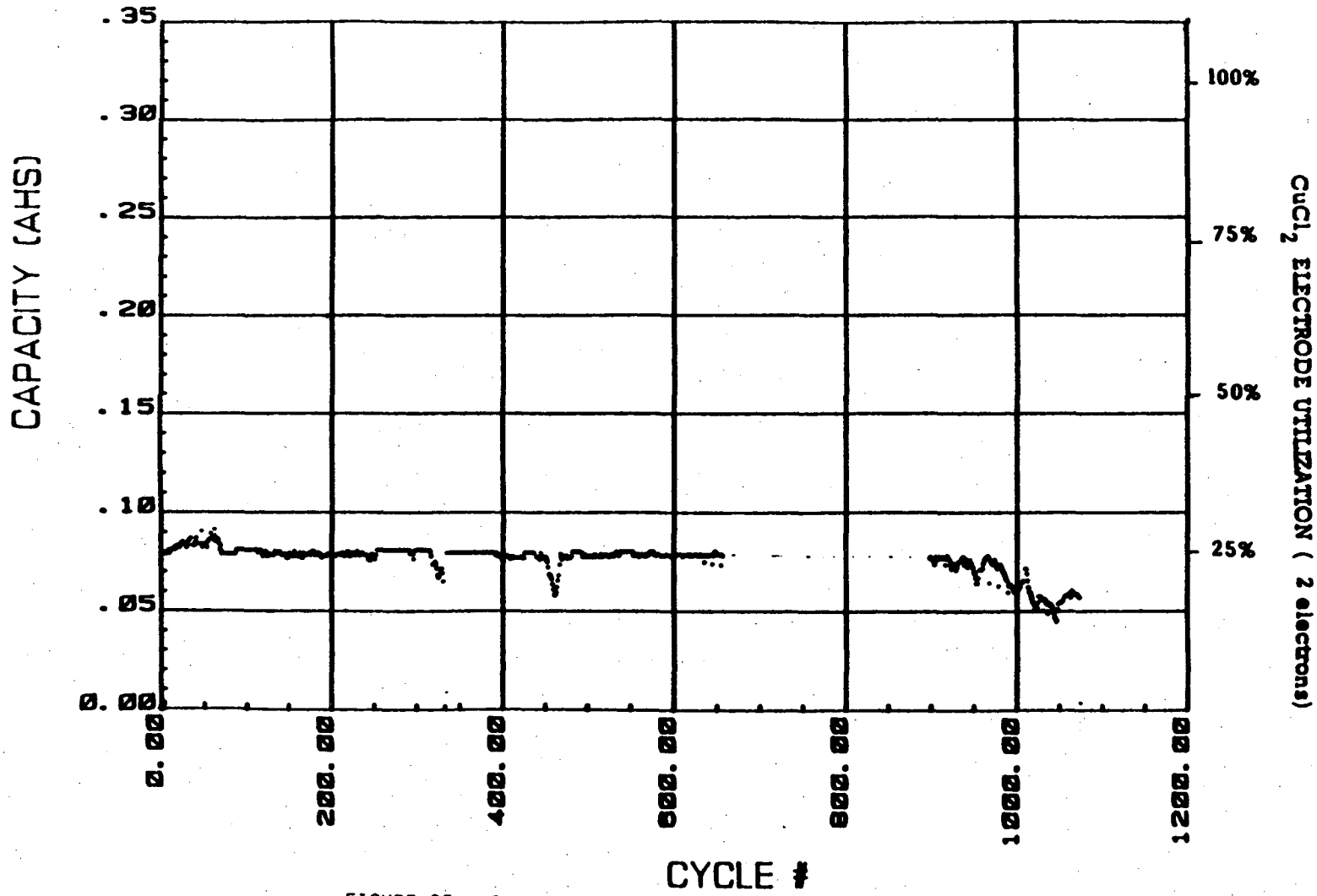

FIGURE 85. Cycling Performance of an Experimental $Li/CuCl_2$ Cell with $LiAlCl_4$-$3SO_2$ Electrolyte, Discharged at 2 mA/cm^2 to 25% Depth (2 Electron Reduction) and Charged at 1 mA/cm^2.

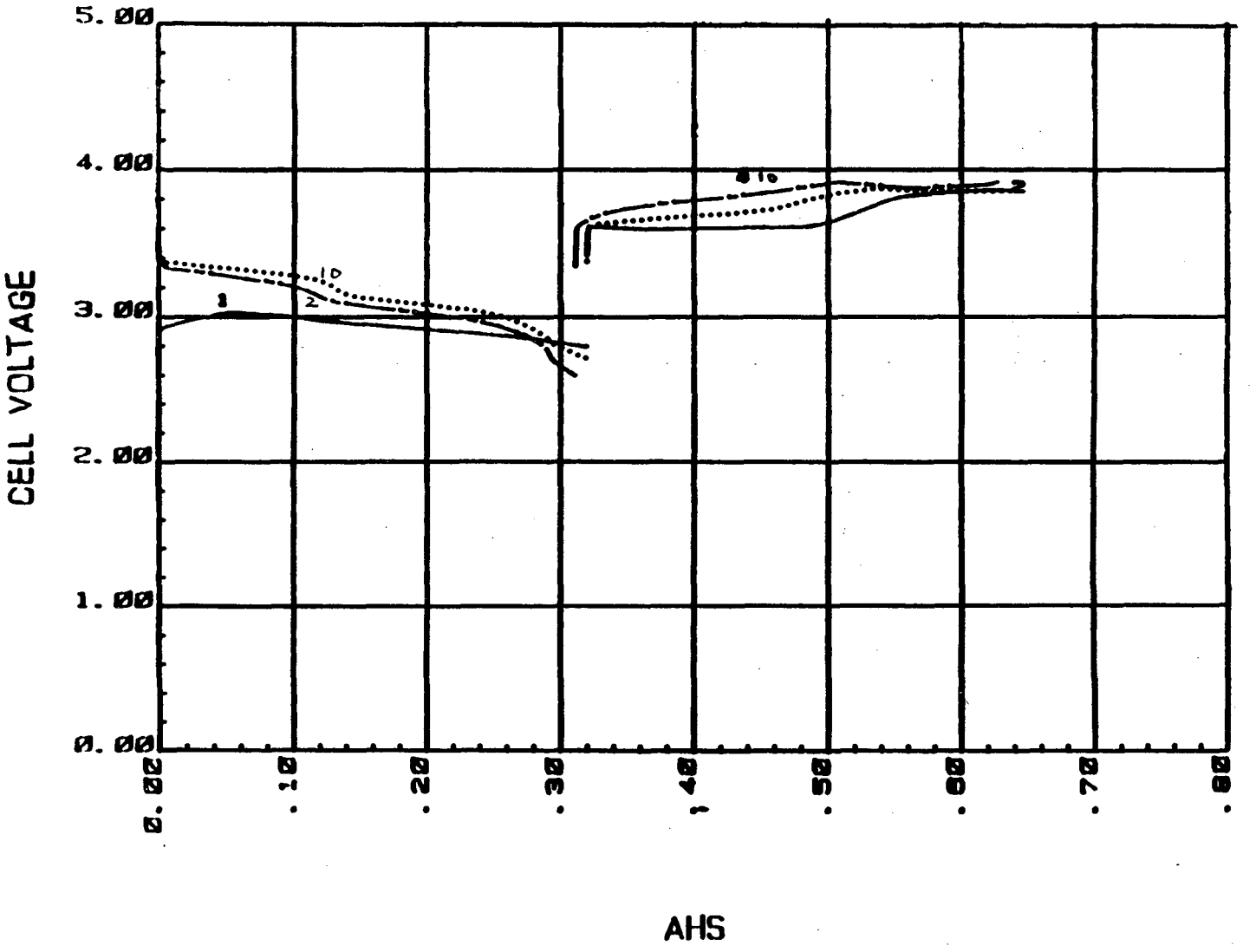

FIGURE 86. Voltage Characteristics of an Experimental $Li/CuCl_2$ Cell with $LiAlCl_4$-$3SO_2$ Electrolyte after 2 Weeks Storage at 71°C, Discharged at 2 mA/cm^2 and Charged at 1 mA/cm^2.

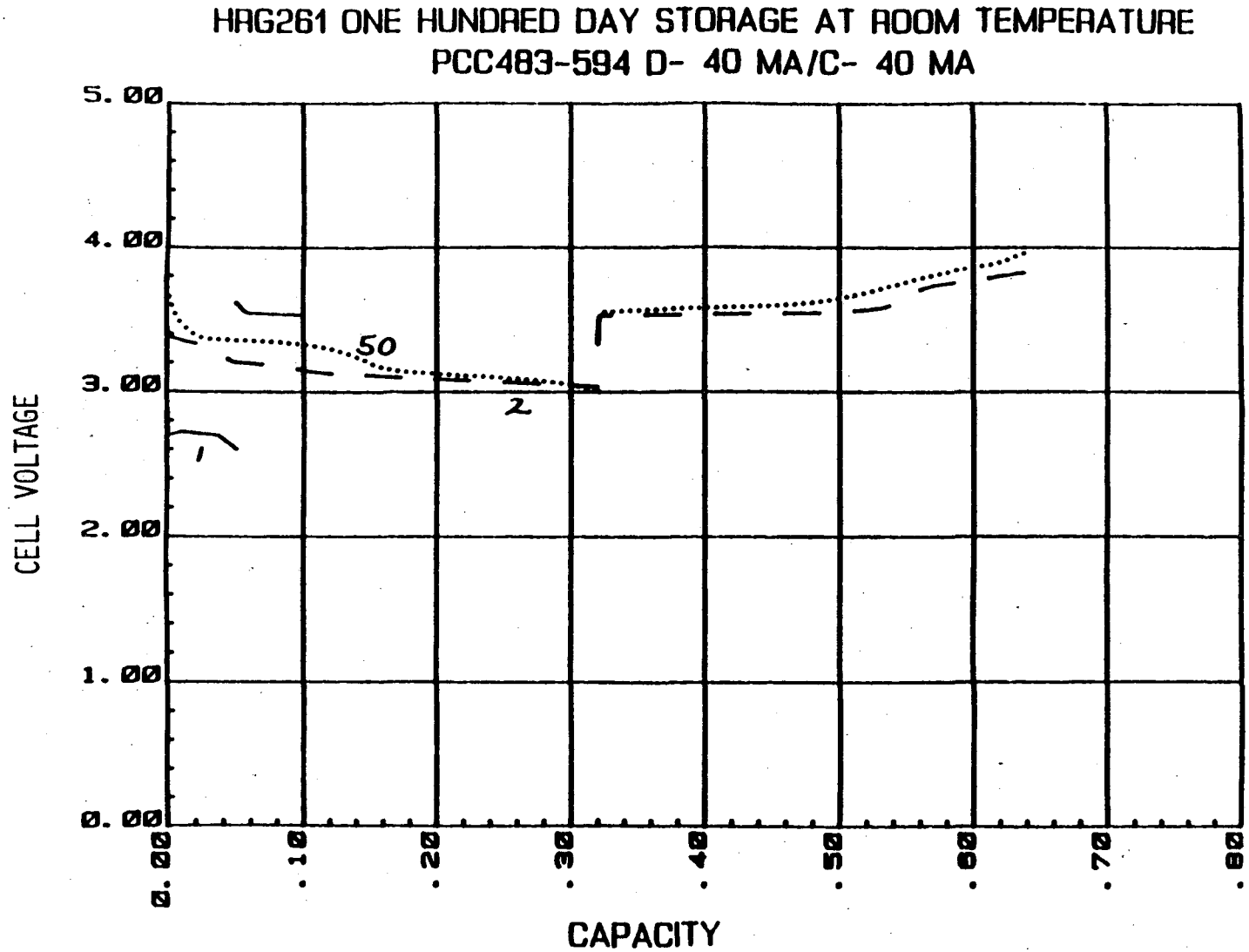

FIGURE 87. Voltage Characteristics of an Experimental $Li/CuCl_2$ Cell with $LiAlCl_4$-$3SO_2$ Electrolyte after 100 Days Storage at Ambient Temperature, Discharged at 2 mA/cm^2 and Charged at 1 mA/cm^2.

The initial loss of capacity and the decrease in cell votage were probably related to the formation of a thick film on lithium after storage. A dark film was usually observed on the surface of lithium after it was stored for a short period at elevated temperature in electrolyte containing $CuCl_2$ positive electrode (i.e. 70^o for 2 weeks). The film was mainly composed of LiCl as identified by SEM/EDX and only a small amount of Cu was detected. For checking the source of Cu, the solubilities of $CuCl_2$ and CuCl in the solvated $LiAlCl_4$-$3SO_2$ electrolyte were studied. The results are shown in following:

	Room Temperature	55^oC
$CuCl_2$	3×10^{-5} M	5×10^{-4} M
CuCl	1×10^{-4} M	5×10^{-2} M

Although the solubilities of both $CuCl_2$ and CuCl seem low at ambient temperature, the CuCl has significant high solubility at elevated temperature. Trace amounts of CuCl might be present in the fresh positive electrode and cause minor storage problem.

We also made a cell to cycle at 55^oC continuously at 2 mA/cm^2 discharge/charge rates and 75% depth. Figure 88 shows the voltage characteristics of the cell at the selected cycles. Although no significant decrease of discharge voltage on cycling was

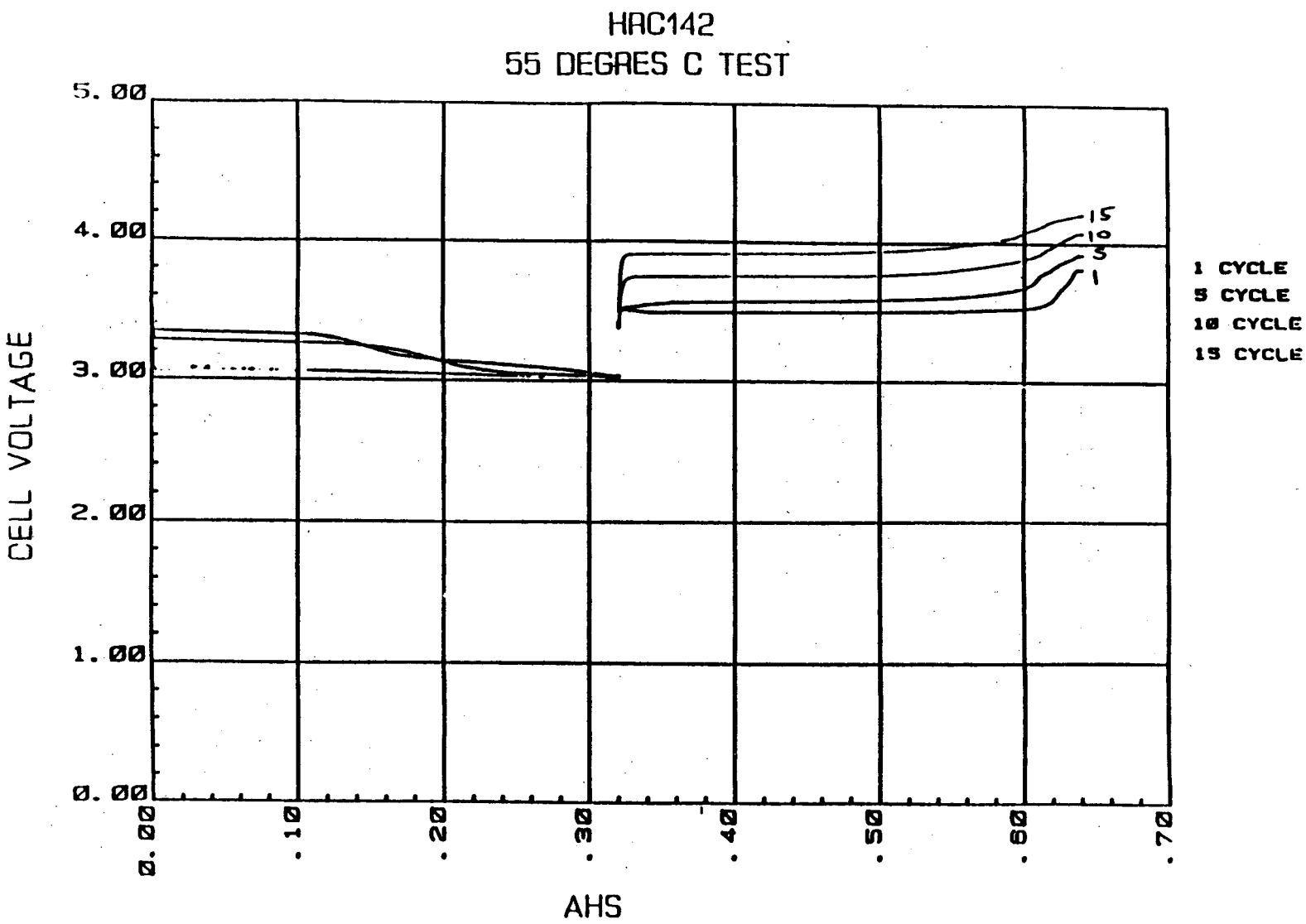

FIGURE 88. Voltage Characteristics of an Experimental $Li/CuCl_2$ Cell with $LiAlCl_4$-$3SO_2$ Electrolyte, Cycled at 55°C, Discharged at 2 mA/cm^2 and Charged at 1 mA/cm^2.

observed, the charge voltage increased obviously with cycling as shown in the figure. The cell operated for about 25 cycles and shorted internally.

4. With Other Tetrachloroaluminate/SO_2 electrolytes

Experimental Li/$CuCl_2$ cells were also made and filled with $NaAlCl_4$-$2.8SO_2$, $Ca(AlCl_4)$-$5.5SO_2$ and $Sr(AlCl_4)_2$-$5.6SO_2$ electrolytes for evaluation. The positive electrodes had a weight of 2 gm and a composition of $CuCl_2$ 60%, Carbon 30% and PTFE 10%. Figures 89 to 91 show the voltage profiles of the first discharge cycle at 1 mA/cm^2 or 2 mA/cm^2 rate with the respective electrolytes. All showed two discharge voltage plateaus corresponding to cupric and cuprous reductions similar to that of the cell with $LiAlCl_4$-SO_2 electrolyte. However, since an electrolyte containing lithium salt was preferred for lithium plating, cells were filled with various tetrachloroaluminates mixed with different amounts of lithium tetrachloroaluminate for cycling evaluation. Cells were cycled at 2 mA/cm^2 discharge rate to 2.6 V cutoff and 1 mA/cm^2 charge rate. The test results were summarized in Table 22. Most cells failed due to gradual loss of capacity. Figure 92 and 93 show two typical cycling performance of the cells, one with $(0.3LiAlCl_4.0.7NaAlCl_4)$-$3.0/SO_2$ electrolyte, the other with $(0.5LiAlCl_4.0.5Ca(AlCl_4)_2$-$5.6SO_2$ electrolyte. Although most alkali or alkali earth metal tetrachloroaluminate/SO_2 electrolytes were suitable for

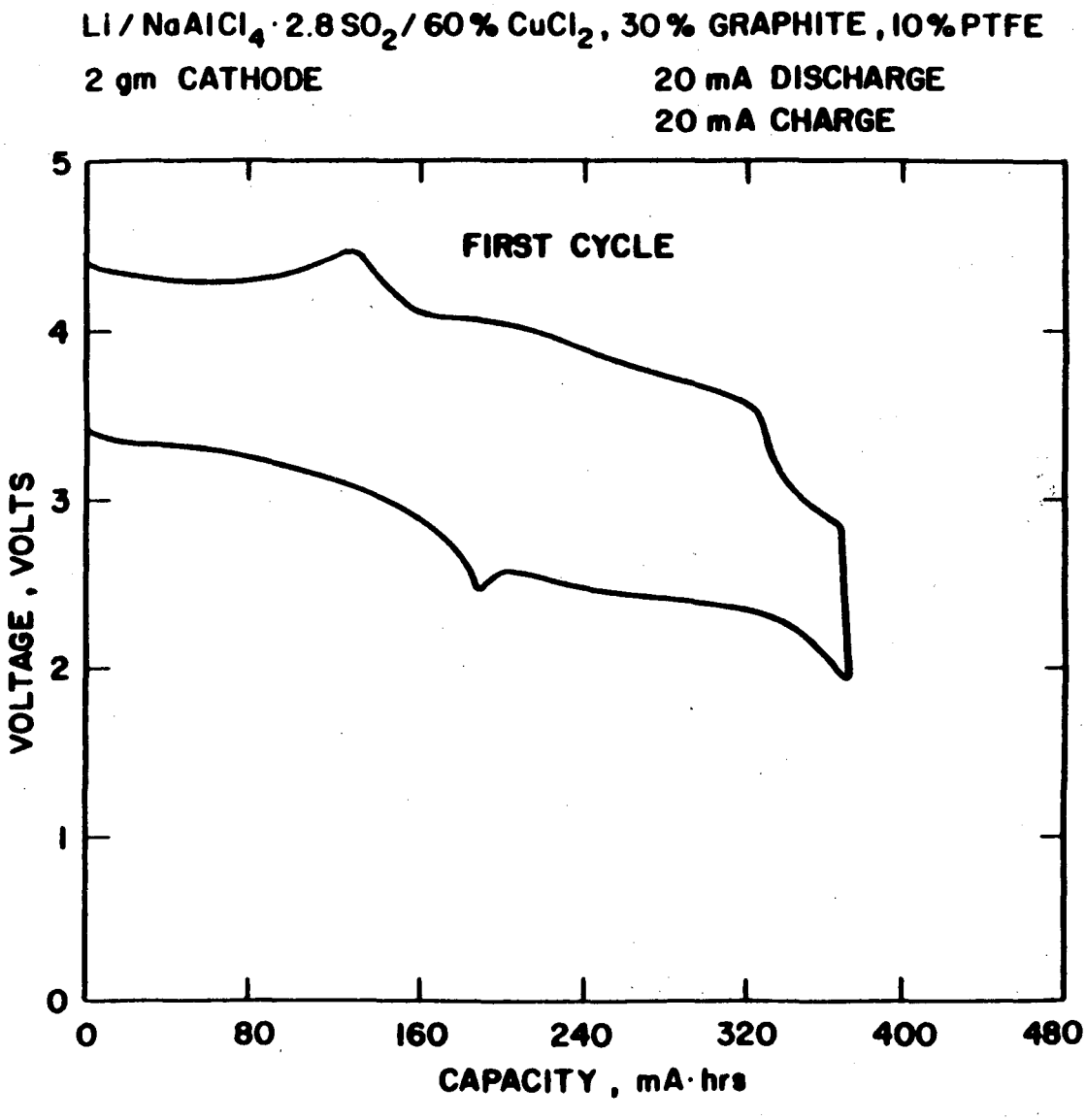

FIGURE 89 Voltage Characteristics of an Experimental $Li/CuCl_2$ Cell with $NaAlCl_4$-$2.8SO_2$ Electrolyte, Discharged at 1 mA/cm^2 and Charged at 1 mA/cm^2.

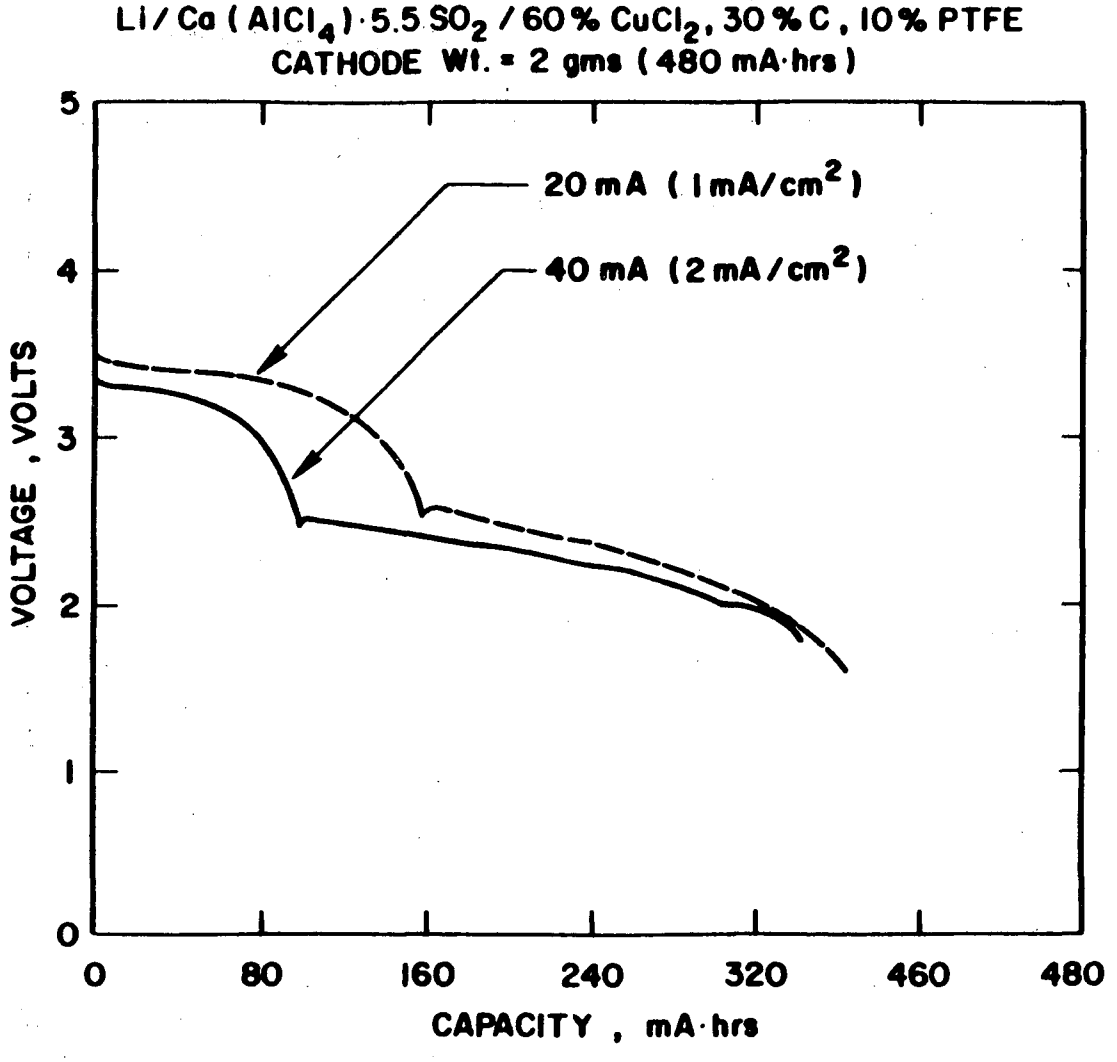

FIGURE 90. Voltage Characteristics of an Experimental $Li/CuCl_2$ Cell with $Ca(AlCl_4)_2$-$5.5SO_2$ Electrolyte, Discharged at 1 mA/cm^2 and 2 mA/cm^2.

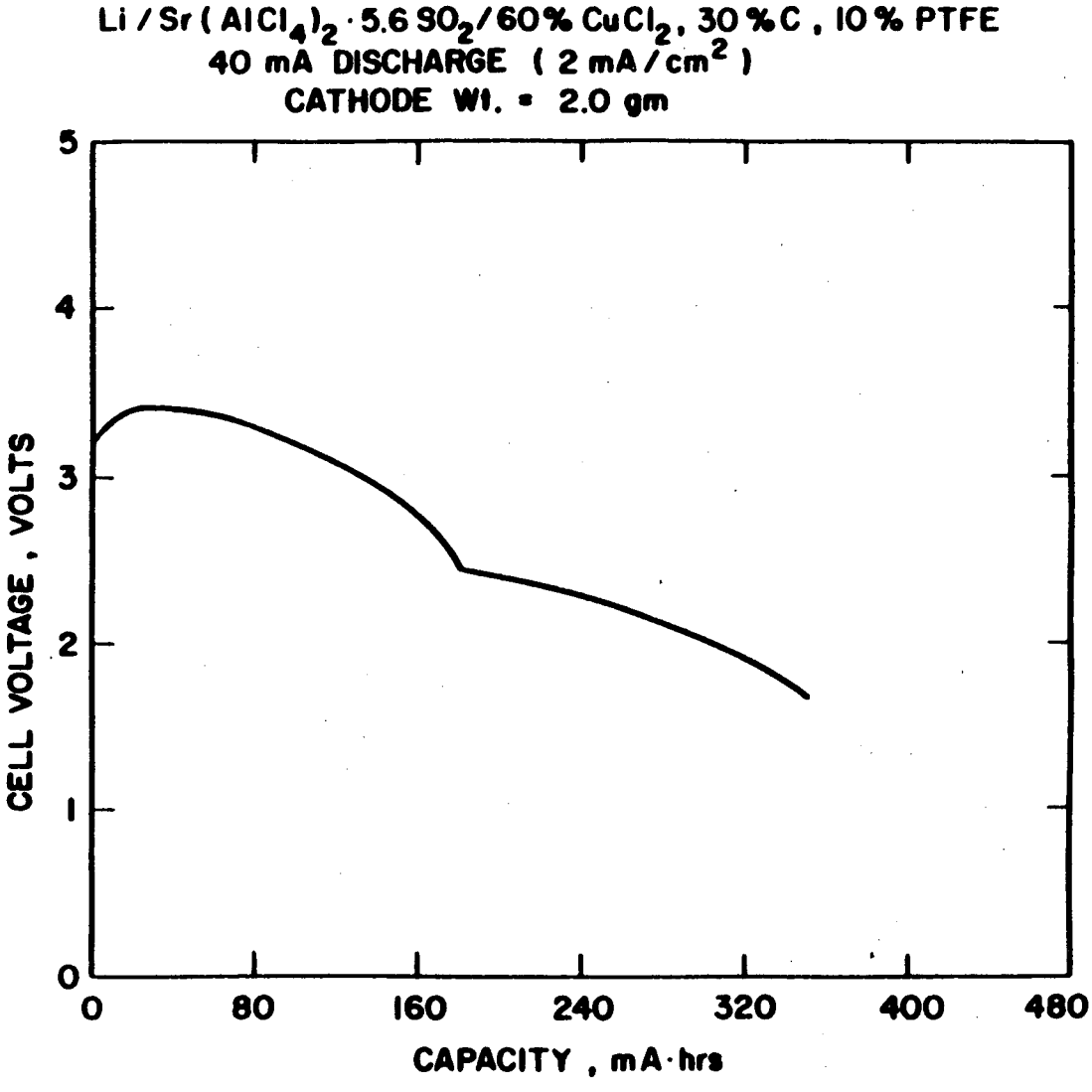

FIGURE 91. Voltage Characteristics of an Experimental $Li/CuCl_2$ Cell with $Sr(AlCl_4)_2$-$5.6SO_2$ Electrolyte, Discharged at 2 mA/cm^2.

TABLE 22. PERFORMANCE OF $Li/CuCl_2$ CELLS FILLED WITH MIXED ELECTROLYTES

Cell No.	No. of Cycles Delivered
A. 0.2 $LiAlCl_4$-0.8 $NaAlCl_4$-2.8SO_2	
HRA271	190
HRA272	192
HRA273	202
HRA274	151
HR7221	48 (shorted)
HR7191	357
HR8271	32 (shorted)
B. 0.3 $LiAlCl_4$-0.7 $NaAlCl_4$-2.8SO_2	
HR6096	96
HR6095	66
C. 0.8$LiAlCl_4$-0.2 $NaAlCl_4$-2.8SO_2	
HR6091	180
HR6092	182
HR7192	45
D. 0.8 Ca $(AlCl_4)_2$-0.2 $LiAlCl_4$-5.6 SO_2	
HR8101	94
HR8102	53
HR8171	81
E. 0.5 Ca $(AlCl_4)_2$-0.5 $LiAlCl_4$-5.6 SO_2	
HR628E	64
HR628F	151
F. 0.2 Ca $(AlCl_4)_2$-0.8 $LiAlCl_4$-5.6 SO_2	
HR628D	119
G. 0.5 Sr $(AlCl_4)_2$-0.5 $LiAlCl_4$-5.6 SO_2	
HR7144	74
HR7142	100
H. 0.2 Sr $(AlCl_4)_2$-0.8 $LiAlCl_4$-5.6 SO_2	
HR7143	70
HR7144	114

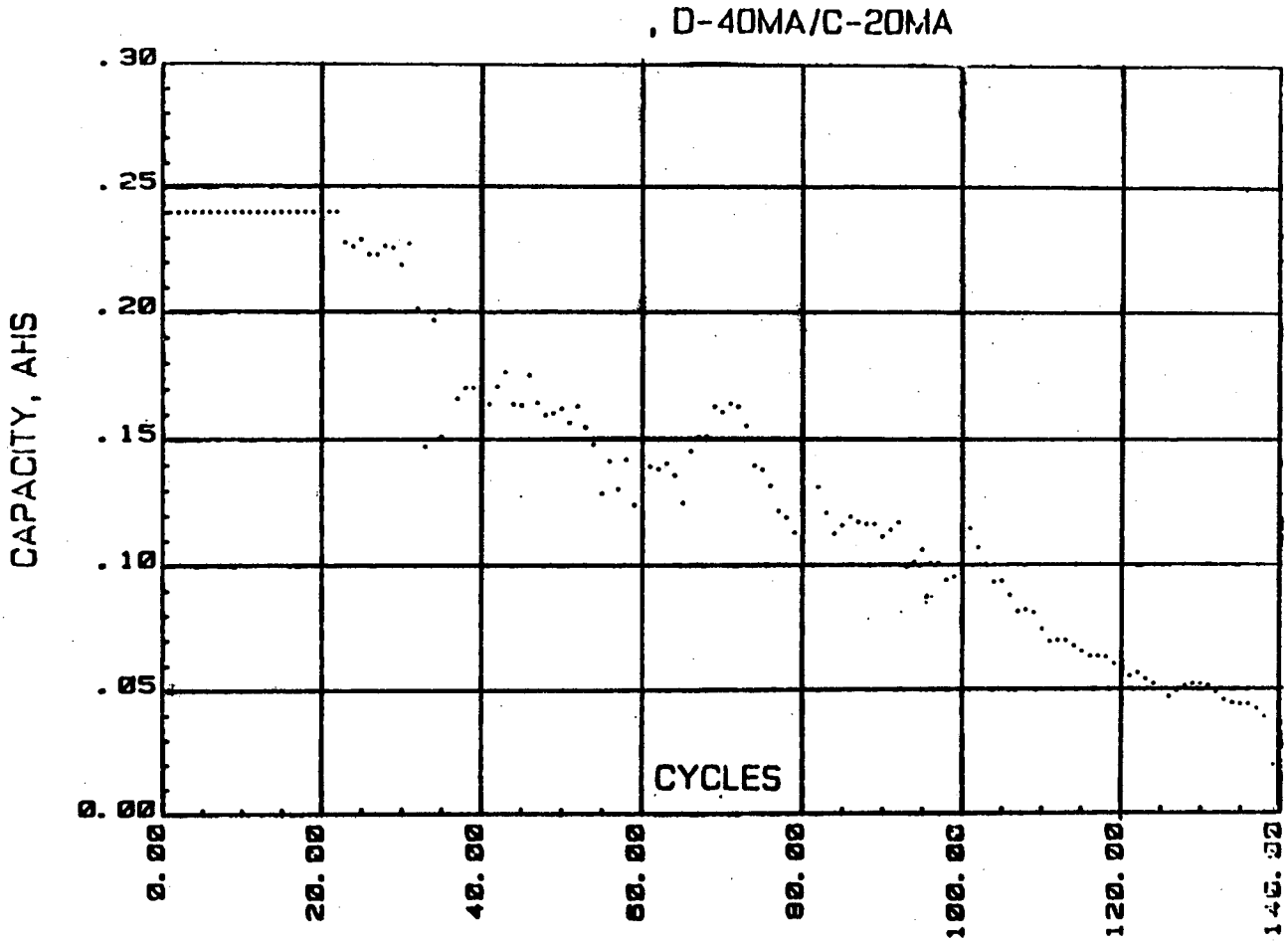

FIGURE 92. Cycling Performance of an Experimental $Li/CuCl_2$ Cell with $(0.3LiAlCl_4\text{-}0.7NaAlCl_4)\text{-}3.0SO_2$ Electrolyte, Discharged at 2 mA/cm^2 and Charged at 1 mA/cm^2.

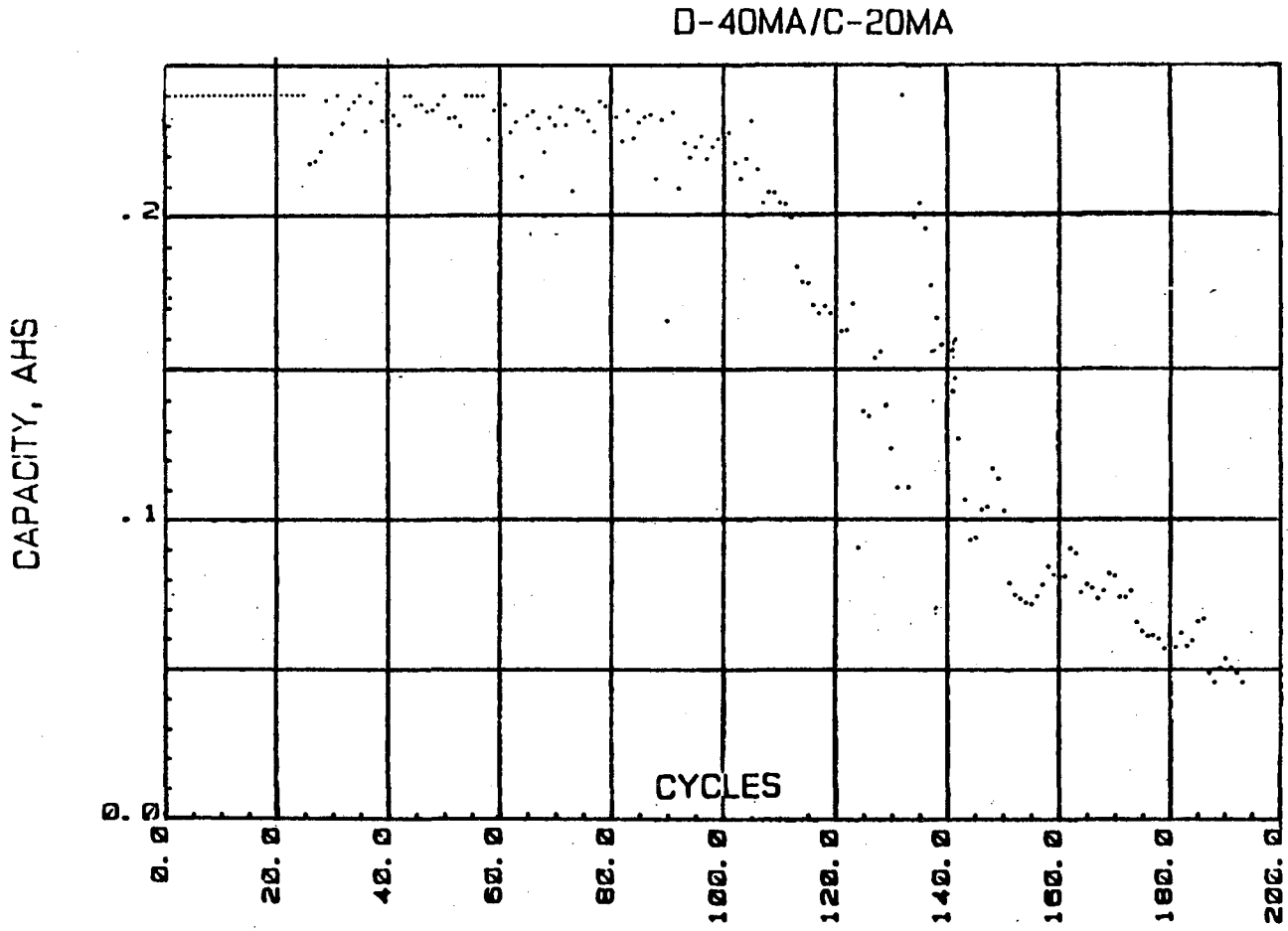

FIGURE 93. Cycling Performance of an Experimental Li/$CuCl_2$ Cell with $(0.5LiAlCl_4\text{-}0.5Ca(AlCl_4)_2)\text{-}5.6SO_2$ Electrolyte, Discharged at 2 mA/cm^2 and Charged at 1 mA/cm^2.

operating $CuCl_2$ positive electrodes, $LiAlCl_4/SO_2$ electrolyte provided the best cycling performance.

5. 2/3A Size Cells with Wound Electrode Design

2/3A size prototype cells with wound electrode design and $LiAlCl_4$-SO_2 electrolyte were made for evaluation using Duracell L032S hardware. The flexible $CuCl_2$ positive electrodes were made by mixing $CuCl_2$ powder 80%, Teflon 10%, carbon 10% with a proprietary solvent and pressing on nickel exmet followed by drying in oven at 140°C overnight. The positive electrode had a thickness of about 20 mils. Cells were made by winding a strip of positive electrode of about 8 inches in length and a strip of lithium electrode of 10 mil thickness separated by 2 layers of Celgard. The positive electrode was connected to the center post on the cover insulated from rest of the can. The cover was welded to the can by laser welder. The finished cells were filled with $LiAlCl_4$-$3SO_2$ electrolyte through the fill port on the bottom of the can.

Figure 94 shows the typical performance of the cells on primary discharge at various rates. The cells delivered about 1.0 Ah capacity with near 100% capacity utilization based on the amount of active $CuCl_2$. The discharge voltage profiles showed clearly two discharge steps corresponding to the reductions of cupric and cuprous chlorides respectively.

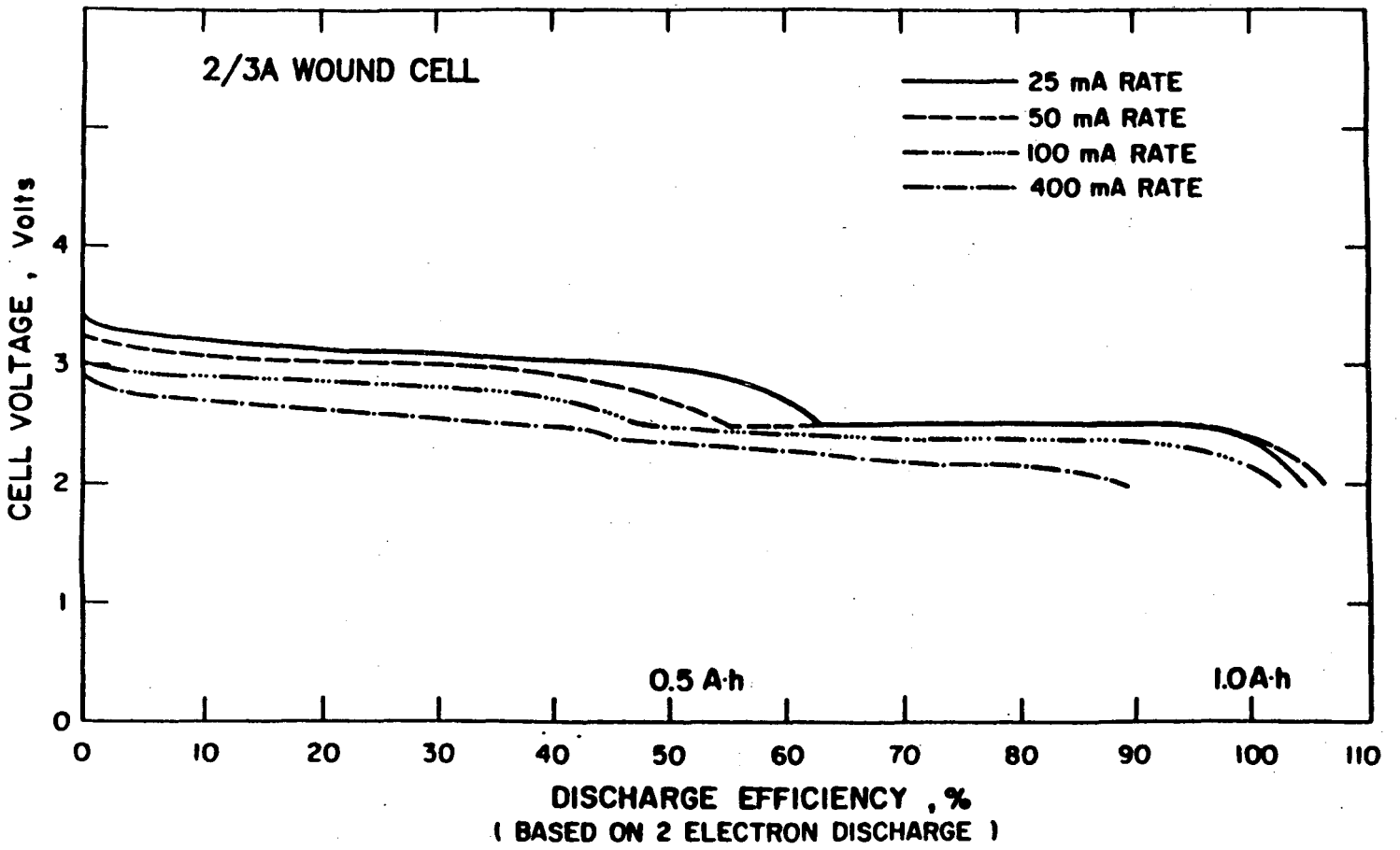

FIGURE 94. Discharge Characteristics of 2/3A Size $Li/CuCl_2$ Wound Cells with $LiAlCl_4$-$3.0SO_2$ Electrolyte at Various Rates.

Similar to the results obtained with experimental prismatic cells, the wound cells discharged deeply to a 2.0 V cutoff showed severe loss of capacity on cycling. Cells delivered only 5-10 cycles. Cells operated to 2.6 V cutoff performed somewhat better and were able to deliver 10-20 cycles as shown in Figure 95. The cycle life of the wound cells was significantly worse than the performance of the prismatic cells having dry pressed positive electrode. The poor cycling performance of the wound cells was probably caused by the preparation process of the flexible $CuCl_2$ positive electrode which involved the use of a solvent. It is believed that the performance of the wound cells can be further improved with proper fabrication process of the positive electrode.

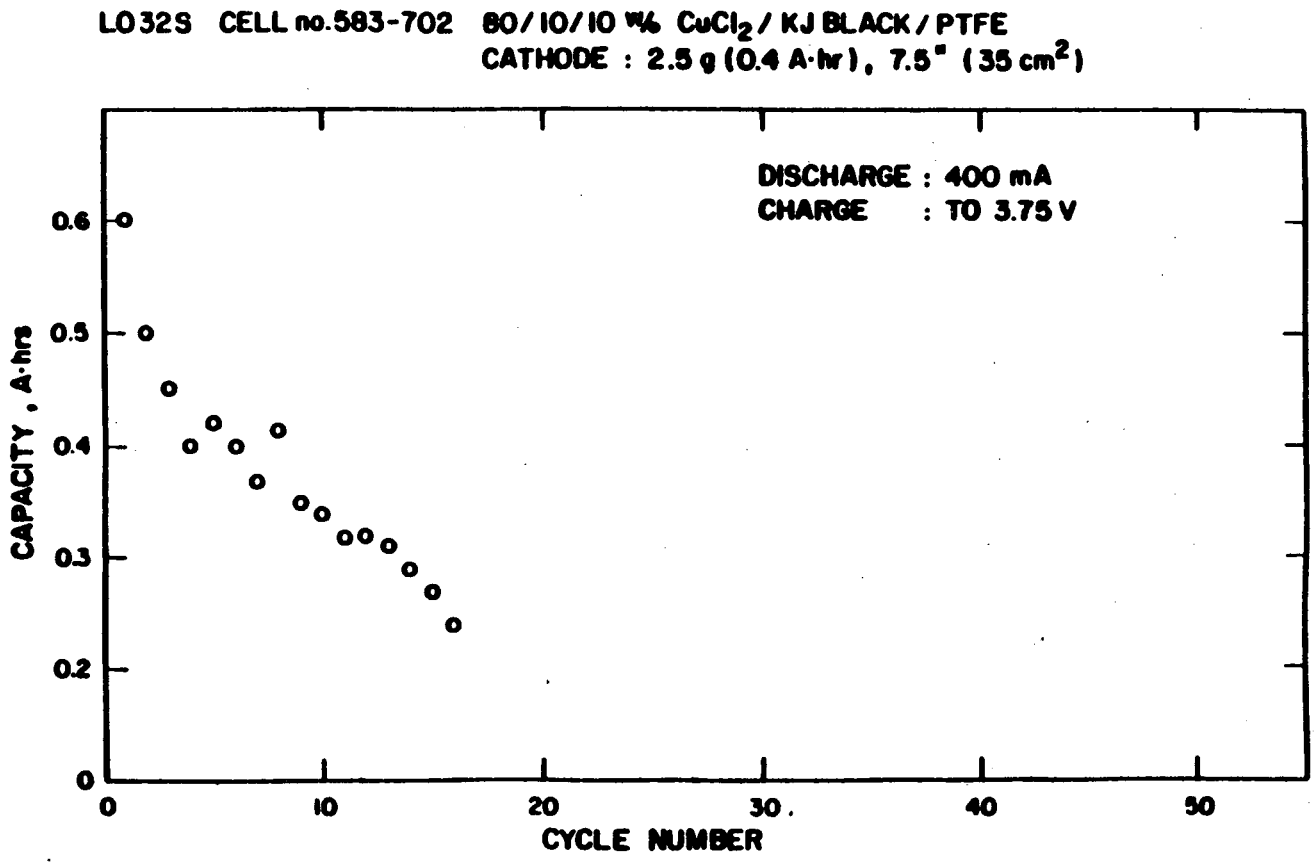

FIGURE 95. Cycling Performance of a 2/3A Size Li/$CuCl_2$ Wound Cell with $LiAlCl_4$-3.0SO_2 Electrolyte.

VI. CONCLUSION

Continuing efforts on research and development of ambient temperature rechargeable lithium batteries with the inorganic SO_2 electrolytes have made several significant achievements and discoveries as highlighted in following:

1. In addition to the $Li_2B_{10}Cl_{10}$ and $LiGaCl_4$ electrolyte salts, several low cost alkali and alkaline-earth metal tetrachloroaliuminates have been found to dissolve readily in SO_2 to provide high conductivity. A conductivity of about 1×10^{-1} $ohm^{-1}cm^{-1}$ at room temperature can be obtained with $LiAlCl_4/SO_2$ and $NaAlCl_4/SO_2$ electrolytes, which is significantly higher than the conductivities obtained with organic electrolytes.

2. Most alkali and alkaline-earth metal tetrachloroaluminates can form highly conductive liquid solvates with SO_2, which have significantly lower vapor pressure than the pressurized SO_2 electrolytes.

3. SO_2 solvated $LiAlCl_4$ electrolytes ($LiAlCl_4$-$3SO_2$ or $LiAlCl_4$-$6SO_2$) can provide excellent lithium cycling efficiency. A plating/stripping efficiciency of lithium above 96% has been obtained with the solvated electrolytes.

4. Li/SO_2 cell with $Li_2B_{10}Cl_{10}/SO_2$ or $LiGaCl_4/SO_2$ electrolyte can provide good primary energy or capacity. However the cycle life is poor due to degradation of the positive electrode.

5. The Li/Carbon system with $LiAlCl_4/SO_2$ electrolyte has an OCV of 3.2 V and discharges with the formation of a complex with the tetrachloroaluminate on the carbon surface. The system has a theoretical energy density of about 540 Wh/kg. The cell capacity is limited by either carbon or the $LiAlCl_4$ salt. Carbon with high surface area and high pore volume (DBP adsorption), such as Ketjen Black EC carbon, can provide better capacity utilization.

6. $Li/LiAlCl_4$-xSO_2/carbon system has shown good cycle life in experimental cells containing excess electrolyte. 2/3A size wound cells have shown good cycle life on partial discharge but poor cycle life (40-60 cycles) on deep discharge. A capacity fading of about 1-2% per cycle has been observed on deep discharge presumably due to exhaustion of the

electrolyte salt at the end of deep discharge which causes insufficiency of charge or degradation of the carbon positive electrode.

7. The inorganic SO_2 electrolytes can be used with active solid positive electrode materials such as $CuCl_2$, $NiCl_2$, $CoCl_2$ and MoO_3 etc.

8. The $Li/CuCl_2$ system with the SO_2 solvated $LiAlCl_4$ electrolyte has shown excellent cycling performance in experimental cells with dry pressed electrodes. Cells have demonstrated near 400 cycles to 2.6 V cutoff on discharge. However, wound cells made with rolled $CuCl_2$ positive electrode, which involved the use of solvents, have shown poor cycling performance and storage life.

Table 23 compares the specific energy densities of the systems with the inorganic SO_2 electrolyte to other conventional rechargeable systems. The lithium rechargeable systems with the inorganic electrolytes have certainly the advantage of high energy density. Another important advantage of the rechargeable systems using SO_2 electrolyte with the $LiAlCl_4$ salt is that the systems are capable of taking limited overcharge. Recombination ot the overcharge products to reform the electrolyte salt is the cell balancing mechnaism. However, a separator which is chemically inert

TABLE 23. COMPARISON OF THE ENERGY DENSITIES OF VARIOUS RECHARGEABLE SYSTEMS

ENERGY DENSITIES OF VARIOUS RECHARGEABLE BATTERIES

System	Voltage	Energy Density, W.hr/kg		Comparison Ratio
		Theoretical	Practical	
Pb/Acid	2.0	170	28	1
Ni/Cd	1.3	210	30	1
Ni/Zn	1.6	321	50	1.6
Li/SO_2	2.9	1095	200	6.7
$Li/CuCl_2$	3.4	606 (1 electron)	120	4
$Li/LiAlCl_4 .6SO_2$/Carbon	3.2	524	100	3.3

to the overcharge products, Cl_2 and $AlCl_3$ is required. Degradation of the separator and formation of internal shorts after numerous cycles might cause venting violently.

Further study of the inorganic rechargeable systems with modification of the electrolyte composition and development of new separator materials to improve the cycle life and safety characteristics is recommended.

VII. REFERENCES

1. U.S. Patent 4,010,240, P. R. Mallory & Co. Inc., 1977.

2. U.S. Patent 4,071,604, P. R. Mallory & Co. Inc., 1978.

3. U.S. Patent 4,139,680, P. R. Mallory & Co. Inc., 1979.

4. U.S. Patent 3,567,515, American Cyanamid Company, 1971.

5. F. A. Cotton & G. Wilkinson "Advanced Inorganic Chemistry", 3rd Ed., 247, Interscience, N.y.

6. W. H. Knoth, H. C. Miller, J. C. Sauer, J. H. Balthis, Y. T. Chia and E. L. Muetterties, Inorg. Chemistry, 3, 159 (1964).

7. "All Inorganic Ambient Temperature Rechargeable Lithium Battery", Final Report, LBL Contract No. 4507410, 1980.

8. W. Bowden "Electrochemical Oxidation of Polyhedral Boron Halide Anions" J. Electrochem. Soc. 129 (6), 1249, 1982.

9. A. Simon, K. Peters, E. M. Peters, H. Kuhnl and B. Koslowski, Z. Anorg. Allg. Chem. 469, 94 (1980).

10. B. Koslowski, Dissertation, The University of Hanover, 1979.

11. Mallory Battery Company, "Lithium Battery Product Bulletin" #479, Duracell Inc., Elmsford, NY.

12. A. N. Dey, J. Power Sources 5, 57 (1980).

13. P. Bro, H. Y. Kang, C. Schlaikjer and H. Taylor, Tenth IECEC Record, 432 (1975).

14. A. N. Dey and W. Bowden, Duracell Final Report on Contract 4507410 to Lawrence Berkeley Laboratory, University of California, 1981.

15. G. Nickless, Inorganic Sulfur Chemistry, p 521.

LAWRENCE BERKELEY LABORATORY
TECHNICAL INFORMATION DEPARTMENT
UNIVERSITY OF CALIFORNIA
BERKELEY, CALIFORNIA 94720